DOCTOR OF PHILOSOPHY

Surface pre-treatment methods for improving adhesion ability in wood plymer composite for frame and furniture construction applications

Dimitriou, Athanasios

Award date:
2015

Awarding institution:
Bangor University

Surface pre-treatment methods for improving adhesion ability in Wood Polymer Composite for frame and furniture construction applications

A thesis submitted in partial fulfilment of the requirements of the Bangor University for the degree of Doctor of Philosophy

---

Submitted by

Dimitriou Athanasios

SCHOOL OF ENVIRONMENT, NATURAL RESOURCES AND GEOGRAPHY,

BANGOR UNIVERSITY,

BANGOR GWYNEDD, UNITED KINDOM

May, 2015

DECLARATION AND CONSENT

Details of the Work

I hereby agree to deposit the following item in the digital repository maintained by Bangor University and/or in any other repository authorized for use by Bangor University.

Author Name: *Athanasios Dimitriou*…….……..

Title: *Surface pre-treatment methods for improving adhesion ability in Wood Polymer Composite for frame and furniture construction applications*……..…….

Supervisor/Department: *Dr. Michael D. Hale, Dr. Morwenna Spear*.....

Funding body (if any):.....

Qualification/Degree obtained: *Doctor of Philosophy*……..…….

This item is a product of my own research endeavours and is covered by the agreement below in which the item is referred to as "the Work". It is identical in content to that deposited in the Library, subject to point 4 below.

Non-exclusive Rights

Rights granted to the digital repository through this agreement are entirely non-exclusive. I am free to publish the Work in its present version or future versions elsewhere.

I agree that Bangor University may electronically store, copy or translate the Work to any approved medium or format for the purpose of future preservation and accessibility. Bangor University is not under any obligation to reproduce or display the Work in the same formats or resolutions in which it was originally deposited.

Bangor University Digital Repository

I understand that work deposited in the digital repository will be accessible to a wide variety of people and institutions, including automated agents and search engines via the World Wide Web.

I understand that once the Work is deposited, the item and its metadata may be incorporated into public access catalogues or services, national databases of electronic theses and dissertations such as the British Library's EThOS or any service provided by the National Library of Wales.

I understand that the Work may be made available via the National Library of Wales Online Electronic Theses Service under the declared terms and conditions of use (http://www.llgc.org.uk/index.php?id=4676). I agree that as part of this service the National Library of Wales may electronically store, copy or convert the Work to any approved medium or format for the purpose of future preservation and accessibility. The National Library of

Wales is not under any obligation to reproduce or display the Work in the same formats or resolutions in which it was originally deposited.

Statement 1:

This work has not previously been accepted in substance for any degree and is not being concurrently submitted in candidature for any degree unless as agreed by the University for approved dual awards.

Signed …….. (candidate)

Date ……..

Statement 2:

This thesis is the result of my own investigations, except where otherwise stated. Where correction services have been used, the extent and nature of the correction is clearly marked in a footnote(s).

Other sources are acknowledged by footnotes giving explicit references. A bibliography is appended.

Signed ……. (candidate)

Date …….

Statement 3:

I hereby give consent for my thesis, if accepted, to be available for photocopying, for inter-library loan and for electronic repositories, and for the title and summary to be made available to outside organisations.

Signed ……. (candidate)

Date …….

NB: Candidates on whose behalf a bar on access has been approved by the Academic Registry should use the following version of **Statement 3:**

Statement 3 (bar):

I hereby give consent for my thesis, if accepted, to be available for photocopying, for inter-library loans and for electronic repositories after expiry of a bar on access.

Signed …… (candidate)

Date ……

Statement 4:

Choose **one** of the following options

a)	I agree to deposit an electronic copy of my thesis (the Work) in the Bangor University (BU) Institutional Digital Repository, the British Library ETHOS system, and/or in any other repository authorized for use by Bangor University and where necessary have gained the required permissions for the use of third party material.	✓
b)	I agree to deposit an electronic copy of my thesis (the Work) in the Bangor University (BU) Institutional Digital Repository, the British Library ETHOS system, and/or in any other repository authorized for use by Bangor University when the approved **bar on access** has been lifted.	
c)	I agree to submit my thesis (the Work) electronically via Bangor University's e-submission system, however I **opt-out** of the electronic deposit to the Bangor University (BU) Institutional Digital Repository, the British Library ETHOS system, and/or in any other repository authorized for use by Bangor University, due to lack of permissions for use of third party material.	

Options B should only be used if a bar on access has been approved by the University.

In addition to the above I also agree to the following:

1. That I am the author or have the authority of the author(s) to make this agreement and do hereby give Bangor University the right to make available the Work in the way described above.

2. That the electronic copy of the Work deposited in the digital repository and covered by this agreement, is identical in content to the paper copy of the Work deposited in the Bangor University Library, subject to point 4 below.

3. That I have exercised reasonable care to ensure that the Work is original and, to the best of my knowledge, does not breach any laws – including those relating to defamation, libel and copyright.

4. That I have, in instances where the intellectual property of other authors or copyright holders is included in the Work, and where appropriate, gained explicit permission for the inclusion of that material in the Work, and in the electronic form of the Work as accessed through the open access digital repository, *or* that I have identified and removed that material for which adequate and appropriate permission has not been obtained and which will be inaccessible via the digital repository.

5. That Bangor University does not hold any obligation to take legal action on behalf of the Depositor, or other rights holders, in the event of a breach of intellectual property rights, or any other right, in the material deposited.

6. That I will indemnify and keep indemnified Bangor University and the National Library of Wales from and against any loss, liability, claim or damage, including without limitation any related legal fees and court costs (on a full indemnity bases), related to any breach by myself of any term of this agreement.

Signature: …… Date : ……

ABSTRACT

This study was held to investigate the possibility of improving the WPC adhesion ability by pre-treatment of the material surface. Pre-treatments are used by the polymer industry to oxidize and alter the polymer's surface to improving the surface energy and adhesion ability, resulting in more effective surface for painting and coating. In some cases, the pre-treatment methods that the polymer industry uses require expensive and complicated equipment like corona, plasma, and fluorination treatments, and in some cases dangerous chemicals like chromic acid. The adhesion improvement of the WPC is essential for coating, frame construction and furniture manufacture. The lack of effective WPC adhesion limits the potential usage of the material, to constructions like decking, and the only substantial joining method which are available from today's manufacturers market, are metallic and plastic fasteners, including nails and screws. Pre-treatments for improving adhesion could provide the possibility of building structures within a small workshop, increasing the variety of WPC applications. The increase of the WPC usage, could be environmentally beneficial because it is a part renewable material with the possibility to be part produced from recycled and waste materials. Moreover, it is a weather resistance material with minimum need of preservation.

In this study, hydrogen peroxide, hot air gun, flame and halogen heating lamps pre-treatment methods, which could be applied without the usage of sophisticated and expensive equipment, were investigated. In order to evaluate the effectiveness of each treatment to produce higher adhesion strength a series of experiments were undertaken. Lap joint shear strength of the bonding line was the main test to evaluate the adhesion ability changes of the WPC material. To investigation the reasons that lead to efficient adhesion, surface characterization was also performed. The surface characteristics that were study were Surface roughness, scanning electron microscopy (SEM), surface energy and FTIR-ATR spectroscopy. The aesthetic aspect of the surface after the pre-treatments was also studied by light microscopy and colour determination. All the treatment methods, except the halogen heating lamp, are able to increase the adhesion strength of the WPC material.

All treatments except of the halogen heating lamps, which was reducing the adhesion strength to values lower than the control samples, were increasing the WPCs adhesion ability to values that causing material failure and not just to bonding line.

Surface characterization showed cluster relationships between the adhesion strength and the surface chemistry and morphology but there was not any specific trend that could

explain the adhesion behaviour with confidence. However all the treated samples showed some morphologically and chemically modification.

The aesthetic investigation of the treated samples showed that there were treatment methods which were causing colour differences which in some cases like flame treatment, were the treatment was more aggressive, the samples appeared to have a more “bunt” appearance. However the bleaching ability of the hydrogen peroxide caused the highest colour difference.

ACKNOWLEDGEMENTS

I would like to express my appreciation to my supervisors Dr. Mike D. Hale and Dr. Morwenna Spear for supervising my research. Their support, advice and guidance has been essential for completing this research. I would like to thank them for making this happen and also for all their scientific and technical support. I would also like to thank Professor Dr. George Ntalos for supervising my research in Greece and also the school of Wood and Furniture Design and Technology of the Technical Educational Institute of Larissa branch of Karditsa which offered me their laboratories and equipment to run a series of experiments of this research.

I would like to give special thanks to Kompetenzzentrum Holz GmbH Austria for supplying me the WPC material which was produced under the European research project ERA-NET Cornet/2006/01. I would also like to thank Assistant Professor Dr. Eleni Pavlidou of the Department of Physics of the Aristotle University of Thessaloniki for the use of SEM.

Many thanks to Professors Dr. Ioannis Kakaras, Dr. Sotiris Karastergiou, Dr. George Madanis, Dr. Ioannis Papadopoulos and Dr. Marios Trigas for their support. Also I would like to thank Evangelia Agnantopoulou, MSc for guidance in the literature research. Special thanks to Loukas Argiriadis MSc for helping me with the software editing.

A special thanks to my family for their incredible support which was more than I could ever imagine. It is not possible to find a way to express my gratitude to my family. I would also like to thank my friends who have supported me all these years.

TABLE OF CONTENTS

LIST OF TABLES

LIST OF FIGURES

LIST OF ABBREVIATIONS

AFM	Atomic force microscopy
ANOVA	Analysis of variance
CCA	Chromated copper arsenate
CI	Confidence interval
CPGC	Comingled polymer glass fibre composite
EOS	Equation of state
ESCA	Electron spectroscopy for chemical analysis
F-test	Distribution population for null hypothesis
FTIR	Fourier transform infra red
FTIR-ATR	Fourier transform infra red-attenuated total reflectance
FTIR-PAS	Fourier transform infra red-photo acoustic spectroscopy
HDPE	High density polyethylene
Hj	Roughness height from peak to valley
LDPE	Low density polyethylene
LLDPE	Linear low density polyethylene
LMWOM	Low molecular weight oxidized material
MAPE	Maleic anhydride grafted on polypropylene
MAPP	Methylacetylene propadiene propane
MOE	Modulus of elasticity
MOR	Modulus of rupture
P	Pigment
PE	Polyethylene
PET	Polyethylene terephthalate
Post-Hoc HSD	Tukey honestly significant difference
PP	Polypropylene
PPM	Permanganate potassium
PS	Polystyrene
PU	Polyurethane adhesive
PVA	Polyvinyl acetate
PVC	Polyvinyl chloride
Ra	Roughness average
RH	Relative humidity
Rq	Roughness square mean of deviation

Rz	Roughness mean of biggest peak to valley
SD	Standard deviation
SEM	Scanning electron microscopy
SEM-EDS	Scanning electron microscopy-energy dispersive X-ray Spectrometer
SIMS-FABMS	Secondary ion mass spectrometry-fast atom bombardment mass spectroscopy
UV	Ultra violet radiation
UVA	Ultra violet absorber
WPC	Wood polymer composite
XPS	X-ray Photoelectron Spectroscopy

CHAPTER 1: INTRODUCTION

During recent years there has been a special interest on developing plastics made with cellulose fibres as reinforcing fillers (Son et al 2001). The term lignocellulosic material is referenced to every substance composed of lignin and cellulose (Rowell 1996, Johnson et al 2005). Lignocellulosic materials are derived from wood, agricultural crops like cereal straw, wooden stem of cotton-plant, vine, sunflower, tobacco-plant, linen e.g. (Grigiriou 1999, Johnson et al 2005). Despite the fact that the usage of lignocellulosics materials to reduce the price and to improve the mechanical behaviour of plastics is not a new application, in the last decade there has been an increased interest in these materials because of the plastic costs and the desire to use renewable materials (Rowell 2007). In the past years for the polymer and biopolymer production, a variety of other materials like fibreglass, talc fillers, calcium carbonate have also been used as reinforcing fillers (Johnson et al 2005, Clemons and Stark 2007). Although there has been usage of the conventional fillers in the polymer industry, the interest of the lignocellulosics in composite production as reinforcing fillers has recently significantly increased because of various advantages as below (Son et al 2001, Carvalho et al 2003, Rohmány et al 2003, Sombatsompop and Chaochanchaikul 2004, Ashori 2008):

- lignocellulosics are recyclable raw materials produced everywhere lignocellulosics are natural and biodegradable
- lignocellulosic fibres do not normally cause skin and respiratory system irritation
- their use allows the utilization of a large amount of waste like crop waste and recycled paper
- because of its low relative density, the formed products have a low weight; low weight is desirable for many different applications
- it is a low cost material
- lignocellulosic fibres cause less damage on the cutting machinery during production, less tool wear
- lignocellulosics require small energy consumption for their production and utilization

Recycled polymers combined with lignocellulosic materials offer a solution to the large problem of the polymer waste management. Recycled polymers are a notable material

for composites production because plastics are the main city waste (Cui et al 2008, Adhikary et al 2008a). The main polymers derived from solid waste are low density polyethylene (LDPE), linear low density polyethylene (LLDPE), high density polyethylene (HDPE), polypropylene (PP), polyethylene terephthalate (PET) and polystyrene (PS). These polyolefins, which are mainly packaging waste, can be recycled. Recycled plastics usually have good properties, although, their usage in many applications is limited because they appear to be less effective concerning stiffness and creep resistance in contrast to virgin polymers. However wood or similar natural fibres combined with recycled plastics provides a significant improvement in stiffness and creep resistance resulting in composites with wider uses (Selke and Wichman 2004).

Wood Plastic Composite (WPC) is a material which may be composed of lignocellulosics fibres and thermoplastic polymers in various percentages (Stark and Matuana 2007a). The most important aspect for selecting the right thermoplastic polymer for WPC production is its processing temperature which must not exceed 180-200^{o}C because temperatures above 200^{o}C cause thermal decomposition of the lignocellulosics (Clemons and Stark 2007, Rowell 2007). This is an issue that defines the most suitable polymers for WPC production as the polyolefins which have low processing temperatures. Thus the most commonly used polyolefins for WPC production are low density polyethylene (LDPE), high density polyethylene (HDPE), polypropylene (PP), polyvinyl chloride (PVC) and polystyrene (PS) (Son et al 2001, Clemons and Stark 2007, Stark and Matuana 2007a).

The percentages of the contained polymer in WPC composites are about 50% and 60% (Clemons and Stark 2007, Stark and Matuana 2007a). There are some cases in which the polymer percentage could exceed 70% (Clemons and Stark 2007). For the WPC production the lignocellulosics material is used in the form of a flour (Rowell 2007, Clemons and Stark 2007, Stark and Matuana 2007a) and could be derived from wood-working processing waste (Clemons and Stark 2007). The most common species which are used for the WPCs manufacture in the United States are pine, oak and maple with a particle size in the range of between 10-80 μm (Clemons and Stark 2007).

The usage of these species is down to availability and the minor colour differences. In contrast species like red oak are not preferred because of their extractives which could come to the composite surface as spots by moisture penetration. Additionally the use of salt cedar and juniper perform similarly to other species but the composite is darker, limiting the ability to produce various material colorizations (Clemons and Stark 2007). Beside wood, agri-based

fibres from agricultural crops are also used for polymer composites (Rowell 1996). Rice husk (Premalal et al 2002, Yang et al 2004) and paper sludge waste (Son et al 2001, Son et al 2004) have also been studied as additional fillers for WPC production.

1.1 PURPOSE OF STUDY

WPCs development presents a new age of material production by the association of polymer and forest products industry which were previously two totally different industries (Clemons 2002). Growing interest and development in biomass/polymer composites is due to the need for durable wood products with the minimum preservation for outdoor exposure (Steckel et al 2007). Despite the fact that WPC is a biodegradable material it appears to be a sustainable and durable material with no need for use of toxic and environmental harmful substances application after production (Ashori 2008). The WPC promotion has been more significantly influenced by the fact that can be produced using recycled polymers and wood industry waste (Cui et al 2008). The polymer methods which are used for WPC production are providing designers the ability to manufacture products with more complicated forms and characteristics which were not possible with conventional wood processing, resulting in additional reasons for promoting these products (Clemons and Stark 2007).

Even with all the advantageous properties of the WPC products there is an essential need for further study concerning their behaviour in fire (Stark et al 2007), chemical contact (Tajvidi et al 2006), adhesion and treatments for improving adhesion possibilities (Oporto et al 2007). Furthermore the WPC recycling is a major issue that has to be investigated in depth (Winandy et al 2004) for evaluation of these products, forced by the need of the recent "green products" revolution.

The adhesion ability of the material is an important factor for aesthetic improvements like painting and coating and creation of adhered joints in WPC for constructions such as furniture and frame-build products. There is very limited research held about the WPC adhesion (Oporto et al 2007). In this study the WPC surface modification for improving its adhesion ability is investigated. Hydrogen peroxide, flame, hot air and halogen heating lamp treatments have been applied to WPCs to improve the material's surface energy and adhesion strength. The treatment methods mentioned above are selected due to their simplicity and the limited needed for equipment. The idea is that those methods could be easily applied by a carpenter in a simple wood working workshop. These methods do not require sophisticated and expensive equipment and machinery like in corona discharge and plasma treatment and also there is no need to handle hazardous chemicals such as chromic acid.

To investigate the effectiveness of the studied methods, lap joint shear strength testing has been used to determinate the achieved adhered strength. Also contact angle measurements, SEM, FTIR and roughness topography have been performed to the treated samples to help understand the mechanism of the chemical and morphological issues which are taking place during the surface modification and how these improve the adhesion ability of the WPC. Macroscopic observation by a stereoscopic microscope and colour difference determination has also performed to detect potential visible surface changes. These tests have been used to provide data to determine the chemical and the morphological factors responsible for improvements in the WPC adhesion behaviour.

CHAPTER 2: LITERATURE REVIEW

2.1 WPCS PRODUCTION AND IMPROVEMENT METHODS

WPC production methods are the extrusion, injection moulding and compression moulding which are also the most commonly used methods for plastic manufacture (Stark et al 2004, Bengtsson et al 2006, Clemons and Stark 2007, Rowell 2007). Extrusion is the most conventional method for WPC production (Clemons and Stark 2007). The equipment for the extrusion process is called "extruder". The extruder is comprised of a funnel for the raw material feeding. In the funnel the materials are mixed together by screws and the polymer−lignocellulosics mixture is formed in a homogenized mass in a heated cylinder in which the polymers melt. Shear forces due to rotation of the single or the multi screws increases the rate of melting of mixing/homogenisation. Afterwards the composite mass is passed through a cooling formation matrix where the final WPCs profile is produced. The moulding methods are initially similar to extrusion procedure, with the difference that it takes place in several stages and it is not a continuous in-line procedure (Grigoriou 1999). WPC manufacturers except those using the immediate compression moulding method, are also using pre-blended mixture of polymer-lignocellulosic material in pellet form which are heated over to produce desirable profiles. The ready mixed pellets are useful for non in-line production systems like injection moulding procedures (Clemons 2002, Clemons and Stark 2007).

Processing temperature and pressure are the most influential parameters for controlling the material flow during production and for controlling the WPCs morphology and physical properties (Stark et al 2004). Increasing the extrusion temperature the composite properties are improved because better wettability among the polymer-lignocellulosics materials is accomplished (Son et al 2001). However, as mentioned before, increasing the processing temperature above 200°C may cause thermal decomposition of the lignocellulosic material. The polymer-lignocellulosic mixing process time is also a significant parameter for improving the composite properties because of the lignocellulosic fibre breakage during its compression in the mixing funnel (Bledzki and Gassan 1999). WPCs processing conditions are determined which produce minimum damage and decomposition during production procedures.

Rates associated with the lignocellulosic materials also negatively affect the WPC production procedure. Therefore lignocellulosic materials require pre-drying to a 2% contained moisture in a drying chamber prior to blending. It is noticed in many cases that a

small amount of humidity from the wooden material is released in the extruder which causes material mixing problems. As a solution to this problem, a venting port is installed in the extruder mixing section. The material ventilation removes the remaining humidity and some volatile wood extractives, including terpenes and acetic acid which could cause problems during the extrusion process (Stokke and Gardner 2003).

For improving processing and the composite properties small amounts of additives are used (Clemons and Stark 2007, Rowell 2007). Coupling agents (chemicals for improving the bondability of the wood and the polymer) are the most commonly used additives. The hydrophobic nature of the polymers causes bond incompatibility with the hydrophilic lignocellulosic material. Improving the bonds between wood and polymer is an issue which has attached great research interest and there are a large number of publications on this specific subject. Maleic anhydride grafted on polypropylene (MAPP) or polyethylene (MAPE) is the most conventional used chemical system for polymer-biomass composite bondability improver (Lee et al 2004, Selke and Wichman 2004, Nachtigall et al. 2007, Adhikary et al 2008a, Adhikary et al 2008b Nourbakhsh and Ashori 2008). When the MAPE or MAPP contacts the biomass surface it reacts with the lignocellulosic hydroxyl groups and creates an ester bond. During the thermoplastic melting the PP or PE end of the MAPP or MAPE molecule is able to interact with the matrix polymer and provides an entanglement between the composite components (Rowell 2007). There are also studies which have investigated the potential of using silane technology for enhancing fibre matrix interactions in WPCs (Bengtsson et al 2005, Bengtsson and Oksman 2006, Bengtsson et al 2006, Cui et al 2008).

During WPCs production, other additives like UV stabilizers, colorants, lubricants, antioxidants, reinforcing agents, fire resistance agents and antimicrobials are added to improve the aesthetic, mechanical and physical composites properties (Rowell 2007, Ashori 2008). The outdoor usage of the WPC necessitates that products have good resistance to UV radiation, are able to endure high temperatures, limited shrinkage-swelling, have good resistance to humidity penetration, are able to resist mechanical stresses and have resistance to biological attack. In outdoor exposure there is more than one environment condition affecting the material, giving use to the major need for using these additives (Rowell 2007).

The most important physical characteristic of the WPC in outdoor exposure which must be considered is the humidity absorption related to materials swelling (Stark 2001, Neagu et al 2005, Najafi et al 2008). Water absorption causes lignocellulosic material to

swell. Because of the biomass swelling the wood fibres shear and microcracks can appear on the WPC surface and degradation of the fibre matrix interface could also occur. This degradation could cause the WPC density to decrease and to reduce the mechanical properties (Stark and Matuana 2006, Stark and Matuana 2007a). Water absorption limitation could be achieved by reducing the wood content within the composite (Stark 2001, Steckel et al 2007, Adhikary et al 2008a) and by decreasing the wood particles size (Steckel et al 2007). In many cases reducing the biomass amount and lignocellulosic size is not desirable because of mechanical properties issues, so adding coupling agents or acetylation can reduce water absorption (Adhikary et al 2008a, Steckel et al 2007). Chemical modification by silane also provides reduction of the composites absorption of water vapour (Bengtsson et al 2005). Coupling agents form bonds with the biomass hydroxyl groups, resulting in a reduction of the number of free hydroxyls on the lignocellulosic material surface. This reduces the sites available for water to form bonds with the wood particles; consequently the water absorption is reduced (Nachtigall et al 2007).

Limitation of the water absorption is influenced also by the polymer type. HDPE appears to be less effective than PP in resisting water absorption (Najafi et al 2007, Adhikary et al 2008, Najafi et al 2008). The water absorption of WPCs produced from recycled thermoplastics, in contrast with virgin polymers, does not appear give consistent results. In some cases recycled polymers have greater humidity absorption than virgin thermoplastics (Najafi et al 2007, Najafi et al 2008). Other studies claim that recycled thermoplastics have less water absorption than virgin polymers, however the water absorption values of recycled and non-recycled polymers do not appear to have significant deviations, resulting in ambiguous conclusions (Adhikary et al 2008).

The WPC production method also affects the composite's water absorption ability. Injection moulded material is more effective in humidity absorption protection than material from extrusion. It is reported that this occurs because in injection moulding, a thicker layer of polymer is formed on the composite exterior surface. Thus, the hygroscopic hydroxyl groups in the lignocellulosic mass are protected by the polymer, so the biomass is protected from humidity absorption (Clemons and Ibach 2004, Stark et al 2004, Stark and Matuana 2007a). To achieve an exterior surface with a polymer protective layer, a co-extrusion production method has been used. In co-extrusion two extruders supply two different materials into a single composite profile. A clear polymer layer adds a protective cover to the WPC product. Despite the fact that water absorption is significantly limited by the co-extrusion method,

microcracks on the cover layer reported to have appeared by photodegradation, and eventually pathways for humidity penetration were created during weathering tests (Stark and Matuana 2007b).

The combination of UV radiation and water absorption is the most important problem occurring with outdoor exposure of WPCs. The composite degradation appeared to be more significant when UV radiation and humidity absorption occurred together. Water spray during weathering has a cleaning effect and causes degraded mass removal. Furthermore, the oxidation reactions occurring and the microcracks formed by biomass swelling result in the deeper exposure into the WPCs layers and UV radiation occurs beneath the initial surface (Stark and Matuana 2006). It is important to mention that the WPCs biomass performs as a UV stabilizer limiting the photooxidation, but in extended UV irradiation wood mass degradation causes chromophoric formations which are accelerating the composites degradation by light reversing its UV protection ability (La Mantia and Morreale 2008).

For UV radiation protection of WPCs, UV absorbers (UVA) and pigments (P) are used (Stark and Matuana 2003, Stark and Matuana 2006). Both UVA and P offers a protecting effect to the composite against UV radiation. The UVA absorbs the UV radiation, limiting the occurrence of photodegradation. The pigments reflect the UV radiation, achieving the same result as the UVA, but by a different method. The combination of UVA and P together provide WPCs maximum UV protection (Stark and Matuana 2006). Darker pigments appear to give less composite bleaching, resulting in a more efficient UV protection, in contrast to lighter colours (Kiguchi et al 2007). Big differences between the colour of biomass and the polymer can make the wood fibres appear as light spots on the composite surface. To control this colour inhomogeneity, when pigments are used in WPC production, in some cases it is necessary to add the colorant to the component materials individually before the production process to limit the coloration dissimilarities (Rowell 2007).

Water absorption limitation within the composite interface also influences biodegradation. The more moisture the composites contain, the more significant the extent of biodegradation. Therefore, the methods for limiting the water absorption that were discussed above, also operate for biological decay protection (Ibach and Clemons 2002, Wang and Morell 2004). Adding antimicrobial agents to WPC production is also a viable method for fungal and microbial decay protection (Wechsler and Hiziroglou 2007). WPCs produced from wood particles treated with chromated copper arsenate (CCA), derived from out of service products, have been studied for improving the biodegradation decay resistance. These

materials appear to perform with high resistance to biological decay due to the presence of the arsenic and copper components. Despite the advantageous performance of CCA treated wood particles in WPC production, the toxicity of the materials used limits the end-use of the final products to those with minimum contact with humans and water resources (Kamdem et al 2004). Also the availability of CCA treated wood will decline in future due to the prohibition of CCA for wood treatments.

2.2 WPCS MECHANICAL PROPERTIES

The WPCs mechanical properties variation is influenced by the fibre volume proportion, the lignocellulosic material morphology and the production methods (Kumari et al 2007). If the proportion of biomass in WPC is produced without compatibilisers, the modulus of elasticity (MOE) is improved but the tensile strength and the modulus of rupture (MOR) are decreased (Lee et al 2004, Chotirat et al 2007). Elongation of the WPC during rupture is also decreased by the composites polymer volume proportion increment (Chotirat et al 2007). The MOE improvement could be explained by the wood fibre's higher stiffness. Furthermore, the increment of the lignocellulosic fibres in the polymer matrix results in a blend of high stiffness material which causes a brittle and a limited elongated ability composite product (Georgopoulos et al 2005). Composite strength decrease can also occur because of poor fibre dispersion, existence of fibre agglomerates and the formation of voids between the biomass and the hydrophobic polymer (Chotirat et al 2007). Agglomerate formation during polymer and biomass mixing is the most important problem in WPC production. The presence of agglomerates within the composite due to poor dispersion of lignocellulosics means that reinforcing ability of the biomass is reduced. The low dispersion could be confronted by adding lubricants into the WPCs during mixing, and by chemical modification (Bledzki and Gassan 1999).

The increased amount of lignocellulosic in WPCs produced with compatibilisers results in a increase of the composite strength (Lee et al 2004, Bengtsson et al 2005, Bengtsson and Oksman 2006, Bengtsson et al 2006, Wechsler and Hiziroglou 2007, Cui et al 2008, Nourbakhsh and Ashori 2008) not only in the MOE (Lee et al 2004, Bengtsson et al 2005, Cui et al 2008, Nourbakhsh and Ashori 2008) but other mechanical properties. This increment is due the better bondability between the biomass and the polymer, providing a better transfer of the stress form the weaker plastic component to the stronger wood particles (Bengtsson and Oksman 2006). Likewise the increment of biomass within the composite appears to decrease the elongation during rupture for modified components in contrast with

non-modified (Bengtsson et al 2005). Modified components also provide a higher impact strength to composites surface (Bengtsson et al 2006, Bengtsson and Oksman 2006) and lower materials creep response (Lee et al 2004, Bengtsson and Oksman 2006, Bengtsson et al 2006).

The lignocellulosic form is as well a significant influential factor which affects the WPCs properties. In general WPCs produced with wood fibres appeared to resist better in elongation, tensile strength and impact strength than wood flour composites (Clemons 2002). On the other hand the use of increased levels of wood fibres alters the WPCs properties, depends on the processing conditions, because an amount of the lignocellulosic material is degrading during composites production and the fibre quality changes and dimension loss can occur (Rowell 2007, Cui et al 2008). Despite the beneficial impact of the wood fibres within the WPC, wood flour is most commonly used as the WPCs filler. This is because of the difficulties that longer lignocellulosic fibres appear to have during feeding into the plastic production equipment (Clemons and Stark 2007). Thus wood flour with aspect ratio lower than 10 is mostly used for WPCs production preventing the processing problems that wood fibre could cause (Rowell 2007).

The fibre length seems to affect the WPCs flexural strength. The fibres length increment causes a decrease of the composites flexural strength. This could be explained by the fact that reducing fibres length, for the same wood fibre weight, the biomass surface area increases and results in a more homogeneous stress transfer between the fibres and the polymer. Smaller fibres also provide a better dispersion within the composites matrix which produces a stronger WPC interface. Thus the stress transfer while load is applied to the material is transferred better between the wood and the polymer, producing a stronger matrix than larger fibres (Cui et al 2008).

WPCs mechanical properties produced by recycled polymers do not seem to have great dissimilarities with those made by virgin polymers. It is important to mention that in some studies wood-recycled polymer composites appeared to have better mechanical properties than WPCs made by virgin polymer (Adhikary et al 2008b). Moulding method also affects the composites MOE and MOR properties. Composites produced by injection and extrusion moulding method have greater mechanical properties than those made by compression moulding (Kumari et al 2007). For improving the wood-polymer composites mechanical properties it is possible to use within the composites matrix nanoclay as polymer reinforcement agent (Faruk and Matuana 2008) and mixture of polymer and glass fibres like

commingled polymer glass fibre composite (CPGC) (Jiang et al 2007). Of course WPCs with reinforcing materials like glass fibres are only produced for applications with high resistance needs (Jiang et al 2007).

Fasteners which have been developed for wood, metal and for polymeric materials seem to be an effective and quick method for joining WPC (Farid et al 2002). It is important to mention that solid WPC appears to have similar, and in some cases higher resistance, to screw and nail withdrawal in comparison with wood based panel products like plywood, particleboard and fibreboard (Falk et al 2001).

2.3 WPC ADHESION PROPERTIES

2.3.1 ADHESION MECHANISM

Adhered bonding is an advantageous technique in contrast to joining with fasteners, nails, screws and bolts, because it is weightless and distributes the adhesive forces better to the material. Also adhered joints have greater aesthetic value because it can be hidden. Adhesion mechanisms are a very complex scientific area which consists of a number of scientific fields (Pizzi and Mittal, 1994). The main adhesion factors that are responsible for the adhesion properties are:

- Mechanical factors
- Electronic theory
- Theory of boundary layers
- Thermodynamic theory
- Diffusion theory
- Chemical bonding theory

The mechanical factor is that the adhesion strength can be increased by the surface cavities, pores and roughness of the material, resulting in an anchoring of the adhesive into the material surface.

The electronic theory suggests that there is an electron transportation between the adhesive and the material. This forms double electrical surfaces between the adhered materials and the adhesive which are attracted by electrostatic bonds.

The boundary layer theory is that the adhesion strength is influenced by the weak boundary cohesive strength of the material. According to this theory the weakest boundary

layers of the material are the most probable cause of bond failure, than the interface of the adhesive. The formation of weak boundary layer is a result of chemical and physicochemical phenomena and must be strongly considered when adhesion strength is investigated.

Thermodynamic theory is the most used theory for investigating the adhesion properties. The thermodynamic theory is based on the interface forces which are taking place at an interatomic and intermolecular level, such as van der Waals and Lewis acid-base interaction forces. Those forces can be related to adhesive and material surface free energy. According to thermodynamic theory, wettability is essential to effective adhesion because the adhered joint is produced by a solid-liquid contact stage. However, the wettability is an important factor for good bonding but it alone is not enough.

The theory of diffusion suggests that there is a shared diffusion among the interface macromolecules which results to polymers auto-adhesion. According to this theory it is possible the macromolecular chain segments of the adhered material to be shared by the joint materials. This adhesion mechanism is mainly affected by factors like the contact time and temperature.

The chemical bond theory is the formation of chemical bonds between the material and the adhesive. Those bonds are considered to be the strongest among the rest of the adhesion theories. Covalent and hydrogen bonds are most prevalent in the majority of wood adhesives, however metallic and ionic bonding may be appropriate in specific situations.

2.3.2 POLYMER ADHESION PROPERTIES

WPC has the advantages and the disadvantages of the contained polymer. Because polyolefins have low surface energy and limited polarity (Papirer et al 1993, Ritter 2000, Pijpers and Meier 2001), this also gives WPC surface energy values, around 31 mN m^{-1} (Gupta et al 2007). Ritter et al (2000) reports that acceptable adhesion could be attained with surface energy values 40 mN m^{-1} and higher. Wood for example has a surface energy in the range of 40-60 mN m^{-1} (Gupta et al 2007). Surface energy has a correlation with adhesion strength (Mirabedini et all 2004, Papirer et al 1993). Therefore applications such as film coating, paint and bonding, which could increase the WPC usage, could not be satisfactorily achieved (Gatenholm et al 1990, Gupta et al 2007). For that reason, surface treatments for improving the adhesion ability of polyolefins and WPC is used in polymer industry (Zhang et al 1998, Sun et al 1999). Despite the fact that surface energy is related to adhesion strength, chemical bonds most affect the polymers bondability (Papirer et al 1993). The most

well-known and commonly used treatments for polyolefin surface modification are: flame treatment, corona discharge, plasma and chemical etching and UV irradiation (Pinto et al 2008). There have been many studies which sought to investigate treatment methods for surface modification to cause an increase in polymer surface energy and wettability, to achieve adhesive bonding improvement. Chromic acid treatment, fluorination, microwave treatment, corona discharge, plasma treatment, flame treatment and simple abrasion are some of these cases, and most of the treatments show some beneficial effect on the bonding strength of the polymers. The polymer surface energy increase been by surface modification is in most cases due to oxidation processes (Oporto et al 2007).

2.3.3 SURFACE PRE-TREATMENT METHODS FOR IMPROVING POLYMER ADHESION

2.3.3.1 Flame treatment

Flame treatment appears to be the most common surface treatment for polymer adhesion improvement in order to achieve material painting and coating. Garbassi et al (1987) investigated the surface chemical changes that occurred on polypropylene surfaces after flame treatment. They applied a flame several times over the PP surface to produce different levels of treatment intensity. To monitor the surface modification, fast atom bombardment mass spectroscopy (SIMS-FABMS) and Fourier transform infrared-photo-acoustic spectroscopy (FTIR-PAS) were used. To correlate the surface oxidation to adhesion improvement, surface tension and paint adhesion tests were also performed. After flame treatment hydroxyl and carbonyl groups are formed on the PP surface as oxidation products. Importantly the appearance of the contained oxygen on the surface does not significant change as the flame treatment increases, leading to the conclusion that oxygen containing moieties are just modified to different functional groups. Cations CH_2OH^+, H_2O^+ and anions C_2OH^-, $C_2O_2H_3^-$ appeared on the PP surface. The CH_2OH^+ increases during the first treatments and then decreases after several treatments; this is in contrast with H_2O^+ which keeps increasing. The anions are both increasing after continued treatments, with the C_2OH^- stabilized after second treatment of the overall four. Accordingly the anion and cation behaviour that is outlined above, the route is most likely as follows:

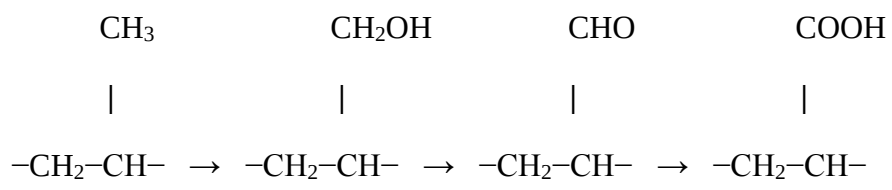

In this route oxidation processes lead to a hydroxyl formation on the methyl group. Further oxidation gives an aldehyde or carbonyl group and further oxidation adds another hydroxyl to give a carboxylic acid group. By this route it is possible to explain the observed carboxyl increase and the hydroxyl decrease because of the transformation of the hydroxyl groups to carboxyl groups by the extended oxidation through the repeated flame treatments. Furthermore this study showed that there was no significant change in the surface tension as the several treatments occurred. Surface tension was increased by the first treatment and then almost stabilized despite the further flame treatment applications. It was noticed that the surface tension was probably more affected by the formation of the hydroxyl than the aldehyde and carboxyl groups. The paint adhesion also improved after the first treatment and then become almost stable, with a slight decrease at the fourth treatment. In order to explain the adhesion behaviour, this study concluded with the hypothesis that the formed groups are alike in affecting the adhesion mechanism, or that the amount of oxidization products which are required for improving the adhesion process are achieved very fast and there is no need for further oxidation. Although there is no proof that the oxidation products are clearly affecting the adhesion properties, this study indicates that the hydroxyl groups could be responsible for the adhesion improvement, as the majority of the hydroxyls were formed after the first treatment.

Papirer and Schultz (1993) studied the adhesion improvement of flame treated polypropylene and polyethylene. They applied several fast flame treatments over PP and PE material and they did shear strength tests and surface characterization in order to link adhesion properties with surface modification. It was apparent that flame treatment could change the polyolefin's surface. Contact angle measurement, scanning electron microscopy (SEM) observation, electron spectroscopy (ESCA), Fourier transform infra-red spectroscopy (FTIR) and peel strength measurements were used to investigate positional surface changes that might have occurred. According to this study, flame treatment can increase the surface polarity by the presence of formed polar groups. The peel strength test shows that after flame treatment the adhesion strength was immediately increased. By the surface chemical analysis it was observed that oxidation scissions had appeared over the polyolefin's surface, which

was related to an increase in surface energy. The comparison between the ESCA and the FTIR results showed that in the case of PP the oxidation scission rapidly occurred at the surface to a small depth and is stabilized even with extended treatment. On the other hand PE oxidation scission is augmented and goes deeper into the material after continuous treatments. Therefore the oxidation products are more likely to remain on the PE rather than the PP surface after treatment.

In another study, Pijpers and Meier (2001) reported that if flame treated PP surfaces were reheated the surface oxygen which has been formed by the treatment reduced significantly (from 12% to 2% oxygen concentration). That could prevent the advantageous effect of the flame treatment if the treatment happens repeatedly. In this study it was reported that oxygen concentration is quickly increased as the treatment speed rises, until the highest point beyond which it slowly decreases to levels similar to untreated values. Flame distance also affects the oxygen concentrations. In the case of the flame distance factor, it was revealed that oxygen concentration increased in a similar way to the effect of treatment speed, from low to high distance from the treated PP.

Air/propane ratio was also investigate by this study. The oxygen concentration increased as the air/propane became richer in air and decreased at ratios from 23 to 29. They concluded that air/propane ratio, treatment speed and flame distance could produce an increase in surface oxygen which hypothetically would benefit the adhesion ability. The air/propane ratio was found to be the most significant factor for surface modification with less chemical impact. On the other hand, flame distance appeared to have more effect on the surface chemically. Moreover treatment speed seemed to provide wide variation between treatment flame contact duration. However the polymer additives, and especially antioxidants, could lead to unexpected results in adhesion ability, despite the fact that flame treatment provides a better surface energy and polarity.

2.3.3.2 Corona treatment

Corona treatment is another well-known surface modification method for improving the adhesion strength and reducing the hydrophobic behaviour of polymers like polyolefins (Gatenholm et al 1990, Strobel et al 1991, Jones et al 2005). Corona treatment or corona discharge is a procedure in which gases passing through an electric field are transformed into a state of cold plasma (Guimond and Wertheimer 2004). This high voltage electric field usually happens between two parallel electrodes in which the electrons are moving very fast and some of them hit the gas molecules and force the orbital electrons of the gas molecule to

be deposited in an unstable state creating a reactive gas mixture full of electrons (Zhang et al 1998). If a material is placed between the arc electrodes, the electron gas mixture in the plasma state impacts with the material and surface modification occurs (Zhang et al 1998, Guimond and Wertheimer 2004.). During corona treatment it is possible to use various gases like atmospheric air, O_2, CO_2, N_2, H_2, He and A (Zhang et al 1998). Corona treatment produces higher surface energy, improving the wettability and the adhesion ability when applied to low surface energy materials (Sun et al 1999).

Corona discharge treatment is an effective method for surface modification used for adhesion and paint properties improvement, and occurs through surface oxidation and scission (Gatenholm et al 1990, Zhang et al 1998, Guimond and Wertheimer 2004, Jones et al 2005). The polymer oxidation through corona treatment is confirmed by an increase in the oxygen/carbon (O/C) ratio as shown by XPS ESCA studies. Gatenholm et al (1990) report that as the energy of the corona increases, the O/C ratio is increased by 20% at lower energy and reaches 90% at the highest investigated treatment energy. Jones et al (2005) also confirmed that the O/C ratio increased during corona discharge and suggested the formation of low molecular weight oxidized material (LMWOM): a comment also reported by Guimond and Wertheimer (2004) in an earlier study. XPS and atomic force microscopy (AFM) studies revealed that from 0.1 J/cm^2 corona treatment energy, the water soluble LMWOM appearing and increasing as the treatments energy became higher resulted in an increase of O/C ratio (Jones et al 2005). LMWOM is a weakly bonded material with the appearance of nodules or droplets which is noticed to be formed on the corona treated polymers possibly resulting in insufficient adhesion, but this is easy to remove by washing the surface with polar solvents like water or wiping the material (Guimond and Wertheimer 2004). The oxidation which takes place during the corona discharge forms groups which are the same as the flame treatment, despite the gas which is used. Zhang et al (1998) reported that oxygen containing formations on the surface of the treated polymer appeared with all gases used for the corona treatment without being necessary for the gas to contain oxygen molecules. This excludes hydrogen corona however, which does not produces oxygen contained formations and did not produce polar groups on the polymer for improving the adhesion.

Surface energy is significantly increased during corona treatment as a result of the polar groups which are formed on the polymer treated surface (Gatenholm et al 1990). The surface energy which represents the material wettability is reduced over time after the corona treatment due to an aging process (Strobel et al 1991, Sun et al 1999, Guimond and

Wertheimer 2004). It was reported by Strobel et al (1991) that the surface energy was not affected by the time of water rinsing for the removal of LMWOM, and the treated PP seemed to have the same surface energy even the washing happened just after treatment or after a few days. However, the same study revealed that the presence of LMWOM on the air corona treated surface might protect the material wettability from aging effect, because PP which was washed just after treatment and then aged for 7 days had the same surface energy as other samples which were washed after 7 days and then left for another 7 days. Guimond and Wertheimer (2004) showed that N_2 corona treated polyolefins retained the high surface energy for longer periods of time than the air corona treatment.

Excluding the chemical changes there are also morphological changes which happen on the surface, such as development of roughness and polymer cross-liking (Zhang et al 1998, Sun et al 1999, Jones et al 2005). To investigate the potential changes that occurred on the polymer surface Atomic Force Microscopy (AFM) and Scanning Electron Microscopy (SEM) are normally used by many researchers (Gatenholm et al 1090, Zhang et al 1998, Guimond and Wertheimer 2004, Jones et al 2005). Jones et al (2005) and Guimond and Wertheimer (2004) noticed the same globular mounds in AFM observation of their corona treated polymer surfaces, which they concluded was LMWOM. Those mounts have a diameter of approximately 10 nm, and these get bigger to diameters of about 50 nm as the corona energy is increased (Guimond and Wertheimer 2004). On the other hand, according Jones et al (2005) study, a "bead-like" appearance noticed on PP surface after corona treatment without the existence of LMWOM. Corona discharge creates small holes on the surface through the attack by the electrons and this could lead to an increase of the bonding surface area, resulting in higher adhesion strength (Zhang et al 1998). When oxygen-less gases like N_2 are used for corona treatment, there is no significant formation of LMWOM on the treated surface and the morphology does not seem to have great dissimilarities with the untreated polyolefins (Guimond and Wertheimer 2004). Zhang et al (1998) also agree that gases like H_2, He, A and N_2, when they are used for corona discharge treatment, do not lead to significant visual surface modification, so the surface roughness is mostly related with the presence of oxygen in the corona treatment gases.

2.3.3.3 Fluorine gas treatment

Surface treatment of polyolefins with fluorine gas mixtures could also result in wettability and adhesion ability increase. According to du Toit and Sanderson (1999) the

fluorine reacts with the hydrocarbon polymer surface forming a layer of fluorocarbon on the surface. The reaction which taking place on the surface is as follows:

$RH + F_2 \rightarrow R^{\bullet} + HF + F^{\bullet}$.

When the fluorination happens without the presence of other reagents, the reactive particles which are formed result in a further formation:

$R^{\bullet} + F_2 \rightarrow RF + F^{\bullet}$

The RF formation is responsible for the surface tension increment.

The factors that affect the depth and the characteristics of the fluorine modification are the treatment duration, the process temperature and the amount of fluorine within the applied gas mixture. The most commonly used gases for mixtures with fluorine are N_2 and He. While the polymer is subjected to fluorination treatment its weight is increased due to the presence of fluorine/fluorocarbon in the surface structure. The weight gained reveals the treatment degree.

There is also the oxyflourination treatment in which oxygen is used within the gas mixture as diluting gas. Oxyflourination has a slower effect on weight gain than fluorination with N_2 gas. This happens because of the very reactive nature of oxygen which means that it reacts with the radicals and forms peroxides as follows:

$R^{\bullet} + O2 \rightarrow ROO^{\bullet}$

Despite the oxyflourination slower effect on the weight gain in contrast with N_2 Fluorination, the impact on the contact angle increment is more dramatic during oxyflourination. In both fluorination methods the surface tension is increased at the treatments start, but over time it is decreased to values almost similar to the untreated polymer. Fluorine gas is a procedure that today is not harmful to apply and is cost effective (du Toit and Sanderson 1999).

2.3.3.4 Microwave treatment

Polyolefin surface modification can also be achieved by microwave irradiation in presence of potassium permanganate (PPM). Mirabedini et al (2004) showed that microwave irradiation seems to be a more effective catalyst for surface modification than conventional heating processes because of the extremely short time needed for surface energy increase. During microwave irradiation treatment the surface energy and the adhesion strength is increased. This could be explained by the C=O formation, which increases polarity of the

polymer surface. The surface morphology also changes to a rougher matrix resulting in an increase in bonding area. Mirabedini et al (2004) also showed that chromic acid treatment seems to have a better impact on the surface energy and adhesion strength than microwave irradiation treatment.

2.4 WPCS APPLICATIONS

WPCs applications are defined according to manufacturing technologies (polymer type, wood/fibre content, recycled or non-recycled polymer, biomass species morphology and shape, additives, moulding method). These affect the final product abilities and properties resulting in high performance material for specific uses.

The main WPC market is oriented to produce products for applications like decking, railing, automotive, windows and doors, fencing, siding, roofing, picnic tables and industrial flooring (Jiang and Kamden 2004, Stark and Matuana 2007a, Tungjitpornkull and Sombatsompop 2009, Youngquist 1995). A variety of small items like flashlight cases and hangers are also produced by biomass polymer composites manufacturers (Youngquist 1995). Since the CCA treated wood restriction and the higher cost for relative more environmental friendly methods for producing high durability wood, WPC has been found to be the alternative product for demanding environment exposure applications (Winandy et al 2004, Rowell 2007).

WPC products are a fast growing market in America. Products produced by WPC like decking boards, railings, fencings and outdoor exposure application materials have recently become popular (Clemons and Stark 2007). Europe is also an increasing market for WPC products for various applications, despite the fact that the majority of the WPC manufacturers until recently focused on automotive parts (Stokke and Gardner 2003, Ashori 2008). Because of the WPC good strength/weight and stiffness/weight ratios the automotive industry has achieved an up to 20% weight reduction by using WPC parts like dashboards and door panels which is resulting in recyclable and more environmental friendly vehicles with less fuel consumption responding to the European Guideline 200/53/EG for automotive recycled and renewable material usage (Ashori 2008).

CHAPTER 3: MATERIALS AND METHODS

Adhesion of WPC is important to extend the usages of the plastic material. Painting and coating can significant improve the WPC aesthetic appearance. The only aesthetic approach that the WPC manufacturers have undertaken till today, are the colour, which is added during the production of the material, and the wood-like texture on the surface. More complex and desirable surface effects, with almost unlimited variety, can be achieved with painting and coating. At present they cannot be used today by WPC manufacturers because of the poor adhesion of the material.

Furthermore, the joining systems which are used today on WPCs products are metallic and plastic fasteners. These joining systems limit the material use to constructions like decking and railing with specific WPC profiles to fit to the fasteners. The use of screws also, is another joining system that can to produce effective WPC joints, because the screw withdraw strength of WPC is higher in some cases than wood-based panels (Falk et al 2001). Glued joints however, can produce a greater variety of more complex constructions with hidden bond-lines. Non-visible joints are necessary for furniture, because the aesthetic manner of those products is essential. The possibility of producing adhered joints with WPC could broaden the material usage to traditional carpentry. Outdoor furniture made by WPC could minimise the usage of potentially environmentally harmful substances; non-durable solid wood outdoor furniture needs preservatives. Frame construction and furniture are a huge variety of products with unlimited designs, shapes, joining types and dimensions which cannot be produced by a single WPC manufacturer. However, the production of solid WPC beams in a variety of dimensions, and the development of a simple and cheap adhesion system with pre-treatment that could be performed even in a small traditional carpentry workshop, could deliver a wide variety of products as furniture and frame constructions.

This study was undertaken to investigate possible WPC surface pre-treatment methods for improving adhesion ability. The four methods that were selected to be tested were:

- treatment with hydrogen peroxide in the presence of NaOH
- application of hot-air on the surface
- application of flame treatment to the surface
- and heat treatment with the usage of halogen heat lamps

All four pre-treatments which are mentioned above are expected to cause surface oxidation and increase the adhesion ability of the material. To evaluate the effectiveness of each treatment lap joint shear strength evaluation according EN 205/1991 standards were done. It is also expected the surface to change morphologically and chemically during the pre-treatments. The surface changes that might appear on the material after the pre-treatments, could be the reasons of which the shear strength of the lap joints may possibly improved. Therefore, to further understand the modification mechanism which is taking place at the WPC surface, a series of surface characterization experiments was undertaken. These experiments looked at:

- Surface contact angle
- Surface roughness
- Light microscopy
- Scanning electron microscopy
- Fourier transform infrared spectroscopy (FTIR-ATR)
- Colour changes

3.1 MATERIALS

A WPC containing 60% of 35 mesh spruce flour, 35.5% polypropylene, 2% coupling agent, 1.5% UV-stabilizer and 1% colour pigment was used. This was sourced from Kompetenzzentrum Holz GmbH Austria and was produced under the European research project ERA-NET Cornet/2006/01. The WPC was an extruded square shaped pipe (Figure 3.1) allowing samples to be cut from the sides. WPC samples were cut with dimensions 40 mm X 20 mm X 5 mm (Figure 3.2). The samples were systematically cut from several pipes in order to achieve material diversity for the tests. All samples were sanded with P220 glass paper to remove the excess polymer from the surface and to produce a smother surface for better bondability. In order to avoid heat transfer by friction during sanding which might unexpected modify the samples surface, all samples were sanded by pressing the handheld vibration sander on the surface for 30 sec and then left to cool down for further 1 min. The sanding procedure was repeated four times on every sample. The samples were rinsed with deionised water after sanding and before every treatment to remove possible remaining dust from the surface and placed in a conditioning room at 20 °C and 65% R.H. until the weight stabilized at equilibrium moisture content.

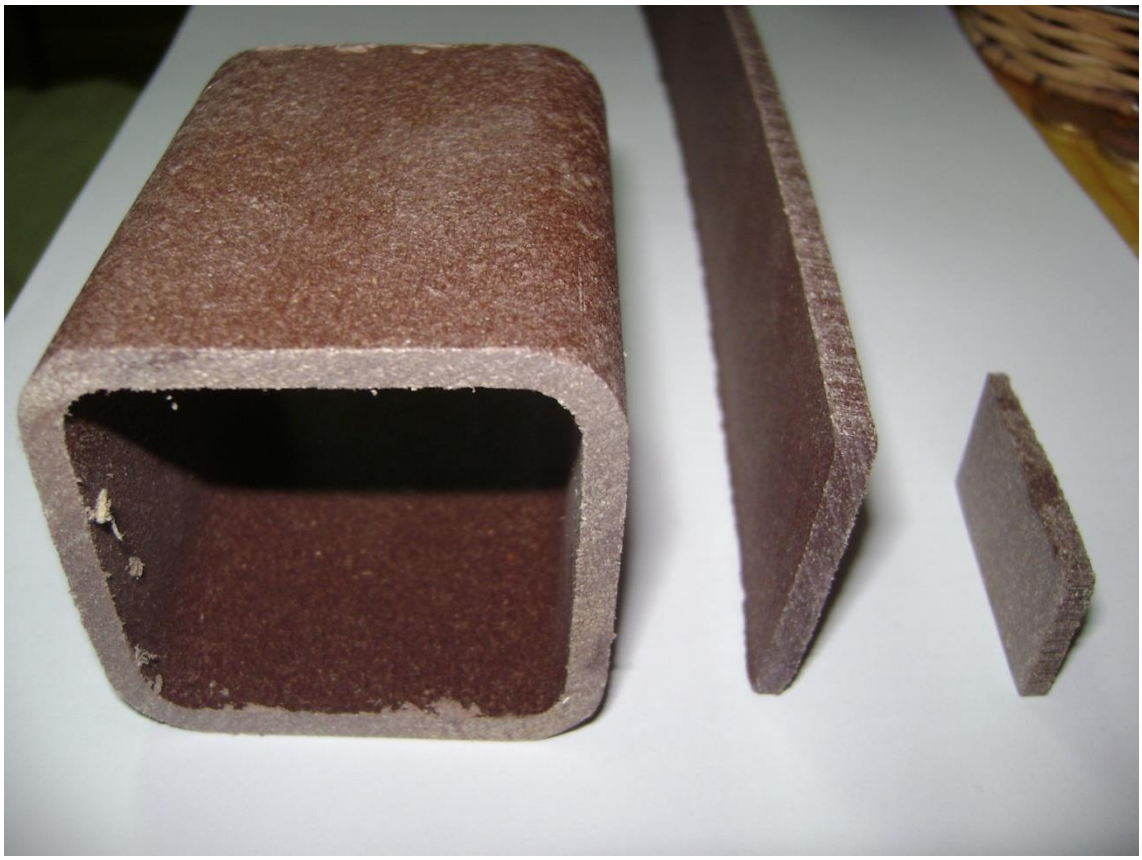

Figure 3.1: WPC pipe sliced to prepare flat strips sample.

Figure 3.2: WPC sample.

Three adhesive systems were investigated for lap joint test. These were a two component commercial epoxy resin SALDA TUTTO MIX provided by PATTEX, a commercial PVA No 35 FAST SETTING CRYSTALLINE WOOD ADHESIVE provided by DUROSTICK and an one part commercial PL PREMIUM POLYURETHANE CONSTRUCTION ADHESIVE provided by LOCTITE.

30% w/v hydrogen peroxide and 1 M sodium hydroxide were obtained from Panreac Quimica SAU and used without further purification for the hydrogen peroxide treatment.

For the hot air treatment a DEWALT DW 340K 2000W hot air gun was used. According to the manufacturer the maximum temperature that the gun can produce at the nozzle is approximately 600 °C.

A methylacetylene-propadiene-propane (MAPP) gas flame torch provided by TurboTorch was used to produce flame treated samples (Figure 3.3). The identical flame intensity, during the treatments replication, was guaranteed by a line which was marked on the operating valve and the body of the torch (Figure 3.3). When the torch was fired up to perform the treatment, the valve was turned to complete two circles until the marked line on the valve aligned to the line on the torch body. The gas tank also was changed with a new one after 3 treatment runs, to minimum possible flame intensity deviation by the decrease of the tank gas pressure.

Figure 3.3: MAPP gas torch.

For the heat treatment, three halogen heat lamps of 400 W each were used. These were combined in one single unit with 8 cm distance between them. Figure 3.4 shows this combined unit.

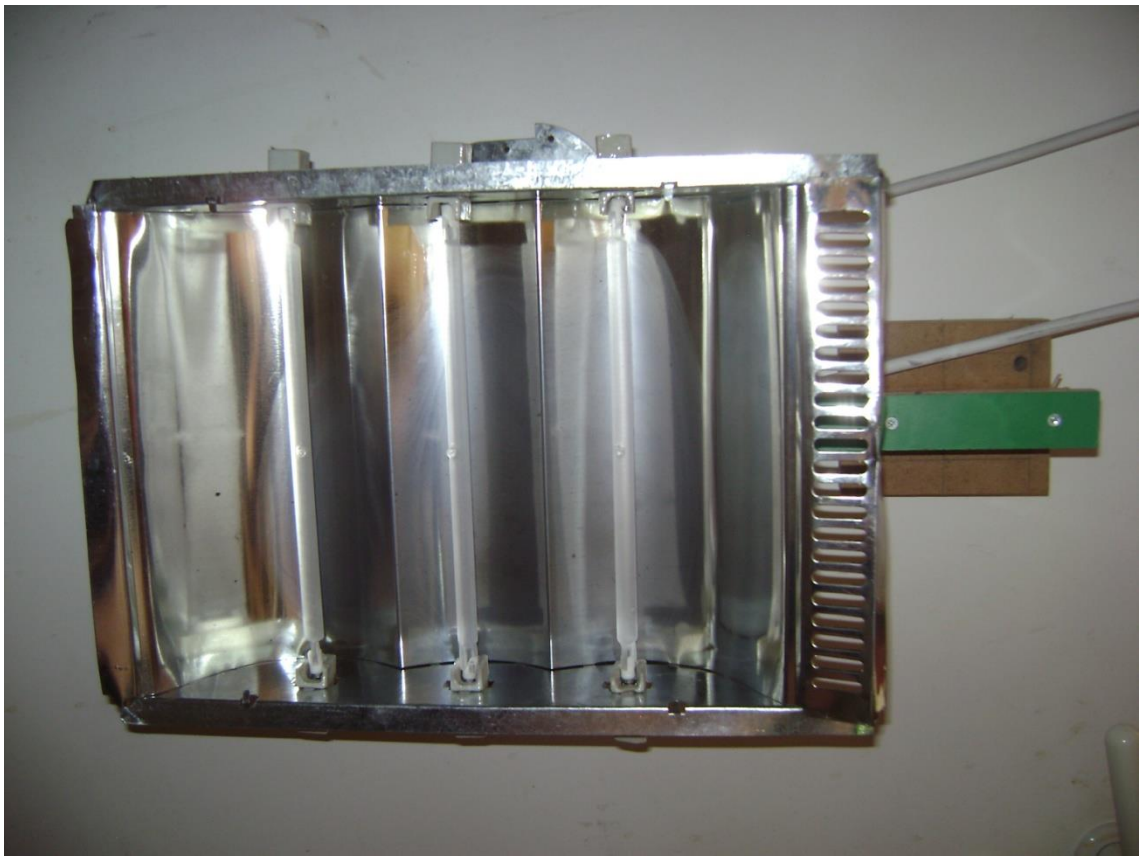

Figure 3.4: Halogen heating lamps.

A STAUBLI TX90 robotic arm was used to apply the hot air, flame and the halogen heat lamps treatments (Figure 3.5). The robotic arm was programmed to execute a specific routine. This routine allowed accuracy to the treatment speed and the distance from the samples of the hot air gun, flame and halogen heating lambs. The speed ranged from 10 mm s^{-1} to 250 mm s^{-1} as will be reported in the methods section. The distance from the lower edge of every attached equipment, for every pre-treatment method, was accurate controlled by an electronic calliper at 2.5 cm for hot air gun treatment, 5 cm for flame treatment and 2 cm for halogen heating lamps treatment. In case of the halogen heating lamps, the distance from the lower edge of the equipment was 2 cm but the distance from the lamps was 5 cm.

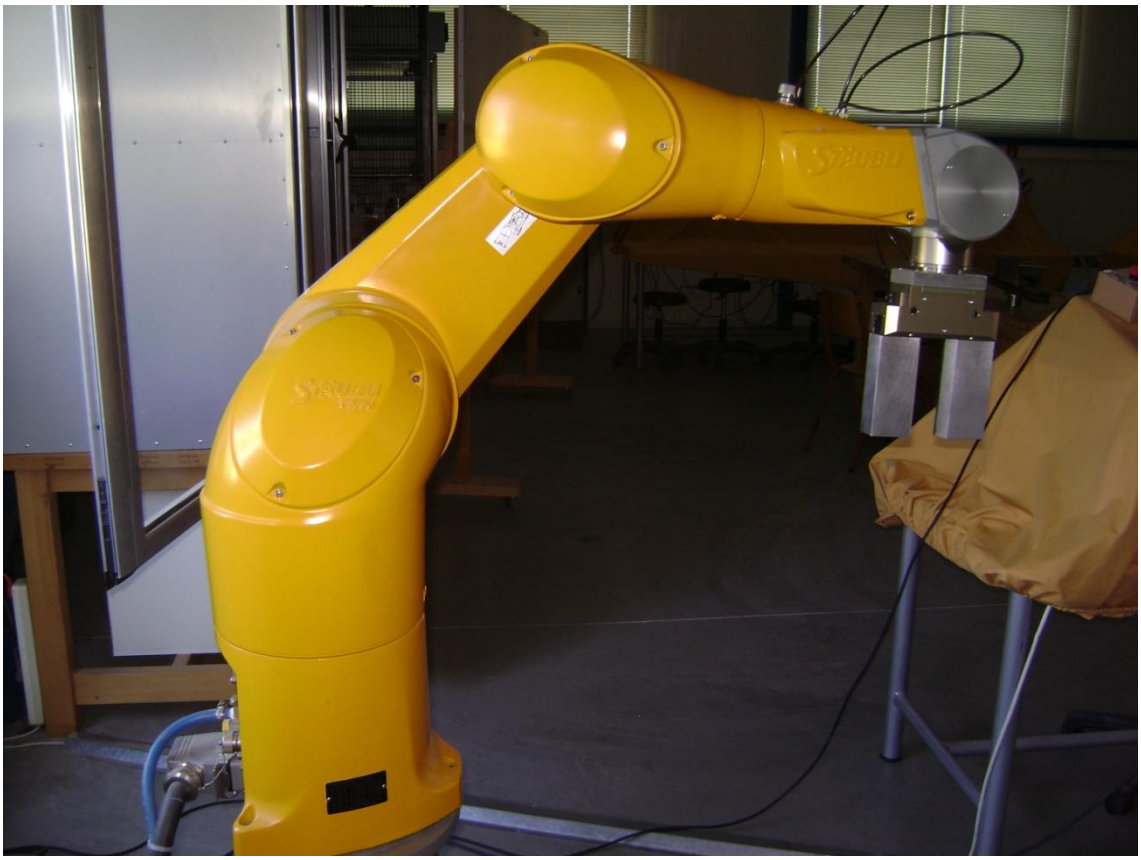

Figure 3.5: Robotic arm.

3.2 METHODS

3.2.1 TREATMENT PROCEDURES

To determine the limits between each treatment parameters that would be examined, a series of pilot testing according to adhesion strength were done. The optimum range was determined to be between the extreme parameter ends of which the adhesion strength was reduced.

3.2.1.1 Adhesives type comparison

A lap joint shear strength evaluation test was undertake to compare the adhesion effectiveness of different adhesive types, namely, a two component epoxy adhesive, a PVA and a PU adhesive. All samples were prepared by sanding the bonding surface and rinsed with deionised water to remove the dust. After that, the samples were conditioned in a conditioning room at 20 °C and 65% R.H, until weight stabilization, and adhesive was applied to both bonding surfaces. All samples were glued to the outer side of the pipe because the surface was smoother and therefore less sanding was required. After 48 hours in the conditioning room, for the best adhesive curing, the samples were drilled and placed on the universal testing equipment for the shear strength measurement.

3.2.1.2 Hydrogen peroxide treatment

A 30% w/v H_2O_2 solution was used for the treatments. The pH of the treatment solution was adjusted by adding drops of 1 M NaOH into the solution at 20 °C and monitoring pH using a pH meter (CONSORT C532) at 5, 6, 6.5, 7, 7.5, 8, 8.5 and pH 9. All hydrogen peroxide treatments took place in conditioned room at 20 °C and 65% R.H.

Approximately 300 ml of solution was poured into a 500 ml beaker container. This was enough to cover 40 samples. The samples were soaked in the treatment solution for 30 minutes. To ensure that the samples did not float and remained under the solution throughout the treatment, a conical flask with bottom diameter to fit into the beaker was filled with water to increase weight and was placed on top (Figure 3.6). Every 10 minutes the samples in the solution were stirred with a glass rod to ensure that the samples had the same amount of contact time with the solution on each side of the material during the treatment period. After each treatment period ended, the samples were removed and washed with deionised water. The excess water was removed by touching each side of the sample on absorbent paper. All samples were weighed and placed in a conditioning room at 20 °C and 65% R.H until weight stabilization.

Figure 3.6: Samples placed into the hydrogen peroxide solution.

3.2.1.3 Hot air treatment

The samples were placed on a metallic plate under the hot air gun. The hot air gun was attached to the robotic arm with a 2.5 cm vertical distance from the samples (Figure 3.7). In order to ensure that the hot air gun had reached a steady temperature, it was switched on and left working for 2 min before the first treatment. The samples were treated with different speeds of the hot air gun in a straight line direction. The speeds that were used for the treatments were 115 mm s^{-1}, 75 mm s^{-1}, 67.5 mm s^{-1}, 37.5 mm s^{-1}, 31 mm s^{-1}, 25 mm s^{-1}, 18.5 mm s^{-1}. Another treatment regime used 2 times passage with 75 mm s^{-1}speed (2x75 mm s^{-1}). After treatment the samples were placed in the conditioning room at 20 °C and 65% R.H to cool down for 15 minutes and then rinsed with deionised water. The excess water was removed from the sample sides with absorbent paper. The samples were again conditioned until weight stabilization.

Figure 3.7: Hot air treatment.

3.2.1.4 Flame treatment

All samples were placed on a metallic surface under the robotic arm. A MAPP flame torch was attached to the robotic arm with the flame nozzle facing down, and being 5 cm over the samples surface. The treatment speeds which were applied on the samples were

125 mm s^{-1}, 150 mm s^{-1}, 175 mm s^{-1}, 200 mm s^{-1}, 225 mm s^{-1} and 250 mm s^{-1}. All samples were placed in the conditioning room at 20 °C and 65% R.H to cool down for 15 minutes and then rinsed with deionised water to remove potential dust and water dissolving materials which could be formed on the surface, and which might affect the adhesion and replaced in the conditioning room at 20 °C and 65% R.H until weight stabilization.

3.2.1.5 Halogen heat lamps treatment

The samples were placed on a metallic beam. The halogen lamp unit (Figure 3.4) was attached to the robotic arm at a distance of 2 cm above the samples. Similar to hot air gun, to ensure steady temperature during the treatments the halogen heating lamps were switched on 5 min before the first treatment. Samples were treated with speeds of 10 mm s^{-1}, 20 mm s^{-1}, 30 mm s^{-1}, 40 mm s^{-1} and 50 mm s^{-1} (Figure 3.8). After treatment the samples were placed into the conditioning room for 15 minutes to cool down. Then they were rinsed with deionised water to remove potential dust and water dissolving materials which could affect the adhesion. After washing with water the samples were replaced in the conditioning room at 20 °C and 65% R.H until weight stabilization.

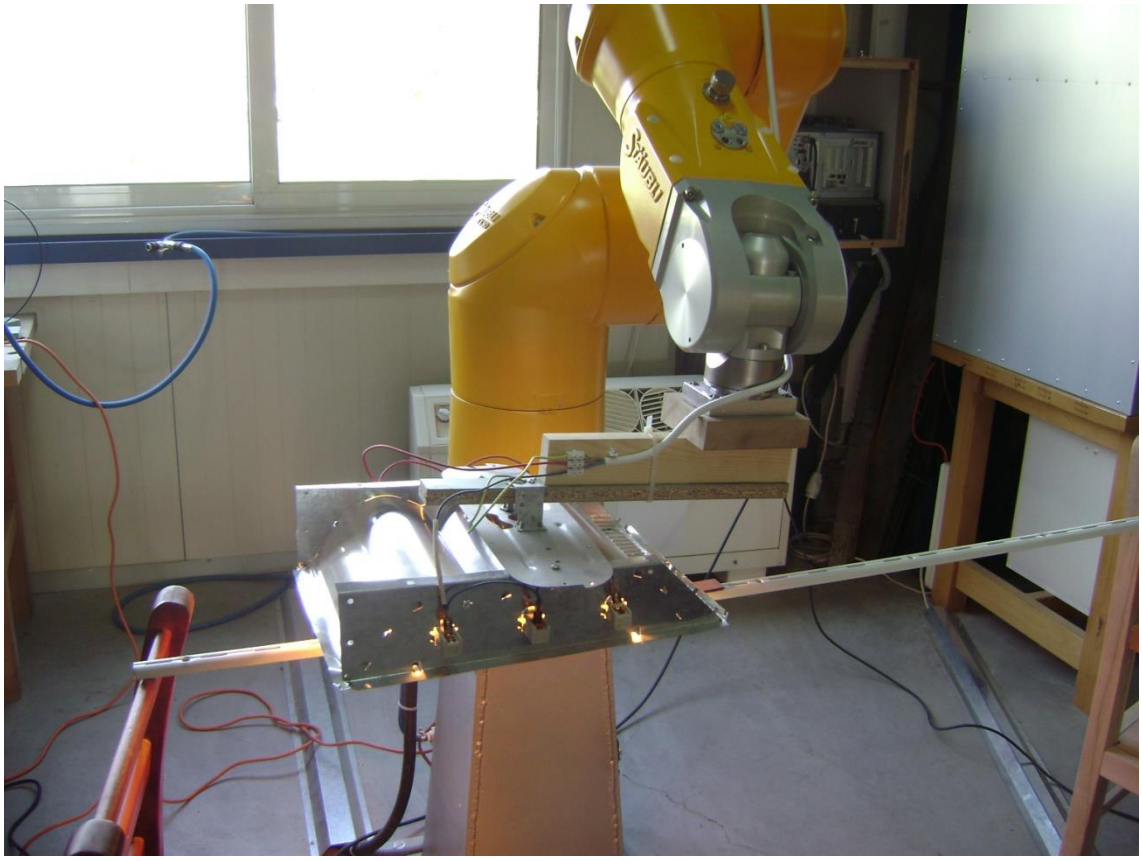

Figure 3.8: Halogen heating lamps treatment.

3.2.2 LAP JOINT PREPARATION

Sets of 40 samples were prepared to be bonded and to produce sets of 20 lap joints. All samples (including control samples) which were prepared to be used as lap joints were rinsed with deionised water and placed into the conditioning room at 20 °C and 65% R.H until weight stabilization before the adhesive application. The epoxy adhesive components were mixed with resin:hardener 1:1 w/w ratio and then applied to both sample surfaces. The other adhesives were directly applied to both sample surfaces of the lap joint. Then the samples were placed together to form the desired joint and then pressed. To avoid variations between samples, pneumatic clamps were used to apply uniform pressure to the bonding joints for 15 minutes, which is the minimum pressuring time according the manufacturer (Figure 3.9).

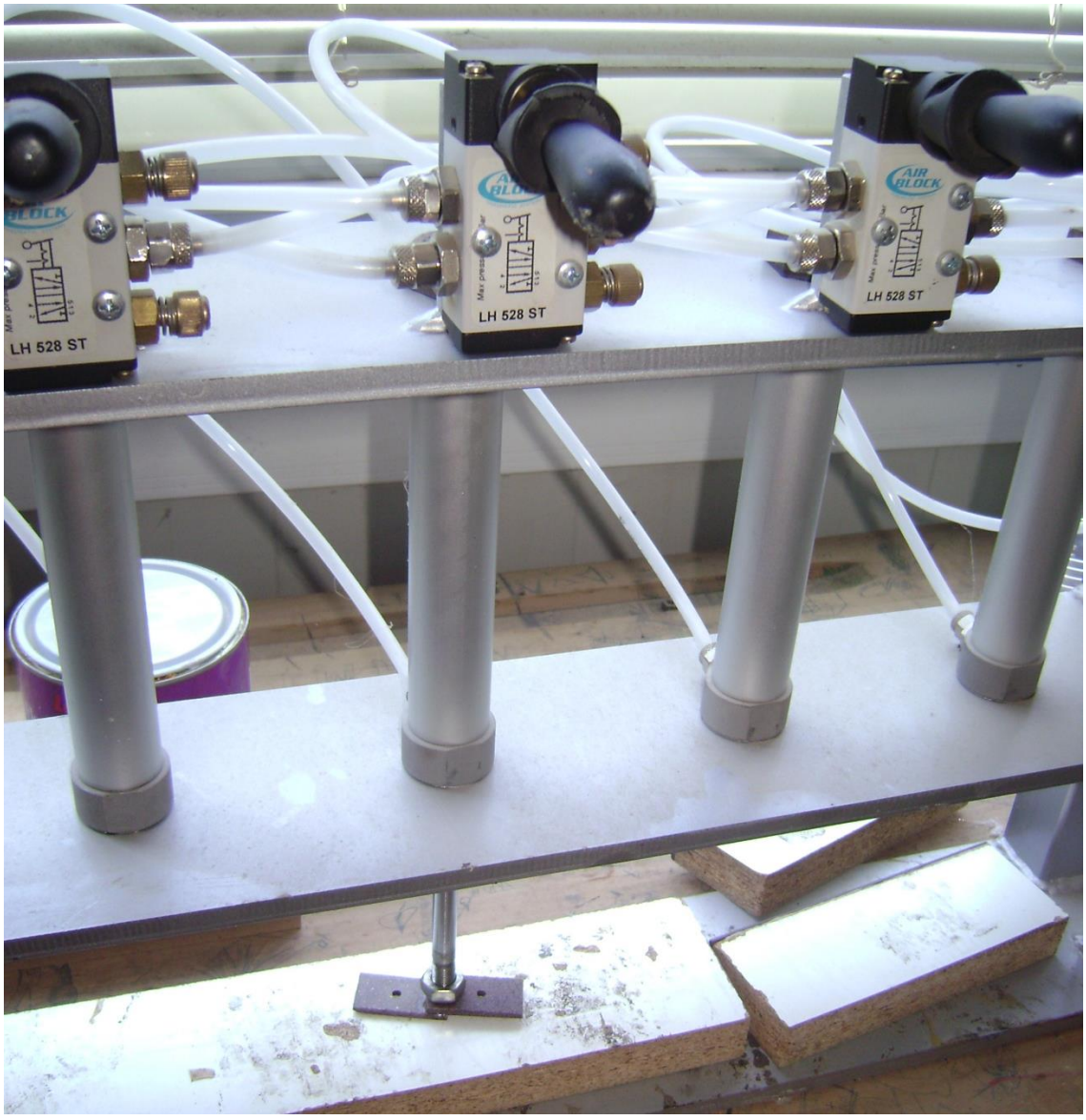

Figure 3.9: Pneumatic clamps applying uniform pressure to a lap joint specimen.

The bonding area of each sample was 10 mm X 20 mm. To avoid even small variations at the bonding area, which can have big influence on shear area, the samples were placed in a mould, which ensured that the bonding area of every lap joint was the same. After the adhesive curing, the bonding area was checked with a digital calliper with ±0.2 mm accuracy, to ensure that the lap joint bonding area was 10 mm X 20 mm. All the adhered lap joint samples were placed into the conditioning room at 20 °C and 65% R.H for 48 hours as recommended by the manufacturer for best adhesion due to curing. For the bonding shear strength evaluation a Zwick/Roell Z020 universal testing machine was used (Figure 3.11). The mechanical properties were determined according to EN 205/1991 standards at 1.5 mm min^{-1} cross head speed. For every treatment 20 lap joint samples were used according to standards. 20 lap joint samples of untreated WPC were also tested to determine the control value. Each sample was drilled (Figure 3.10), to allow mounting in the universal testing machine. A U-shaped shackle was used as sample holder and a steel nail was used to secure the sample in place as shown in Figure 3.12. When the samples were placed on the testing instrument they were pre-loaded to ensure that the strength would be applied directly at the start of the test by tightening the bolts over and under the instrument grips. The freedom of movement of the sample holders was ensuring that the force would be applied parallel and through the bonding line. It is important to mention that all the samples failed within the material did not shown any elongation. The failure pattern was similar in all cases and was occurring catastrophically at the edge of the bonding area.

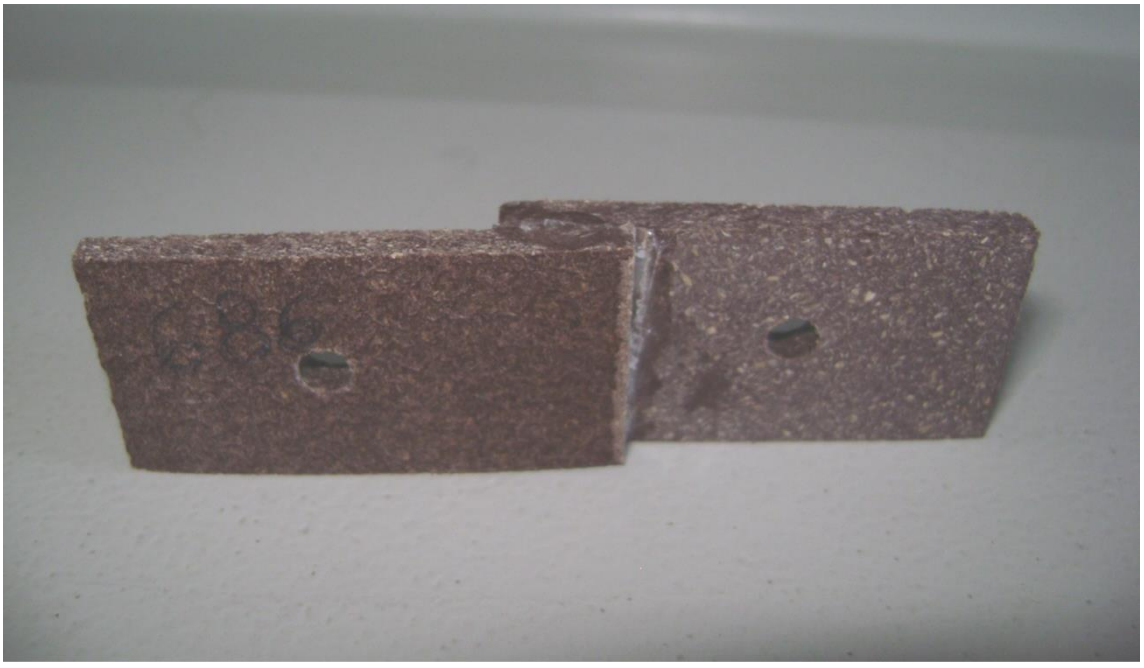

Figure 3.10: Lap joint with bonded area 10 X 20 mm, and holes to allow mounting in test machine.

Figure 3.11: The Zwink/Roell Z020 universal testing machine used for the evaluation of bonding shear strength.

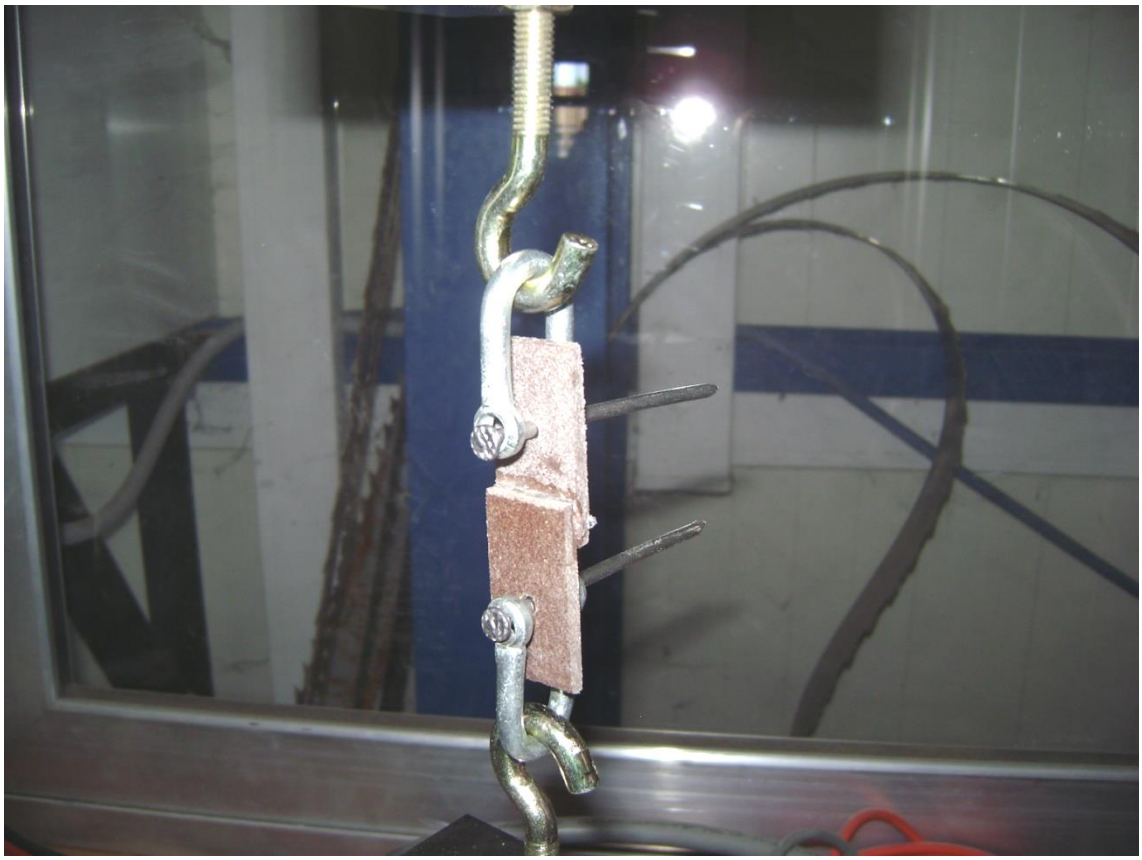

Figure 3.12: Samples attached on the mechanical properties instrument.

3.2.3 LIGHT MICROSCOPY OBSERVATION

For light microscopy observations, a Leica DFC280 microscope camera installed on a Leica MZ6 stereoscopic light microscope was used. Three samples of every set of H_2O_2 treatment, flame treatment, halogen heat lamp and hot air gun treatment were observed and pictures taken before and after treatment. This allowed comparison of the possible surface differences which may have occurred due to treatment. The samples were washed with deionised water before treatment to remove any dust present, but they were dried without being rinsed with water after treatment. The reason for samples not being rinsed with water after treatment is to observe potential water soluble material formation on sample surfaces.

3.2.4 SURFACE ROUGHNESS

The surface roughness was determined using a Mitutoyo SurfTest SJ-210 instrument. The pin radius was 2 μm and the measuring range was from -200 μm to 160 μm. The samples were placed on a surface which was calibrated as parallel to the instrument testing pin using a spirit level (Figure 3.13). Every sample was tested along the two diagonals to cover as much surface as possible. Two samples of every treatment parameter were used for roughness determination. The testing pin speed was 0.5 mm s^{-1} and the testing length was 25 mm.

Moreover the tested surface was divided into 6 segments for the surface roughness determination. The evaluation of the roughness was made according to ISO 1997 standards.

From each test three values were obtained; Ra, Rz and Rq. Roughness average (Ra) is the roughness mean of the all the measured area. Rz is the mean of the biggest peaks to valleys of the tested surface and Rq refers to the square means of the deviation from the mean line. Ra is a typical value to illustrate the general view of the surface roughness of a material. For that reason Ra value was used to compare the change of the WPC roughness due to treatments. The Ra measurement equation is:

$$\mathrm{Ra} = \frac{1}{n}\sum_{i=1}^{n} \mathrm{Hj} \qquad \textbf{[3.1]}$$

n refers to the measurement segments and Hj the distance from a peak to valley of every segment.

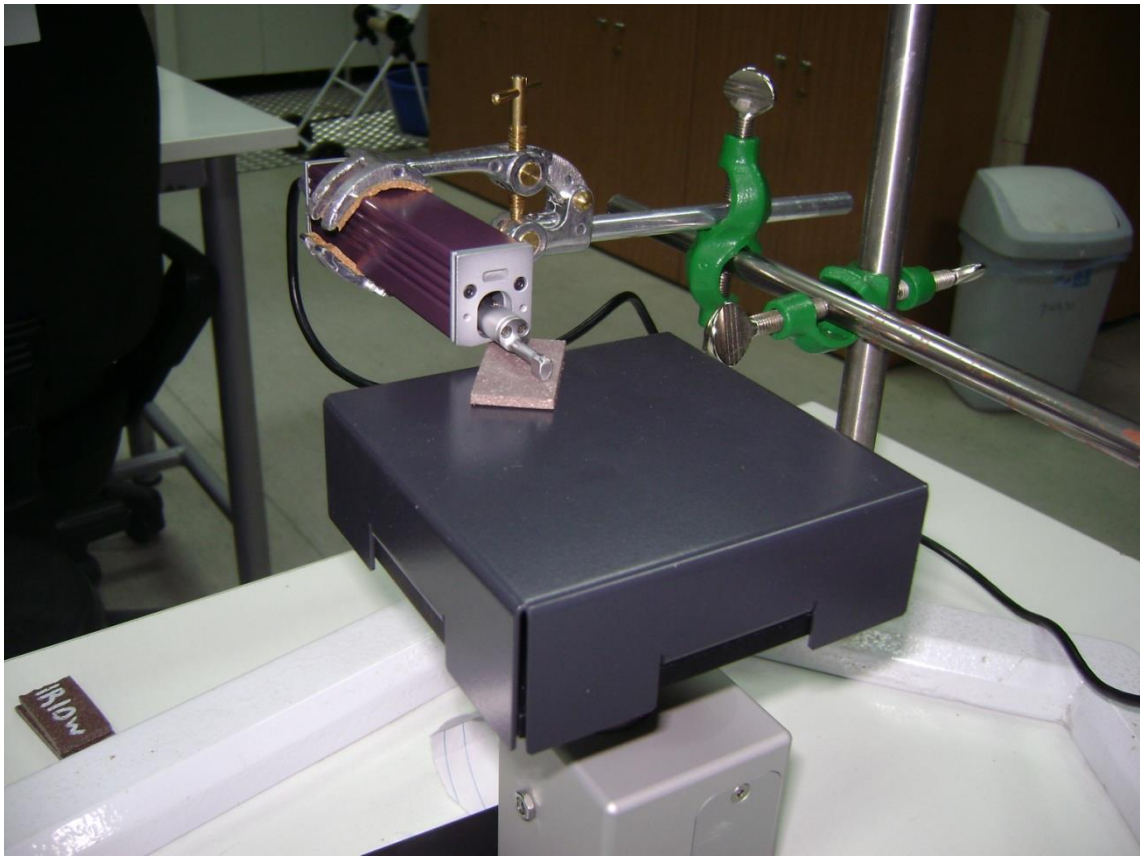

Figure 3.13: Roughness determination along the diagonal of a treated sample.

3.2.5 CONTACT ANGLE MEASUREMENTS

Contact angle was determined using a Kruss easy drop instrument (Figure 3.14). A high definition camera attached to the instrument was used to observe the liquid drop on the surface. Computer software provided by the manufacturer was also used to calculate the contact angle and the surface energy. The liquid which was used for the contact angle determination was deionised water. The reason for using only water for the surface energy determination, was that the main interest for this test was the penetration of the adhesive into the material surface which is more related to the wettability of the material and not to the chemistry which affecting the surface energy. Five samples of every treatment were tested. Contact angles were recorded every 1 s for the first 4 s from the moment that the drop contacted the material's surface. Untreated samples were also tested to calculate the surface energy and contact angle as control values. The instrument automatically delivers a specific dose of water drop on the surface. The camera records the drop on the surface and calculates the contact angle and the surface energy according the equation of state (EOS). The EOS with known surface tension of the liquid is the most suitable method for determine the surface energy of solids with the use of a single liquid contact angle measurement.

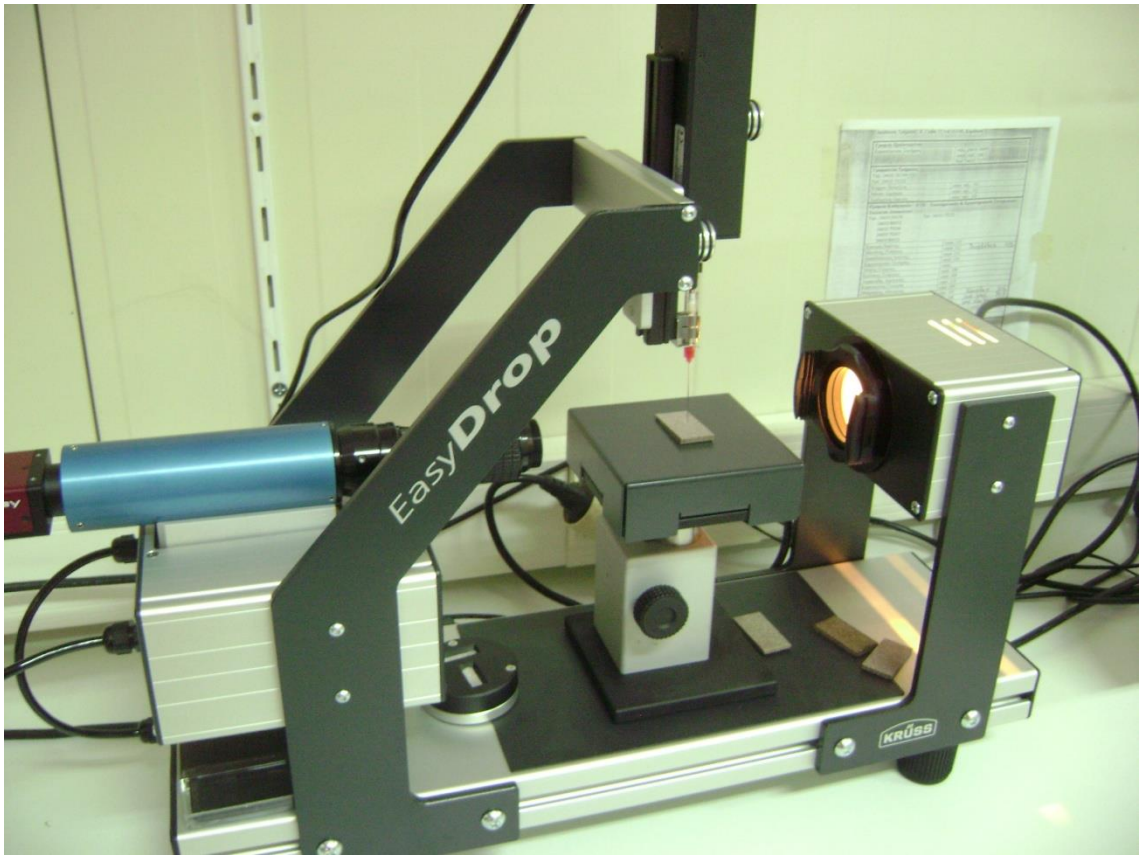

Figure 3.14: Contact angle determination instrument.

The contact angle which is measured is the formed angle between the tangent of the drop and the surface line (Figure 3.15). The larger the θ angle is, the more hydrophobic the material is.

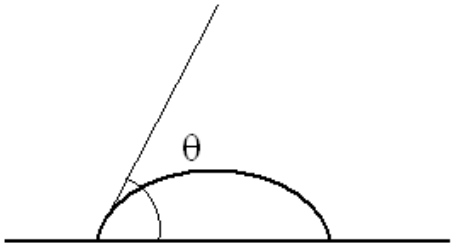

Figure 3.15: Contact angle measurement of a liquid drop. θ is the angle which is measured.

The EOS is derived from the equation of Young.

$$\sigma_s = \gamma_{sl} + \sigma_l * \cos\theta \quad \textbf{[3.2]}$$

σ_s: surface tension of the solid.

σ_l: surface tension of the liquid.

γ_{sl}: interfacial tension between the solid/liquid.

To measure the γ_{sl} a series of contact angle data were taken and experimental resulted to the following equation:

$$\gamma_{sl} = \sigma_l + \sigma_s - 2\sqrt{\sigma_l * \sigma_s} * e^{-\beta(\sigma_l - \sigma_s)^2} \quad \textbf{[3.3]}$$

The constant β was determined at the value of 0.0001247. Therefore by the combination of the equations [3.2] and [3.3] derives a new equation as follows:

$$\cos\theta = -1 + 2\sqrt{\frac{\sigma_s}{\sigma_l}} * e^{-\beta(\sigma_l - \sigma_s)^2} \quad \textbf{[3.4]}$$

Thus if the surface tension of the liquid (σ_l) is known and a single contact angle (θ) is measured it is possible to calculate the surface tension of the solid (σ_s) by the equation [3.4].

The characteristics of the deionized water which was used for the surface energy determination are presented in Table 3.1.

Table 3.1: Water characteristics for the surface energy determination. Values refer to 25 ^{0}C temperature.

IFT (mN m^{-1})	72.8
Disperse component	21.8
Polar component	51
Density (g cm^{-1})	0.998
Viscosity (mPa s)	1.002

(KRUSS GmbH, Hamburg 2004-2011, Software for Drop Shape Analysis DSAI V.1.92 for contact angle measurement systems. User Manual. V. 1.92-05)

3.2.6 COLOUR CHANGES

The treatments cause mechanical and chemical changes on the sample surfaces and also change its appearance. One important factor related to the aesthetic value of the material is the colour difference. To investigate the possible colour changes that might have occurred during treatments, a BYK Gardner colour-guide instrument was used. The colour changes were determined by CIE Lab standard. For the colour difference determination 2 samples of every treatment and 2 samples of untreated WPC were used.

The instrument provides three variables L^*, a^* and b^*. The L^* variable takes values from 0 to 100. L^* value indicates how white the colour is (0 for absolute black and 100 absolute white).

The a^* variable is between -100 to +100 and indicates how red or green is the colour. a^* values above 0 refers to red and below 0 to green.

The b^* variable takes values from -100 to +100 just as in a^* variable. For positive values the colour is tending to yellow and for negative values to blue.

To mathematically calculate the colour difference between treated and untreated samples equation 2 was used:

$$\Delta E=[(\Delta L)^2+(\Delta a)^2+(\Delta b)^2]^{1/2} \quad \textbf{[3.5]}$$

ΔL, Δa and Δb refers to the arithmetical differences between treated and untreated sample values. ΔE value indicates the significant colour difference after treatment.

3.2.7 SEM OBSERVATION

The microscopic observation of the surface structure was held by SEM-EDS method at the Aristotelian University of Thessaloniki department of Physics. The electronic microscope was a JEOL JMS-840A attached to an energy dispersive X-ray (EDS) INCA micro analytical system. The samples were cut at 20 X 20 mm dimensions and carbon coated under vacuum with a JEOL JEE-4X vacuum evaporator. The SEM was carried out with accelerated voltage of 20kV and probe current 45nA. The counting time was 60 sec. To scan the sample surface two types of electron spectrum (primary [backscattered] and secondary electron) were used. The primary electron scanning provides a more clear view of the surface without distinguishing the material components distributions. The surface morphology is more obvious with the primary electron scan rather than the secondary electron scan.

The secondary electron spectrum presents a view of the basic chemical components which are present on the materials surface. Lighter areas indicates that the surface contains oxygen. That means that the lighter areas are the wood fibres, because of the cellulose and the hemicellulose, which are containing oxygen. The PP does not contain any oxygen in the polymeric chain. Therefore, the secondary electron spectrum offers a better view of the wood fibres condition after the treatment.

3.2.8 FTIR CHEMICAL ANALYSIS

A Nicolet 8700 FTIR (Thermo Scientific) with GladiATR vision (Pike Technologies) was used for the surface chemical analysis. The FTIR spectrometry was performed directly on the material surface using the ATR reflector and not in a form of pellet. There were an average of 32 scans for the collection of every spectra and the wavenumbers varied from 4000 to 600 cm^{-1}. For the FTIR-ATR investigation one sample was used of every treatment and scanned 5 times on different areas on the surface. From the 5 spectra of every treated sample an average spectrum was produced to see the chemical changes occurring on the surfaces. To avoid the spectra noise and the formed peaks which might have occurred as a result of environment changes like CO_2, background spectra were taken for every two spectra.

3.2.9 STATISTICAL ANALYSIS

SPSS statistics version 17.0 software was used to carry out one way ANOVA analysis of variance on the shear strength values, surface roughness and contact angle of treated and untreated samples. The shear strength values were analyzed with the treatment factors and untreated material (control) as independent variable. Homogeneity variance, F-test and Tukey

test were performed to investigate the possible statistical significant differences within treatment factors compared to control.

The samples that they were used during this study are presented detailed in the Table 3.2. All samples that they used were 861. For the control 30 samples were used during all testing; 234 for hydrogen peroxide treatment; 234 for heat treatment; 176 for flame treatment; 147 for halogen heating lamps treatment and 40 for the adhesives comparison test.

Table 3.2: Table of all samples used during treatments and testing

	Lap joints	Light microscopy	Surface roughness	Contact angle	Colour	SEM	FTIR-ATR	Total
Control	20	3	2	1	2	1	1	30
Hydrogen peroxide tereatment	160	24	16	8	16	2	8	234
Heat gun treatment	160	24	16	8	16	2	8	234
Flame treatment	120	18	12	6	12	2	6	176
Halogen heating lamps treatment	100	15	10	5	10	2	5	147
Adhasives comparison	40							40
Total samples used	861							

CHAPTER 4: RESULTS

4.1 MECHANICAL PROPERTIES DETERMINATION

To evaluate the effectiveness of the treatments methods, the mechanical properties of the bonded samples were the most important parameter to be tested. Therefore the lap joint shear strength test was performed to untreated samples and treated samples. From the comparison of the untreated (control) and the treated samples, it is possible to evaluate the treatments efficiency to improve WPCs adhesion ability.

4.1.1 ADHESIVE TYPE LAP JOINT SHEAR STRENGTH RESULTS

The samples that broke within the material rather the bond line were excluded from the mean values determination. This is because the breaking strength value of a sample which broken in the material refers to the sample shear strength and not to the bonding shear strength. Therefore the amount of samples available for statistical analysis of bond strength differed between treatments. Samples which broke at the surface and not at the bonding line could be an indicator of the adhesion effectiveness, as the strength that required to pull apart the adhered joint is higher than the materials internal shear strength. For that reason, material failure expressed as % percentage was reported for each set of joints. To evaluate the shear strength values and be able to compare the effectiveness of treatments one way ANOVA statistical analysis was performed.

A PVA, PU and 2 component epoxy adhesive were used to determine which adhesive type produces the most effective adhesion. The results are shown in Figure 4.1.

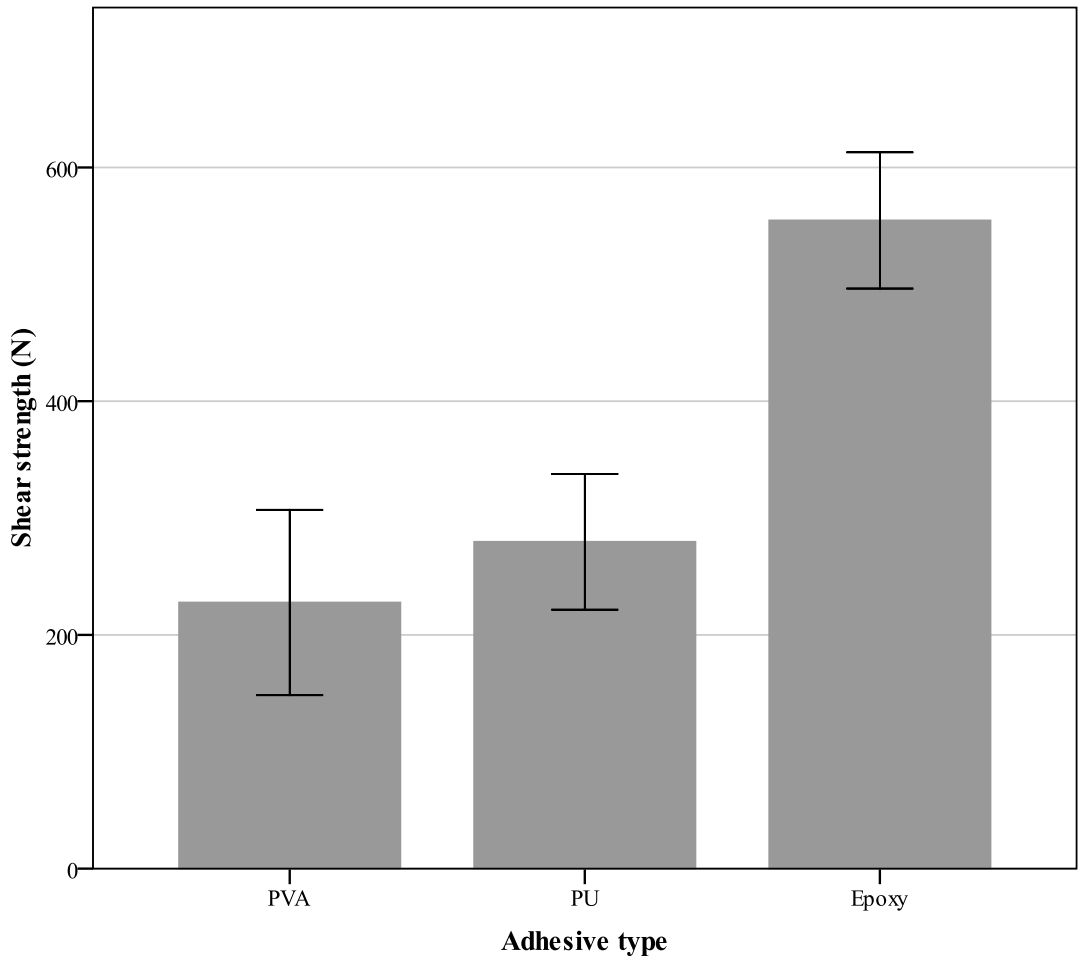

Figure 4.1: Adhesive type lap joint tensile strength (N). Error bars represent the SD (+/- 1).

The homogeneity of variance was tested with Levene test. Levene test of the adhesive comparison shear strength results revealed that the null hypothesis could not be eliminated (Levene statistic=1.119, p=0.334). The failed elimination of the null hypothesis means that the differences between the samples shear strength, might be random, by equal variances within the compared samples. In case of null hypothesis rejection ($p<0.05$), the variances of the tested samples did not occur randomly, which confirms the relation of the sample sets and the shear strength deviations. However, the Levene test is not an important factor for comparing values (Norusis 2005).

The descriptive statistics (Table 4.1)) show that the PVA adhesive has mean value 227.73 N following the PU 279.7 N and the 2 component epoxy had the highest bonding strength with mean value 554.7 N. The Polyurethane adhesive has the smallest standard deviation (SD=58.1) and PVA has the greatest scales (SD=79.3).

Table 4.1: Mean values of adhesive type in N. Standard Deviation (SD), Minimum and maximum values and the boundaries of the 95% CI of the lap-joint. Material failure refers to the samples that failed on the material rather the bonding line.

Shear strength (N)		PVA	PU	Epoxy
Average		227.73	279.70	554.70
min		120.52	173.83	443.56
Max		418.34	390.61	660.53
CI 95%	Lower Bound	188.29	252.51	526.60
	Upper Bound	267.18	306.89	582.80
SD		79.32	58.10	58.30
Material failure %		0%	0%	5%

Despite the fact that Levene test is not significant the null hypothesis could be eliminated because the F-test is significant for F=135.1 and at significance level p<0.001.

The differences between the lap joint shear strength of the different adhesives were investigated with the Tukey HSD multiple comparisons, and presented in Table 4.2. PVA and PU adhesives are statistically different from the 2 component epoxy adhesive (p<0.001). The PVA with the 2 component epoxy adhesive has the highest mean difference (-326.96) among all samples. PVA with PU are also statistically different (p<.05) and having the smallest mean difference among all samples (-51.96).

Table 4.2: Adhesive type multiple comparison test results. Statistical significant difference for p<0.05

p values	PU	Epoxy
PVA	0.047	0.000
PU		0.000

One way ANOVA clearly shows that the 2 part Epoxy adhesive had the stronger bond strength for joining WPC compared to the PVA and the PU adhesives. The Epoxy adhesive caused the joints to break in the material rather in the bonding line in 5% percentage of the tested samples in contrast to none of the PVA and PU adhesives. 5% of the 20 samples that were tested is only one sample which might not be that significant. It is however clear that the 2 part epoxy adhesive is significantly stronger than the PVA and the PU. Additionally 10% of the PVA adhesive joints were too weak to sustain the joint until the shear strength evaluation, and they broke just by trying to install them on a Zwink/Roell Z020 universal testing machine. Following the tensile test mentioned above, the epoxy adhesive was chosen as the adhesive to be used for the rest of the lap joint tests.

4.1.2 EFFECT OF PH ON HYDROGEN PEROXIDE TREATMENT LAP-JOINT SHEAR STRENGTH RESULTS

Hydrogen peroxide solutions at 8 different pH values (5, 6, 6.5, 7, 7.5, 8, 8.5, 9) were used as pre-treatments and compared with the untreated (control) set (Figure 4.2).

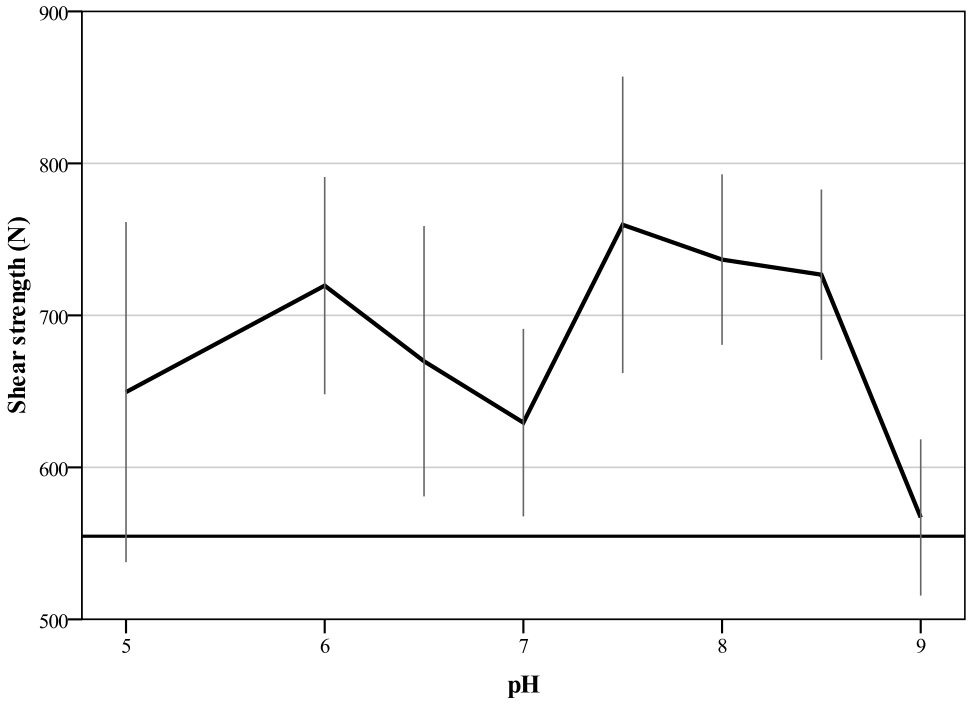

Figure 4.2: Effect of pH on hydrogen peroxide treatment lap joint tensile strength (N). The flat line present the control mean value (554.70 N). Error bars represent the SD (+/- 1).

The Levene test was not statistically significant, therefore the null hypothesis could not be eliminated (Peroxide treatment Levene statistic=1.102, p= 0.305) but one way ANOVA was done anyway. The descriptive statistics for the hydrogen peroxide treatment method are presented in Table 4.3.

Table 4.3: pH of hydrogen peroxide treatment lap joint tensile strength mean values (N). Standard Deviation (SD), Minimum and maximum values and the boundaries of the 95% CI of the lap-joints. Material failure refers to the samples that failed on the material rather the bonding line.

Treatment pH		control	5	6	6.5	7	7.5	8	8.5	9
Average		554.70	649.52	719.58	669.82	610.33	759.59	714.12	673.09	564.40
Min		443.56	479.52	604.46	451.76	464.42	700.57	556.89	567.29	375.31
Max		660.53	854.94	874.59	804.72	736.58	872.17	827.42	800.97	713.94
95% CI	Lower Bound	526.60	589.90	685.11	622.42	569.72	517.31	670.29	631.90	524.74
	Upper Bound	582.80	709.15	754.04	717.22	650.95	1001.88	757.96	714.27	604.06
SD		58.30	111.90	71.50	88.95	78.99	97.53	79.15	64.82	77.14
Material failure %		5%	15%	5%	15%	10%	80%	25%	40%	10%

The mean values ranged from 564.4 N (pH 9) to 759.59 N (pH 7.5). The minimum standard deviation among the hydrogen peroxide treated samples was observed in the pH 8.5 samples (SD=64.82) and the maximum in the samples treated with pH 5 solution (SD=111.9). High standard deviations were seen in all tests.

All treatments seem to have a positive effect on WPC adhesion ability, with an exception of the pH 9 treatment, which has a mean shear strength value similar to the control (Figure 4.2). The samples treated at pH 6, pH 7.5, pH 8 and pH 8.5 have around the same high values, all are over 700 N but the highest overall is at pH 7.5. It is very important to mention that 80% of the pH 7.5 samples failed by fracture in the WPC material rather than the glue line, in contrast with only 5% of the control samples. This is a further indication of good bonding with this surface treatment.

The F-test comparing treatments revealed that pH level of the hydrogen peroxide solution was statistically significant, as for peroxide treatment $F=10.734$ for significance level $p<0.001$, related to the WPCs shear strength. Consequently the null hypothesis, that the deviation among the treatment parameters and the control samples occurred randomly, could be eliminated for the hydrogen peroxide treatment method.

To investigate the differences between the treatment variances the Post-Hoc HSD multiple comparisons test was used. The statistically significant difference, between the pH of hydrogen peroxide treatment solution, is presented in

Table 4.4. The acidic solutions all had means which were significantly different to the control at $p<0.05$ level, with pH 5 showing significant difference at $p<0.05$ and having the smallest mean difference (-94.82) among all samples, and pH 6 and pH 6.5 having significant difference at $p<0.001$ and $p<0.005$ respectively. The pH 7 solution is not statistically significant different from the control samples but shows significant difference to pH 6 and pH 8 at $p<0.005$. For the alkaline solutions, all were significantly different from the control, excluding the pH 9 solution means, at $p<0.001$ including pH 7.5 at $p<0.005$ which had the highest mean difference (-204.89) among all samples. The pH 9 solution is statistically significantly different to pH 6, 6.5, 8, 8.5 at $p<0.001$ and pH 7.5 at $p<0.01$.

Table 4.4: Hydrogen peroxide treatments pH multiple comparison test results (p values). Statistical significant differences for p<0.05. Values with fainter text are >0.05.

Treatment pH	pH 5	pH 6	pH 6.5	pH 7	pH 7.5	pH 8	pH 8.5	pH 9
Control	0.019	0	0.001	0.496	0.002	0	0.003	1
pH 5		0.211	0.999	0.896	0.427	0.389	0.998	0.069
pH 6			0.666	0.003	0.997	1	0.82	0
pH 6.5				0.462	0.698	0.838	1	0.008
pH7					0.084	0.011	0.498	0.766
pH 7.5						0.993	0.765	0.005
pH 8							0.924	0
pH 8.5								0.014

All solutions except for the pH 7 and pH 9 solutions were advantageous giving an increase in the lap joint shear strength. Although there were differences between the treatments mean shear strength values, the multiple comparison test show that there were no significant differences between the advantageous treatments namely pH 5, 6, 6.5, 7.5, 8 and 8.5 (Table 4.4). Thus ANOVA cannot provide a clear view of the single best treatment solution pH, but does indicate several potential treatments to improve the adhesion ability of WPC material. It is possible however to present as the best treatment the solution with the highest material failure percentage during lap joint tests (Table 4.3). The pH 7.5 solution appeared to have the highest material failure at 80% of the tested samples; this also had the highest mean shear strength. Next the pH 8.5 treatment with 40% material failure showed acceptable performance. Then pH 8 with 25%, pH 5 and pH 6.5 with 15% and pH 6 with 5% material failure also had good mean shear. On the other hand pH 7 and pH 9 solutions had 10% material failure, which was higher than the control material failure percentage (5%), but these were not statistically significant different to the control. According to the material failure during lap joint test, pH 7.5 was the most effective pH for hydrogen peroxide treatment to improve the WPCs adhesion.

4.1.3 HOT AIR TREATMENT LAP-JOINT SHEAR STRENGTH RESULTS

The samples were exposed in 8 different hot air gun treatment speeds (115 mm s^{-1}, 75 mm s^{-1}, 67.5 mm s^{-1}, 37.5 mm s^{-1}, 31 mm s^{-1}, 25 mm s^{-1}, 18.5 mm s^{-1} and two times passage with 75 mm s^{-1} speed) and compared with the untreated samples. Results are presented in Figure 4.3.

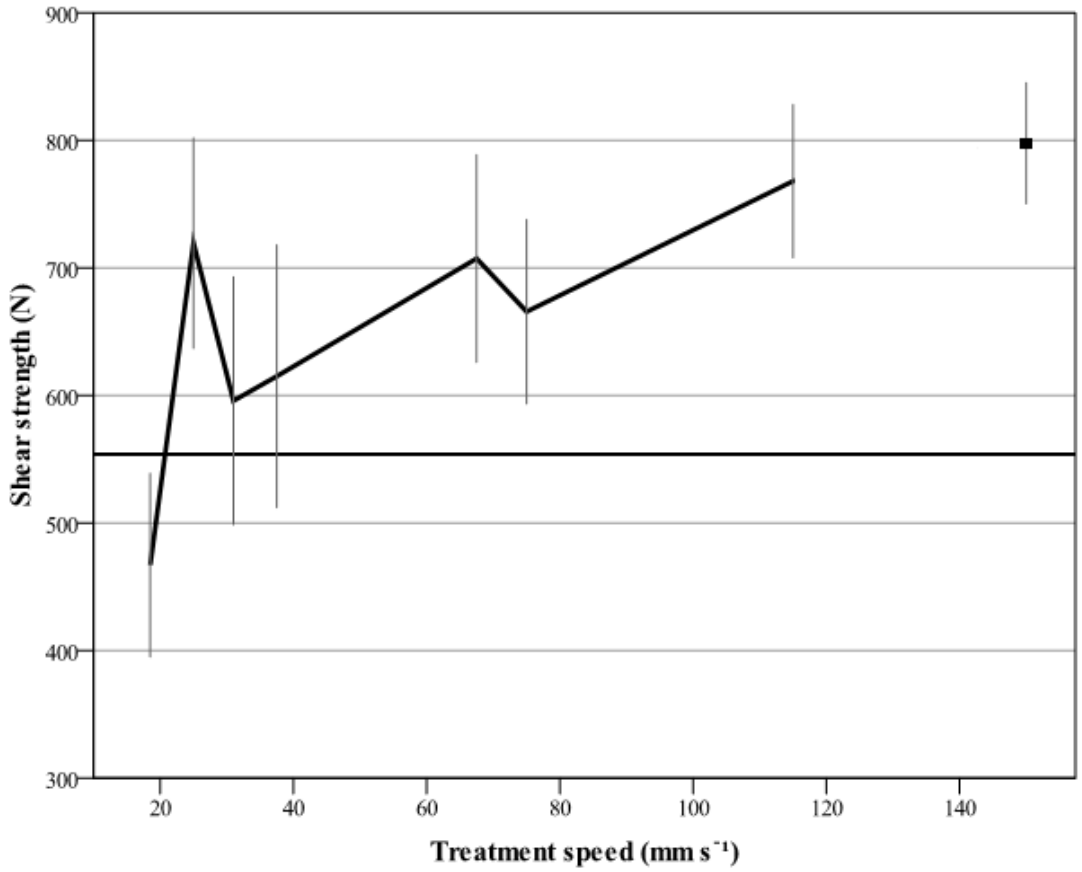

Figure 4.3: Hot air treatment lap joint tensile strength (N). The mean value at the 150 mm s^{-1} treatment speed refers to the samples treated twice with the speed of 75 mm s^{-1}. The flat line present the control mean value (554.70 N). Error bars represent the SD (+/-1).

The Levene test for the hot air treatment method appeared not to be statistically significant, and the null hypothesis could not be eliminated (Hot air treatment Levene statistic=0.886, p=0.531).

The hot air treatment tensile strength descriptive statistics are shown in Table 4.5.

Table 4.5: Mean values of hot air treatment in N. Standard Deviation (SD), Minimum and maximum values and the boundaries of the 95% CI of the lap-joints. Material failure refers to the samples that failed on the material rather the bonding line.

Treatment speed (mm s^{-1})		control	115	75 (X2)	75	67.5	37.5	31	25	18.5
Average		554.70	768.08	797.78	665.73	707.37	615.10	595.90	719.47	467.01
Min		443.56	699.67	716.72	524.56	622.10	513.09	422.65	555.30	271.43
Max		660.53	850.84	862.80	835.84	878.88	832.47	733.88	864.95	548.86
95% CI	Lower Bound	526.60	725.09	763.83	625.71	658.18	552.84	534.12	675.48	427.14
	Upper Bound	582.80	811.08	831.72	705.76	756.57	677.36	657.68	763.47	506.87
SD		58.30	60.11	47.45	72.28	81.41	103.03	97.23	82.57	71.98
Material failure %		5%	50%	50%	25%	25%	30%	30%	5%	10%

The mean values varied from 467.01 N (18.5 mm s^{-1}) to 797.78 N (2X75 mm s^{-1}). Samples treated with the 2X75 mm s^{-1} hot air gun speed appeared to have the smallest standard deviation (SD=47.4) and the 37.5 mm s^{-1} treatment the largest standard (SD =103).

The hot air treatment had a positive effect on the adhesion shear strength (Table 4.5 and Figure 4.3). The samples that were treated with hot air with speeds of 115 mm s^{-1}, 2X75 mm s^{-1}, 75 mm s^{-1}, 67.5 mm s^{-1} and 25 mm s^{-1} seemed to have an advantageous effect on the bonding strength. Samples treated with speed 18.5 mm s^{-1} had the opposite effect on the adhesion strength, with a mean value which was lower than the control. The samples that treated with speeds 37.5 mm s^{-1} and 31 mm s^{-1} did not clearly effect the shear strength because of their high standard deviation. It is important to mention that the samples which were treated with the speed of 75 mm s^{-1} had mean shear strength lower than the samples treated by two times passes of the hot air at the same treatment speed. Thus it could be more effective to apply the hot air over the WPC surface twice, although other two pass systems were not examined.

The F test showed that the hot air treatment speed did affect the adhesion ability of the WPC for $F=25.430$ and for significance level $p<0.001$. Therefore the null hypothesis, that the differences between the samples shear strength might be random, could be eliminated.

The significant differences between hot air treatment speeds as determined by the Post-Hoc HSD multiple comparison test are presented in Table 4.6.

Table 4.6: Hot air treatment multiple comparison test results (p values). Statistical significant differences for p<0.05. Values in a fainter text are >0.05

Treatment speed (mm s^{-1})	115	75 (X2)	75	67	37.5	31	25	18.5
Control	0.000	0.000	0.002	0.000	0.423	0.874	0.000	0.033
115		0.994	0.038	0.630	0.000	0.000	0.819	0.000
2X75				0.002	0.128	0.000	0.000	0.230
75				0.884	0.721	0.324	0.583	0.000
67.5						0.066	0.012	1.000
37.5							0.999	0.012
31							0.002	0.001
25								0.000

All samples treated with hot air except those treated at speeds of 37.5 mm s^{-1} and 31 mm s^{-1} are significantly different to the control samples. In particular, the samples treated at the speeds of 115 mm s^{-1}, 2X75 mm s^{-1}, 67.5 mm s^{-1} and 25 mm s^{-1} are different to the control for significance level $p<0.001$ and the samples treated at the speed of 75 mm s^{-1} for significance level of $p<0.005$. The samples treated at the speed of 18.5 mm s^{-1}, are significantly different to the control for significance level $p<0.001$ but with shear strength mean lower than the control. Despite the fact that there are treatment speeds which are significantly different to the control samples, there are no significant differences among the samples which are causing the shear strength to increase. The only significant differences among the treated samples which are increasing the shear strength, are the samples treated at the speeds of 115 mm s^{-1} and 75 (X2) mm s^{-1} with the samples treated at the speed of 75 mm s^{-1} ($p<0.05$ and $p<0.005$ respectively). The samples treated with the speeds of 67. mm s^{-1} and 25 mm s^{-1} are not significantly different to the samples treated at the speeds of 115 mm s^{-1}, 75 (X2) mm s^{-1} and 75 mm s^{-1}. To go over the main points, the samples treated with the speeds of 115 mm s^{-1} and 75 (X2) mm s^{-1} give the best treatment, followed by the samples treated at speeds of 67.5 mm s^{-1}, 25 mm s^{-1} and 75 mm s^{-1}.

Hot air treatment results for multiple comparisons were also not able to illustrate one best treatment speed. However it clearly appeared that 115 mm s^{-1}, 75 (X2) mm s^{-1}, 67.5 mm s^{-1} and 25 mm s^{-1} have a beneficial effect while 18.5 mm s^{-1} reduces the material bond-ability. The 115 mm s^{-1} and 75 (X2) mm s^{-1} speeds had the same material failure rate of 50%, the 67.5 mm s^{-1} treatment speed of 25% and the 25 mm s^{-1} treatment had only 5% (Table 4.5).

4.1.4 FLAME TREATMENT LAP-JOINT SHEAR STRENGTH RESULTS

The samples were exposed to 6 different flame treatment speeds (250 mm s^{-1}, 225 mm s^{-1}, 200 mm s^{-1}, 175 mm s^{-1}, 150 mm s^{-1} and 125 mm s^{-1}). The treated lap joints sets were tested and compared with the control samples. The results are presented in Figure 4.4. The plot below shows an increase in bonding strength with increasing flame treatment up to a pass speed of 175 mm s^{-1} but above this value reduces. All treatments seem to have a positive effect on WPC adhesion ability, with an exception of the speed of 125 mm s^{-1}, which has mean shear strength value lower of the control.

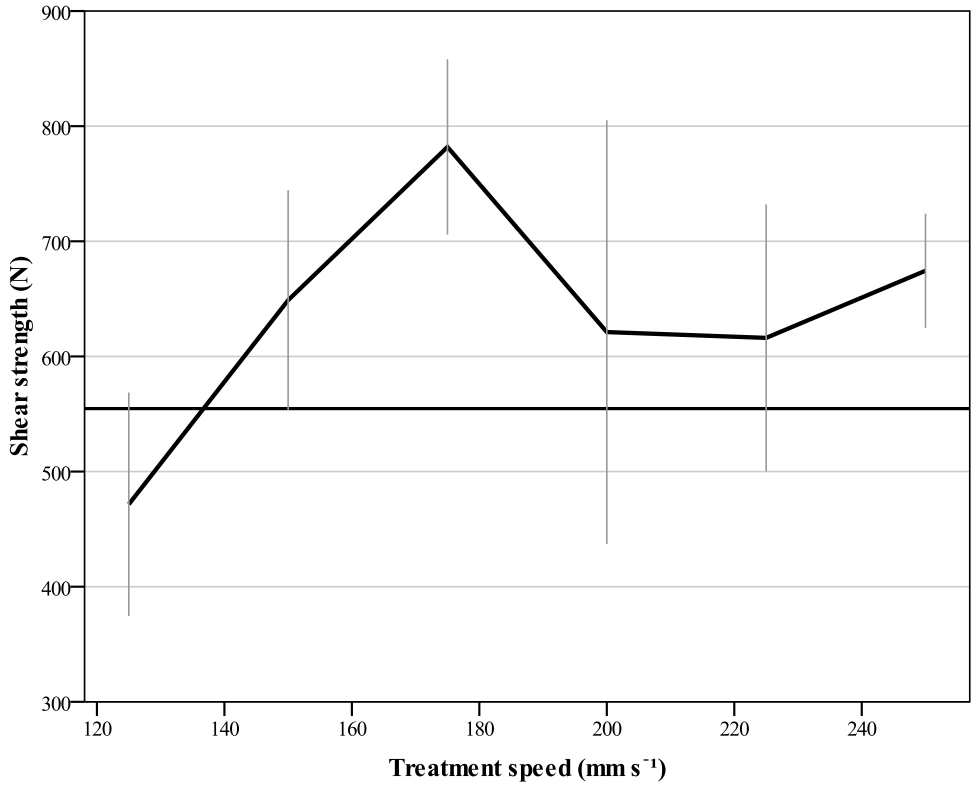

Figure 4.4: Flame treatment lap joint tensile strength (N). The flat line present the control mean value (554.70 N). Error bars represent the SD (+/- 1).

The homogeneity of variance was tested with Levene test, which was statistically significant. Therefore the null hypothesis could be eliminated (Levene statistic=6.29, $p<0.001$). The descriptive statistics of the flame treatment are presented in Table 4.7.

Table 4.7: Mean values of flame treatment in N. Standard Deviation (SD), Minimum and maximum values and the boundaries of the 95% CI of the lap-joints. Material failure refers to the samples that failed on the material rather the bonding line.

Treatment speed (mm s^{-1})		control	250	225	200	175	150	125
Average		554.70	674.43	616.11	621.15	781.93	648.85	471.57
Min		443.56	592.21	450.08	322.55	626.69	515.43	320.31
Max		660.53	735.35	799.45	892.48	850.64	792.68	700.46
95% CI	Lower Bound	526.60	644.46	551.89	526.54	711.52	597.95	424.78
	Upper Bound	582.80	704.41	680.33	715.75	852.35	699.75	518.36
SD		58.30	49.60	115.97	184.00	76.14	95.52	97.08
Material failure %		5%	25%	5%	10%	65%	20%	0%

The minimum SD was observed at 250 mm s^{-1} samples (SD=49.6) and the maximum at samples treated at 200 mm s^{-1} (SD=184). The shear strength mean values ranged from 320.3 N (125 mm s^{-1} minimum) to 892.5 N (200 mm s^{-1} maximum). The flame treated samples seemed to have an altered WPC adhesion, producing high standard deviation values. The standard deviation mean for the hydrogen peroxide treated samples was 83.75; for the hot air treated samples was 77.01; and for the flame treated samples was 103.05. The material does not seem to have a stable reaction following flame treatment. This could be explained by the different nature of the constituent materials. The polymer might react differently than the wood flour under the treatment flame so the WPC adhesion behaviour is related to the heterogeneity of the materials that are present on the surface. However the samples treated at 250 mm s^{-1} and 175 mm s^{-1} clearly increased their bond strength in contrast to the control values, and the standard deviation of these was close to the control.

The F-test revealed that flame treatment speed was statistically significantly related to the WPC shear strength, as F=10.008 for significance level $p<0.001$. Consequently the null hypothesis could once more be eliminated verifying the Levene test.

To investigate the differences between the treatment variances the Post-Hoc HSD multiple comparisons test was used. The statistically significant differences between flame speeds are presented in and Table 4.8.

Table 4.8: Flame treatment multiple comparison test results (p values). Statistical significant differences for p<0.05. Values with fainter text are >0.05.

Treatment speed (mm s^{-1})	250	225	200	175	150	125
Control	0.042	0.656	0.526	0.000	0.150	0.225
250		0.789	0.834	0.351	0.996	0.000
225			1.000	0.019	0.980	0.004
200				0.022	0.990	0.001
175					0.106	0.000
150						0.000

The post-Hoc HSD multiple comparison confirms that the samples treated at 250 mm s^{-1} and 175 mm s^{-1} were the only flame treated samples which clearly increased the shear strength ($p<0.05$ and $p<0.001$), but there was no statistically significant difference between them to clarify which of the speeds gave the best treatment.

The samples treated at 250 mm s^{-1} were only significantly different to the control and the 125 mm s^{-1} samples ($p<0.001$) which had mean value lower than the control. On the other hand the samples treated at 175 mm s^{-1} were significantly different to the samples treated at the speeds of 225 mm s^{-1} and 200 mm s^{-1} ($p<0.05$) which might be an indication that 175 mm s^{-1} is slightly better from the other treatment speeds.

ANOVA showed that during flame treatment the only treatment speeds that confirmed statistically significant differences in lap-joint shear strength were 250 mm s^{-1} and 175 mm s^{-1}. Samples that were treated with other speeds did not clearly affect the adhesion properties of the WPC. However the samples treated at 175 mm s^{-1} also appeared to have the higher percentage of material failure 65% (Table 4.7) which could indicate that this is the best treatment speed. The second best treatment speed according to material failure is the 250 mm s^{-1} flame speed with 25% material failure, followed by the 150 mm s^{-1} speed with 20%, 200 mm s^{-1} with 10%, 225 mm s^{-1} with 5% and 125 mm s^{-1} with 0%. Therefore according to material failure observation most of the treatment speeds seem to provide better bondability than the control except for the 225 mm s^{-1} treatment speed which was similar to control and 125 mm s^{-1} which was lower than control.

4.1.5 HALOGEN HEATING LAMP TREATMENT LAP-JOINT SHEAR STRENGTH RESULTS

The samples were exposed to 5 different treatment speeds under halogen heating lamps (10 mm s^{-1}, 20 mm s^{-1}, 30 mm s^{-1}, 40 mm s^{-1} and 50 mm s^{-1}) and compared with the control samples (Figure 4.5, Table 4.9).

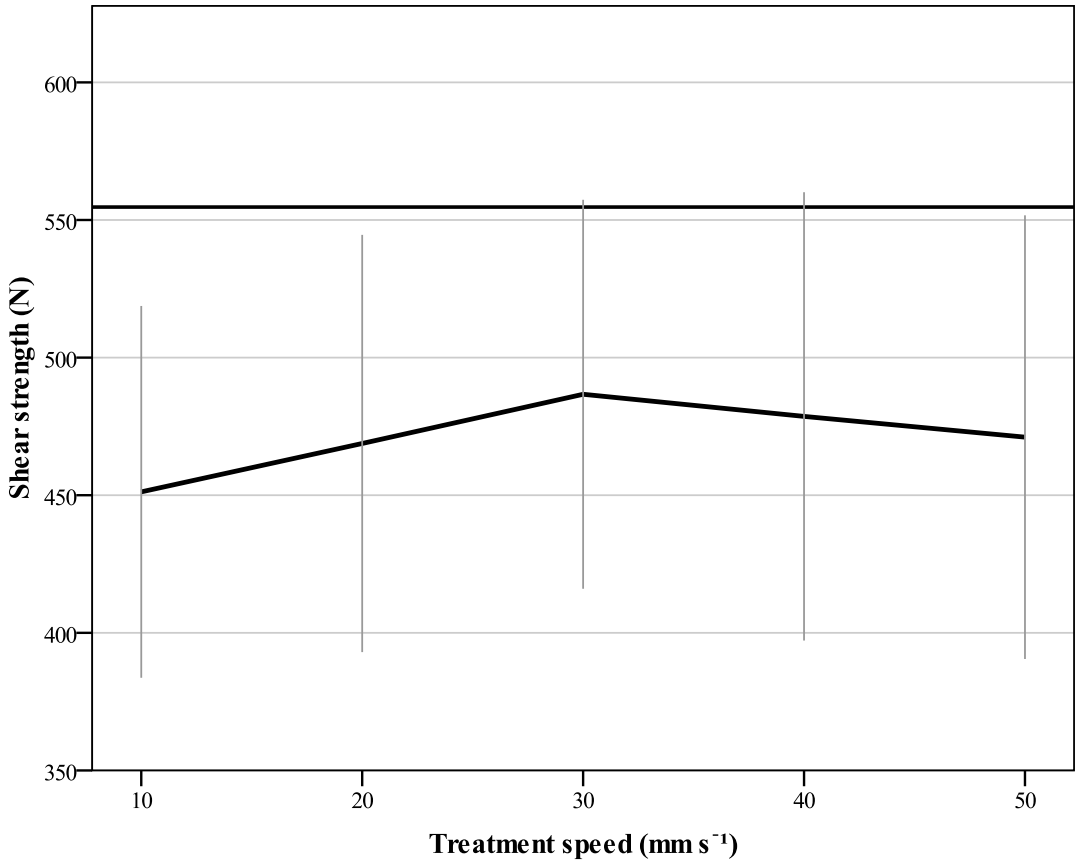

Figure 4.5: Halogen heat lamp treatment lap joint tensile strength (N). The flat line present the control mean value (554.70 N). Error bars represent the SD (+/-1).

Homogeneity of variance, which was tested by Levene test, showed that for the halogen heat lamp treatment method were not statistical significant and the null hypothesis could not be eliminated (Halogen Heat lamp treatment Levene statistic=1.005, p=0.418).

All of the halogen heat lamp treated samples had reduced adhesion ability with the worst at the 10 mm s^{-1} (reduced shear strength from a mean value of 554.7 N from the control to 451.21 N). Then as the treatment speed increased the mean values slightly increased up to the 30 mm s^{-1} treatment speed (486.57 N) but at faster treatment speeds minor decreases occurred. All of these treatments resulted in high variability.

The halogen heat lamp treatment descriptive statistics are shown in Table 4.9. The samples treated with the speed of 10 mm s^{-1} appeared to have the smallest standard deviation (SD=58.30) and the samples treated with halogen heat lamp speed of 40 mm s^{-1} had the maximum deviation (SD =81.44). The SD of the treated samples is not significant different from the control samples in contrast with the other treatment methods.

Table 4.9: Mean values of halogen heating lamp treatment in N. Standard Deviation (SD), Minimum and maximum values and the boundaries of the 95% CI of the lap-joints. Material failure refers to the samples that failed on the material rather the bonding line.

Treatment speed (mm s^{-1})		control	10	20	30	40	50
Average		554.70	451.21	468.79	486.67	478.64	471.10
Min		443.56	356.81	357.46	359.71	334.97	341.75
Max		660.53	551.41	593.72	585.01	633.88	593.24
95% CI	Lower Bound	526.60	419.60	433.32	453.60	440.52	433.38
	Upper Bound	582.80	482.82	504.27	519.75	516.76	508.82
SD		58.30	67.54	75.80	70.66	81.45	80.60
Material failure %		5%	0%	0%	0%	0%	0%

The F-test revealed that halogen heat lamp treatment speed was statistically significant related to WPCs shear strength as F=4.701 for significance level p<0.005. Consequently the null hypothesis could once more be eliminated verifying the Levene test.

To investigate the differences between the treatment variances the Post-Hoc HSD multiple comparisons test was used. The statistical significant differences between the halogen heating lamp treatment speeds are presented in Table 4.10. All the samples treated with the halogen heating lamp show statistically significant differences to the control. However there was no statistically significant differences among the sets of the treatment speeds.

Table 4.10: Halogen heating lamp treatment multiple comparison test results (p values). Statistical significant differences for p<0.05. Values with fainter text are >0.05.

Treatment speed (mm s^{-1})	10	20	30	40	50
Control	0.000	0.005	0.048	0.018	0.007
10		0.973	0.641	0.841	0.955
20			0.971	0.998	1.000
30				0.999	0.984
40					0.999

One way ANOVA clearly shows that the halogen heat lamp treated samples behaved differently from the untreated WPC samples in their adhesion ability. All the treated samples had a reduced bond strength. The halogen heating lamp treatment did not appear to have any positive effect on bond strength. None of the treated samples broke in the material during shear strength evaluation. There is no indication which treatment speed provides better or worst bonding strength, because of high variance in the data.

4.1.6 ADHESION STRENGTH RESULTS SUMMARY

The shear strength results showed adhesion strength improvements for all treatments as compared to the controls except the halogen heating lamps, which gave lowered adhesion strength. The optimal treatment for each type of surface activation (hydrogen peroxide, hot air gun and flame) gave similar mean results. In some instances where high increases in bond shear strength occurred, appreciable numbers of failures occurred within the material. Those values were excluded from the determination of the mean values as mentioned in the methods chapter. However the material failure could be an indication of the efficient bonding as the adhered bond was stronger than the material itself. The highest adhesion strength mean value was observed at the samples treated twice with hot air at the speed of 75 mm s^{-1} followed by the flame treated samples at the speed of 175 mm s^{-1} and finally the samples treated in hydrogen peroxide solution at pH 7.5.

4.2 SURFACE CHARACTERIZATION

The mechanical, physical and the chemical properties of the surface are very important factors for adhesion. The surface morphology is allows the resin to lock into the surfaces resulting in good mechanical bonds for adhesion. Also chemical alteration at the surfaces can enhance the adhesive bonding. Thus to the material surface was characterized, by surface roughness determination test, contact angle and surface energy measurements, light and scanning electron microscopy (SEM) observation and chemical analysis by FTIR spectroscopy. The surface roughness and the SEM, could provide information about the mechanical factors that might be responsible for any change of the adhesion strength after the pre-treatments. Additionally the chemical alteration, caused by surface pre-treatments and be related to the adhesion strength, might be revealed by the contact angle measurements and FTIR spectroscopy.

4.2.1 CONTROL SAMPLES

Because of the limited deviation of the surface roughness results within treatments only two samples of every treatment were used. Each sample was tested twice at diagonally opposing directions. The surface roughness is presented as Ra values. The Ra is the average height, between the peaks and the troughs, of the tested surface and is presented in μm.

4.2.1.1 Surface roughness determination results

The untreated samples were subjected to surface roughness test, after they were washed with deionised water and placed in a conditioning room at 20 °C and 65% R.H until

weight stabilization. The untreated WPC had surface roughness mean of 2.30 μm. The values ranged from 2.08 μm to 2.80 μm (SD= 0.34). The 95% CI boundaries ware vary from 1.76 μm to 2.84 μm.

4.2.1.2 Scanning Electron Microscopy (SEM) observation

For the SEM observation two untreated samples were used. The untreated samples under X134 magnification (X100 equipment indication) seemed to have rough surfaces and the wood particles were not clearly visible (Figure 4.6a).

Figure 4.6b shows the surface under secondary electron scanning. The lighter colour indicates the presence of oxygen, which is predominantly in the wood particles. The darker area is the polypropylene on the surface. The white spots are points on the surface that were not completely covered with carbon during the sample preparation and charged under the electron beam. There are damaged wood particles on the surface which could have been formed by the sanding operation. The wood particles in general seem to be in good condition, except for the edges, which are ravelled. The same observation is also visible at the Figure 4.7 which show that the wood particles edges have been degraded.

a) b)

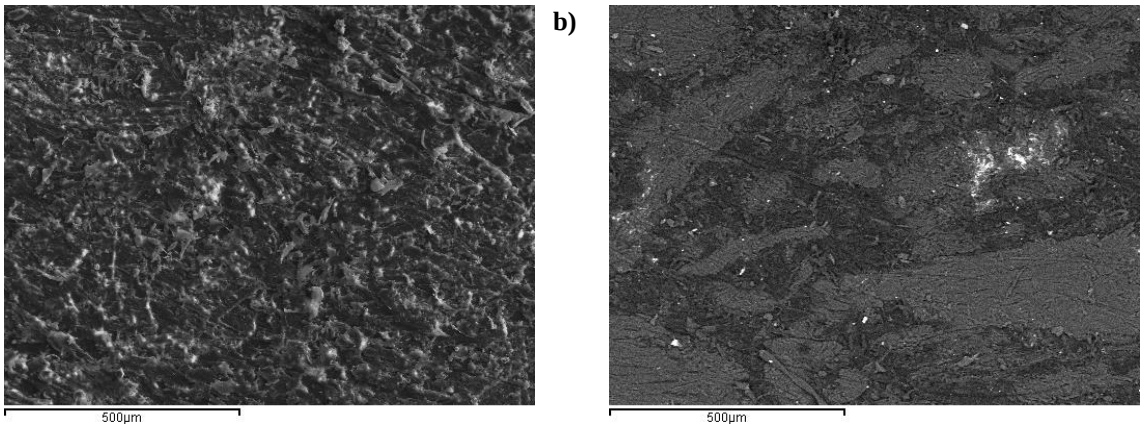

Figure 4.6: Control sample under X134 magnification (X100 equipment indication). a) photo is showing the surface under SEM primary electron scanning. b) photo shows control sample under secondary electron scanning. The photos are from the same region.

a) b)

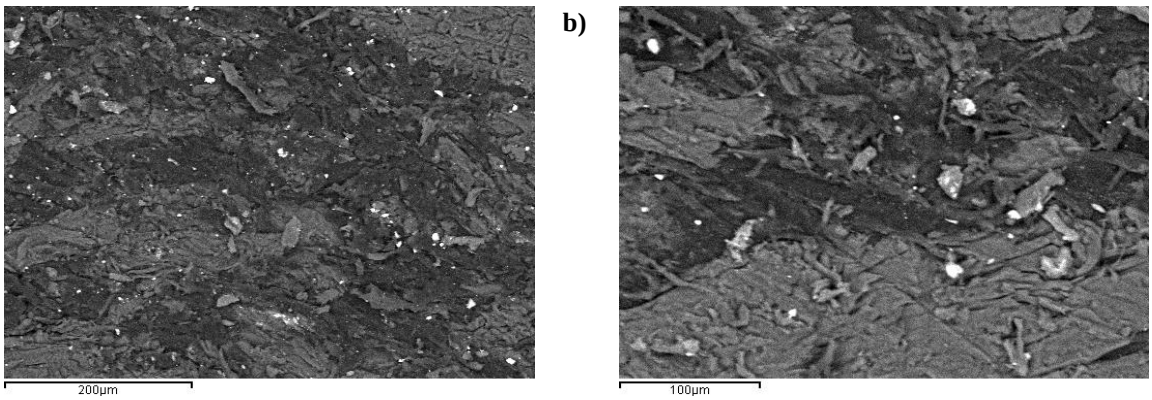

Figure 4.7: Secondary electron scanning microscopy untreated WPC photo under X265 magnification (X200 equipment indication) a) and under X400 magnification (X300 equipment indication) b)

4.2.1.3 Contact angle and surface energy determination

Two samples of untreated WPC were used to determine contact angle. Five sessile drops of deionised water were used on each sample. The surface energy was determined by the equation of state method (EOS). The untreated WPC had surface energy mean of 14.76 mN m^{-1}. The values ranged from 11.30 mN m^{-1} to 16.05 mN m^{-1} and the standard deviation was 1.50. The 95% CI boundaries varied from 13.68 mN m^{-1} to 15.83 mN m^{-1}.

4.2.1.4 FTIR ATR spectroscopy

FTIR-ATR spectroscopy was performed on the WPC sample surfaces. From every sample, 5 spectra were taken (wavenumber 400 – 4000 cm^{-1}), and by them an average spectrum was produced.

The WPC which was used in this study was produced from spruce and polypropylene. The PP, spruce and WPC spectra are presented in Figure 4.8. The spectra of the PP sample had some characteristic peaks. The peaks of the PP spectra which were observed between the

wavenumbers of 2800 cm^{-1} and 3000 cm^{-1} (2947cm^{-1}, 2915cm^{-1}, 2863cm^{-1} and 2834 cm^{-1} which are the CH_3, CH_2 asymmetric stretch and CH_3, CH_2 symmetric stretch respectively), and of 1300 cm^{-1} and 1500 cm^{-1} (1450 cm^{-1} and 1375 cm^{-1} which are CH_3 asymmetric bend and CH_3 in phase "umbrella" bend respectively) mainly refer to the CH geometry of the polymeric chain. The peaks between the wave numbers of 800 cm^{-1} and 1300 cm^{-1} refer to the regularity bands of the PP.

On the other hand, the peaks which occur in the WPC spectrum, observed between 2800 cm^{-1} and 3500 cm^{-1}, and of 800 cm^{-1} and 1200 cm^{-1} clearly relate to the wood, and in particular to the cellulose component of this. These are the most characteristic peaks of the spruce spectra. The rest of the main peaks are presented in Table 4.11.

In Figure 4.8, the WPC spectra, is a combination of the PP and the spruce spectra. The most characteristic peaks of the PP and the spruce spectra appear on the WPC spectra.

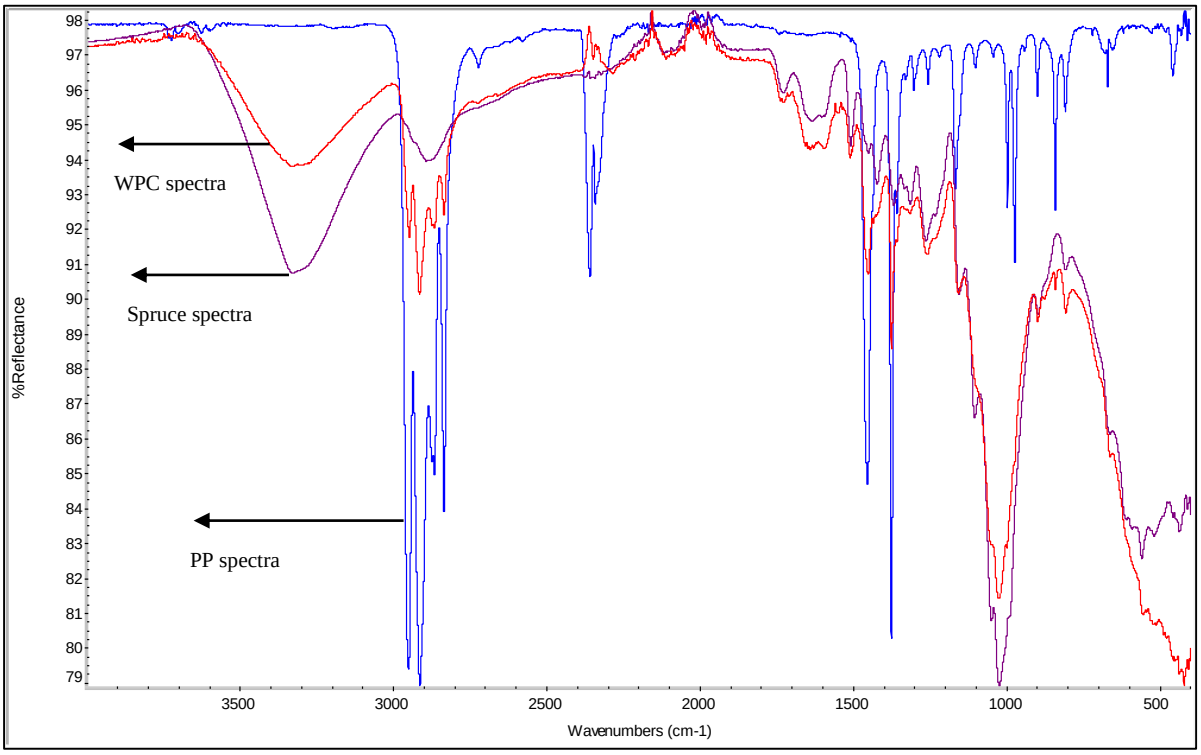

Figure 4.8: Spectra of WPC, PP and spruce samples.

Table 4.11: FTIR wavenumbers of lignocellulosic materials (Bykov 2008, Jaaskelainen et al 2003, Liu et al 2006 and Sun et al 2004).

Wavenumbers cm^{-1}	Indicative of
677	CELLULOSE
782	α-linkage α-pyranoside
897	CELLULOSE C-O-C stretching of glycosidic link
903	β-anomers β-glycosidic linkages
1030	CELLULOSE C-C stretching and C-O stretching of C_6
1049	Glycosidic linkage in XYLAN
1064	CELLULOSE C-O stretching at C_3
1106	CELLULOSE
1168	CELLULOSE C-O-C stretching of glycosidic link
1208	C-O-H in plane bending at C_6
1223	LIGNIN
1273	LIGNIN
1341	C-H and OH
1378	CELLULOSE CH bending
1427	CELLULOSE C-H and OH
1430	LIGNIN aromatic ring vibration
1433-1460	CH_2 bend
1467	LIGNIN CH_2 and HEMICELLULOSE pyran ring
1520	LIGNIN aromatic ring vibration
1600	LIGNIN aromatic ring vibration
1635	Absorbed water
1656	LIGNIN carbonyl stretch
1708	LIGNIN carbonyl stretch
1730-1740	Ester carbonyl
2913-2936	CELLULOSE OH stretching
3417-3436	CELLULOSE CH stretching

The most interesting peaks which were investigated are presented in Figure 4.9. To monitor the potential changes that might occur due to the treatments, the peak heights had to be measured. The peak heights were measured from a base line drawn between two points on the spectrum at wavenumbers of 3656 cm^{-1} and 1900 cm^{-1}. These two points were considered as stable in every sample, even after the treatments. Moreover, to ensure that the height differences of the tested samples would be at the same scale a specific ratio was used. This ratio was calculated by dividing the absorption band with the band of 2833 cm^{-1} wavenumber, which was used as a reference band.

$$\text{Ratio: Ar} = \frac{A_{peak}}{A_{2833}} \quad \textbf{[4.1]}$$

The band of the 2833 cm^{-1} is the CH_2 symmetrical stretch in the polypropylene spectrum, and therefore is considerably stable because for every polypropylene monomer there is a CH_2 unit. The peak height ratios of the untreated sample is presented in

Table 4.12. These ratios were used as control values and compared with the ratios of the treated samples to monitor the chemical changes, due to the treatment methods. In order to

have a clearer view of the changes the percentage of each ratio was calculated according the following equation:

$$Ar\% = \frac{Ar - Arcontrol}{Arcontrol} * 100\% \quad \textbf{[4.2]}$$

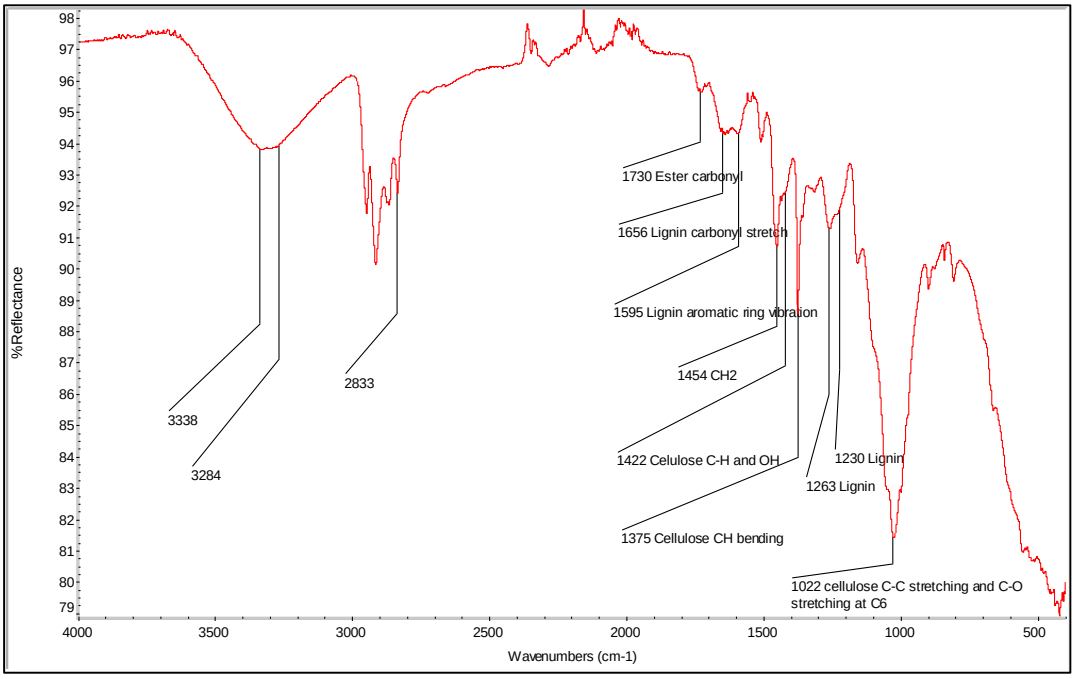

Figure 4.9: Average spectrum for untreated WPC sample, with labels showing the peaks investigated and reference peak at 2833 cm^{-1}.

Table 4.12: FTIR ATR peaks height A_{bs}/A_{2833} ratio of the untreated samples.

Wavenumber cm^{-1}	A_{bs}:A_{2833}
3338	0.80
3284	0.78
1732	0.25
1656	0.55
1595	0.55
1454	1.34
1422	0.97
1375	1.83
1263	1.20
1230	1.10
1022	3.40

4.2.2 EFFECT OF PH ON HYDROGEN PEROXIDE TREATED SAMPLES

4.2.2.1 Surface roughness determination results

The surface roughness of samples treated in the hydrogen peroxide solution at 8 different pH values was determined and the and the values were compared with the untreated samples. The surface roughness values are presented for each treatment pH in Figure 4.10.

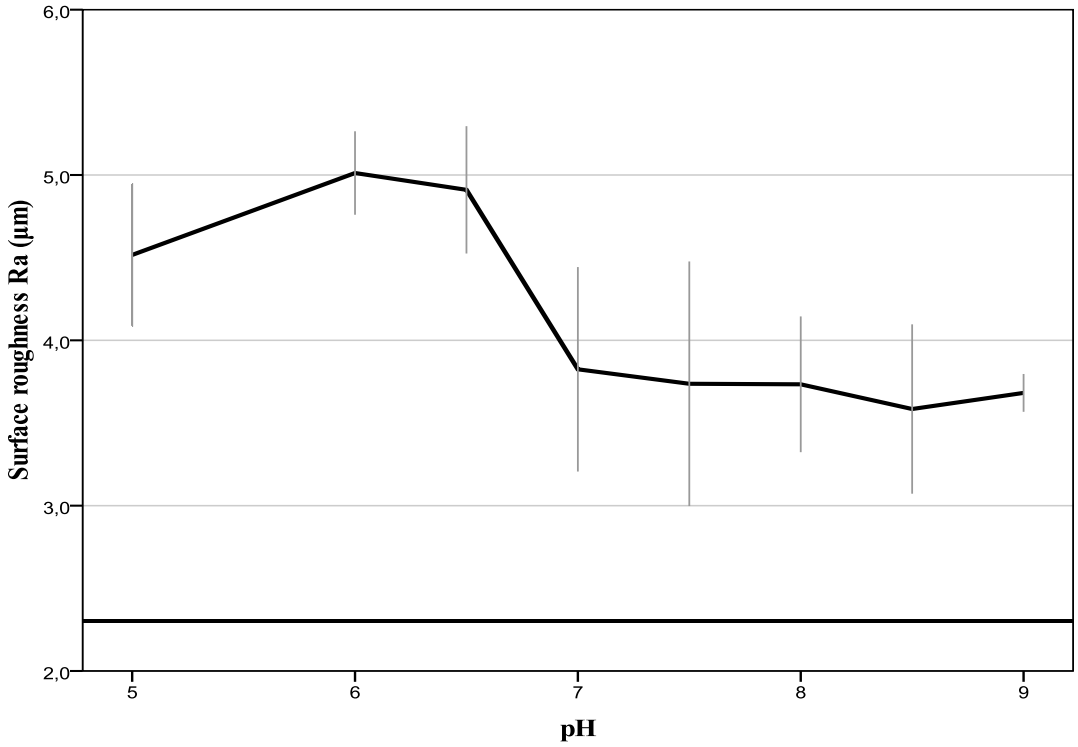

Figure 4.10: Hydrogen peroxide treatment surface mean roughness (µm) The flat line represent the control value (2.3 µm). Error bars represent the SD (+/-1).

The homogeneity of variance according the Levene test was not statistically significant, therefore the null hypothesis could not be eliminated (Peroxide treatment surface roughness Levene statistic=1.663, p= 0.154).

The descriptive statistics for the hydrogen peroxide treatment surface roughness are presented in Table 4.13 and shows that the sample roughness mean values differed from 3.58 µm (pH 8.5) to 5.01 µm (pH 6). The smallest standard deviation was observed in the samples treated at pH 9 (SD=0.11) and the highest at samples treated in pH 7.5 (SD=0.74).

Table 4.13: Surface roughness mean values of hydrogen peroxide treatment in µm. Standard Deviation (SD), Minimum and maximum values and the boundaries of the 95% CI.

Treatment pH		control	5	6	6.5	7	7.5	8	8.5	9
Average		2.30	4.52	5.01	4.91	3.82	3.74	3.73	3.58	3.68
Min		2.08	4.19	4.76	4.54	3.00	3.08	3.44	3.11	3.52
Max		2.80	5.11	5.27	5.32	4.32	4.77	4.34	4.09	3.77
95% CI	Lower Bound	1.76	3.83	4.61	4.30	2.84	2.56	3.08	2.77	3.50
	Upper Bound	2.84	5.20	5.41	5.52	4.81	4.91	4.39	4.40	3.86
SD		0.34	0.43	0.25	0.39	0.62	0.74	0.41	0.51	0.11

All treatments gave increased surface roughness in comparison to the control. Samples treated with acidic hydrogen peroxide solutions, produced the roughest surfaces (Figure 4.10). At alkaline and neutral pH values the surface roughness is also greater than the control but is clearly lower than the samples treated with acidic solutions.

The F-test revealed that the hydrogen peroxide solution pH is statistically significantly related to WPC surface roughness as F=12,913 for significant level $p<0.001$. Therefore the null hypothesis could be eliminated.

To investigate the differences between the treatment variances the Post-Hoc HSD multiple comparisons test was used. The statistically significant differences between pH solutions roughness are presented in Table 4.14.

Table 4.14: Hydrogen peroxide treatment surface treatment multiple comparison test results (p values). Statistical significant differences for p<0.05. Values with fainter text are >0.05.

Treatment pH	5	6	6.5	7	7.5	8	8.5	9
control	0.000	0.000	0.000	0.002	0.004	0.004	0.012	0.006
5		0.831	0.946	0.470	0.319	0.314	0.138	0.241
6			1.000	0.025	0.013	0.013	0.004	0.009
6.5				0.051	0.028	0.027	0.009	0.018
7					1.000	1.000	0.998	1.000
7.5						1.000	1.000	1.000
8							1.000	1.000
8.5								1.000

All treated samples were statistically significant different to the control samples at least $p<0.05$ or better. The samples treated in pH 6 and pH 6.5 solutions were statistically significant different to the rest of the treated samples. Although the pH 6 values gave the highest roughness values, they were similar to those of the pH 6.5 values and were not significantly different, even at $p>0.05$. Even though there were not any statistically significant difference between the samples treated in pH 6 and pH 6.5 solution, pH 6 treated samples were statistically significant difference with the samples treated in pH 7 solution ($p<0.05$) while the samples treated in pH 6.5 solution were not statistically significant difference with pH 7 treated samples. Thus the samples treated in pH 6 solution might have slightly greater surface roughness.

One way ANOVA shows that all samples treated with hydrogen peroxide solutions were statistically significant and had rougher surfaces than the control. Although pH 5, pH 6 and pH 6.5 solutions seemed to have a rougher surface than the samples treated with the rest of the solutions, according to Tukey HSD multiple comparisons, pH 5 does not clearly produce a rougher surface than the samples treated with other H_2O_2 solutions. Samples treated with pH 6 solution did differ significantly from all the samples treated with the other

solutions, with an exception of pH 5 and pH 6.5. Therefore the pH 5 seemed to have a slightly rougher surface from the samples treated in pH 7 and higher but still less rough than the samples treated in pH 6 and pH 6.5 solutions.

4.2.2.2 Scanning Electron Microscopy (SEM) observation

For the SEM observation two samples of two selected parameters for every treatment were used. The treatment parameters which provide the best and the lowest adhesion results were chosen to be studied, in order to observe any possible difference in the material surfaces that could provide an explanation in terms of surface morphology and adhesive bond formation.

In the samples treated with hydrogen peroxide solution at pH 9 the wood particles were more readily visible than in the control (Figure 4.11 and Figure 4.12). This observation was in good agreement with observation by eye. The surface becomes smoother, but according to the roughness test the hydrogen peroxide treatment actually produces a rougher surface (Figure 4.10). The wood particles have internal cracks and show regions of separation from the polypropylene after the hydrogen peroxide treatment. Figure 4.11 and Figure 4.12 clearly show that the wood particles are degraded. As will be discussed later, this may be from a swelling effect caused by the swelling solvent and subsequent shrinkage after reconditioning. This might be the reason that the surface is rougher after treatment.

In Figure 4.13 the wood particle separation from the polymer is more visible under higher magnification. The wood particle in Figure 4.13a is surrounded by a gap which is more visible (Figure 4.13b). There are also some cracks visible within this partially detached wood particle, and the rest of the wood particles are to be scuffed, most probably by sanding. Figure 4.14 shows a wood particle which is more damaged than in Figure 4.13 while in Figure 4.14 has a bigger crack along its length and some fibrillation. There are also small detached wood pieces scattered around the edges and around the WPC surface which indicates the damage which has been caused on the surface by the hydrogen peroxide treatment.

The Figure 4.15, Figure 4.16 and Figure 4.17 show the wood particles condition under higher magnification (X400). The wood degradation is very visible. All wood particles are seriously damaged, and the fibres contained within the particles seem to be separated from each other. This is particularly true were the particle orientation presents the transverse view of fibres, as in Figure 4.16. The wood particles appear to be losing their consistency. In Figure 4.16 and Figure 4.17 the damaged wood particle surfaces are more intense and clearly visible.

Figure 4.18 shows a formation of the crystalline material on the surface under X67 magnification (X50 equipment indication) just as was observed by the light microscopy which will be discussed later in chapter 4.3.2.1, however during SEM there no crystalline formations were observed. However it could also be a fragmented tissue fibre. The samples which were rinsed with deionised water did not differ from the samples that were not washed with water.

a) **b)**

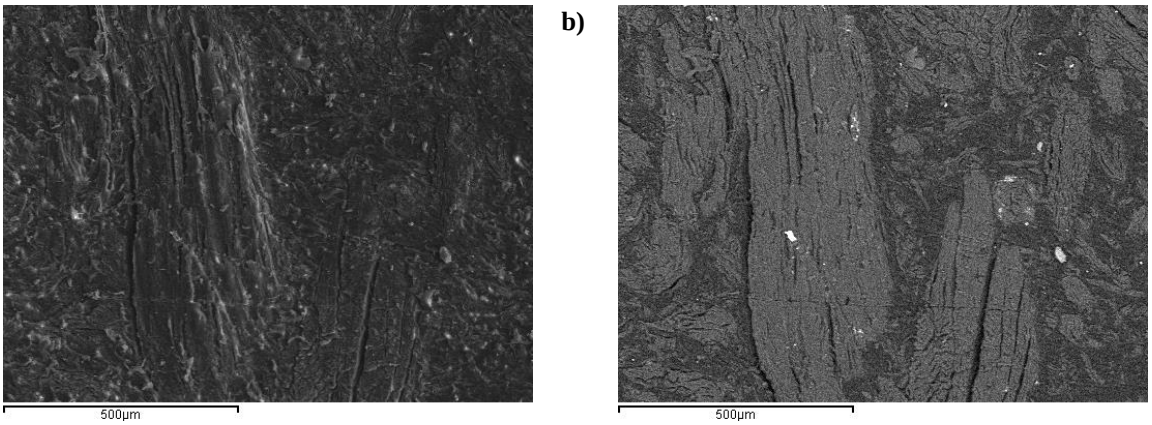

Figure 4.11: pH 9 solution treated sample under X134 magnification (X100 equipment indication). a) photo is showing the surface under SEM backscattered electron image. b) photo shows a secondary electron image of the same region

a) **b)**

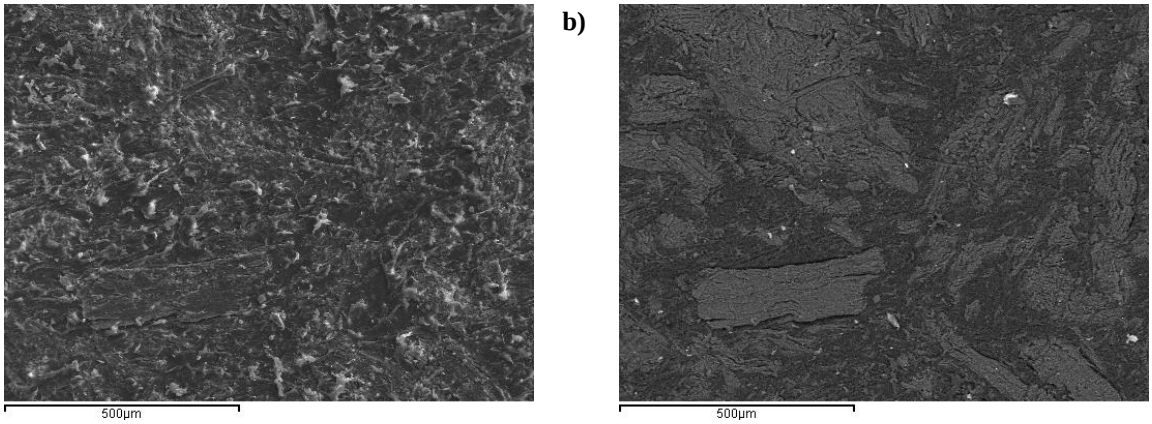

Figure 4.12: pH 9 solution treated sample under X134 magnification (X100 equipment indication). a) photo is showing the surface under SEM backscattered electron image. b) shows a secondary electron image of the same region.

a) b)

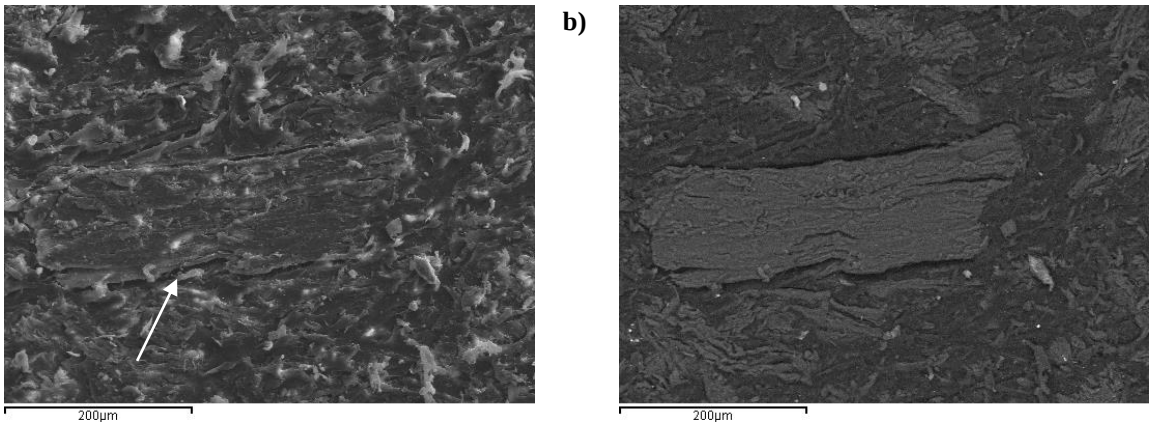

Figure 4.13: pH 9 solution treated sample under X265 magnification (X200 equipment indication), detail of Figure 4.19. a) Backscattered image of the surface. b) same region seen as a secondary electron image. The arrow in photo a) shows the separation of wood fibre and from PP

a) b)

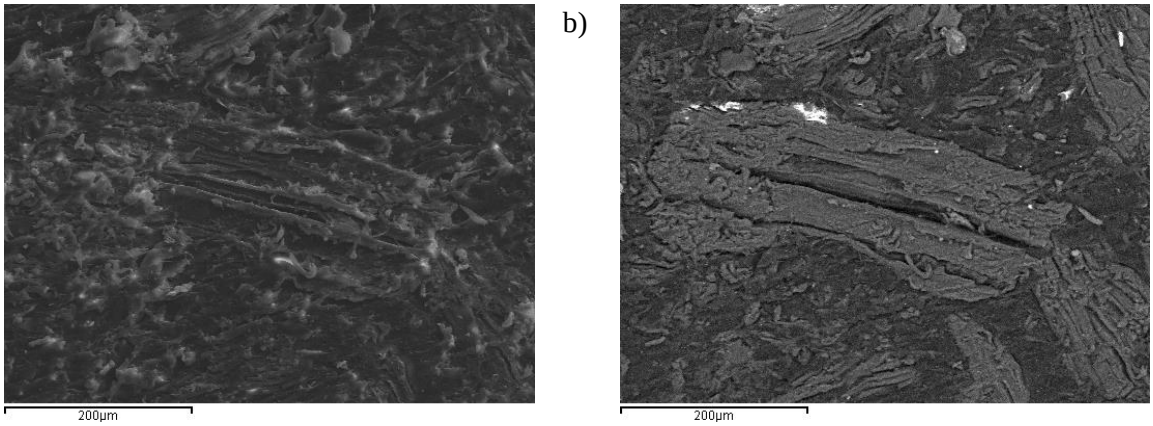

Figure 4.14: pH 9 solution treated sample under X265 magnification (X200 equipment indication). a) Backscattered image of the surface. b) same region seen as a secondary electron image.

a) **b)**

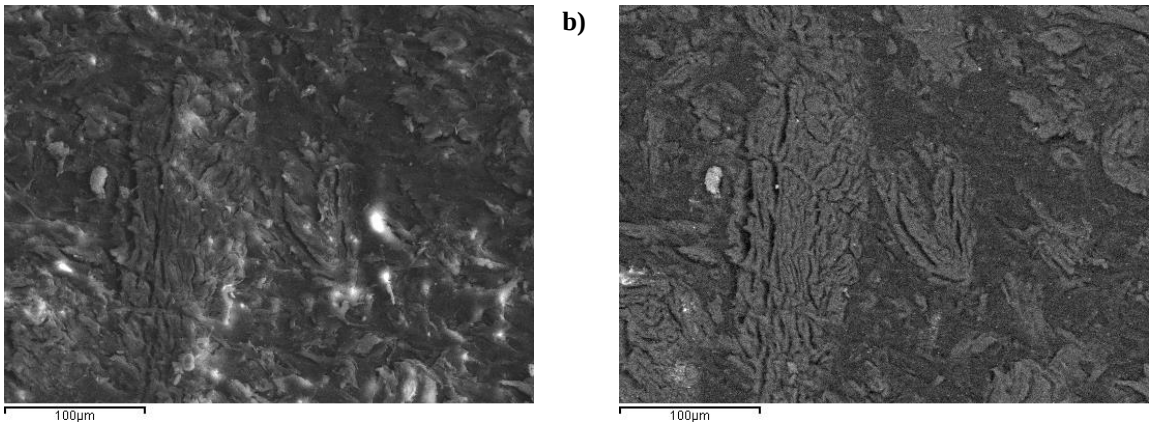

Figure 4.15: pH 9 solution treated sample under X400 magnification (X300 equipment indication). a) Backscattered image of the surface. b) same region seen as a secondary electron image.

a) **b)**

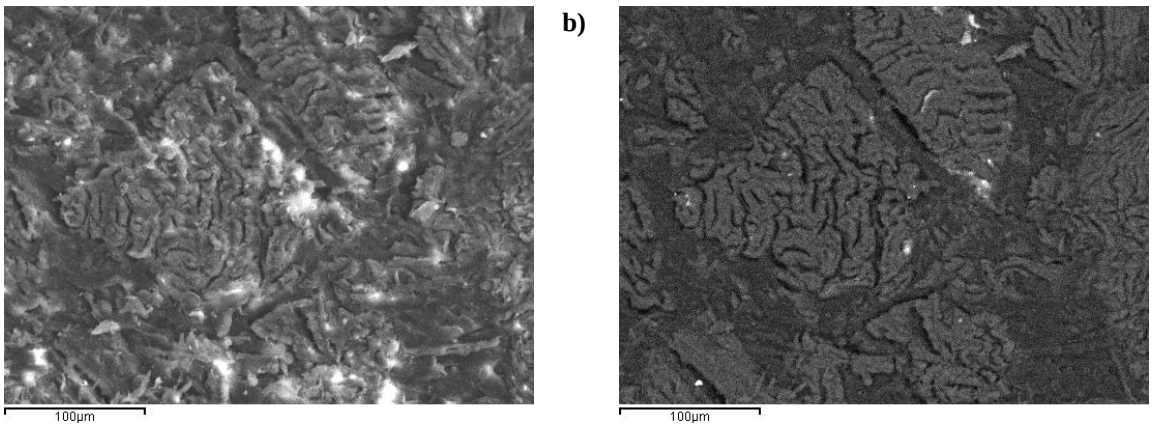

Figure 4.16: pH 9 solution treated sample under X400 magnification (X300 equipment indication). a) Backscattered image of the surface. b) same region seen as a secondary electron image.

a) b)

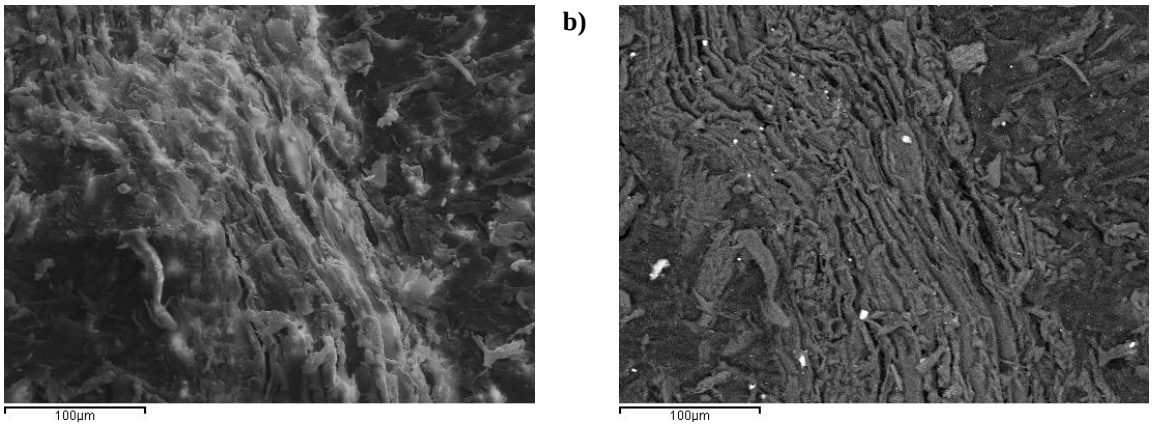

Figure 4.17: pH 9 solution treated sample under X400 magnification (X300 equipment indication). a) Backscattered image of the surface. b) same region seen as a secondary electron image.

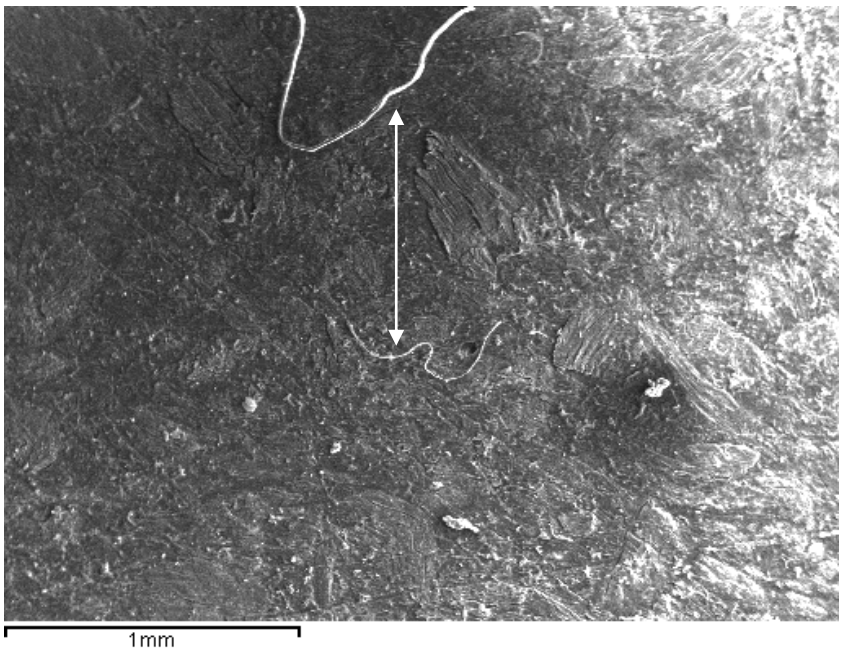

Figure 4.18: pH 9 solution treated sample under X67 magnification (X50 equipment indication) on SEM. The arrows points the appearance of crystalline material.

The samples treated with hydrogen peroxide solution at pH 7.5 did not appear to have any significant differences from the samples treated with pH 9. Figure 4.19, Figure 4.20 and Figure 4.21, all under X134 magnification, show that the surface seems slightly smoother than the samples treated with pH 9 solution. In Figure 4.19 the wood particles seem to have separated from the polymer matrix just as in samples treated with pH 9 solution. The wood degradation in the form of cracks and separation is also visible in Figure 4.19 to Figure 4.21, and it is more clearly visible at higher magnifications (Figure 4.22, Figure 4.23-Figure 4.25). In Figure 4.26 shows extensive internal cracking within an individual wood particle.

Consequently there are no visible difference between pH 9 and pH 7.5 treated samples that could be explaining the different adhesion behaviour, i.e. pH 7.5 shear strength mean 759.59 N and pH 9 564.40 N. The shear strength mean of the pH 9 samples was similar to that of the control (554.7 N).

a) **b)**

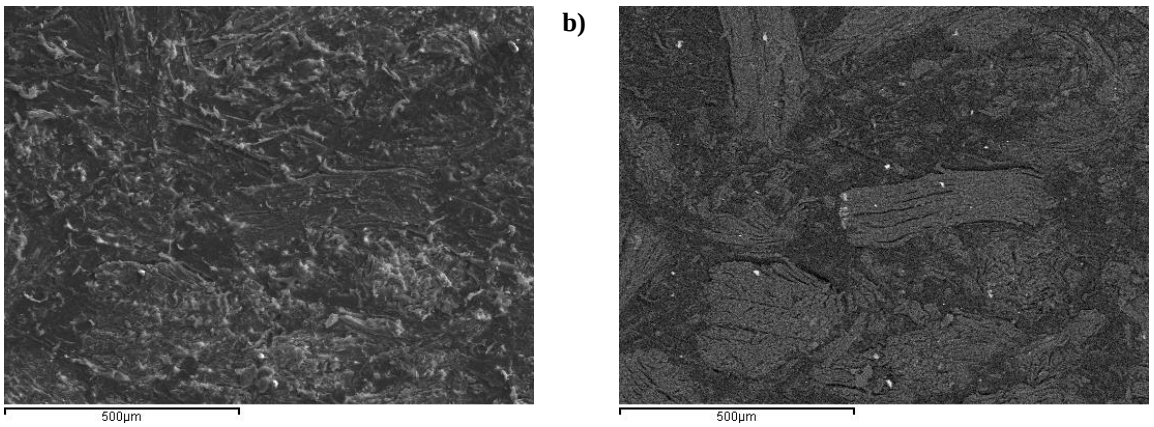

Figure 4.19: pH 7.5 solution treated sample under X134 magnification (X100 equipment indication). a) Backscattered image of the surface. b) same region seen as a secondary electron image.

a) **b)**

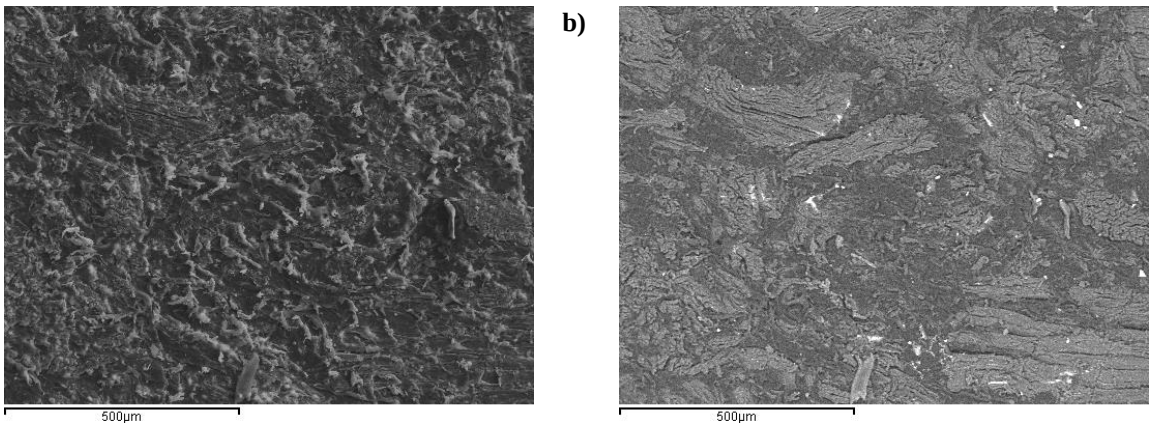

Figure 4.20: pH 7.5 solution treated sample under X134 magnification (X100 equipment indication). a) Backscattered image of the surface. b) same region seen as a secondary electron image.

a) b)

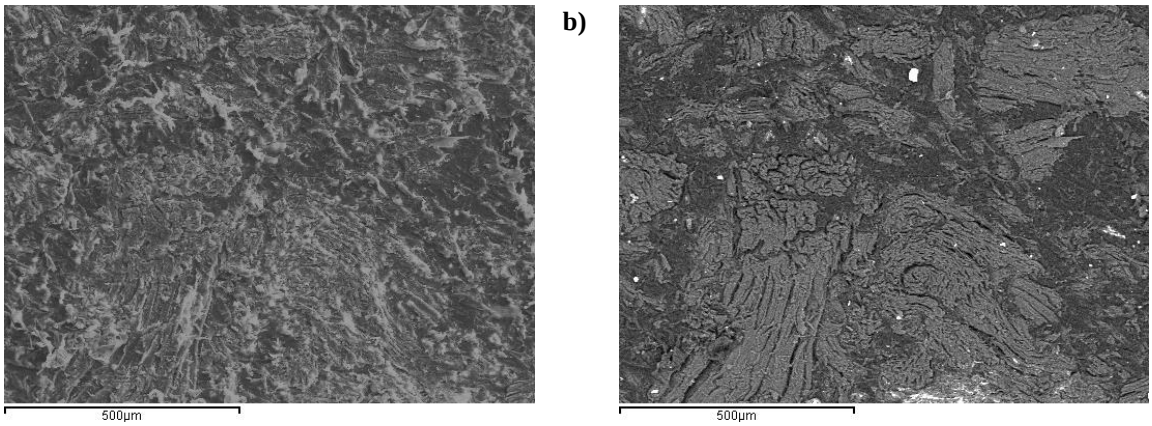

Figure 4.21: pH 7.5 solution treated sample under X134 magnification (X100 equipment indication). a) Backscattered image of the surface. b) same region seen as a secondary electron image.

a) b)

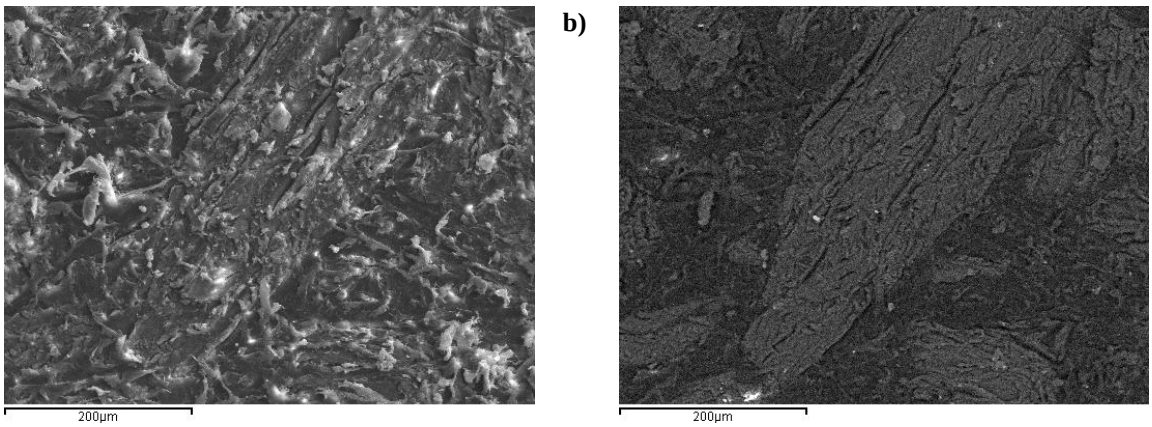

Figure 4.22: pH 7.5 solution treated sample under X265 magnification (X200 equipment indication). a) Backscattered image of the surface. b) same region seen as a secondary electron image.

a) b)

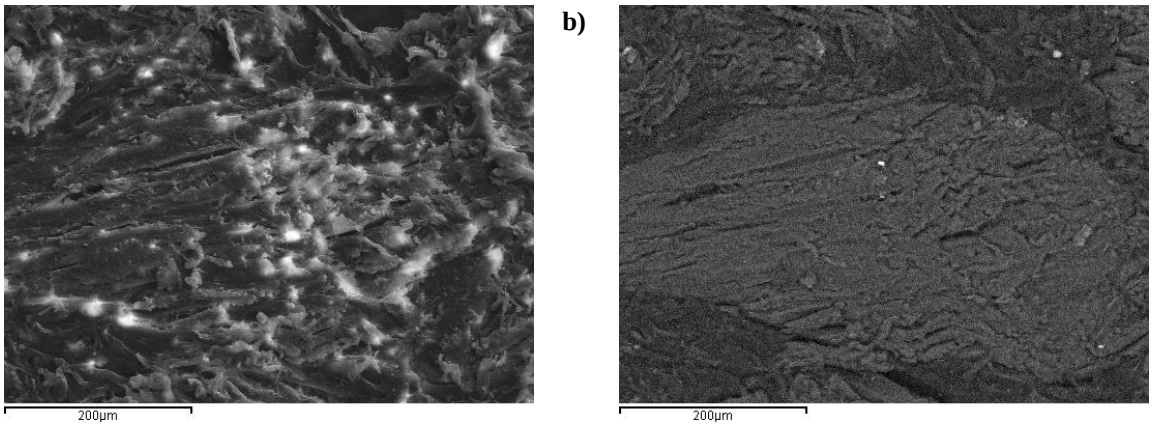

Figure 4.23: pH 7.5 solution treated sample under X265 magnification (X200 equipment indication). a) Backscattered image of the surface. b) same region seen as a secondary electron image.

a) b)

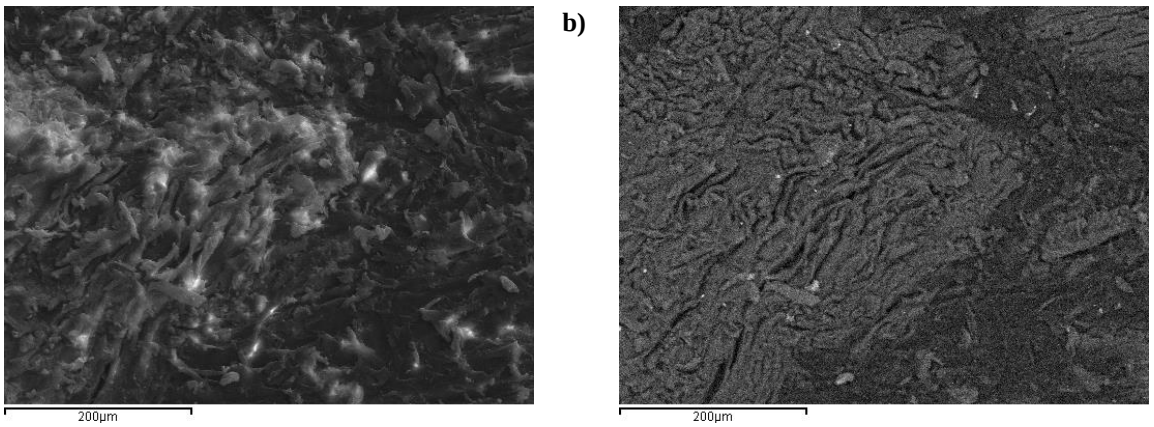

Figure 4.24: pH 7.5 solution treated sample under X265 magnification (X200 equipment indication). a) Backscattered image of the surface. b) same region seen as a secondary electron image.

a) b)

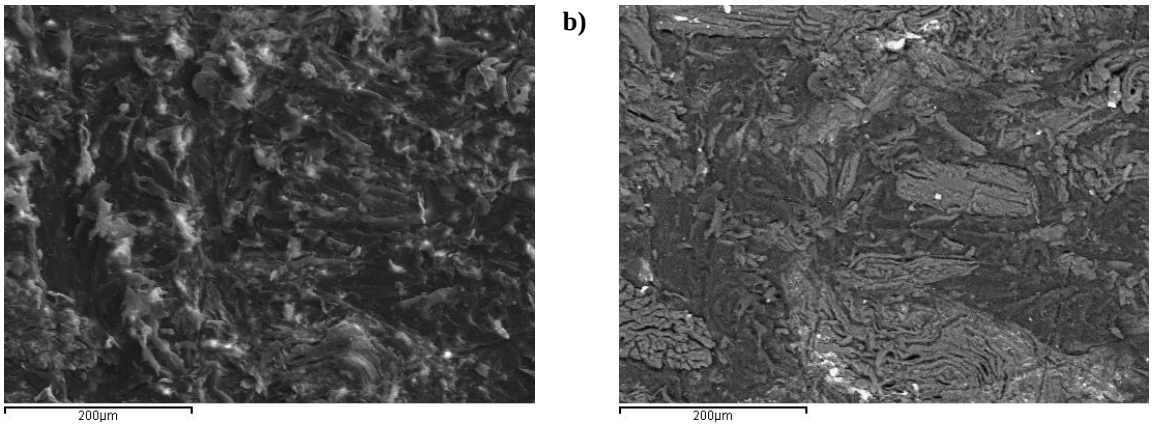

Figure 4.25: pH 7.5 solution treated sample under X265 magnification (X200 equipment indication). a) Backscattered image of the surface. b) same region seen as a secondary electron image.

a) b)

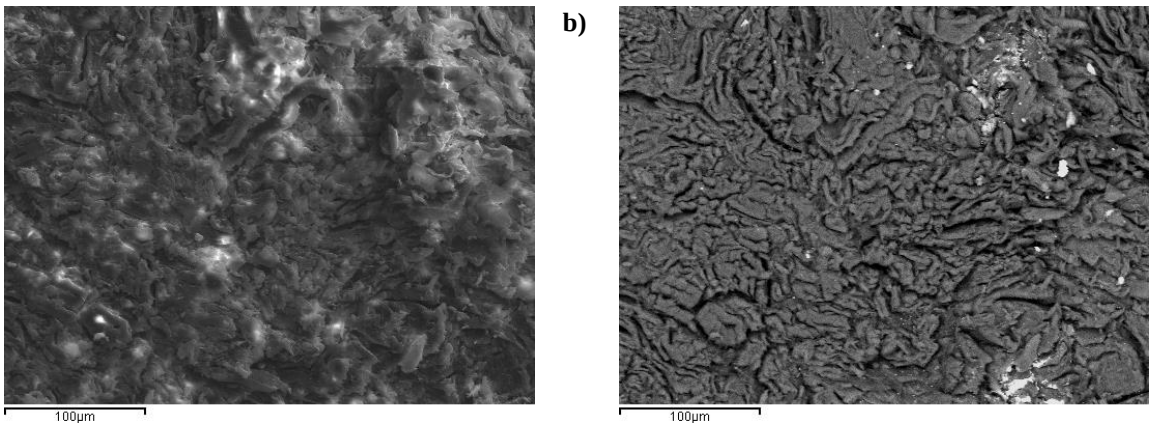

Figure 4.26: pH 7.5 solution treated sample under X400 magnification (X300 equipment indication). a) Backscattered image of the surface. b) same region seen as a secondary electron image.

4.2.2.3 Contact angle and surface energy determination

The hydrogen peroxide treated samples were subjected to surface energy determination test. The Levene test was not statistically significant, therefore the null hypothesis could not be eliminated (Peroxide treatment Levene statistic=0.32, p= 0.96) but one way ANOVA was done anyway. The surface energy results are presented in Figure 4.27.

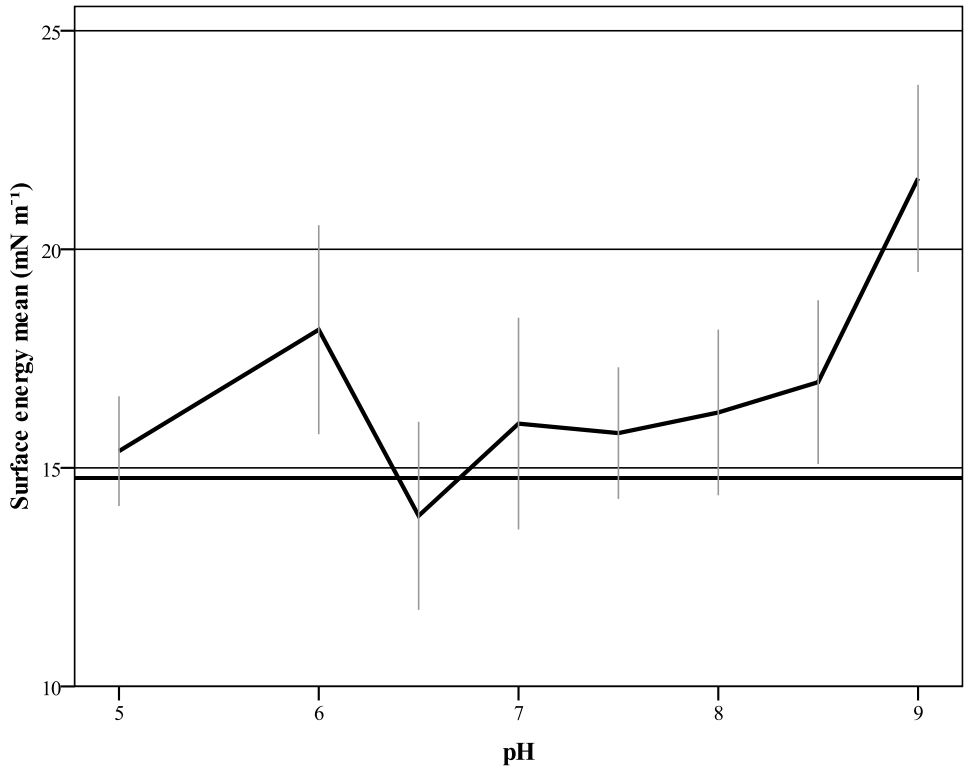

Figure 4.27: Effect of pH and hydrogen peroxide treatment on surface energy (mN m^{-1}). The flat line represent the control mean (14.76 mN m^{-1}). Error bars represent the SD (+/-1).

All treatments seemed to have a positive effect on WPC surface energy, with an exception of the pH 6.5 treatment, which was lower than the control. The samples treated in pH 6.5 and pH 9 solutions had the highest surface energy mean values, while the other treatment pH only had a minor effect.

The descriptive statistics of the pH effect on the hydrogen peroxide treatment method shown in Table 4.15.

Table 4.15: Mean values of surface energy for hydrogen peroxide treatment in mN m^{-1}. Standard Deviation (SD), Minimum and maximum values and the boundaries of the 95% CI of the surface energy

Treatment pH		Control	5	6	6.5	7	7.5	8	8.5	9
Average		14.76	15.38	18.16	13.90	16.01	15.80	16.27	16.96	21.62
Min		11.30	13.75	16.04	9.13	12.29	14.12	13.25	14.59	17.27
Max		16.05	17.81	24.72	16.21	21.13	18.55	20.01	20.16	24.62
95% CI	Lower Bound	13.68	14.48	16.45	12.36	14.28	14.72	14.91	15.62	20.09
	Upper Bound	15.83	16.28	19.87	15.44	17.74	16.87	17.62	18.30	23.15
SD		1.50	1.26	2.39	2.15	2.42	1.51	1.90	1.87	2.14

The sample means ranged from 13.90 mN m^{-1} (pH 6.5) to 21.62 mN m^{-1} (pH 9). The minimum standard deviation among the hydrogen treated samples was observed in the pH 5 samples (SD=1.26) and the maximum in the samples treated with pH7 solution (SD=2.42).

The F-test revealed that the hydrogen peroxide solution pH was statistically significantly related to WPC surface energy as F=13.576 for significance level $p<0.001$. Therefore the null hypothesis could be eliminated.

To investigate the differences between the treatment variances the Post-Hoc HSD multiple comparisons test was used. The statistically significant differences between pH solutions and surface energy are presented in Table 4.16.

Table 4.16: Effect of pH on hydrogen peroxide treatment multiple comparison test results (p values). Statistical significant differences for p<0.05. Values with fainter text are >0.05.

Treatment pH	5	6	6.5	7	7.5	8	8.5	9
Control	0.998	0.006	0.987	0.876	0.955	0.720	0.230	0.000
5		0.049	0.743	0.998	1.000	0.983	0.672	0.000
6			0.000	0.261	0.156	0.429	0.902	0.004
6.5				0.284	0.430	0.157	0.019	0.000
7					1.000	1.000	0.974	0.000
7.5						1.000	0.915	0.000
8							0.997	0.000
8.5								0.000

The only statistically significant difference between the treated samples and the untreated were the samples treated in pH 6 and pH 9 solutions for significance level $p<0.01$ and $p<0.001$ respectively. The samples treated in pH 9 solution, which had the highest surface energy, were statistically significantly different to all of the other treated samples, for a significance level of $p<0.001$ except of the samples treated in pH 6 solution which was

significantly different for $p<0.005$. Therefore it is clear that the pH 9 solution produces treated surface with the highest surface energy.

On the other hand the samples treated in pH 6.5 solution, which had the lowest surface energy and was significantly different to the samples with the highest surface energy (pH 6: $p<0.001$, pH 8.5: $p<0.05$ and pH 9: $p<0.001$).

One way ANOVA shows that the samples treated in pH 9 and pH 6 solutions had higher surface energy than the control. The samples treated in pH 9 solution, according to Tukey HSD multiple comparisons, had the highest surface energy. The pH 6 treated samples had the second highest surface energy. The samples treated in pH 6.5 solution seemed to have the lowest surface energy, but did not significantly produce surface energy lower than the control.

4.2.2.4 FTIR ATR spectroscopy

From each sample, five spectra were taken. The average of the 5 spectra (Figure 4.28) was used to measure the absorption band height ratio of each sample.

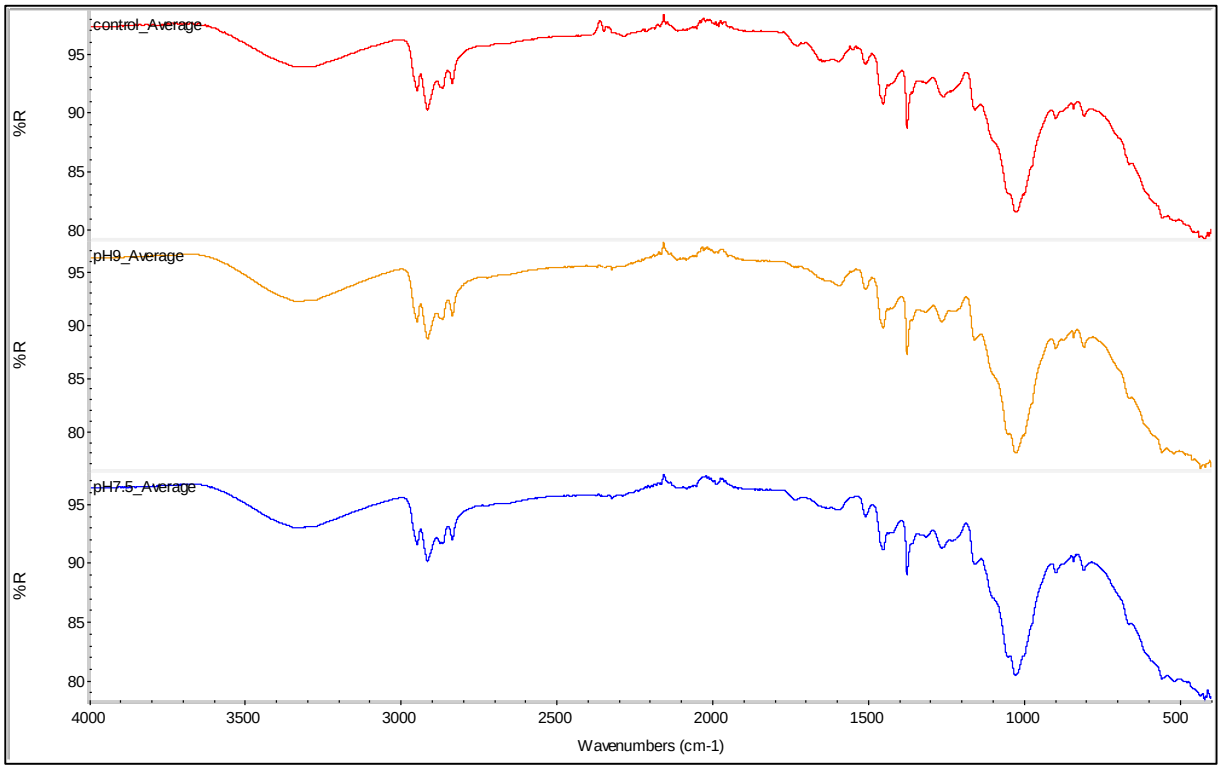

Figure 4.28: FTIR-ATR spectra of untreated samples and treated in pH 7.5 and pH 9 solution

The idea for the hydrogen peroxide treatment was that instead of forming free radicals by heat application or with expensive and complicated equipment like corona discharge, it could be better to simply provide those radicals directly to the material surface. The presence

of NaOH was used as a catalyst to the PP scission at relatively low temperatures (Gijsman et al 1995).

The percentages of the selected bands according to the equation 7 are presented in Table 4.17. The greatest differences occurred at the wavenumbers of 1732 cm^{-1}, 1656 cm^{-1} and 1595 cm^{-1} (Figure 4.29). The absorption band of 1732 cm^{-1} refers to ester carbonyls many of these are in hemicellulose. The absorbance at 1656 cm^{-1} refers to lignin carbonyl stretch and at 1595 cm^{-1} to lignin aromatic ring vibration.

Table 4.17: Peaks height percentages of the samples treated in hydrogen peroxide solutions

	Treatment pH							
Wavenumbers cm^{-1}	**5**	**6**	**6.5**	**7**	**7.5**	**8**	**8.5**	**9**
3338	-9%	16%	18%	-1%	8%	-4%	11%	5%
3284	-10%	15%	18%	-2%	6%	-6%	11%	4%
1732	-4%	15%	2%	-19%	-20%	-53%	-53%	-56%
1656	-33%	-21%	-19%	-35%	-39%	-47%	-35%	-41%
1595	-32%	-13%	-12%	-29%	-27%	-35%	-18%	-20%
1454	-11%	-7%	-5%	-13%	-11%	-14%	-10%	-11%
1422	-21%	-1%	0%	-14%	-12%	-21%	-8%	-12%
1375	-7%	-1%	-2%	-11%	-7%	-10%	-7%	-7%
1263	-13%	13%	10%	-10%	-4%	-16%	-4%	-10%
1230	-14%	11%	8%	-13%	-9%	-23%	-12%	-19%
1022	-9%	21%	17%	1%	8%	-7%	10%	1%

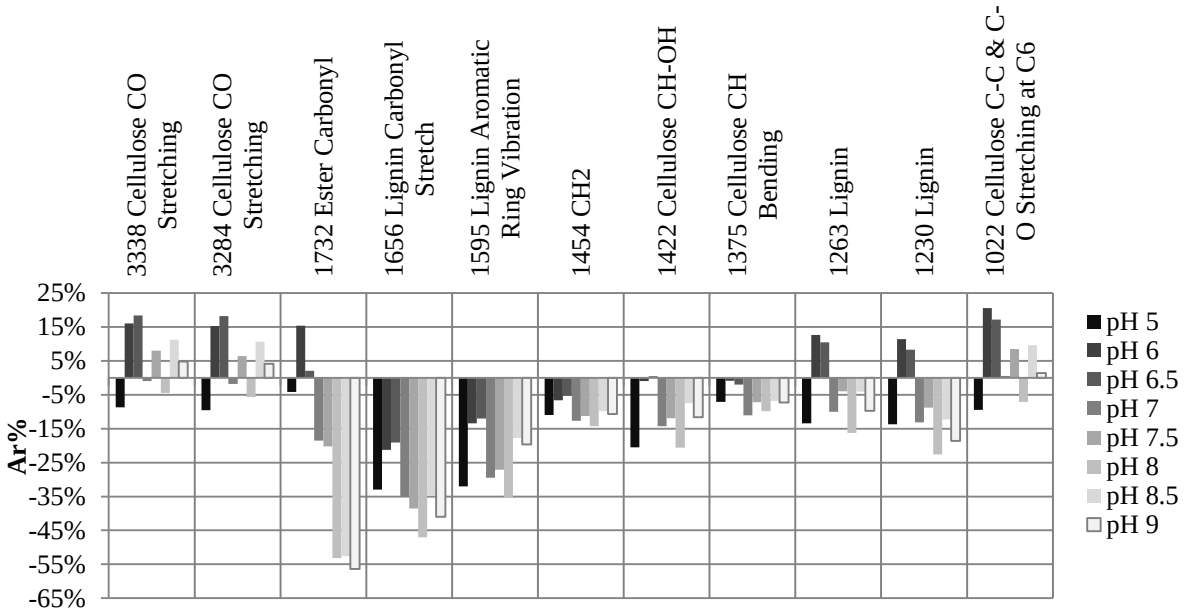

Figure 4.29: FTIR ATR ratio percentage of the hydrogen peroxide treated samples

By studying the peak heights percentages in Figure 4.29, it is possible to categorize the peaks trends into three similar groups. The first group includes the peaks of the 3338 cm^{-1} 3284 cm^{-1} and 1022 cm^{-1} wavenumber bands. Those three bands referred to the cellulose. The second group includes the 1732 cm^{-1} (hemicellulose), 1263 cm^{-1} and 1230 cm^{-1} wavenumber bands which relate to hemicellulose and lignin and the third group includes the wavenumber bands of 1656 cm^{-1} and 1595 cm^{-1} (lignin), 1454 cm^{-1} (CH_2 bend), 1422 cm^{-1} and 1375 cm^{-1} (cellulose) which relate to both the cellulose and the lignin.

Comparison of the wavenumber around 3400 cm^{-1}, Figure 4.8 (cellulose CO stretching), shows a flattening in the peroxide treated WPC spectrum and a slight shift to a lower wavenumber. The peaks at the 3338 cm^{-1} and 3284 cm^{-1} are the two edges of the flat peak. Both of these peaks heights of the samples treated in hydrogen peroxide solutions appeared to have the same trend. The samples treated in pH 5 and pH 8 had peaks height slightly lower (-1% to -9%) than the untreated samples with the samples treated at pH 7 and pH 9 do not present any genuine difference. Furthermore the at the 3338 cm^{-1}peak for pH 8 does not seem to be much different to the control with only a -4% value. The rest of the treated samples appeared to have higher peak heights than the control with the highest values for pH 6.5 (18%) and pH 6 (16%); the other values were lower (5 to 11%). pH 9 treated samples also do not seem to differ much from the untreated samples.

The same pattern is seen for the 1022 cm^{-1} peaks in treated WPC samples, as mentioned before. The peak at 1022 cm^{-1}, refers to the cellulose C-C stretching and C-O stretching at C_6. The highest percentages were 21% (pH 6) and 17% (pH 6.5). Lesser differences occurred for the other treatment solution pH values (pH 8.5: 10%, pH 7.5: 8%).

The second group relates to the esters in hemicellulose (1732 cm^{-1}) and the lignin. The ester carbonyl peak reduced substantially at all alkaline pHs. For the acidic solutions the peak increased substantially in pH 6 samples (15%) but the pH 5 and pH 6.5 samples were similar to the control values. The ester reduction though disagrees with Urbaniak-Domagala (2011), who showed that the esters increase on PP surfaces after hydrogen peroxide treatment. On the other hand Lu (2006) reported that the ester carbonyl peak of bamboo treated in acidic hydrogen peroxide (pH 4, pH 5 pH 6 and neutral pH 7) is slightly reduced, but increased in alkaline conditions (pH 8 and pH 9). At neutral and in alkaline pH values the level of the ester carbonyls reduction increased as the pH goes from the lowest to the highest value (-56% at pH 9). The pH 7 and the pH 7.5 had about the same vales (19% to 20%). Also the pH8, pH8.5 and pH9 were about the same values (-56% to -53%). The ester reduction strongly disagrees

to that which would be expected, i.e. the increase in the carbonyl group as a result of surface oxidation by the H_2O_2. However it is possible these esters (which are contained mostly in hemicellulose, less so in lignin and probably in some lignin polysaccharides covalent bonds) are reduced as a result of the alkaline NaOH. This agrees with the mechanism by which esters are easily cleaved in alkaline condition as mentioned by Sjostrom (1993). The NaOH action hypothesis is also supported by the observation that the ester ratio is decreased as the pH increases; to produce higher pH solutions more NaOH was added.

The peak at 1263 cm^{-1} band is not referred to by previous authors but is close to 1273 cm^{-1} band assigned to lignin (Table 4.11). This peak was reduced by variable amounts across much of the pH range, in the alkaline (-4% to -16%), neutral (-10%) and at the acidic (-13% to 13%) sample spectra. With the slightly acidic conditions the peak increased (pH 6 13%, pH 6.5 10%). However, the pH 8.5 and pH 7.5 do not seem to differ much from the untreated samples. Also the peak at the 1230 cm^{-1} most probably refers to lignin, as a 1223 cm^{-1} band has been assigned to lignin. The percentages trend was similar to the percentages for the 1263 cm^{-1} peak, with the difference that the pH 8.5 and pH 7.5 spectra are more clearly different from the untreated samples at 1230 cm^{-1}. The samples treated in neutral and alkaline solutions had percentage values below zero, ranging from -9% (pH 7.5) to -23% (pH 8). Conclusively, no trend was apparent with change in alkalinity, however the samples treated in acidic solutions at pH 6 and 6.5 showed increases while that at pH 5 showed a decrease.

The lignin carbonyl stretch at 1565 cm^{-1} was also substantially reduced, however under acidic conditions the lignin carbonyl stretch decrease was less (i.e. -19 to -33%) than under neutral (-35%) or alkaline conditions (-35 to -47%). The lignin aromatic ring vibration (wavenumber 1595 cm^{-1}) had almost the same reduction behaviour with pH change as the lignin carbonyl stretch, but was proportionately less.

The peak at the band of 1454 cm^{-1} wavenumber refer to CH_2 groups; this was reduced in all treatments. The CH_2 percentages had the same trend to the peak of the lignin aromatic ring vibration but to a lesser impact. The highest percentage for the CH_2 peaks was -5% (pH 6.5) and the lowest -14% (pH 8). Also the peak of the 1422 cm^{-1} refers to the CH-OH of the cellulose and it had similar trend as observed in the peak at 1454 cm^{-1} with the difference that the pH 6 and pH 6.5 were not significant different from the control. The peak of the CH-OH of the cellulose of all the treated samples except of the samples treated in pH 6 and pH 6.5 was clearly lower than the untreated samples. It was expected that the OH of the

cellulose would be increased, due to the oxidation, but it was not confirmed by the FTIR results. Also the CH bending (1375 cm^{-1}) had the same trend with the 1454 cm^{-1} and 1422 cm s^{-1} wavenumber peaks. All pHs were lower than the control values except of the pH 6 and pH 6.5 which were not significant changed. All the treated samples had about the same values (-11% to -7%).

4.2.3 HOT AIR TREATMENT

4.2.3.1 Surface roughness determination results

The surface roughness values of the hot air treated samples was compared to the untreated samples for homogeneity of variance and found to be significant (Hot air treatment Levene statistic=2.923, p=0.017). Therefore the null hypothesis could be eliminated. The hot air surface roughness results are presented in Figure 4.30.

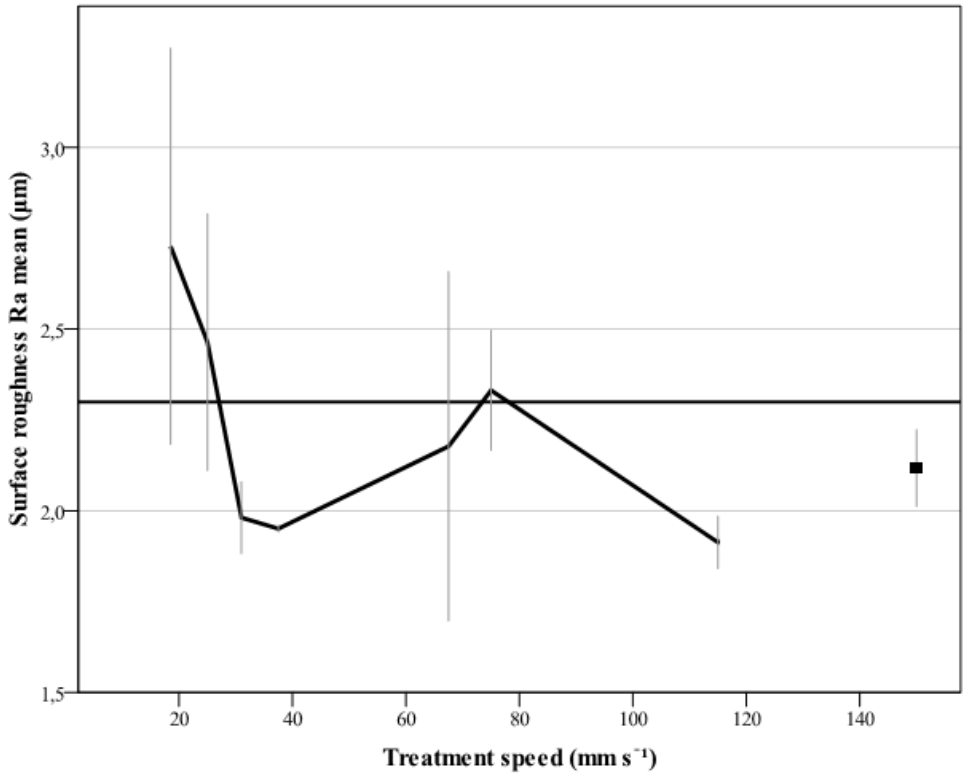

Figure 4.30: Hot treatment surface roughness mean (µm). The mean value at the 150 mm s^{-1} treatment speed refers to the samples treated twice with the speed of 75 mm s^{-1}. The flat line represent the control mean (2.3 µm). Error bars represent the SD (+/-1).

Hot air treatment descriptive statistics for the surface roughness test are, presented in Table 4.18. The roughness means ranged from 1.913 µm (115 mm s^{-1}) to 2.728 µm (18.5 mm s^{-1}). The smallest deviation was observed at samples treated with 37.5 mm s^{-1} speed (SD=0.01) and the highest at treatment speed of 18.5 mm s^{-1} (SD=0.545). The surface

roughness values varied from 1.62 μm (67.5 mm s^{-1} minimum) to 3.43 μm (18.5 mm s^{-1} maximum).

Table 4.18: Surface roughness mean values of hot air treatment in μm. Standard Deviation (SD), Minimum and maximum values and the boundaries of the 95% CI

Treatment speed (mm s^{-1})		control	18.5	25	31	37.5	67.5	75	2X75	115
Average		2.30	2.73	2.46	1.98	1.95	2.18	2.33	2.12	1.91
Min		2.08	2.26	2.15	1.85	1.94	1.62	2.18	2.05	1.82
Max		2.80	3.43	2.96	2.09	1.96	2.79	2.54	2.28	1.99
95% CI	Lower Bound	1.76	1.86	1.90	1.82	1.94	1.41	2.07	1.95	1.80
	Upper Bound	2.84	3.60	3.03	2.14	1.97	2.94	2.59	2.29	2.03
SD		0.34	0.55	0.35	0.10	0.01	0.48	0.17	0.11	0.07

Despite the fact that the roughness mean values are different (Figure 4.30) within hot air treatment speeds is not obvious that there is any effect on the surface roughness during the treatment because of the small mean differences and the high variation in some of the samples sets. Samples treated with the speeds of 31 mm s^{-1}, 37.5 mm s^{-1} and 115 mm s^{-1} seem to have the least rough surface (surface roughness mean<2 μm). The other treated samples did not appear to differ from the control samples roughness mean with an exception of the 18.5 mm s^{-1} treated samples with mean value higher than 2.5 μm.

The F test showed that the hot air treatment speed was statistically significant affecting the WPC surface roughness (F=3.134 for significant level $p<0.05$). Therefore the null hypothesis could be eliminated and agrees with the Levene test.

The significant differences between hot air treatment speed as determined by the Post-Hoc HSD multiple comparison test are presented in Table 4.19.

Table 4.19: Hot air treatment surface roughness multiple comparison test results (p values). Statistical significant differences for p<0.05. Values with fainter text are >0.05.

Treatment speed (mm s^{-1})	18.5	25	31	37.5	67.5	75	2X75	115
Control	0.546	0.997	0.855	0.785	1.000	1.000	0.994	0.682
18.5		0.941	0.037	0.027	0.242	0.647	0.145	0.018
25			0.398	0.322	0.909	0.999	0.785	0.241
31				1.000	0.990	0.775	0.999	1.000
37.5					0.975	0.693	0.997	1.000
67.5						0.998	1.000	0.940
75							0.983	0.583
2X75								0.987

The only statistically significant differences occurred among the treated samples. It appears that the samples with the roughest surfaces (18.5 mm s^{-1}) were significantly different ($p<0.05$) to the least rough (31 mm s^{-1}, 37.5 mm s^{-1} and 115 mm s^{-1}). The smallest mean difference (0.74) was observed between the 18.5 mm s^{-1} treated samples and the 31 mm s^{-1} samples and the highest mean difference (0.815) was observed between the 18.5 mm s^{-1} treated samples and the 115 mm s^{-1} samples. Therefore it is possible to say that if there is a surface roughness alteration the samples treated with the speed of 18.5 mm s^{-1} produces a highly variable rougher surface.

4.2.3.2 Scanning Electron Microscopy (SEM) observation

Samples from the 18.5 mm s^{-1} treatment (poor bonding) and two passes at 75 mm s^{-1} treatment (highest bond strength) were selected for the SEM observation. The samples which were subjected to heat treatment at 18.5 mm s^{-1} do not seem to differ significantly from the untreated samples when observed under the electron microscope. Figure 4.31 shows the appearance of the WPC surface after the heat treatment. Comparison of the hot air treated samples in Figure 4.33 with the hydrogen peroxide treated samples in Figure 4.12 and Figure 4.11, at a similar magnification, it is evident that the wood particles from the hot air treated samples were not damaged in the way they were by the hydrogen peroxide treatment. There is a small area of degradation around the hot air treated sample wood particles (shrinkage spaces, Figure 4.43) but comparison with untreated samples (Figure 4.11) reveals no marked differences.

However the samples treated with heat treatment method appear smoother (Figure 4.33 and Figure 4.34) similar to the hydrogen peroxide treatment (Figure 4.11 and Figure 4.12). Despite this the surface roughness test did not show that the roughness significantly changed after heat treatment.

The heat treated samples with speeds of 18.5 mm s^{-1} (poor bond strength) and 2X75 mm s^{-1} (highest bond strength) did not differ in microscopic appearance. Therefore is not possible to notice any change in surface morphology that could explain the difference in adhesion behaviour.

a) b)

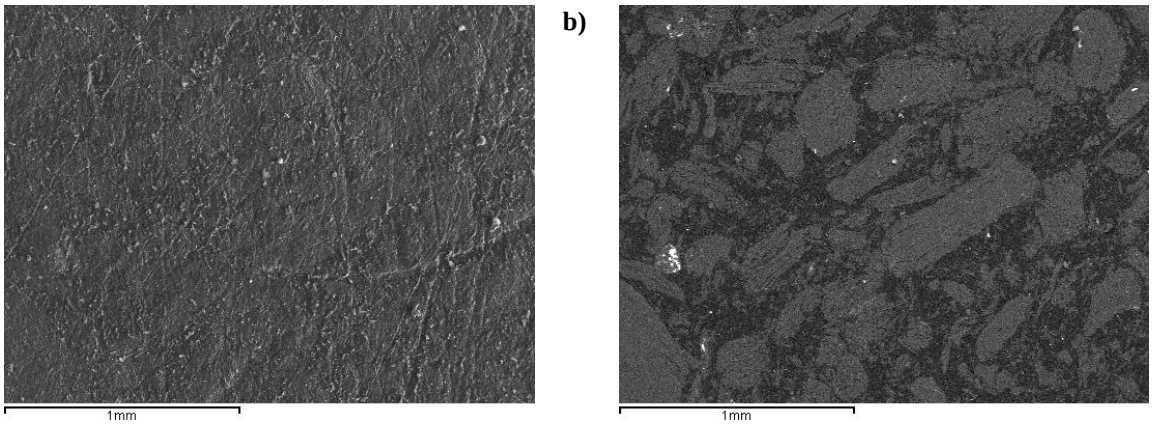

Figure 4.31: 18.5 mm s^{-1} heat treated sample under X67 magnification (X50 equipment indication). a) Backscattered image of the surface. b) same region seen as a secondary electron image.

a) b)

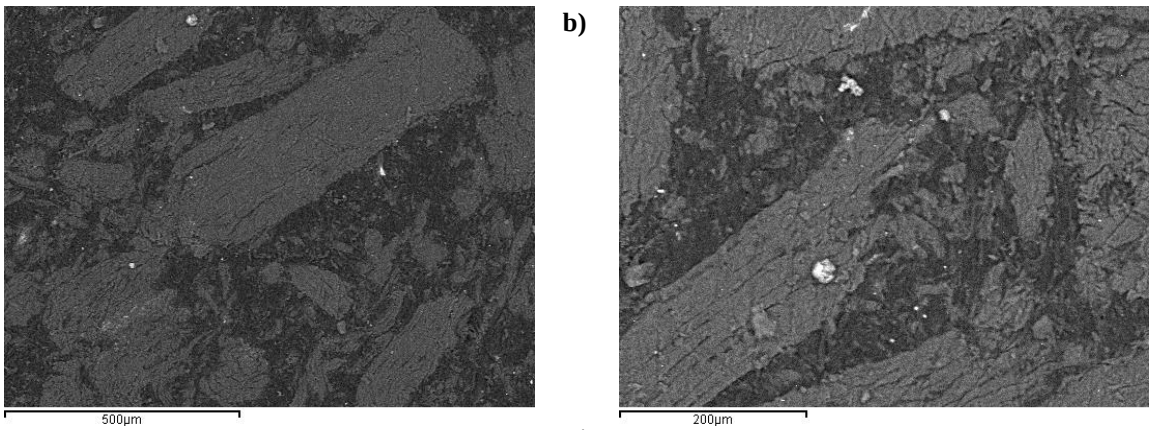

Figure 4.32: Secondary electron image of 18.5 mm s^{-1} heat treated sample under X134 magnification (X100 equipment indication) a) and under X265 magnification (X200 equipment indication) b).

a) b)

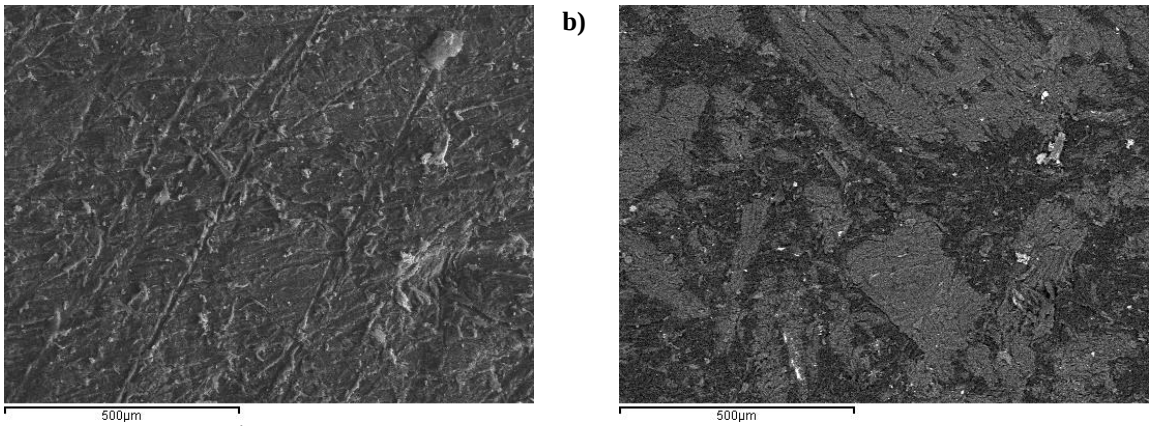

Figure 4.33: 2X75 mm s^{-1} heat treated sample under X134 magnification (X100 equipment indication). a) Backscattered image of the surface. b) same region seen as a secondary electron image

a) b)

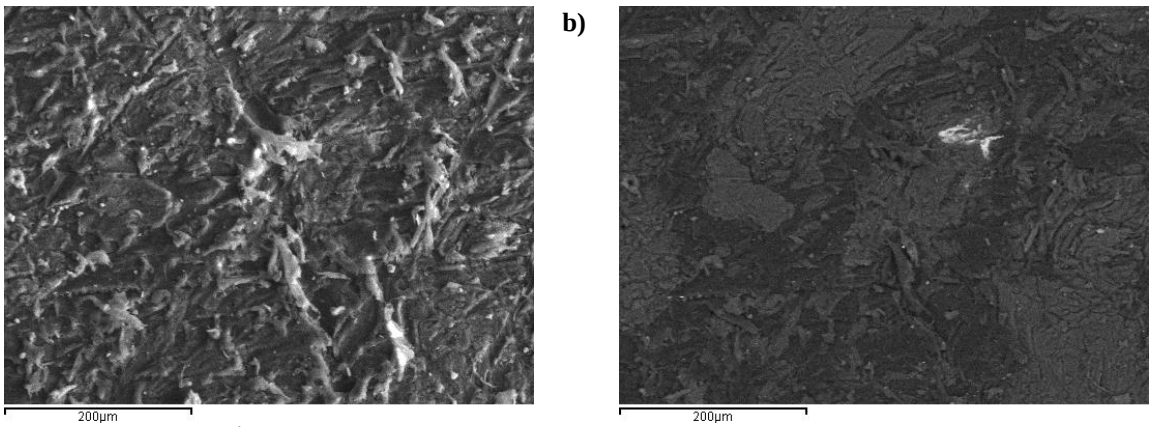

Figure 4.34: 2X75 mm s^{-1} heat treated sample under X265 magnification (X100 equipment indication). a) Backscattered image of the surface. b) same region seen as a secondary electron image.

4.2.3.3 Contact angle and surface energy determination

The hot air treated samples were subjected to contact angle measurements and surface energy determination test. The results are presented in Figure 4.35.

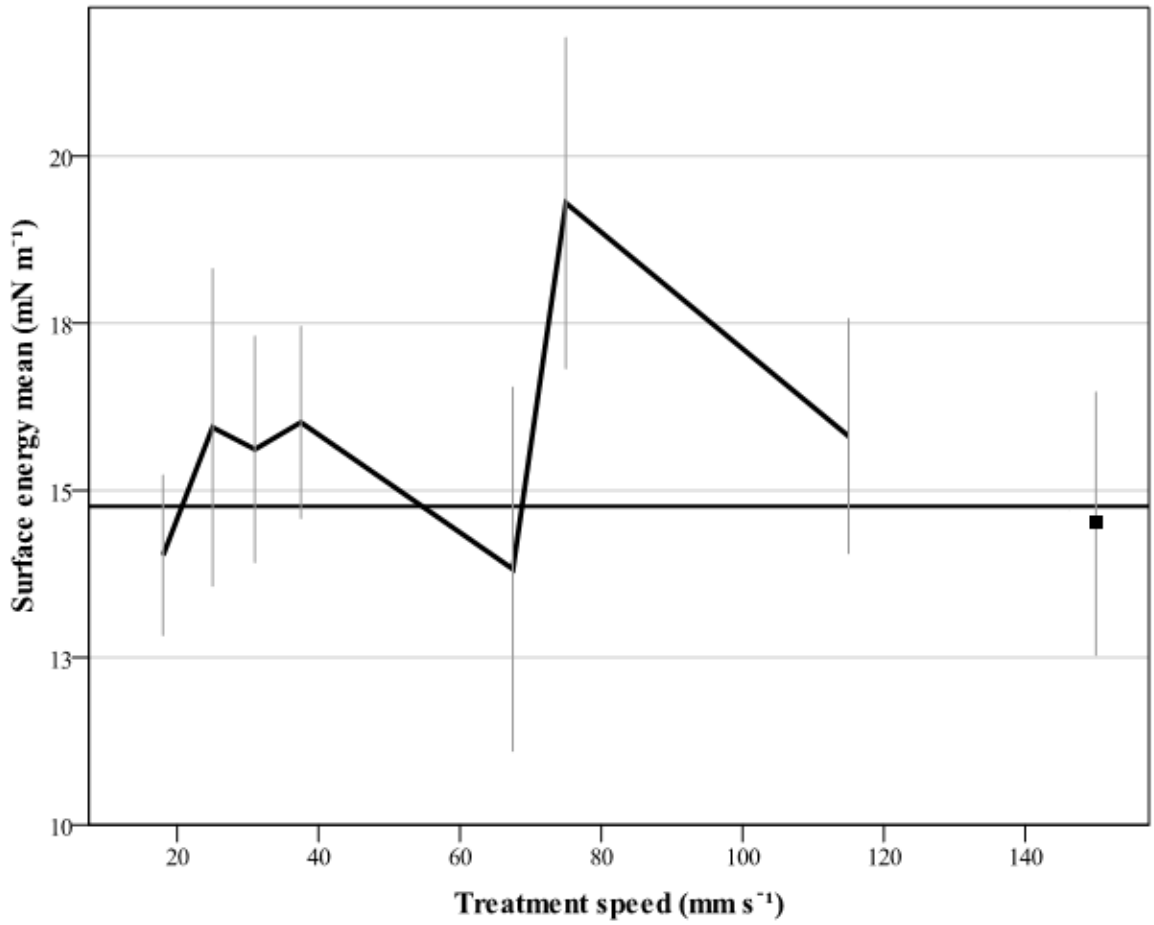

Figure 4.35: Hot air treatment surface energy (mN m^{-1}). The mean value at the 150 mm s^{-1} treatment speed refers to the samples treated twice with the speed of 75 mm s^{-1}. The flat line represent the control value (14.76 mN m^{-1}). Error bars represent the SD (+/-1).

The homogeneity of variance (Levene test) was not statistically significant, therefore the null hypothesis could not be eliminated (Hot air treatment Levene statistic=1.369, p=0.96).

The descriptive statistics for the hot air treatment method are presented in Table 4.20 and shows that the sample means ranged from 13.82 mN m^{-1} (67.5 mm s^{-1}) to 19.30 mN m^{-1} (75 mm s^{-1}). The minimum standard deviation among the hot air treated samples was observed at the samples treated with the speed of 18.5 mm s^{-1} (SD=1.20) and the maximum at the samples treated with the speed of 67.5 mm s^{-1} (SD=2.72).

Table 4.20: Mean values of hot air treatment in mN m^{-1}. Standard Deviation (SD), Minimum and maximum values and the boundaries of the 95% CI of the surface energy

Treatment speed (mm s^{-1})		Control	18.5	25	31	37.5	67.5	75	2X75	115
Average		14.76	14.03	15.94	15.62	16.02	13.82	19.30	14.50	15.81
min		11.30	12.93	12.99	13.56	13.94	10.02	15.26	11.14	13.34
max		16.05	16.58	19.82	18.13	18.12	19.52	22.98	17.82	19.67
95% CI	Lower Bound	13.68	13.18	14.25	14.41	14.99	11.88	17.53	13.10	14.56
	Upper Bound	15.83	14.89	17.64	16.83	17.05	15.77	21.07	15.91	17.07
SD		1.50	1.20	2.37	1.69	1.43	2.72	2.47	1.97	1.75

According to Figure 4.35 most of the treatment speeds seemed to produce a higher surface energy on the WPC, except of the samples treated with the speeds of 18.5 mm s^{-1}, 67.5 mm s^{-1} and 2X75 mm s^{-1}, which had mean surface energy values lower than the control. The samples treated with the speeds of 25 mm s^{-1}, 31 mm s^{-1}, 37.5 mm s^{-1} and 115 mm s^{-1} had mean similar values slightly higher than the untreated samples. The samples treated with the speed of 75 mm s^{-1} had significantly higher surface energy mean than the control. However it was not possible to observe any trend between the surface energy and the treatment speeds.

The F-test revealed that the hot air speed of the treatment was statistically significantly related to WPCs surface energy as $F=6.973$ for significance level $p<0.001$. Therefore the null hypothesis could be eliminated.

To investigate the differences between the treatment variances the Post-Hoc HSD multiple comparisons test was used. The statistically significant differences between treatment speeds and surface energy are presented in Table 4.21.

Table 4.21: Hot air treatment multiple comparison test results (p values). Statistical significant differences for p<0.05. Values with fainter text are >0.05.

Treatment speed (mm s^{-1})	18.5	25	31	37.5	67.5	75	2X75	115
Control	0.996	0.911	0.987	0.879	0.978	0.000	1.000	0.953
18.5		0.430	0.679	0.377	1.000	0.000	1.000	0.529
25			1.000	1.000	0.291	0.008	0.780	1.000
31				1.000	0.520	0.002	0.938	1.000
37.5					0.248	0.010	0.729	1.000
67.5						0.000	0.997	0.375
75							0.000	0.005
2X75								0.857

The only statistically significant difference ($p<0.001$) between the treated samples and the untreated was the samples treated at 75 mm s^{-1} and this treatment was also statistically

significantly different to all of the other treatments. The smallest mean difference was observed between the samples treated with the speeds of 75 mm s^{-1} and 37.5 mm s^{-1} (3.28), and the highest between the samples treated with the speeds of 75 mm s^{-1} and 67.5 mm s^{-1} (5.47).

One way ANOVA Tukey HSD multiple comparisons, clearly showed that the samples treated with the speed of 75 mm s^{-1} produces the highest surface energy. However, there were not any noticeable differences among the rest of the treated samples.

4.2.3.4 FTIR chemical analysis determination

The average of the 5 spectra of the samples treated with hot air using speeds of 2X75 mm s^{-1} and 18.5 mm s^{-1} in comparison to the control are presented in Figure 4.37. Peak height ratios were calculated using 2833 cm^{-1} as reference. Peak height percentages were calculated relative to the untreated WPC control (Equation 7).

Figure 4.36: FTIR-ATR spectra of untreated samples and treated with hot air with the speeds of 18.5 mm s^{-1} and 2X75 mm s^{-1}.

By studying the peak heights percentages in Table 4.22 and Figure 4.37, it is possible to categorize the peaks trends into five similar groups. The first group includes the peaks of the 3338 cm^{-1} 3284 cm^{-1} and 1022 cm^{-1} wavenumber bands. Those three bands referred to the cellulose. The second group includes the 1263 cm^{-1} and 1230 cm^{-1} wavenumber bands. The second group seem to relate the lignin with the esters and the carbonyls. The third group

includes the wavenumber bands of 1656 cm^{-1}, 1595 cm^{-1} and 1422 cm^{-1}. The third group relates to both the cellulose and the lignin. The fourth group includes the peaks of the 1454 cm^{-1} and 1375 cm^{-1} wavenumber bands. The fourth group relates the CH_2 with the cellulose CH bending. Finally, the fifth group is esters which were not seem to have a similar trend to any other band (1732 cm^{-1}).

Table 4.22: Peaks height percentages of the samples treated with hot air

	Treatment speed (mm s^{-1})							
Wavenumbers cm^{-1}	**18.5**	**25**	**31**	**37.5**	**67.5**	**75**	**2X75**	**115**
3338	1%	2%	-27%	-17%	-10%	-13%	-1%	13%
3284	2%	1%	-29%	-17%	-11%	-14%	-2%	12%
1732	25%	13%	-6%	9%	-6%	4%	15%	11%
1656	-8%	-27%	-40%	-25%	-33%	-26%	-25%	-24%
1595	-11%	-22%	-37%	-29%	-33%	-26%	-19%	-15%
1454	-8%	-7%	-11%	-10%	-10%	-7%	-4%	-6%
1422	-7%	-8%	-24%	-18%	-18%	-15%	-5%	-1%
1375	-7%	-2%	-6%	-7%	-5%	-1%	0%	-3%
1263	-3%	0%	-19%	-13%	-10%	-8%	3%	10%
1230	-2%	-1%	-19%	-13%	-10%	-8%	2%	10%
1022	-3%	3%	-18%	-12%	-5%	-6%	6%	20%

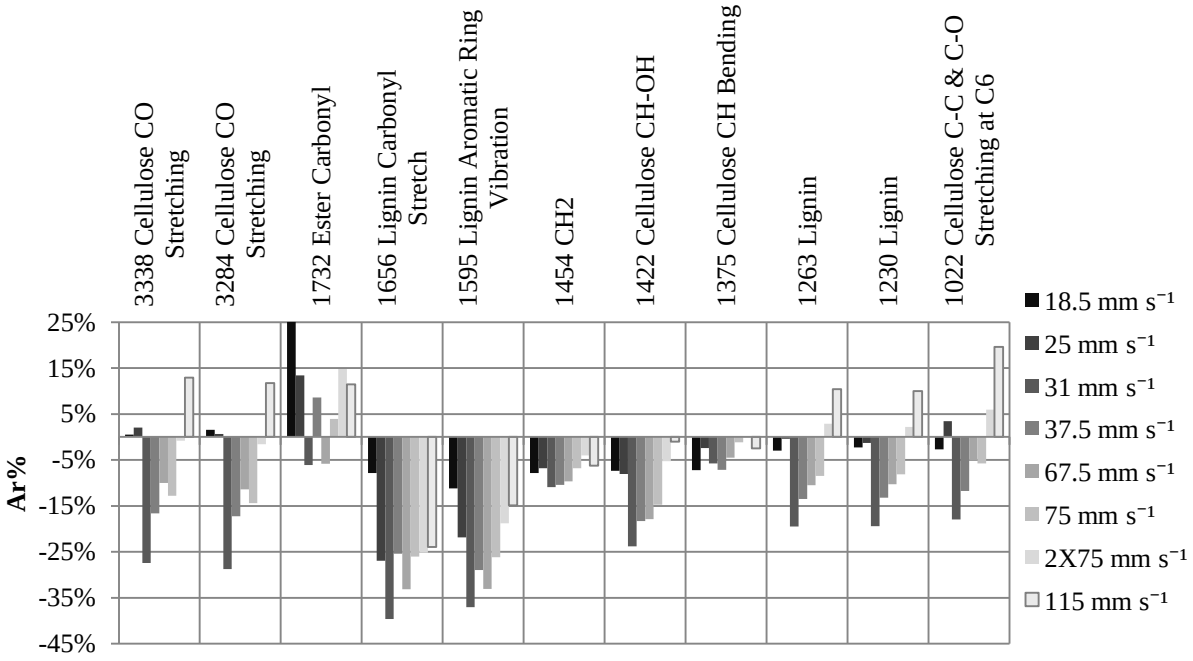

Figure 4.37: FTIR ATR ratio percentage of the hot air treated samples

The first group of the similar peak trends are for the peaks of the 3338 cm^{-1}, 3284 cm^{-1} and 1022 cm^{-1} wavenumbers. The 3338 cm^{-1} and the 3284 cm^{-1} wavenumbers were almost identical. The majority of the treated samples were lower than the untreated, with only the

115 mm s^{-1} samples showing a significant increase (12% to 13%). The samples treated at the speeds of 18.5 mm s-^{1}, 25 mm s^{-1} and 2X75 mm s^{-1} did not appear to be different from the control. The lowest value was observed at the samples treated at 31 mm s^{-1} with values around 30%. The peak height percentage of the cellulose C-C and C-O stretching at C_6 (1022 cm^{-1}) showed a trend similar to the lignin peaks. This pattern was also observed at the 3338 cm^{-1} wavenumber band although the 75 mm s^{-1} treatment showed a reduction from -10% (67.5 mm s^{-1}) to -13%. A similar pattern was observed for the 3284 cm^{-1} wavenumber band, but the effects differed in magnitude.

The 1263 cm^{-1} wavenumber band peak refers to lignin. The peak height percentage of the samples treated with the low treatment speeds of 18.5 mm s^{-1} and 25 mm s^{-1} were at the value of -3% and 0%, but showed a sharp decrease at 31 mm s^{-1} (-19%). At faster treatment speed mean values increased progressively to reach 10% at 115 mm s^{-1}. It was clear that there was a trend between the treatment speeds, from 31 mm s^{-1} to 115 mm s^{-1}, and the lignin increases peak height. The same trend was observed in the 1230 cm^{-1} wavenumber band, as it was expected because it also refers to lignin. although there were slight differences in relative percentages.

The lignin carbonyl stretch (1656 cm^{-1}) is reduced in all treated samples with hot air. The highest peak height percentage was -8% and was observed at samples treated with the speed of 18.5 mm s^{-1}, which was the slowest treatment speed. All of the other treatment speeds produced much greater reductions ranging from -24% (115 mm s^{-1}) to -40% (31mm s^{-1}).

The lignin aromatic ring vibration (1595 cm^{-1}) was also reduced in all treated samples with almost the same pattern with lignin carbonyl stretch (1656 cm^{-1}). The samples treated at the slowest and fastest speeds had the least reductions, i.e. 18.5 mm s^{-1}, -11% and 115 mm s^{-1}, -15%. The other treatments ranged in mean reductions from -37% at the samples treated with the speed of 31 mm s^{-1}. to -29% at 37 mm s^{-1}.

The peak height percentage of the cellulose CH-OH (1422 cm^{-1}) of all the hot air treated samples was also reduced as the two previous peaks but in different magnitude. The peak height percentage of the samples treated with the lowest treatment speeds of 18.5 mm s^{-1} and 25 mm s^{-1}, were similar at -7% and -8% respectively. At a marginally faster speed the effect jumped to -24% but this then declined progressively with increasing treatment speed, to reach -1% at 115 mm s^{-1}.

The CH_2 (1454 cm^{-1}) absorption ratio of all the hot air treated samples was reduced. The peak height percentages of the treated samples varied from -11% to -4%. The small differences between the samples did not reveal a specific trend. Also the cellulose bending peak (1375 cm^{-1}) had the same appearance with the 1454 cm^{-1} peak, with no specific trend and values between 0% to -7%.

The esters (1732 cm^{-1}) of the majority of the hot air treated samples appeared to show an increase in comparison to the control. All the hot air treated samples appeared to produce an increase in ester peak height percentage, except for the samples treated with the speeds of 31 mm s^{-1} and 67.5 mm s^{-1},which decreased marginally (-6%). The highest peak height percentage was 25% (18.5 mm s^{-1}, the slowest treatment speed) and the other peaks were around half of this (15%: 2X75 mm s^{-1},13%: 31 mm s^{-1}, 11%: 115 mm s^{-1}, the fastest treatment speed, and 9%: 37.5 mm s^{-1}. 75 mm s^{-1} only gave a change of 4%. However the esters of the hot air treated samples were mostly increased as was expected. It is possible that ester increscent to be due to a greater exposed woody surface after PP melts. This hypothesis is supported by the fact that the higher ester ratio is observed at the samples treated with the lower speed. The slowest speed is most probably to cause PP melt. However the cellulose seemed to significant reduced which does not agree with the hypothesis that more woody surface was produced. Therefore it is most probably that the ester increase might be occurred by actual esterification.

However, the duration of the treatment alone was not necessarily the main factor that changes the chemical consistency of the surface, but treatment repetition. The hot air of the samples treated with the speed of 37.5 mm s^{-1} is effectively the same as 2X75 mm s^{-1}, but only the peak at 1565cm^{-1} was similar. Papirer et al (1993) also showed that repetition of flame treatment increases the esters, but that work did not compare the effect of one single treatment with the same duration of flame application of multiple treatments.

4.2.4 FLAME TREATMENT

4.2.4.1 Surface roughness of flame treated samples

The surface roughness values of the flame treated samples was compared to the untreated samples for homogeneity of variance and were not found to be significant (Flame treatment Levene statistic=1.237, p=0.328) and the null hypothesis could not be eliminated. The flame treatment surface roughness results are presented in Figure 4.38.

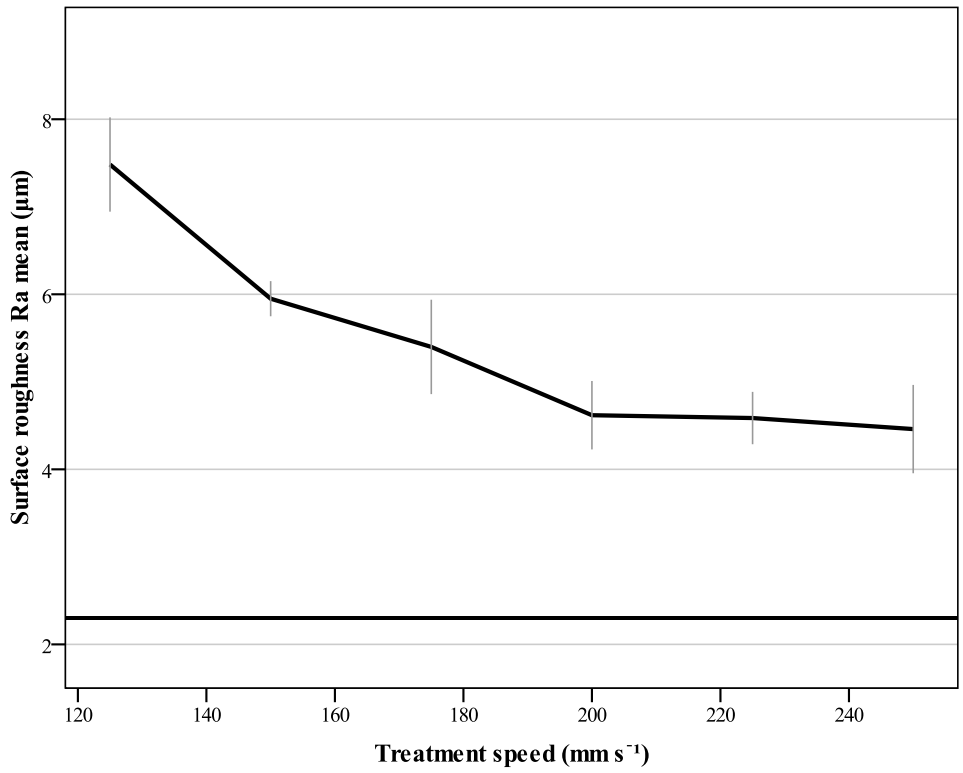

Figure 4.38: Flame treatment surface roughness mean (µm). The flat line represent the control mean (2.3 µm). Error bars represent the SD (+/-1).

The roughness is clearly increased after flame treatment (Figure 4.38) and the means increase with flame duration. At high speeds, low duration, above 200 mm s^{-1}, the effect stabilizes. but at values at least twice that of the control samples.

The surface roughness means varied from 4.46 µm (250 mm s^{-1}) to 7.48 µm (125 mm s^{-1}) (Table 4.23). Samples treated with the speed of 150 mm s^{-1} had the smallest standard deviation (SD=0.2) and the 175 mm s^{-1} treatment had the greatest standard deviation (SD=0.54). The roughness values were varying from 3.76µm (250 mm s^{-1} minimum) to 8.08µm (125 mm s^{-1} maximum).

Table 4.23: Surface roughness mean values of flame treatment in µm. Standard Deviation (SD), Minimum and maximum values and the boundaries of the 95% CI.

Treatment speed (mm s^{-1})		control	125	150	175	200	225	250
Average		2.30	7.48	5.95	5.40	4.62	4.59	4.46
min		2.08	6.91	5.69	4.70	4.05	4.27	3.76
max		2.80	8.08	6.17	5.86	4.91	4.84	4.95
95% CI	Lower Bound	1.76	6.63	5.63	4.54	4.00	4.11	3.66
	Upper Bound	2.84	8.34	6.27	6.26	5.24	5.06	5.26
SD		0.34	0.54	0.20	0.54	0.39	0.30	0.50

Despite that Levene test was not statistically significant, the null hypothesis could be eliminated, due to the F-test, which was statistically significant for F=57.291 for significance level p<.001.

The statistically significant differences, between the roughness values of the flame treatment speeds, were tested by Tukey HSD multiple comparisons and the results are presented in Table 4.24.

Table 4.24: Flame treatment surface roughness multiple comparison test results (p values). Statistical significant differences for p<0.05. Values with fainter text are >0.05.

Treatment speed (mm s^{-1})	125	150	175	200	225	250
control	0.000	0.000	0.000	0.000	0.000	0.000
125		0.001	0.000	0.000	0.000	0.000
150			0.528	0.003	0.003	0.001
175				0.167	0.137	0.060
200					1.000	0.998
225						0.999

All the flame treated samples were statistically significantly different to the control for significance level of p<0.001. The control samples with the samples treated with the speed of 125 mm s^{-1} had the highest mean difference (5.185) among all samples. The samples treated with the speed of 125 mm s^{-1} was also statistically significantly different to all the treated samples for significance level of p<0.001. Therefore the samples treated with the lowest treatment speed of 125 mm s^{-1} had the rougher surface. The samples treated with the speed of 150 mm s^{-1} were statistically significantly different to the samples treated with the speeds of 200 mm s^{-1}, 225 mm s^{-1} and 250 mm s^{-1} for significance level of p<0.005, but it was not different to the samples treated with the speed of 175 mm s^{-1}. Moreover, the smallest mean difference (1.33) among all samples was observed between the samples treated with the speed of 150 mm s^{-1} with the 200 mm s^{-1} treated samples. On the other hand the samples treated with the speed of 175 mm s^{-1} was not statistically significantly different to the samples treated with the speeds of 200 mm s^{-1}, 225 mm s^{-1} and 250 mm s^{-1}. Therefore the samples treated with the speed of 150 mm s^{-1} had the second rougher surface.

One way ANOVA and the Tukey HSD multiple comparisons confirm that the flame treatment, regardless of the treatments speed, produce a rougher surface. The roughest surface was produced by the slowest flame speed used, 125 mm s^{-1}. The Tukey HSD multiple comparisons test confirms the trend which was mentioned by the descriptive statistics study.

4.2.4.2 Scanning Electron Microscopy (SEM) observation

The samples treated with the flame torch were considerably different from the untreated samples. On the surface of the WPC several holes, or pits were formed (Figure 4.39). The pits appeared on the polymer surface, and there are more which are smaller and are noticeable under higher magnification (Figure 4.40 and Figure 4.41). Those pits are most probably formed because of the polymer melting when the flame contacts the material and "fries" the surface. In Figure 4.41 there is pit that is so deep that there is a wood particle visible at the bottom. Zhang et al (1998) also reports pits formed on the polymer surface, due to electron attack by the corona discharge treatment, which increases the bonding area and could result in an increase of the adhesion strength.

The wood however does not appear to be damaged after the treatment. There is wood particle degradation, but it is not considered to be significant compared to the wood degradation seen with the hydrogen peroxide treatment. The wood particles look like the polymer covers them and makes them less visible because there is lees contrast between the polypropylene and the wood particles.

Samples treated at 175 mm s^{-1} have formed smaller pits than the samples treated with 125 mm s^{-1} (Figure 4.42, Figure 4.43 and Figure 4.44) The formation of the pits makes it possible to explain the increase in surface roughness from 2.30 μm (control) to 7.48 μm (125 mm s^{-1}). The hypothesis that the pits related to an increase in the surface roughness could be also supported by the fact that the pits size increases in treatment were the roughness mean was 7.48 μm (125 mm s^{-1}) and decreases in treatment were the roughness mean was 5.40 μm (175 mm s^{-1}) (Figure 4.39 and Figure 4.42).

a) b)

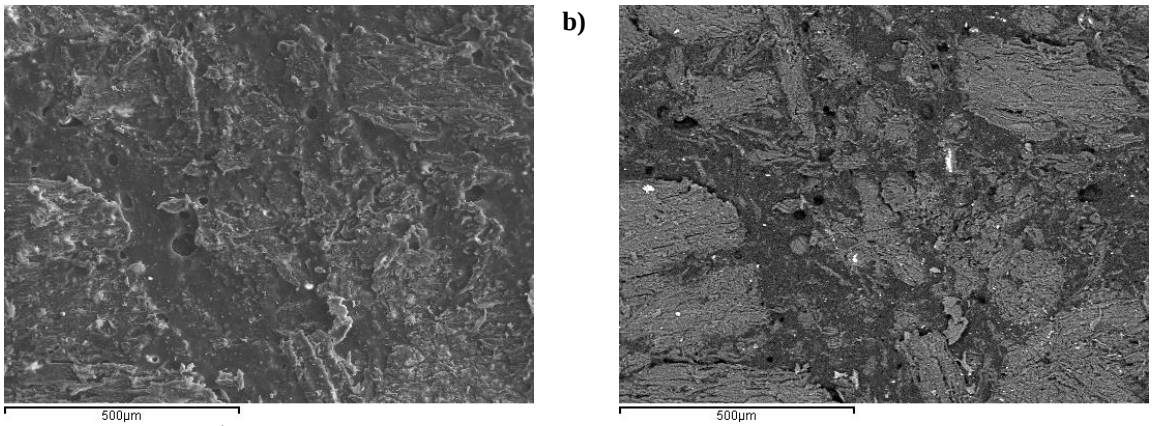

Figure 4.39: 125 mm s^{-1} flame treated sample under X134 magnification (X100 equipment indication). a) Backscattered image of the surface. b) same region seen as a secondary electron image.

b)

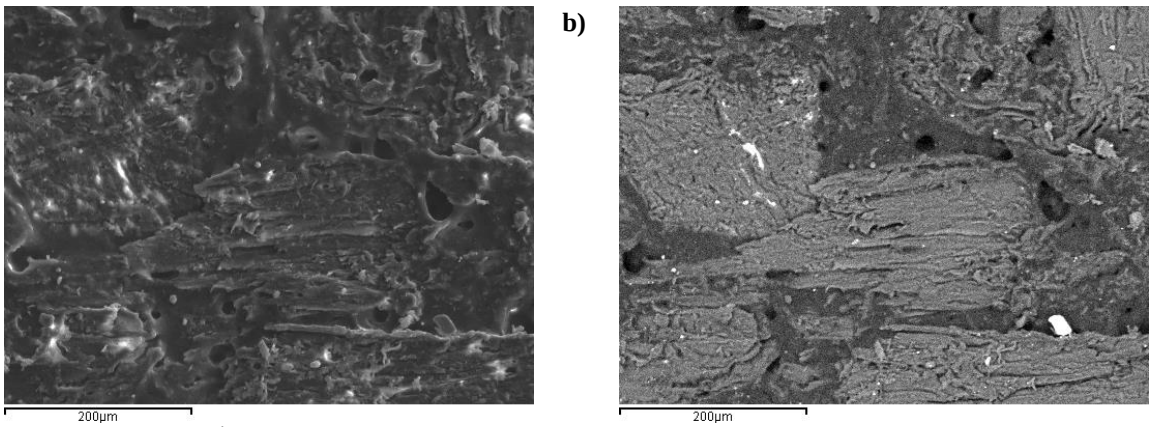

Figure 4.40: 125 mm s^{-1} flame treated sample under X265 magnification (X200 equipment indication). a) Backscattered image of the surface. b) same region seen as a secondary electron image.

a) b)

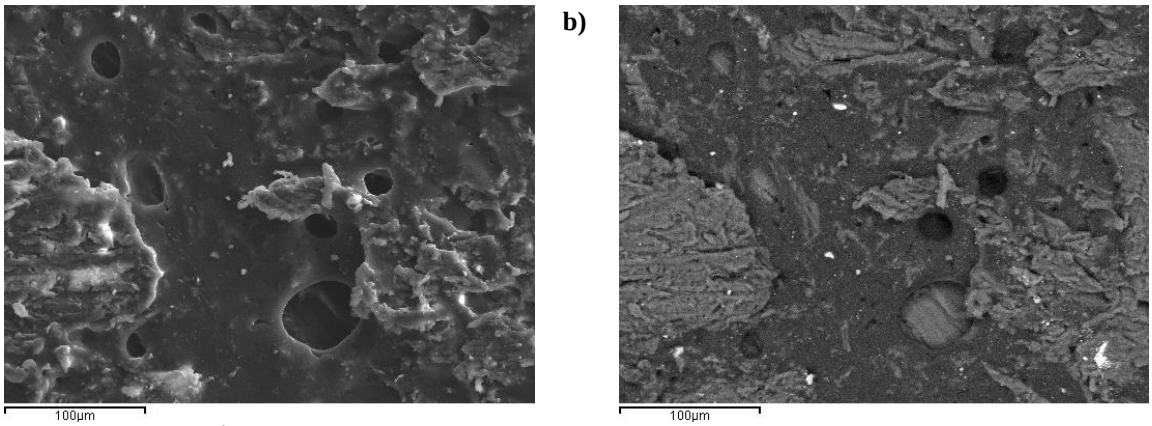

Figure 4.41: 125 mm s^{-1} flame treated sample under X400 magnification (X300 equipment indication). a) Backscattered image of the surface. b) same region seen as a secondary electron image.

a) b)

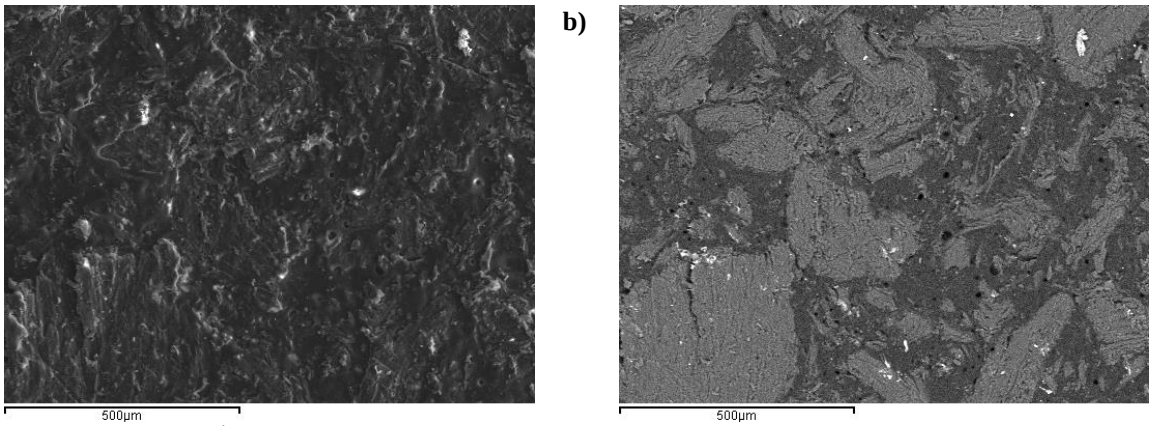

Figure 4.42: 175 mm s^{-1} flame treated sample under X134 magnification (X100 equipment indication). a) Backscattered image of the surface. b) same region seen as a secondary electron image.

a) b)

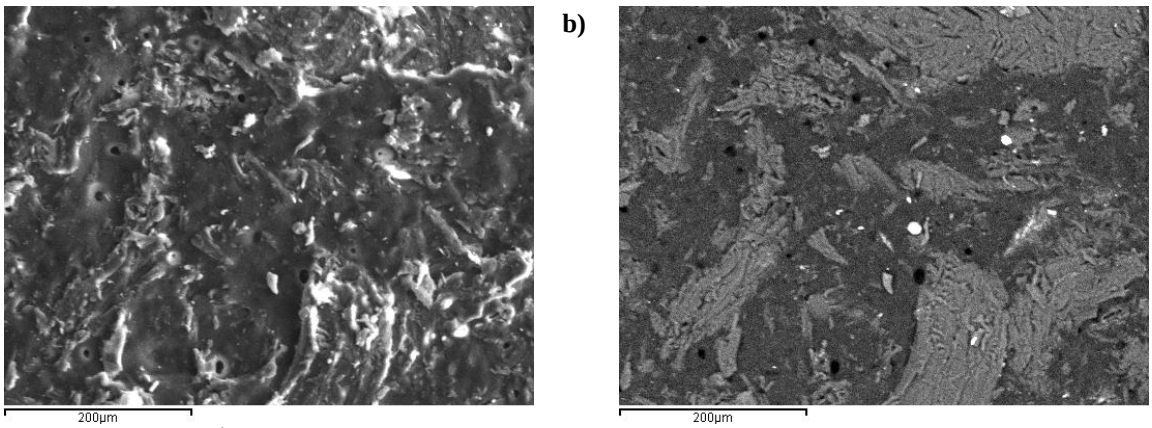

Figure 4.43: 175 mm s^{-1} flame treated sample under X265 magnification (X200 equipment indication). a) Backscattered image of the surface. b) same region seen as a secondary electron image.

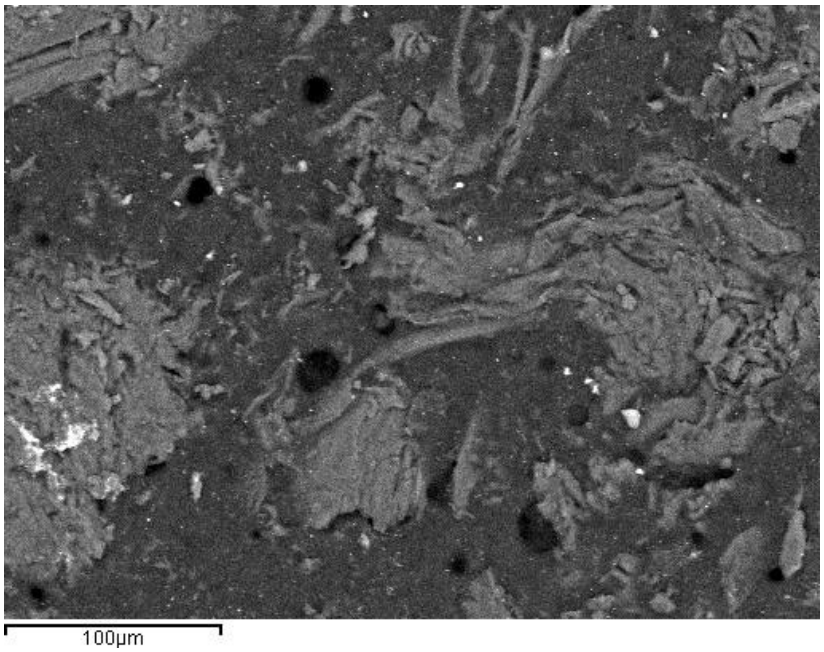

Figure 4.44: Secondary electron scanning microscopy of 175 mm s^{-1} heat treated sample under X400 magnification (X300 equipment indication).

4.2.4.3 Contact angle and surface energy determination

The flame treated samples Levene test was not statistically significant, therefore the null hypothesis could not be eliminated (Flame treatment Levene statistic=1.559, p= 0.176). The flame treatment surface energy results are presented in Figure 4.45. The treated samples means ranged from 15.28 mN m^{-1} (125 mm s^{-1}) to 30.46 mN m^{-1} (250 mm s^{-1}) (Table 4.25). The smallest standard deviation among the flame treated samples was observed at the samples treated with the speed of 125 mm s^{-1} (SD=1.37) and the highest at the samples treated with the speed of 225 mm s^{-1} (SD=3.25).

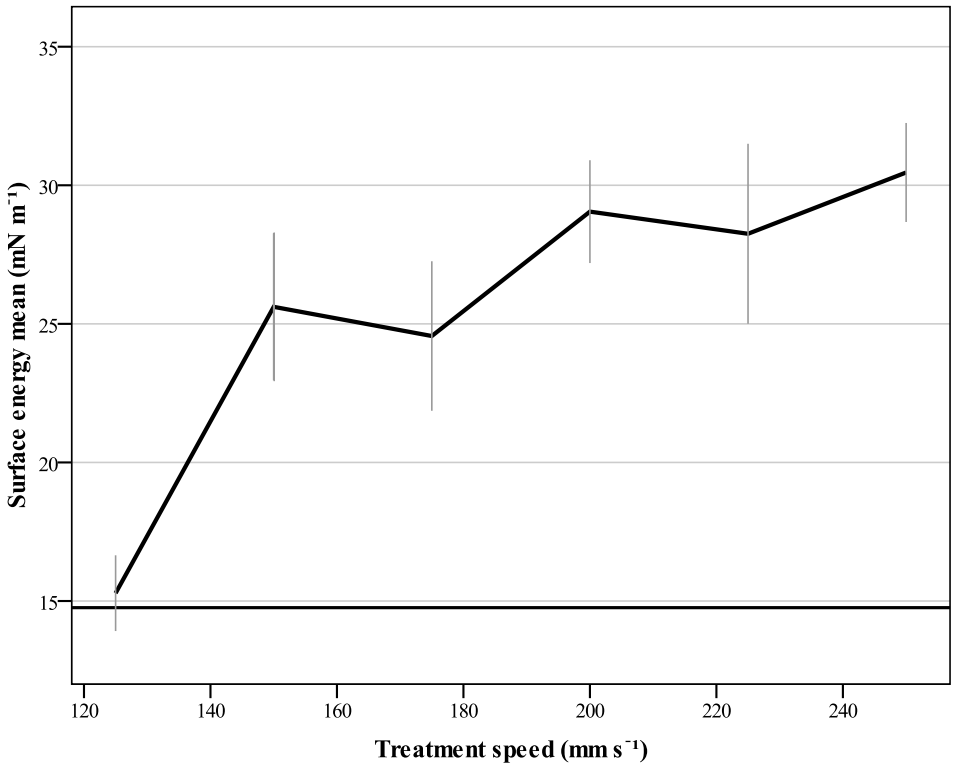

Figure 4.45: Flame treatment surface energy (mN m^{-1}). The flat line represent the control mean (14.76 mN m^{-1}). Error bars represent the SD (+/-1).

Table 4.25: Mean values of surface energy for samples prepared by flame treatment in mN m^{-1}. Standard Deviation (SD), Minimum and maximum values and the boundaries of the 95% CI of the surface energy.

Treatment speed (mm s^{-1})		Control	125	150	175	200	225	250
Average		14.76	15.28	25.61	24.56	29.05	28.25	30.46
min		11.30	13.40	22.09	20.69	26.29	23.07	27.54
max		16.05	17.98	30.50	28.95	32.96	34.29	32.58
95% CI	Lower Bound	13.68	14.31	23.72	22.63	27.72	25.93	29.18
	Upper Bound	15.83	16.26	27.51	26.49	30.38	30.57	31.74
	SD	1.50	1.37	2.65	2.70	1.85	3.25	1.79

All the treated samples seemed to produce a higher surface energy on the WPC except of the samples treated with the speeds of 125 mm s^{-1} which had surface energy mean only slightly higher than the untreated samples. The rest of the treated samples had significantly higher surface energies than the control samples. The samples treated at 250 mm s^{-1} had surface energy mean around 30 mN m^{-1}, twice that of the untreated samples. According to Ritter et al (2000), to produce an acceptable adhesion, the surface energy of the material should have values from 40 mN m^{-1} and higher.

The surface energy seemed to increase as the treatment speed increased. The samples treated at 125 mm s^{-1} had surface energy of 15.28 mN m^{-1}, which was slightly higher than the untreated mean value, and then significantly increased to values around 25 mN m^{-1} for the samples treated at 150 mm s^{-1} and 175 mm s^{-1}. As the treatment speed increases, the surface energy was increased to surface energy mean values of around 28.5 mN m^{-1} for at 200 mm s^{-1} and 225 mm s^{-1}, reaching the highest value of 30.46 mN m^{-1} at 250 mm s^{-1}.

The F-test revealed that the flame speed of the treatment has a significant effect to the WPC surface energy ($F=81.837$ for significant level $p<0.001$). Therefore the null hypothesis could be eliminated.

To investigate the differences between the treatment variances the Post-Hoc HSD multiple comparisons test was used (Table 4.26).

Table 4.26: Flame treatment multiple comparison test results (p values). Statistical significant differences for p<0.05. Values with fainter text are >0.05.

Treatment speed (mm s^{-1})	125	150	175	200	225	250
Control	0.998	0.000	0.000	0.000	0.000	0.000
125		0.000	0.000	0.000	0.000	0.000
150			0.941	0.019	0.139	0.000
175				0.001	0.009	0.000
200					0.985	0.799
225						0.314

One way ANOVA Tukey HSD multiple comparisons, clearly showed that all the treated samples, except of the samples treated with the speed of 125 mm s^{-1}, have surface energy higher than the untreated samples ($p<0.001$). The highest surface energies were observed at the samples treated with the speeds of 200 mm s^{-1} and 250 mm s^{-1}, because they were statistically significantly different to all the other treated samples, except from the samples treated with the speed of 225 mm s^{-1}. The samples treated with the speed of 225 m s^{-1} were not significantly different to the samples treated with the speed of 150 mm s^{-1}.

Therefore, the samples treated with the speed of 225 mm s^{-1}, despite the fact that they were not significantly different to the samples treated at 200 mm s^{-1} and 250 mm s^{-1}, have lower surface energy. Consequently, the one way ANOVA test, showed that the samples treated at 250 mm s^{-1} and 200 mm s^{-1} have the highest surface energy; following the samples treated at 150 mm s^{-1} and 225 mm s^{-1}; and finally the samples treated at 175 mm s^{-1}. However, one way ANOVA did not show which of the treatment speeds is the best treatment speed to produce the highest surface energy.

4.2.4.4 FTIR chemical analysis determination

From each sample 5 spectra were taken. The average of the 5 spectra (Figure 4.46) was used to measure the absorption band height ratio of each sample.

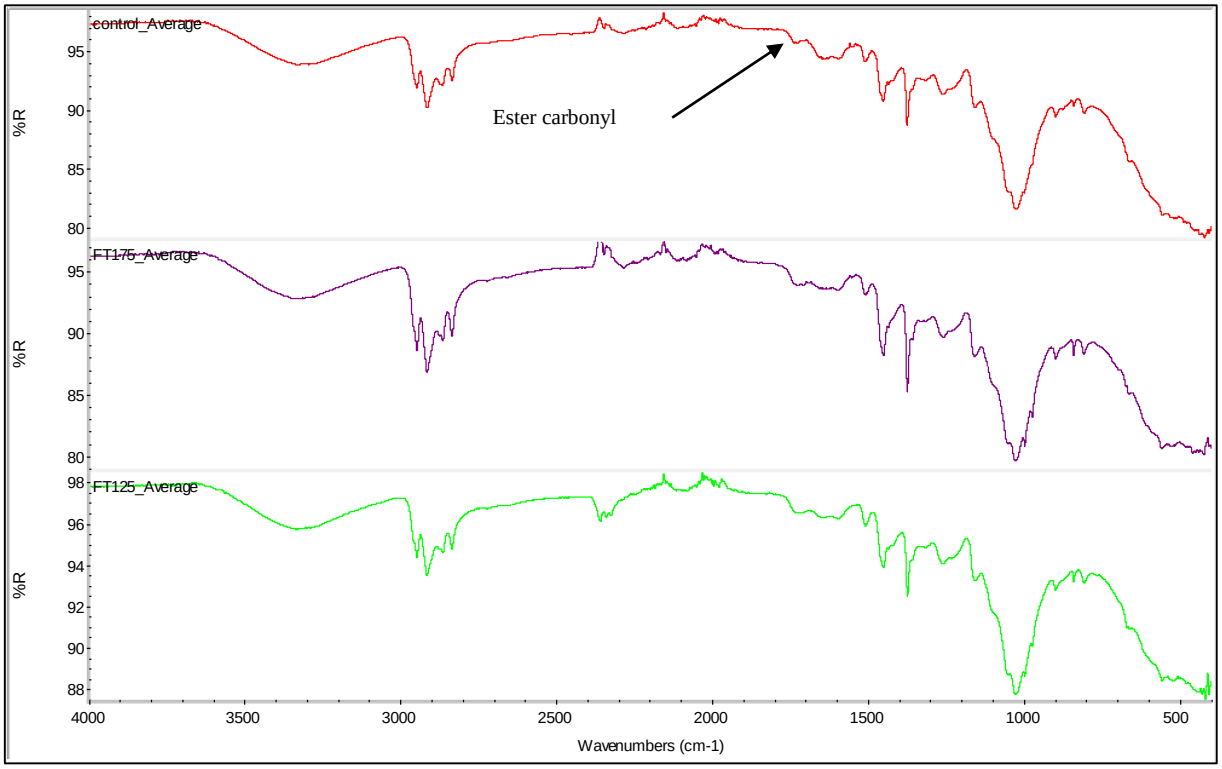

Figure 4.46: FTIR-ATR spectra of untreated samples and flame treated with the speeds of 125 mm s^{-1} and 175 mm s^{-1}.

By studying the peak height percentages in Table 4.27 and Figure 4.47, it was possible to categorize the peak trends into four similar groups. The peaks with the 3338 cm^{-1}, 3284 cm^{-1}, 1263 cm^{-1}, 1230 cm^{-1} and 1022 cm^{-1} wavenumbers appear to have a similar trend but to different magnitudes. All treatment rates caused those peaks to reduce, with the exception of the samples treated at the slowest speed (125 mm s^{-1}); this appeared no different to the untreated control samples. Also the 1656 cm^{-1}, 1595 cm^{-1} and 1422 cm^{-1} peaks showed the same trend to the above peaks but the samples treated at the slowest speed were also

different to the control samples. The 1375 cm^{-1} peak was not different to the untreated control samples and the 1454 cm^{-1} peak was similar but showed slightly more change. Finally, the fourth group, the esters, did not seem to have any similarity to any other band, as all treatment speeds showed a strong increase.

Table 4.27: Peaks height percentages of the samples treated with flame

	Treatment speed (mm s^{-1})					
Wavenumbers cm^{-1}	**125**	**150**	**175**	**200**	**225**	**250**
3338	1%	-13%	-23%	-32%	-16%	-20%
3284	-2%	-16%	-25%	-35%	-19%	-23%
1732	37%	31%	22%	22%	24%	11%
1656	-23%	-31%	-36%	-43%	-36%	-39%
1595	-20%	-29%	-33%	-45%	-35%	-37%
1454	-4%	-6%	-7%	-8%	-9%	-9%
1422	-6%	-15%	-21%	-28%	-20%	-21%
1375	0%	-2%	-3%	-4%	-4%	-3%
1263	2%	-11%	-17%	-26%	-15%	-20%
1230	2%	-11%	-16%	-25%	-15%	-20%
1022	4%	-12%	-21%	-30%	-16%	-21%

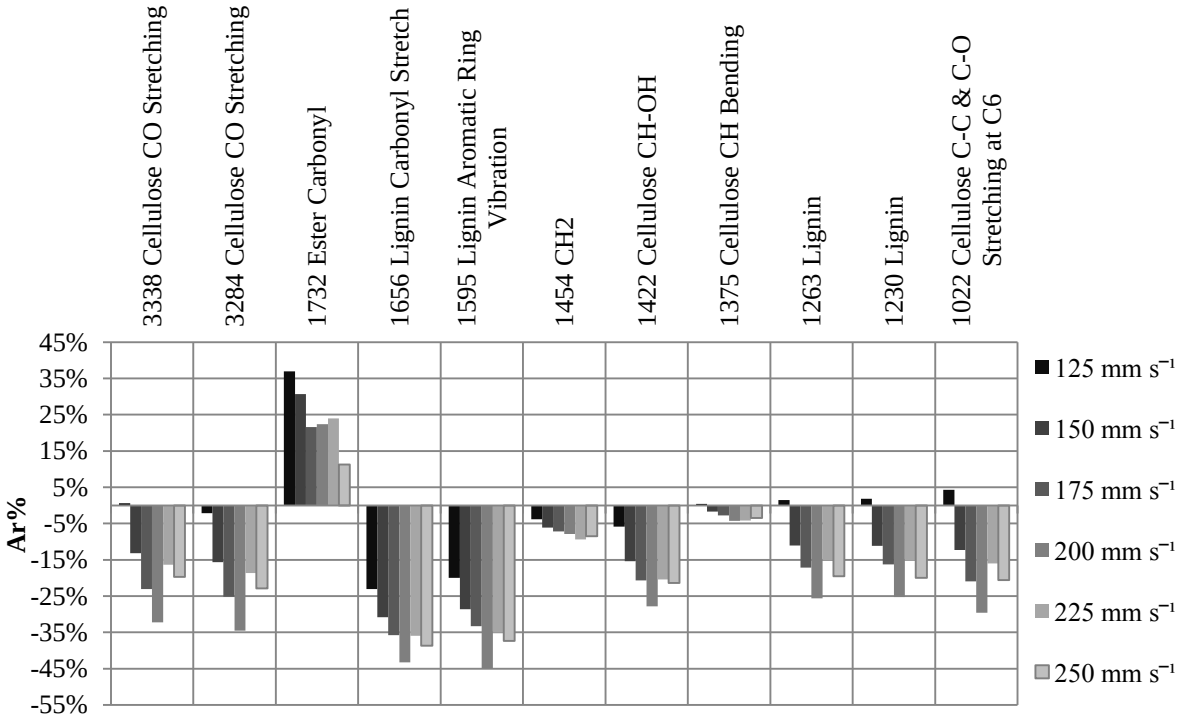

Figure 4.47: FTIR ATR ratio percentage of flame treated samples

The most important data (Figure 4.46) were observed for the ester carbonyl peak (1732 cm^{-1}); this increased in all flame treated samples, in contrast with the previous pre-treatment methods. The highest ester peak heights percentage was 37%, at the slowest

treatment speed (125 mm s^{-1}). This declined to 21.6% as the treatment speed increased to 175 mm s^{-1}. At faster speeds (175-225 mm s^{-1}) there was a similar lesser effect (22-24%) and at the fastest speed (250 mm s^{-1}) the peak was only 11% higher that the control. The FTIR of all the flame treated samples in this study shows that the esters of the WPC were increased, which strongly agrees with the increase of the peak height at 1720 cm^{-1} wavenumber band of flame treated PE as was reported by Papirer et al (1993).

4.2.5 HALOGEN HEATING LAMP TREATMENT

4.2.5.1 Surface roughness determination results

The surface roughness results are presented in Figure 4.48. The surface roughness values of the halogen lamp treated samples were compared to the untreated samples and with the Levene test the differences were not statistically significant and thus the null hypothesis could not be eliminated (Flame treatment Levene statistic=0.382, p=0.854).

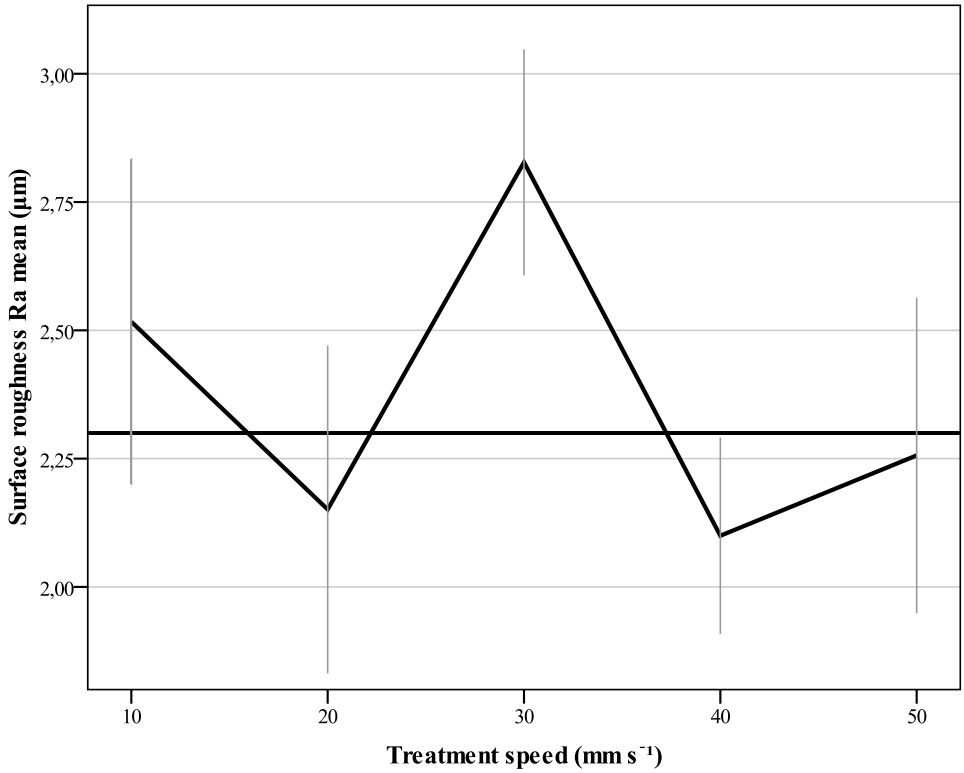

Figure 4.48: Halogen heating lamps treatment surface roughness mean (µm). The flat line represent the control mean (2.3 µm). Error bars represent the SD (+/-1).

The roughness mean values do not seem to differ from the control values (Figure 4.48). The small mean differences among the treatment speeds, and the high standard deviation, does not show that treatment effects surface. The data suggests than 30 mm s^{-1} gives the roughest surface.

The descriptive statistics (Table 4.28) show that the roughness means vary from 2.1 μm (40 mm s^{-1}) to 2.83 μm (30 mm s^{-1}) and ranged from 1.85 μm (40 mm s^{-1} minimum) to 3.14 μm (30 mm s^{-1} maximum). The smallest standard deviation was observed at samples treated with 40 mm s^{-1} speed (SD=0.19) and the highest at the samples treated with the speed of 20 mm s^{-1} (SD =0.32).

Table 4.28: Surface roughness mean values of halogen heating lamp treatment in μm. Standard Deviation (SD), Minimum and maximum values and the boundaries of the 95% CI.

Treatment speed (mm s^{-1})		control	10	20	30	40	50
Average		2.30	2.52	2.15	2.83	2.10	2.26
Min		2.08	2.27	1.86	2.64	1.85	1.99
Max		2.80	2.98	2.60	3.14	2.30	2.65
95% CI	Lower Bound	1.76	2.01	1.64	2.48	1.80	1.77
	Upper Bound	2.84	3.02	2.66	3.18	2.40	2.75
SD		0.34	0.32	0.32	0.22	0.19	0.31

The F-test revealed that this treatment was statistically significant related to treated WPCs surface roughness as F=3.57 for significant level $p<0.05$. Therefore the null hypothesis could be eliminated.

The Post-Hoc Tukey HSD multiple comparisons test was used to illustrate the statistically significantly differences between treatments (Table 4.29).

Table 4.29: Halogen heating lamp treatment surface roughness multiple comparison test results (p values). Statistical significant differences for p<0.05. Values with fainter text are >0.05.

Treatment speed (mm s^{-1})	10	20	30	40	50
control	0.884	0.977	0.147	0.921	1.000
10		0.491	0.652	0.355	0.791
20			0.037	1.000	0.995
30				0.022	0.102
40					0.969

The one way ANOVA and the multiple comparisons revealed that the halogen heating lamp treatment did not change the WPC surface roughness. However there were some differences between the treated samples. The 30 mm s^{-1} gave a significantly different ($p<0.05$) result to 20 mm s^{-1} (with mean difference 0.68) and 40 mm s^{-1} (with mean difference 0.73). Despite the fact that there were some differences, there was no evidence that the halogen heating lamp treatment alters the surface roughness of the WPC.

4.2.5.2 Scanning Electron Microscopy (SEM) observation

The Figure 4.49, Figure 4.50 and Figure 4.51 show the halogen heating lamps treated samples at the slowest speed, 10 mm s^{-1}, which produced the lowest adhesion strength among the treatments method speeds. The halogen heating lamps treatment produced samples with no noticeable changes in surface except that the surface was smoother, which had been observed in almost all treatments methods. The wood particles appear to be slightly less damaged than the control (compare Figure 4.6 with Figure 4.49). There is also a small crack between the polymer and the wood which is more visible in Figure 4.50. Wood decomposition is also observed in Figure 4.51.

Samples treated with a speed of 30 mm s^{-1} seen under low magnification (X134) (Figure 4.52) did not differ from the samples treated at 10 mm s^{-1} but at higher magnifications (X265 and X400) the wood damage is greater. Similar to the control samples, it is clear that the surface is scuffed and particle edges have been picked up during sanding (Figure 4.53b, 4.56). The wood particles are damaged and there are several cracks on the polymer surface.

a) **b)**

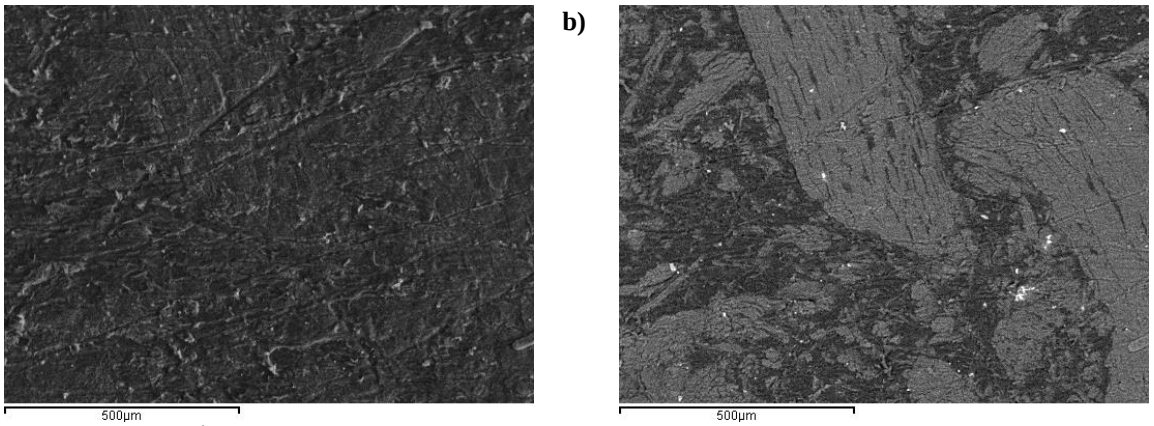

Figure 4.49: 10 mm s^{-1} halogen heating lamps treated sample under X134 magnification (X100 equipment indication). a) Backscattered image of the surface. b) same region seen as a secondary electron image.

a) **b)**

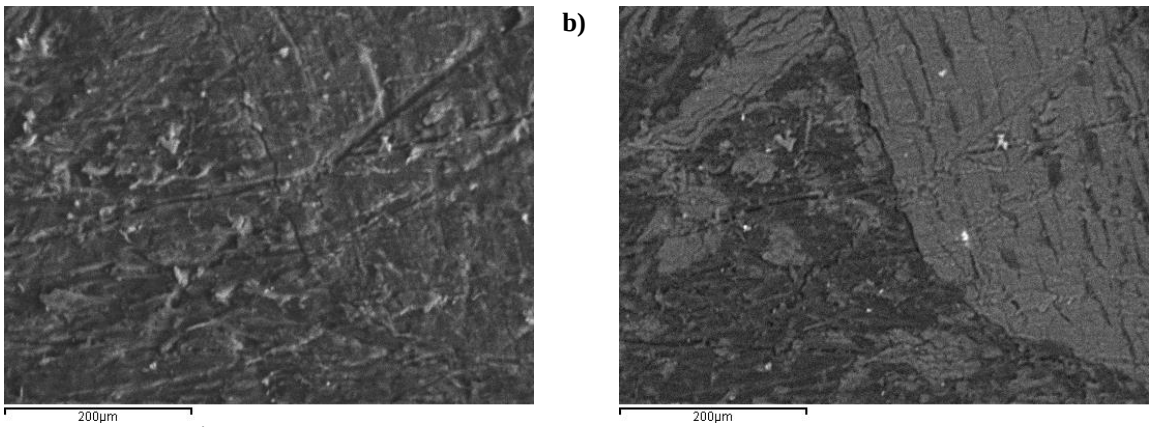

Figure 4.50: 10 mm s^{-1} halogen heating lamps treated sample under X265 magnification (X200 equipment indication). a) Backscattered image of the surface. b) same region seen as a secondary electron image.

a) b)

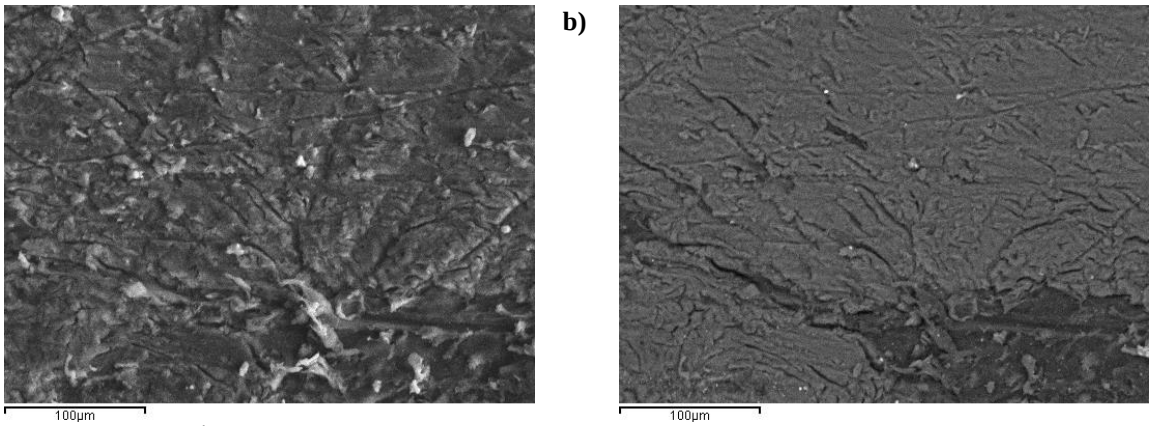

Figure 4.51: 10 mm s^{-1} halogen heating lamps treated sample under X400 magnification (X300 equipment indication). a) Backscattered image of the surface. b) same region seen as a secondary electron image.

a) b)

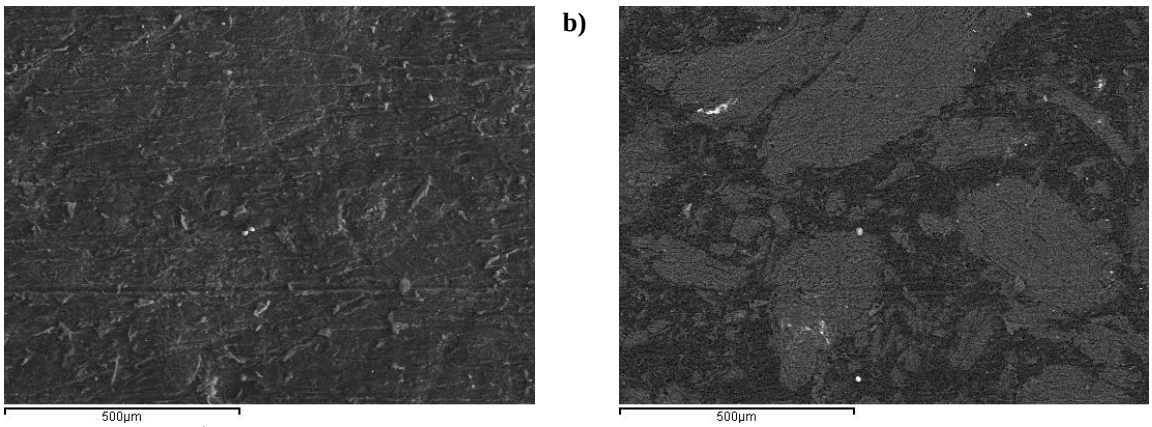

Figure 4.52: 30 mm s^{-1} halogen heating lamps treated sample under X134 magnification (X100 equipment indication). a) Backscattered image of the surface. b) same region seen as a secondary electron image.

a) **b)**

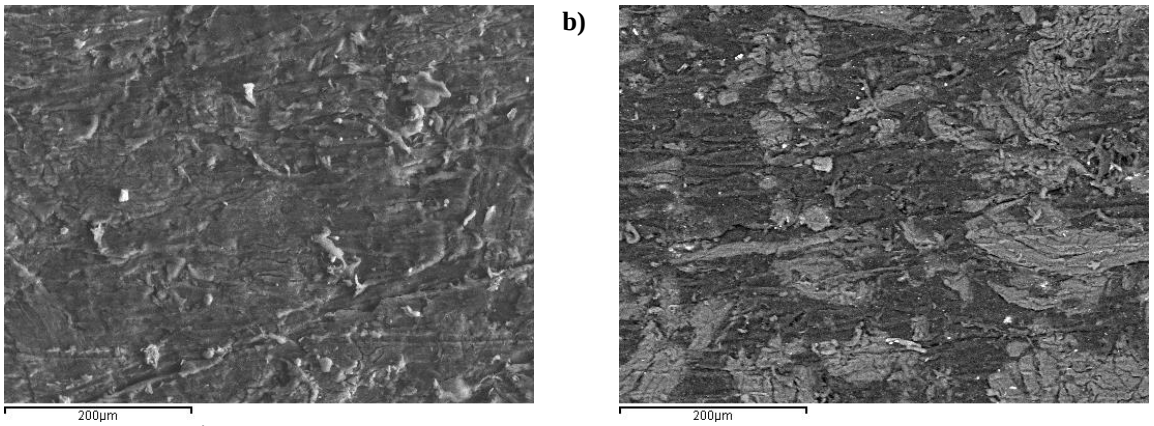

Figure 4.53: 30 mm s^{-1} halogen heating lamps treated sample under X265 magnification (X200 equipment indication). a) Backscattered image of the surface. b) same region seen as a secondary electron image.

a) **b)**

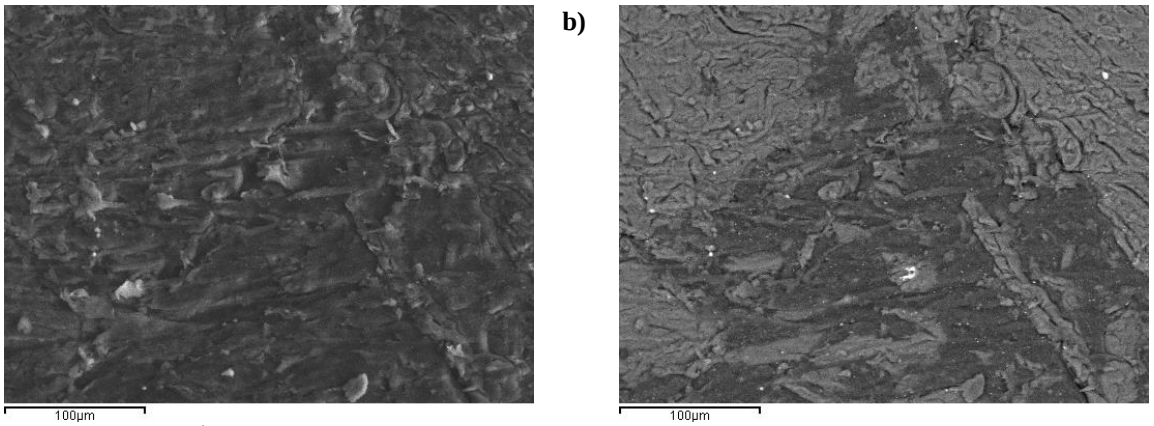

Figure 4.54: 30 mm s^{-1} halogen heating lamps treated sample under X400 magnification (X300 equipment indication). a) Backscattered image of the surface. b) same region seen as a secondary electron image.

4.2.5.3 Contact angle and surface energy determination

The halogen heating lamp treated samples were subjected to contact angle measurements and surface energy determination. The Levene test was not statistically significant, therefore the null hypothesis could not be eliminated (Flame treatment Levene statistic=2.258, p= 0.062). The results of the surface energy tests are presented in Figure 4.55.

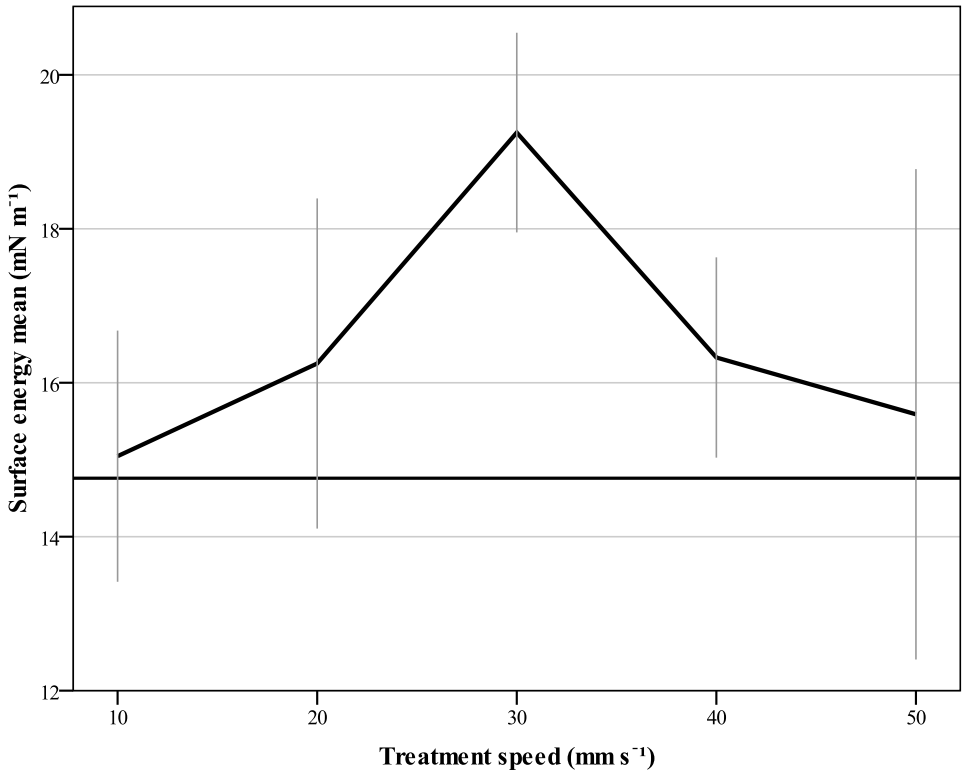

Figure 4.55: Halogen heating lamp treatment surface energy (mN m^{-1}). The flat line represents the control mean (14.76 mN m^{-1}). Error bars represent the SD (+/-1).

All the treated samples seemed to have a higher surface energy on the WPC. It is clearly that there is a trend between the surface energy of the samples treated with the halogen heating lamp and the treatment speed. The surface energy slightly increased from the control values at the slowest treatment speed (10 mm s^{-1}). As the treatment speed increased to 30 mm s^{-1}, the surface energy also increased to the higher surface energy of 19.25 mN m^{-1}. Thereafter, the surface energy decreased as the treatment speed increased. This trend was almost the same with the lap joint shear strength of the samples treated with the halogen heating lamps (Figure 4.5).

The descriptive statistics for the halogen heating lamp treatment method are presented in Table 4.30. The treated samples means ranged from 15.05 mN m^{-1} (10 mm s^{-1}) to

19.25 mN m^{-1} (30 mm s^{-1}). The smallest standard deviation among the halogen heating lamps treated samples was observed at the samples treated with the speed of 30 mm s^{-1} (SD=1.30) and the highest at the samples treated with the speed of 50 mm s^{-1} (SD=3.19).

Table 4.30: Mean values of halogen heating lamps treatment in mN m^{-1}. Standard Deviation (SD), Minimum and maximum values and the boundaries of the 95% CI of the surface energy.

Treatment speed (mm s^{-1})		Control	10	20	30	40	50
Average		14.76	15.05	16.25	19.25	16.33	15.59
Min		11.30	12.75	13.58	17.31	14.41	11.30
Max		16.05	17.26	19.93	21.54	18.15	22.02
95% CI	Lower Bound	13.68	13.88	14.72	18.32	15.40	13.31
	Upper Bound	15.83	16.21	17.78	20.18	17.26	17.87
SD		1.50	1.63	2.14	1.30	1.30	3.19

The F-test revealed that the halogen heating lamp speed of the treatment was statistically significantly related to WPC surface energy as F=6.835 for significance level $p<0.001$. Therefore the null hypothesis could be eliminated.

To investigate the differences between the treatment variances the Post-Hoc HSD multiple comparisons test was used. The statistically significant differences between treatment speeds and surface energy are presented in Table 4.31.

Table 4.31: Halogen heating lamp treatment multiple comparison test results (p values). Statistical significant differences for p<0.05. Values with fainter text are >0.05.

Treatment speed (mm s^{-1})	10	20	30	40	50
Control	0.999	0.534	0.000	0.477	0.930
10		0.742	0.000	0.688	0.989
20			0.014	1.000	0.974
30				0.018	0.001
40					0.958

The only statistically significant difference, of the treated samples with the control samples, was observed at the samples treated with the speed of 30 mm s^{-1}, for significance level of $p<0.001$. Also, the samples treated with the speed of 30 mm s^{-1} were statistically significantly different from all of the other treated samples, whilst there was no difference between any of the other of the treated samples.

Therefore one way ANOVA, clearly showed that the samples treated with the speed of 30 mm s^{-1}, produced the highest surface energy of the samples treated with the halogen

heating lamps. However, it also showed that the other treatment speeds did not statistically significantly change the WPC surface energy.

4.2.5.4 FTIR chemical analysis determination

From each sample 5 spectra were taken. The average of the 5 spectra (Figure 4.56) was used to measure the absorption band height ratio of each sample.

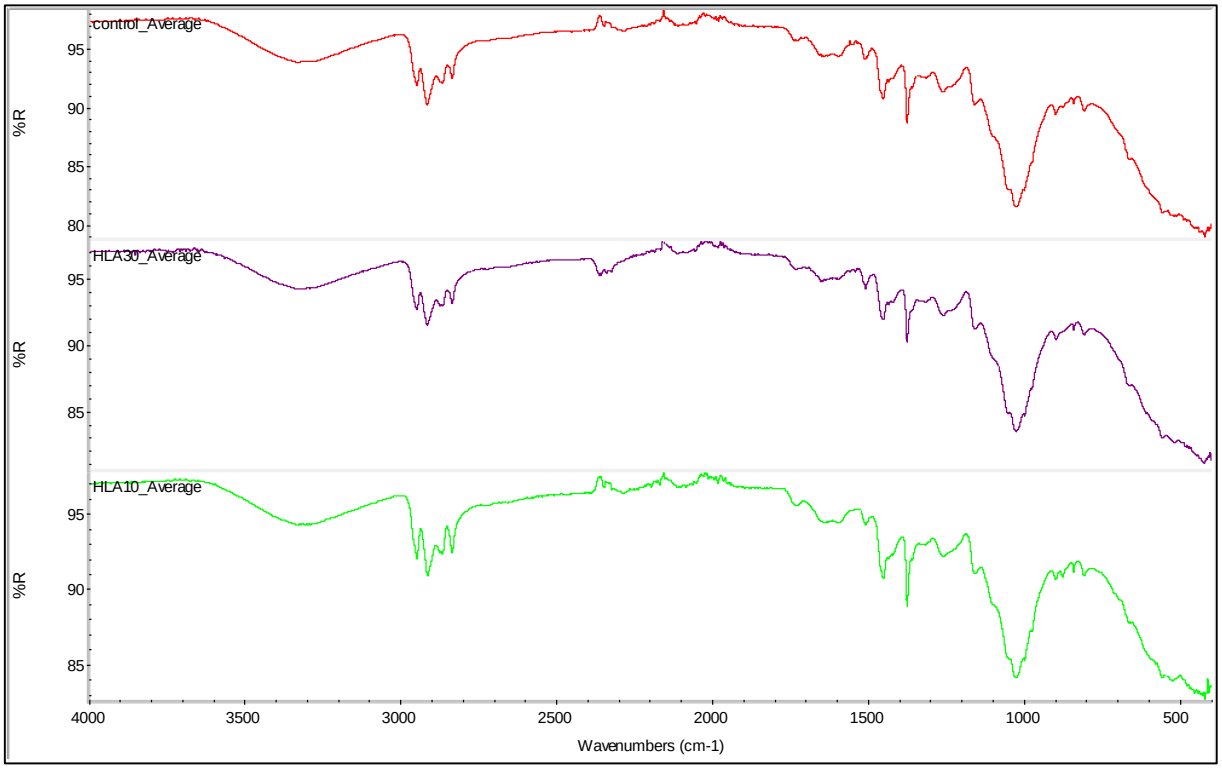

Figure 4.56: FTIR-ATR spectra of untreated samples and halogen heating lamp treated with the speeds of 10 mm s^{-1} and 30 mm s^{-1}.

By studying the peak heights percentages presented in Figure 4.57 and Table 4.32, it was not possible to categorize the peaks trends into groups. The only similar trends seem to be the peaks at 3338 cm^{-1} and 3284 cm^{-1}, and wavenumber bands 1263cm^{-1} with the 1230cm^{-1}, and the 1422 cm^{-1} with the 1454 cm^{-1}.

Table 4.32: Peaks height percentages of the samples treated with halogen heating lamp.

	Treatment speed (mm s^{-1})				
Wavenumbers cm^{-1}	10	20	30	40	50
3338	-17%	-9%	-1%	-10%	-9%
3284	-16%	-10%	0%	-10%	-9%
1732	12%	4%	29%	25%	1%
1656	-6%	-29%	1%	-2%	-22%
1595	-2%	-26%	-7%	-8%	-21%
1454	3%	-8%	5%	-1%	-6%
1422	7%	-13%	2%	-3%	-11%
1375	1%	-3%	-1%	-2%	-3%
1263	-13%	-11%	4%	-6%	-5%
1230	-12%	-12%	5%	-7%	-5%
1022	-14%	-12%	7%	-5%	1%

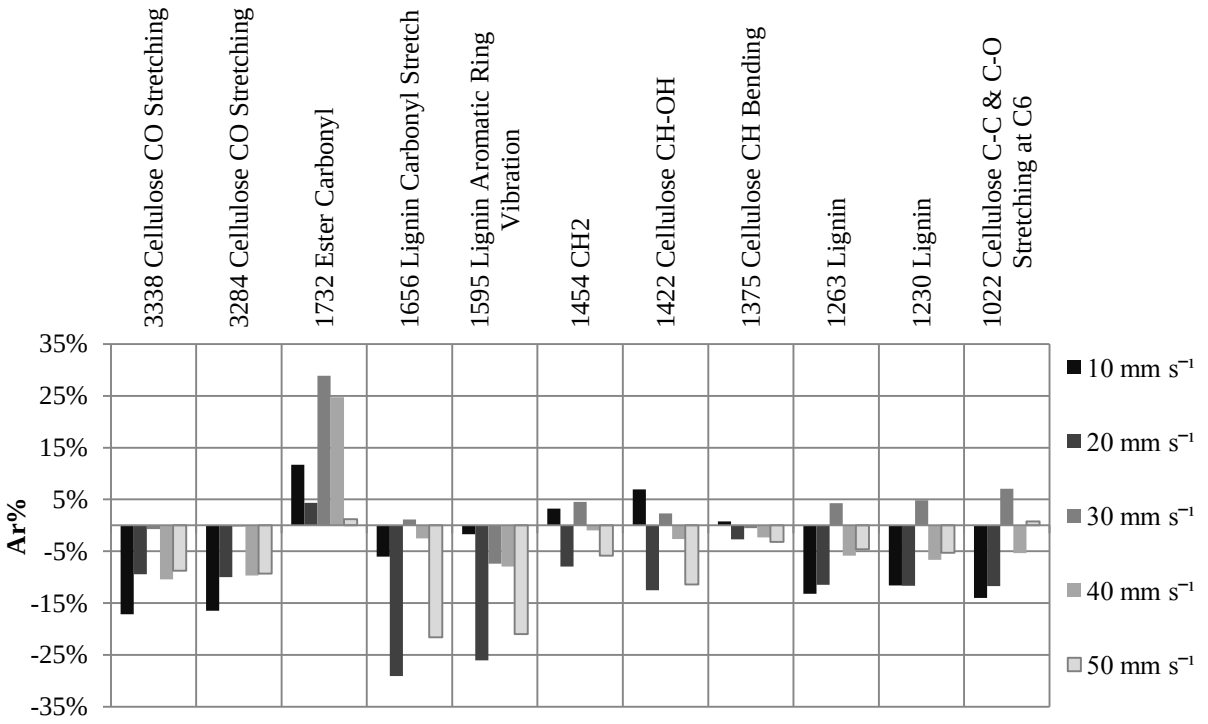

Figure 4.57: FTIR ATR ratio percentage of halogen heating lamp treated samples.

The carbonyl ester peak (1732 cm^{-1}) of all lamp treated samples increased compared to the untreated control samples. The highest percentage change was observed with the 30 mm s^{-1} samples, which also had the highest surface energy. This is the only linkage observed between the esters and the surface energy increment. However despite the fact that the 40 mm s^{-1} samples had almost the same ester percentage as the 30 mm s^{-1} samples, the surface energy was not significantly different from the untreated samples. The peaks heights of the 20 mm s^{-1} and 50 mm s^{-1} treated samples were similar to the untreated control samples.

The peak height percentages for both 3338 cm^{-1} and 3284 cm^{-1} wavenumbers show identical behaviour. The slowest speed samples (10 mm s^{-1}) decreased by *ca*. -16%. The 30 mm s^{-1} treated samples were not different from the untreated samples and the samples treated with the speeds of 20 mm s^{-1}, 40 mm s^{-1} and 50 mm s^{-1} decreased by about -9%.

The 1263 cm^{-1} and 1230 cm^{-1} wavenumbers bands peaks refer to lignin. The peak height percentage of the samples treated with the lowest treatment speeds of 10 mm s^{-1} and 20 mm s^{-1} decreased by around the same value of -12%. The peak heights of the rest of the treated samples were not significantly different from the untreated samples, with values no more than -7%.

The peak height percentage of the CH_2 (1454 cm^{-1}), of the samples treated with the speed of 20 mm s^{-1} and 50 mm s^{-1}, were decreased to about the same percentage of -7%. The rest of treated samples were not significantly different from the control samples. Likewise the peak height percentage of the cellulose CH-OH (1422 cm^{-1}) of the samples treated with the speeds of 20 mm s^{-1} and 50 mm s^{-1} were decreased by about -12%. The only difference from the peak of 1454 cm^{-1} wavenumber was that the samples treated with the speed of 10 mm s^{-1} was slightly increased to 7%. The remaining treated samples were not markedly different to the untreated control samples.

The lignin carbonyl stretch (1656 cm^{-1}) was reduced in all treated samples. The highest differences of the peak heights were observed for the samples treated at 20 mm s^{-1} (-29%) and 50 mm s^{-1} (-22%). The rest of the peak heights were not markedly changed; a slight decrease of -6% occurred for the 10 mm s^{-1} samples.

The lignin aromatic ring vibration (1595 cm^{-1}) was also reduced in all treated samples. The 20 mm s^{-1} and 50 mm s^{-1} samples had similar peaks height percentages (-26% and -21% respectively) and those for 30 mm s^{-1} and 40 mm s^{-1} decreased at almost the same percentage of -7% and -8% respectively.

The peak height percentage of the cellulose CH bending (1375 cm^{-1}) of all the treated samples did not show any difference to the untreated control samples.

The peak heights percentages of the cellulose C-C and C-O stretching at C_6 (1022 cm^{-1}) for 10 mm s^{-1} and 20 mm s^{-1} treatment speeds were around -13% and those for 30 mm s^{-1} increased to 7%. The rest of the treated samples were not different to the untreated samples.

4.2.6 SURFACE CHARACTERIZATION SUMMARY

According to surface roughness the samples treated with flame and hydrogen peroxide appeared to produce the rougher surface in contrast to control among all the treatments. The surface roughness increase of the hydrogen peroxide treated samples could be a result of the wood particles degradation by swelling as it shown in the SEM photos. The flame treated samples showed the highest increase in the surface roughness, probably caused by the formed pits which were observed in the SEM photos. Halogen heating lamps also appear to have a slightly rougher surface than the control samples but significantly smoother than the previous two, without however been any noticeable difference appeared on the SEM photos. The samples treated with hot air on the other hand seemed to produce a smoother than the control samples surface. This might be explained by the partial melt of the polymer which could operate as a filer within the surface peaks and valleys.

The surface energy which is related to the wettability of the material, as the only solvent used was water, revealed that the samples treated with flame and halogen heating lamps had the highest mean values. The flame treated samples however had the highest mean values. The hydrogen peroxide samples and the hot air samples did not seem to cause a significant change in the wettability of the material.

The chemical analysis showed that all treatments seemed to alert the chemistry of the material. In particular the ester peak wais increased in all treatments except of the hydrogen peroxide treated samples. It seems that the hydrogen peroxide treatment reacts differently on the samples surface than the other treatments.

4.3 AESTHETIC SURFACE CHANGES

The aesthetic appearance is an important factor for constructions like furniture. The colour change which might occur on the surface could produce an improper surface for the final product. Another factor that defines the aesthetic appearance of a material, is the texture. The observation with the use of a light microscopy could provide information about potential changes on the surface texture of the material. The different colour of the light microscopy images are due to different settings of the microscopy camera and not caused by the modification.

4.3.1 CONTROL SAMPLES

4.3.1.1 Light microscopy observation

The surface of the control sample seemed scuffed due to sanding (Figure 4.58) and clearly visible are some abrasion lines on the surface (arrowed). However the surface did not have any noticeable texture differences between the wood particles and the polymer.

A 3D model (Figure 4.59) is produced according to the camera focus of the microscope, so the accuracy is not guaranteed. However it may provide a general idea of the surface texture and peaks and troughs are visible on the surface, evenly spread on the surface.

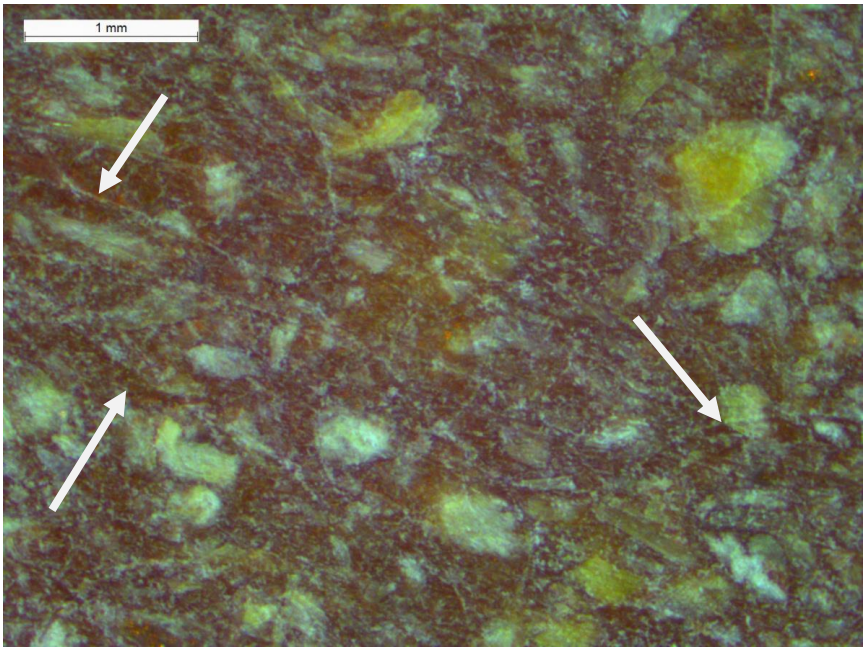

Figure 4.58: Light microscopy (X2.5 equipment indication). Untreated sample. Arrows showing abrasion lines on the surface. Those lines were absence on the surface before sanding.

Figure 4.59: 3D model of untreated sample.

4.3.1.2 Colour determination

For the colour determination test, 2 areas per sample were scanned. The tested area was a circular area with a radius of 1 cm. The colour values of the untreated samples were L^*=40.47, a^*=5.05 and b^*=7.01. The L^* value shows the white-black colour of the sample surface. The a^* value represents the red-green colour of the samples. Because the a^* values are slightly above 0, the samples are more red than green. The b^* value refers to the yellow-blue colour. The positive b^* values shows that the samples colour is more yellow than blue.

4.3.2 HYDROGEN PEROXIDE TREATMENT

4.3.2.1 Light microscopy observation

The figures presented below, show the sample surface appearance before and after hydrogen peroxide treatment. The light microscopy pictures illustrate that the surface modification was more intense as the pH increased (Figure 4.60 and Figure 4.61). The surface seemed to become smoother, and the wood particles became more visible than before the treatment. Clearly the wood particle visibility could be hypothetically explained by the WPC pigment bleaching. H_2O_2 is a strong oxidizing agent and has a great bleaching effect (Lu, 2006).

In addition, in the pH 9 and pH 8.5 treated samples (Figure 4.62) the appearance of crystals which had formed on the surface are clearly observed. This crystalline formation indicates the presence of water soluble material which formed on the surface during treatment. Figure 4.63 shows that the crystal material disappears after being rinsed with water. The formed crystals could be Low Molecular Weight Oxidized Material (LMWOM) which is usually appeared on polymer treated surface after corona discharge treatment causing materials an increase in wetability but a reduction in the adhesion strength (Jones, et al, 2005). However it is more likely to be NaOH on the surface after treatment. This hypothesis is supported by the fact that the deionised water pH increased after rinsing the treated samples. The deionised water pH was measured before and after samples wash, leading to a great increase in pH observation. The crystalline formed material however, did not affect the shear strength results because it had been removed from the surface after water rinsing prior to bonding and testing of the lap joint specimens.

a) b)

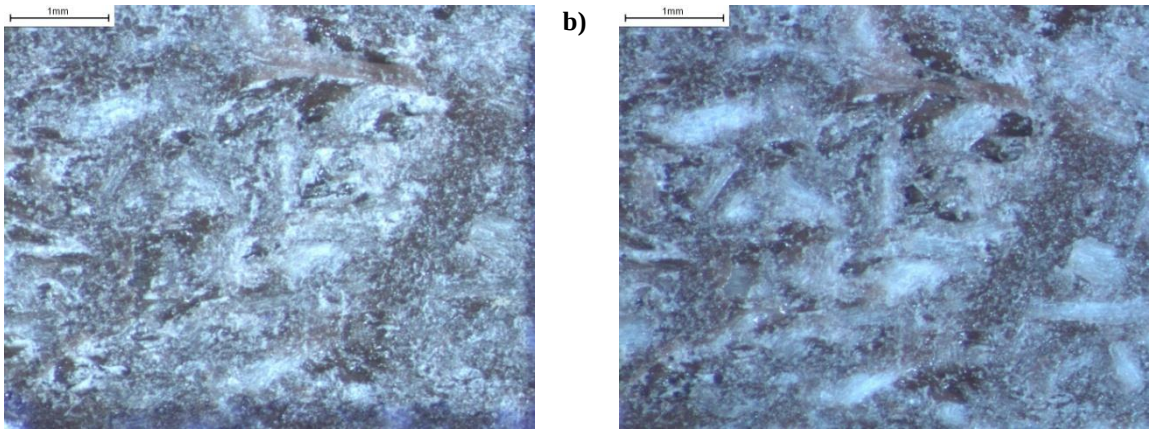

Figure 4.60: Light microscopy (X2.5 equipment indication). Before (photo a) and after treatment in pH 8.5 hydrogen peroxide solution (photo b).

a) b)

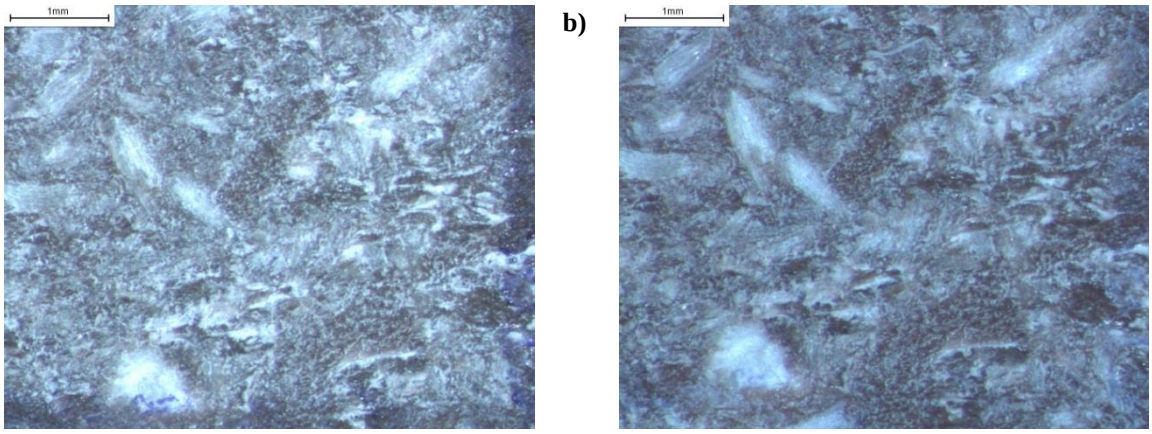

Figure 4.61: Light microscopy (X2.5 equipment indication). Before (photo a) and after treatment in pH 7.5 hydrogen peroxide solution (photo b).

a) b)

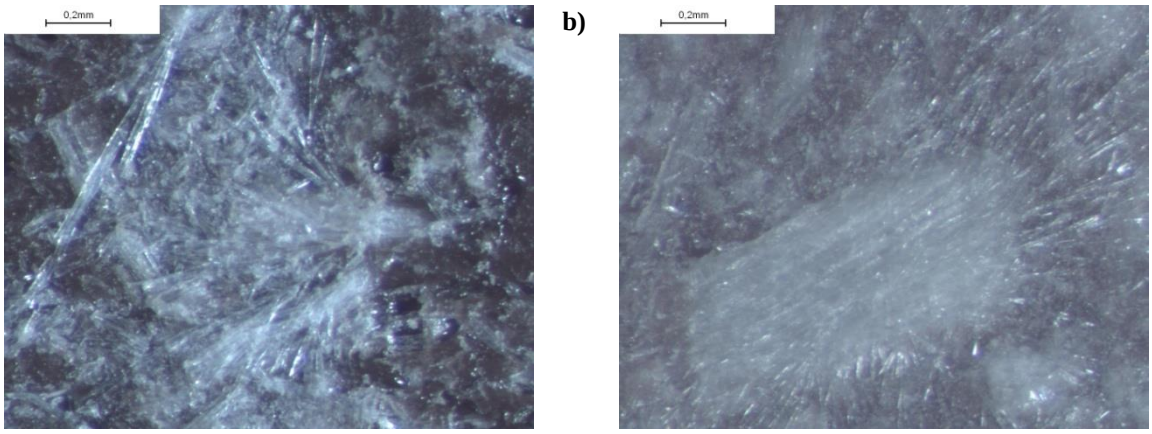

Figure 4.62: Light microscopy (X4 equipment indication). pH 8.5 (photo a) and pH 9 (photo b) hydrogen peroxide treated samples. Appearance of crystalline material.

a) b)

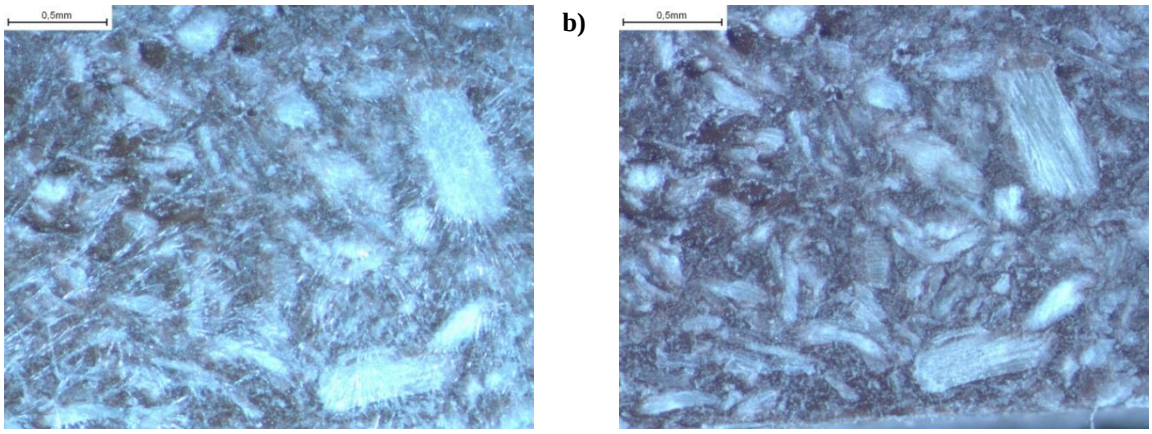

Figure 4.63: Light microscopy (X2.5 equipment indication). Sample treated in pH 9 hydrogen peroxide solution before (photo a) and after rinsed with water (photo b).

Figure 4.64 clearly shows that there are peaks and troughs in the surface of the sample treated in hydrogen peroxide solution. The peaks are mainly wood particles although the surface of the untreated sample did not show wood particles forming peaks (Figure 4.59). This could be the result of wood particle swelling after the hydrogen peroxide treated surface forming peaks caused by water absorption during the treatment procedure.

Figure 4.64: 3D model of treated sample in pH 7.5 solution.

4.3.2.2 Colour changes determination

The colour changes are presented as the ΔE value which is illustrates the grade of the colour change which took place after each treatment in contrast to the untreated WPC colour. It is calculated according the method described in section 3.2.6. Results for hydrogen peroxide measurement are presented in Figure 4.65.

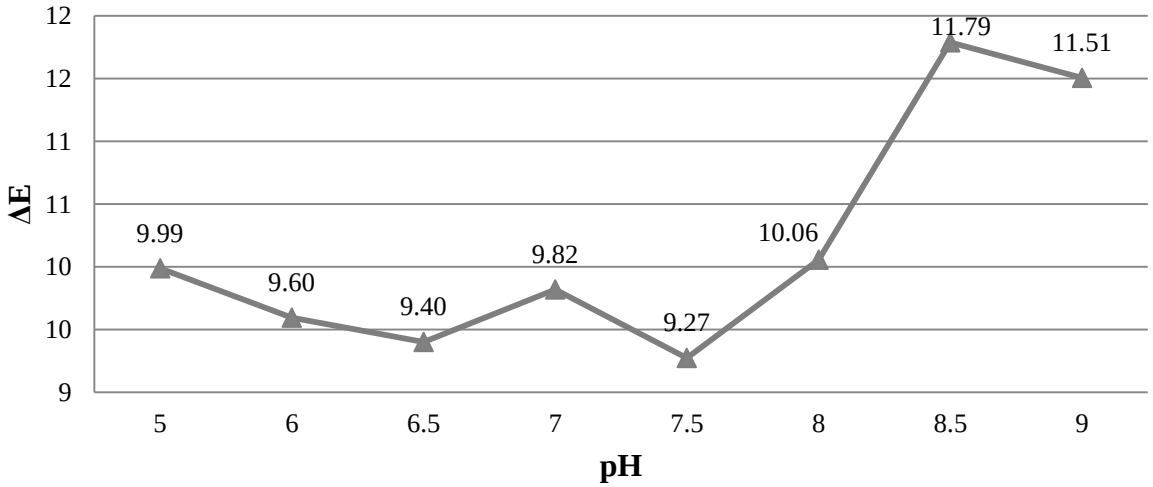

Figure 4.65: Hydrogen peroxide treatment colour changes ΔE.

According ΔE values all samples treated with hydrogen peroxide solutions appear to have changed colour. The ΔE values vary from 9.40 (pH 6.5) to 11.79 (pH 8.5). All hydrogen peroxide treated samples have similar colour difference from the untreated WPC with exception of the samples treated in pH 8.5 and pH 9 solution which are appear to have higher ΔE values (Figure 4.65).

In Figure 4.66 the values that are used to calculate the ΔE value are presented.

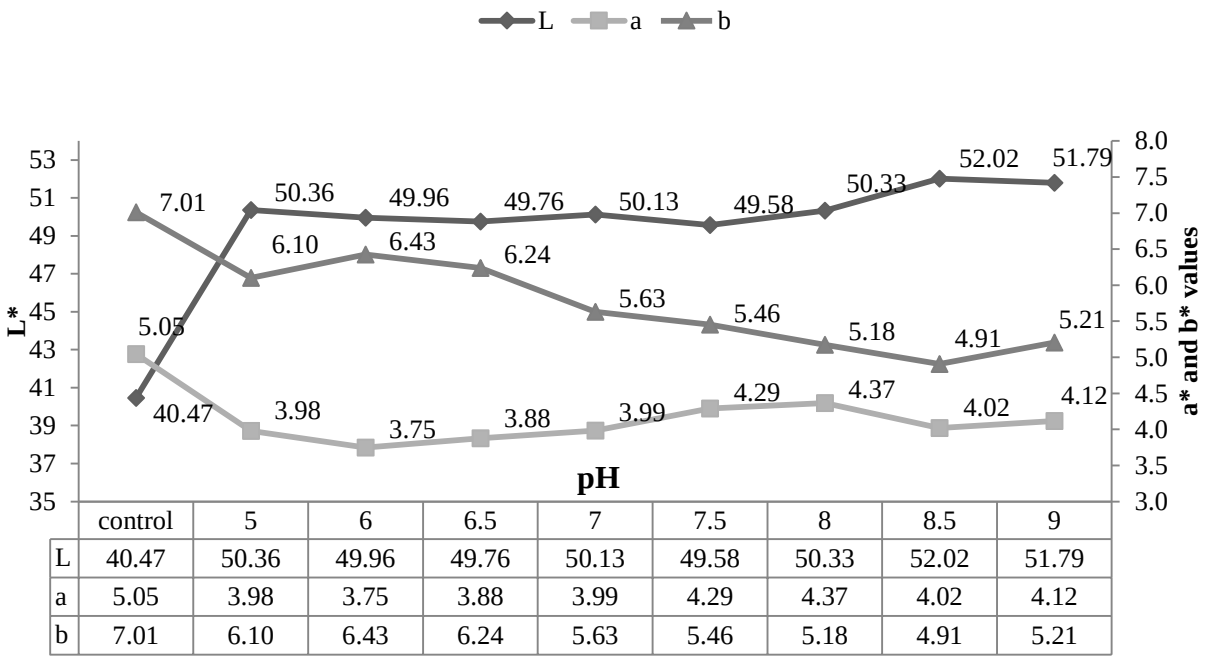

	control	5	6	6.5	7	7.5	8	8.5	9
L	40.47	50.36	49.96	49.76	50.13	49.58	50.33	52.02	51.79
a	5.05	3.98	3.75	3.88	3.99	4.29	4.37	4.02	4.12
b	7.01	6.10	6.43	6.24	5.63	5.46	5.18	4.91	5.21

Figure 4.66: Hydrogen peroxide treatment colour determination values. "a" refers to red for positive values and green for negative. "b" refers to yellow for positive values and blue for negative. "L" refers to white for 100 value and black as the value decreasing to 0.

The L^* value shows the white-black change on the sample surface. The values are varying from 40.47 (control) to 52.02 (pH 8.5). It is clear that the samples treated in hydrogen peroxide solution are becoming whiter than the untreated WPC, but this does not seem to differ with pH. The bleaching effect of the hydrogen peroxide solution shown by the colour changes determination agrees with the study by Lu (2006).

The a^* value represents the red-green colour of the samples. Because the a^* values are slightly above 0, the samples are more red than green. The a^* values vary from 3.75 (pH 6) to 5.05 (control). In all treated samples the a^* value is reduced and stabilized in about the same value so treated samples are less red. The a^* value difference does not seem to be important as the highest difference which occurred between the control samples and the samples treated in pH 6 solution was 1.3.

The b^* value refers to the yellow-blue colour. The positive b^* values shows that the samples colour is more yellow than blue. The b^* values vary from 4.91 (pH 8.5) to 7.01 (control): treated samples are less yellow. There is no big difference of the b^* value among the treated samples but there is a trend of decreasing values as the pH increases. The b^* value does not seem to have significant differences compared to the other treated and untreated samples as the highest difference of b^* value was 2.1 and observed between control and pH 8.5 treated samples. However the highest difference of the b^* value between treated and untreated samples was greater than the highest a^* value difference (1.3).

4.3.3 HOT AIR TREATMENT

4.3.3.1 Light microscopy observation

Figure 4.67 present the appearance of hot air treated samples under light microscopy observation. The samples treated with hot air (Figure 4.67a and b) showed little difference to the untreated sample (Figure 4.58). The only difference was the slightly darker colour of the samples treated with the slowest speed of 18.5 mm s^{-1} (Figure 4.67b) in contrast with the samples treated with two pass of faster hot air speed of 75 mm s^{-1} (Figure 4.67a). However this colour difference could be due to the auto setting configuration of the microscope camera.

a) **b)**

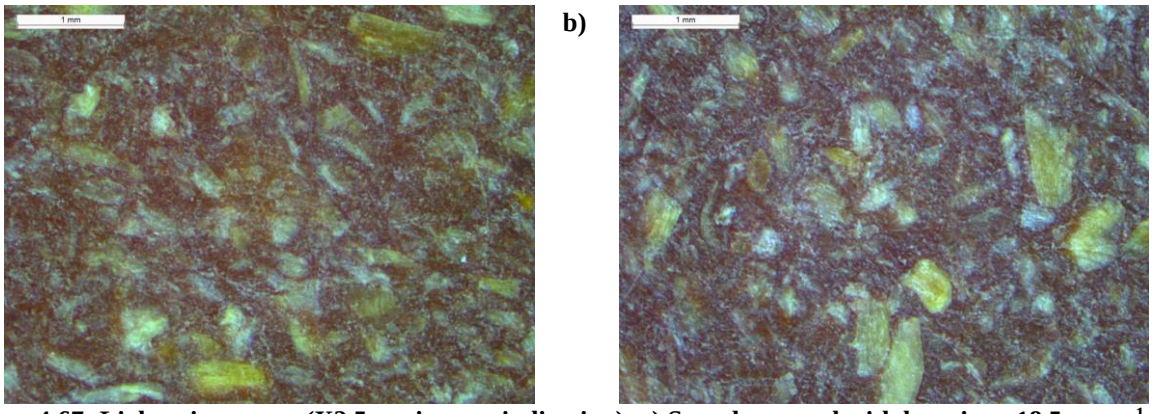

Figure 4.67: Light microscopy (X2.5 equipment indication). a) Sample treated with hot air at 18.5 mm s^{-1}. b) Two times treated samples at 75 mm s^{-1}.

The 3D model (Figure 4.68) shows the surface texture of the hot air treated sample. By comparing the hot air treated 3D with the untreated sample (Figure 4.59) it can be seen that the surface is essentially similar.

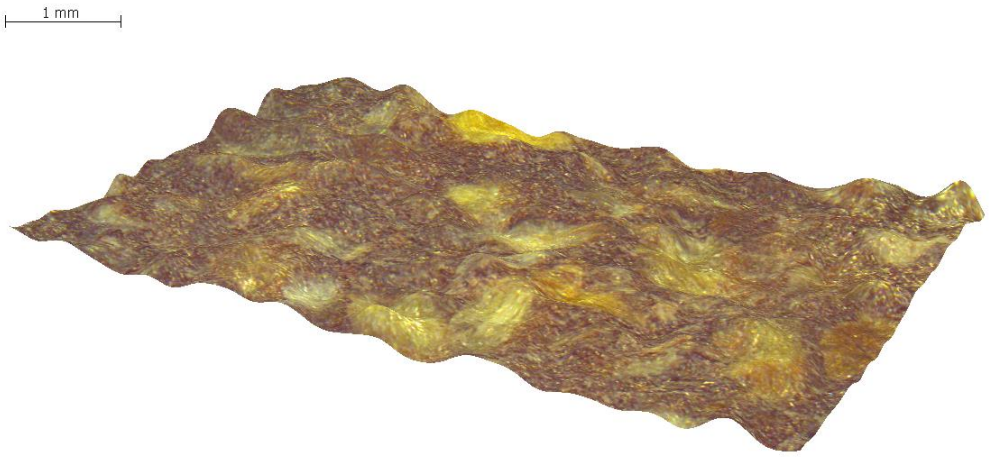

Figure 4.68: 3D model of hot air treated sample with 2 passes at 75 mm s^{-1}.

4.3.3.2 Colour changes determination

The hot air treatment colour differences (ΔE) are presented in Figure 4.69 and the data used to calculate this are in Figure 4.70.

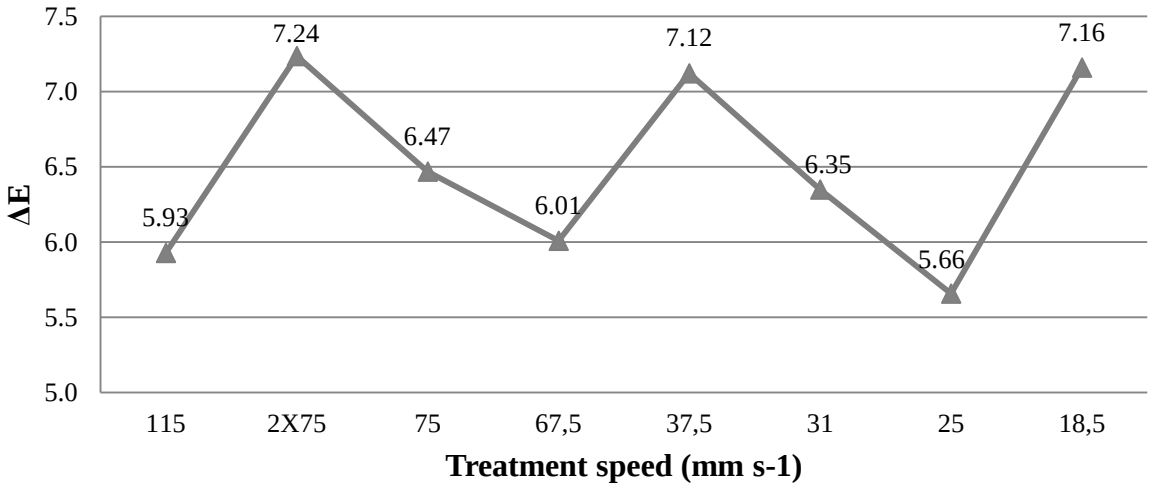

Figure 4.69: Hot air treatment colour changes ΔE.

The ΔE values indicate that some colour changes occur with heat treatment irrespective of treatment speed, although there is no clear trend. The ΔE values vary from 5.66 (25 mm s^{-1}) to 7.24 (2X75 mm s^{-1}) and this variation may be random deviation. However the samples treated with the speed of 37.5 mm s^{-1} had similar ΔE value to the 2X75 mm s^{-1} treated samples. In this case both sets of samples were subjected for the same amount of time to hot air.

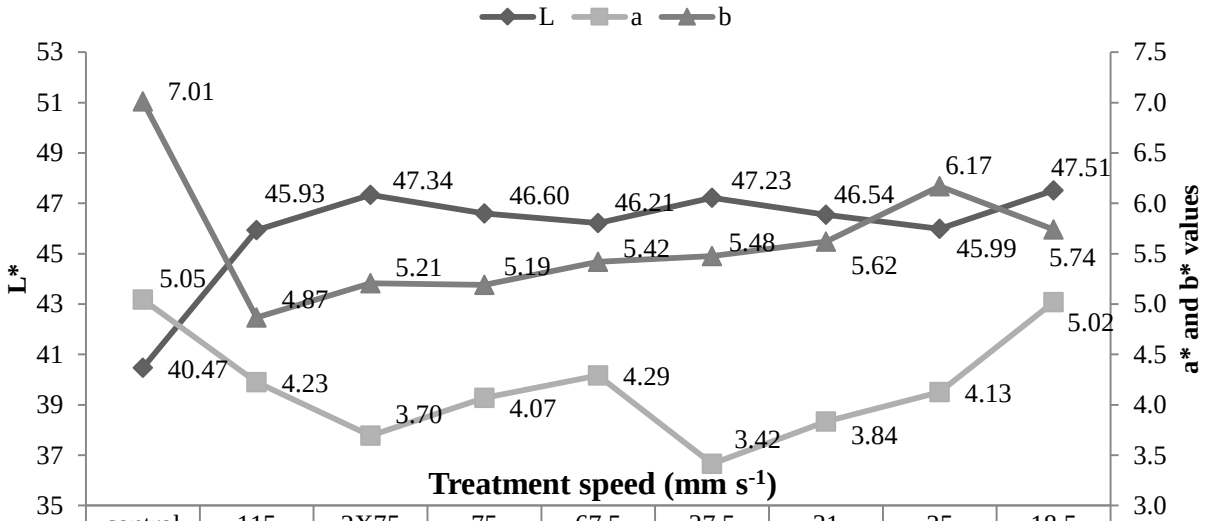

	control	115	2X75	75	67,5	37,5	31	25	18,5
L	40.47	45.93	47.34	46.60	46.21	47.23	46.54	45.99	47.51
a	5.05	4.23	3.70	4.07	4.29	3.42	3.84	4.13	5.02
b	7.01	4.87	5.21	5.19	5.42	5.48	5.62	6.17	5.74

Figure 4.70: Hot air treatment colour determination values. "a" refers to red for positive values and green for negative. "b" refers to yellow for positive values and blue for negative. "L" refers to white for 100 value and black as the value decreasing to 0.

The L^* value of the hot air treated samples vary from 40.47 (control) to 47.51 (18.5 mm s^{-1}) and are consistently higher than the untreated WPC, so the surface becomes slightly brighter. There are no significant differences between the treatment speeds (Figure 4.70).

The a^* value varies from 5.05 (control) to 3.42 (37.5 mm s^{-1}) but this seems to be a small difference between the treated and untreated samples. On the other hand, the b^* values drop by a larger amount when the samples treated with hot air, from 7.01 (control) to 4.87 (115 mm s^{-1}). The hot air treated samples b^* values do not significantly differ as the treatment speed changes. Therefore all hot air treated samples had a less yellow but bluer surface (Figure 4.70).

4.3.4 FLAME TREATMENT

4.3.4.1 Light microscopy observation

Light microscopy clearly reveals appearance of the wood particles in the polymer matrix after flame treatment (Figure 4.71) By comparing the control surface in Figure 4.59 with the samples treated with flame in Figure 4.71a and b, it is apparent that the surface wood fibres were exposed to flame treatment. This surface alteration is more intense on the sample treated with the lowest treatment speed of 125 mm s^{-1} (Figure 4.71a) than the sample treated with highest speed of 250 mm s^{-1} (Figure 4.71b).

a) b)

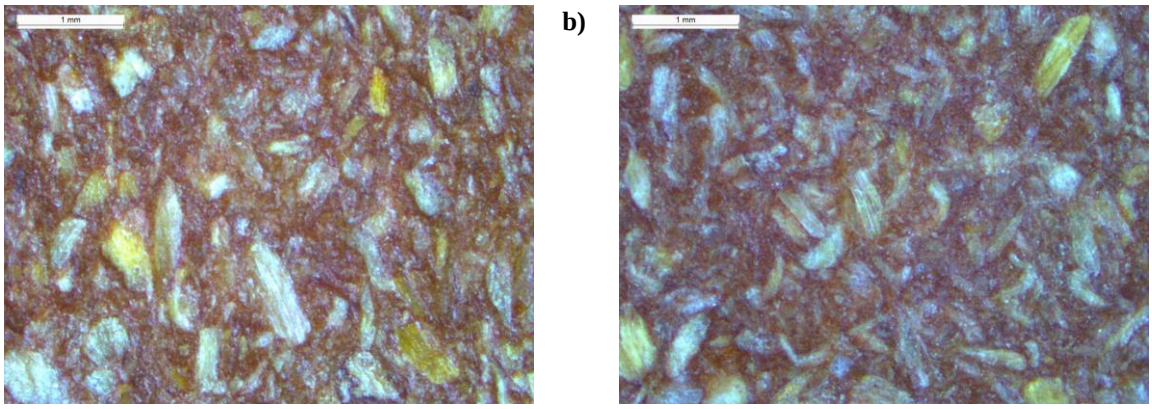

Figure 4.71: Light microscopy (X2.5 equipment indication). a) Flame treated sample with the speed of 125 mm s^{-1}. b) Flame treated sample at 250 mm s^{-1}.

The 3D model of a sample treated at the slowest speed (125 mm s^{-1}) (Figure 4.72) clearly shows that the wood fibres forms peaks on the surface and the polymer forms the troughs. This indicates that the polymer has partly melted due to the flame treatment, and the wood fibres were exposed on the surface. Thus as the speed decreases the wood fibre exposure increases. This could also explain why the surface roughness increases with flame treatment.

Figure 4.72: 3D model of flame treated sample at 125 mm s^{-1}.

4.3.4.2 Colour changes determination

The ΔE values for the flame treated samples (Figure 4.73) have the same colour difference from the untreated WPC, with the exception of the samples treated at the slowest speed (125 mm s^{-1}), where the ΔE is slightly greater.

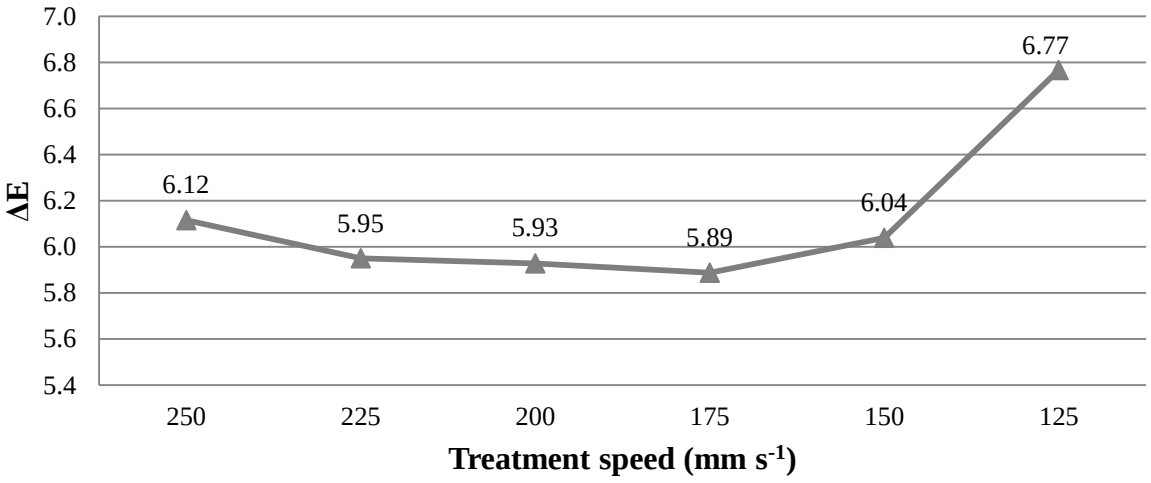

Figure 4.73: Flame treatment colour changes ΔE.

The colour coordinates for the flame treated samples (Figure 4.74) are represented by the L*, a* and b* values.

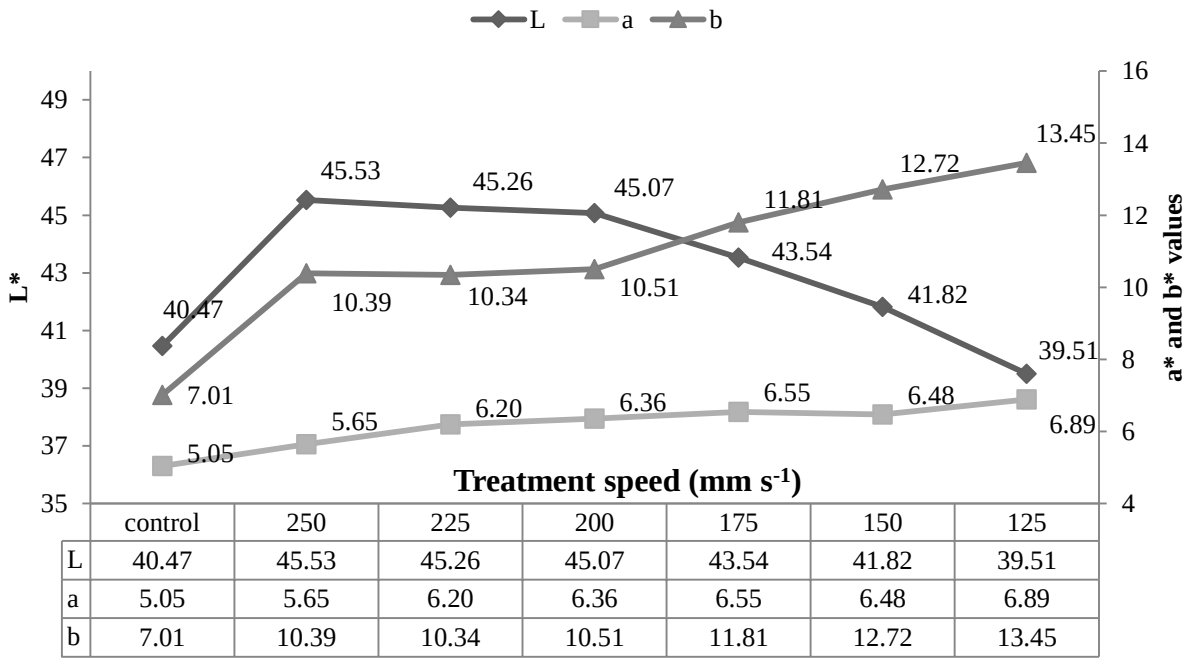

	control	250	225	200	175	150	125
L	40.47	45.53	45.26	45.07	43.54	41.82	39.51
a	5.05	5.65	6.20	6.36	6.55	6.48	6.89
b	7.01	10.39	10.34	10.51	11.81	12.72	13.45

Figure 4.74: Flame treatment colour determination values. "a" refers to red for positive values and green for negative. "b" refers to yellow for positive values and blue for negative. "L" refers to white for 100 value and black as the value decreasing to 0.

The L^* values vary from 39.51 (125 mm s^{-1}) to 45.53 (250 mm s^{-1}). There are L^* value increases relative to the control values at the faster treatment speeds (200-250 mm s^{-1}). This then decreases with decreasing treatment speed to values similar to the control at the slowest treatment speed (125 mm s^{-1}). This confirms the burnt appearance of these specimens.

The a^* values show slight increases with reduced treatment speed. The values vary from 5.05 (control) to 6.89 (125 mm s^{-1}), i.e. samples become redder.

The b^* value also increases with reduced treatment speed. Even at fast treatment speeds (200-250 mm s^{-1}) there is a marked change from the control values and this then further increases at slower speeds, almost linearly. The b^* values vary from 7.01 (control) to 13.45 (125 mm s^{-1}), corresponding to an increase in yellowness as the treatment speed is reduced to 125 mm s^{-1}.

4.3.5 HALOGEN HEATING LAMP TREATMENT

4.3.5.1 Light microscopy observation

Light microscopy reveals little difference of the halogen lamp treated surfaces as compared to the untreated control samples (Figure 4.75).

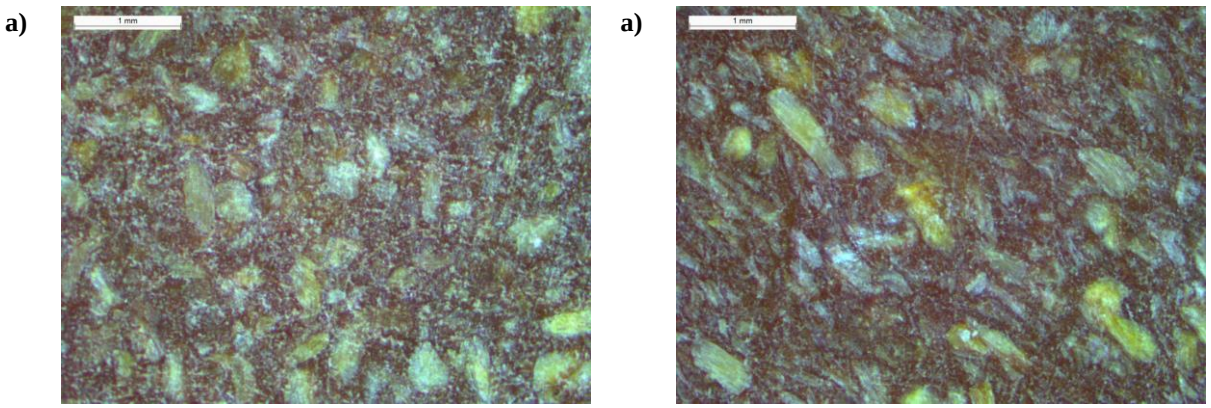

Figure 4.75: Light microscopy (X2.5 equipment indication). a) Sample treated with halogen heating lamps at 10 mm s^{-1}. b) Sample treated with halogen heating lamps at 30 mm s^{-1}.

The 3D model (Figure 4.76), of the treated sample is similar to the untreated control sample.

Figure 4.76: 3D model of halogen heating lamps treated sample with the speed of 10 mm s^{-1}.

4.3.5.2 Colour determination

The halogen heating lamps samples treated show slight colour differences, ΔE, (Figure 4.77) as the treatment speed is changed. The values varied from 4.87 (20 mm s^{-1}) to 6.14 (10 mm s^{-1}). The slowest treatment (10 mm s^{-1}) had the higher colour difference, as the samples had been more exposed to heat.

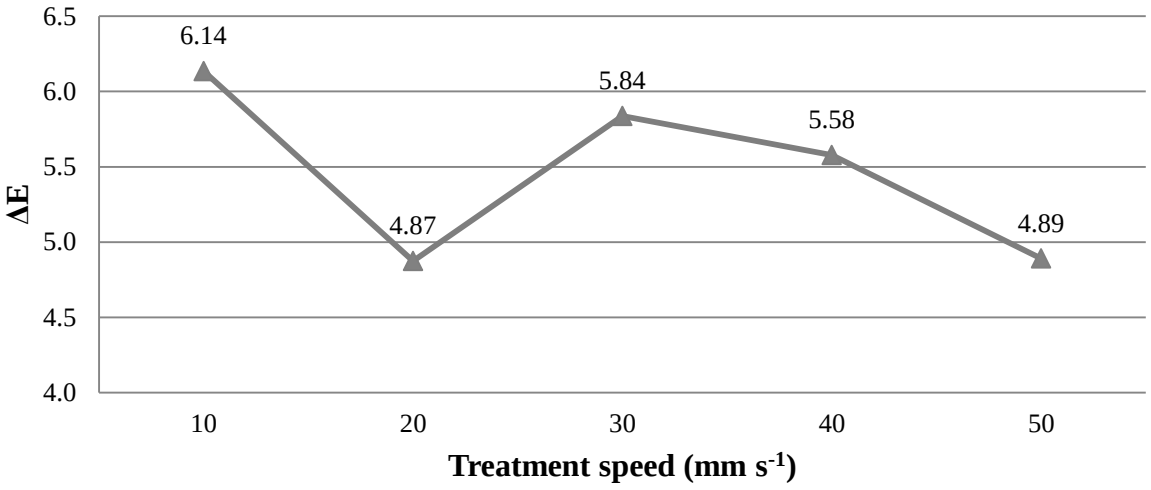

Figure 4.77: Halogen heating lamps treatment colour changes ΔE.

The values that are used to calculate the ΔE value are presented in Figure 4.78.

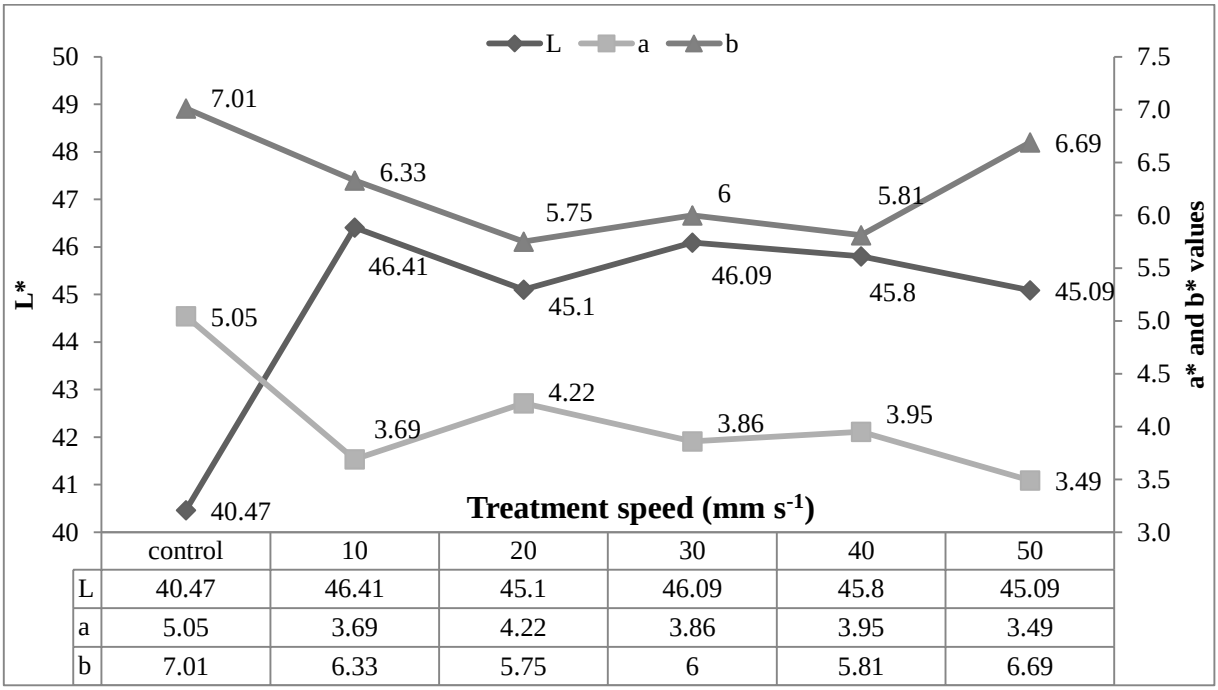

	control	10	20	30	40	50
L	40.47	46.41	45.1	46.09	45.8	45.09
a	5.05	3.69	4.22	3.86	3.95	3.49
b	7.01	6.33	5.75	6	5.81	6.69

Figure 4.78: Halogen heating lamps treatment colour determination values. "a" refers to red for positive values and green for negative. "b" refers to yellow for positive values and blue for negative. "L" refers to white for 100 value and black as the value decreasing to 0.

The L^* value appeared to increase by a similar amount for all treatments.. The control L^* value was 40.47 while treated samples ranged from 45.09 for 50 mm s^{-1} to 46.41 for 10 mm s^{-1}.

The a^* values varied from 3.49 (50 mm s^{-1}) to 5.05 (control), although there are only minor differences in the a^* values of the treated samples. There was a decrease in the a^* values for the halogen heating lamps treated samples, but there does not appear to be any difference between different treatment speeds.

The b^* values only show minor variation, varying in the treated samples from 5.75 (20 mm s^{-1}) to 6.69 (50 mm s^{-1}) as compared to the control, 7.01. The fastest treatment speed caused a small change but slightly slower (20-40 mm s^{-1}) caused marginally greater changes. All value differences however were not markedly different from the untreated WPC.

4.3.6 AESTHETIC SURFACE CHANGES SUMMARY

The light microscopy showed that all treated surfaces except of the samples treated with halogen heating lamps had noticeable differences. The samples treated with hydrogen peroxide appeared to be partial bleached as was expected by the bleaching properties of the hydrogen peroxide. The samples treated with hot air are showed that there was a partial polymer melting which might result to the surface roughness reduction. The flame treated samples under the light microscopy showed that the polymer melting was very intense and therefore the wood particles were exposed on the surface. Also the colour determination test showed that the samples treated with hydrogen peroxide had the highest colour difference followed by hot air, flame and halogen heating lamps respectively.

CHAPTER 5: DISCUSSION

5.1 TREATMENT PROCEDURE EVALUATION

The adhesion shear strength results from the lap joint tests have shown that all treatments methods except for the halogen heating lamps have a beneficial effect on the bonding strength at certain treatment conditions. The hydrogen peroxide treatment appears to produce a WPC surface with greater adhesion strength. The procedure is quite stable and easy, and requires relatively harmless chemicals when handled in low quantities (H_2O_2 and NaOH). The treatment parameters are very easy to monitor, so the advantageous effect of the adhesion improvement is guaranteed by simple equipment, i.e. just a timer and a pH meter. The disadvantage of the hydrogen peroxide treatment is that the material needs to be soaked in the treatment solution, so the treatment will affect the whole material and not just the desired surface for bonding. That means that the wettability improvement by the oxidation process will affect the whole material surface and it could cause undesirable material damage. For example the material will be exposed to conditions similar to weathering such as water absorption, wood swelling and polymer degradation.

The heat treatment with a hot air gun is also a very effective treatment method to improve adhesion bonding strength. It is also an easy applied treatment with excellent results in improving the adhesion strength. It is a quicker procedure than the hydrogen peroxide treatment and does not require chemical handling. However it is crucial that the treatment speed is accurate because it could also lead to a decrease in adhesion strength. The hot air treatment method requires high accuracy in controlling the treatment speed, which is not very practical in a workshop without the use of controlled speed machinery. It also eliminates the disadvantage of hydrogen peroxide treatment as the surface modification is taking place only at the uppermost surface which is exposed to hot air, ensuring that the surface wettability will be only improved on the surface to be bonded.

Flame treatment is one the well known surface modification methods in polymer industry (Garbassi et al 1987, Papirer and Schultz 1993, Pijpers and Meier 2001). It does however also require accuracy in selecting the treatment speed, as incorrect speeds may result to adhesion strength decrease. The flame treatment, has a medium level of risk, as it involves applying a flame on flammable materials. There is a small possibility of producing harmful fumes during the method application. Although these are unlikely for PP; transfer of the technique to other polymers could be hazardous. In the same manner as the hot air treatment,

this flame treatment modification is applied only to the surface to be bonded and does not affect the rest of the material.

The halogen heating lamps treatment does not appear to have any advantageous effect on the WPC adhesion ability. It produces a modified surface that has a reduced adhesion strength, with values lower than the untreated WPC. This treatment is possibly useful to help us understand the mechanisms that negatively affect the adhesion strength of the WPC.

5.2 THE ROLE OF THE SURFACE ROUGHNESS IN THE ADHESION

In order to better understand the mechanisms that affect the adhesion ability of the WPC after each treatment, several tests were made. The surface roughness is one important test that could explain how the material morphology could cause adhesion strength to increase or decrease. In many cases there were correlations between roughness and adhesive bond strength.

The relationship of the shear strength and the surface roughness at different pH values with H_2O_2 treatment is however not entirely simple (Figure 5.1). In this graph, the shear strength (554.7 N)and surface roughness 2.3 μm of untreated control samples are indicated by the continuous lines for reference.

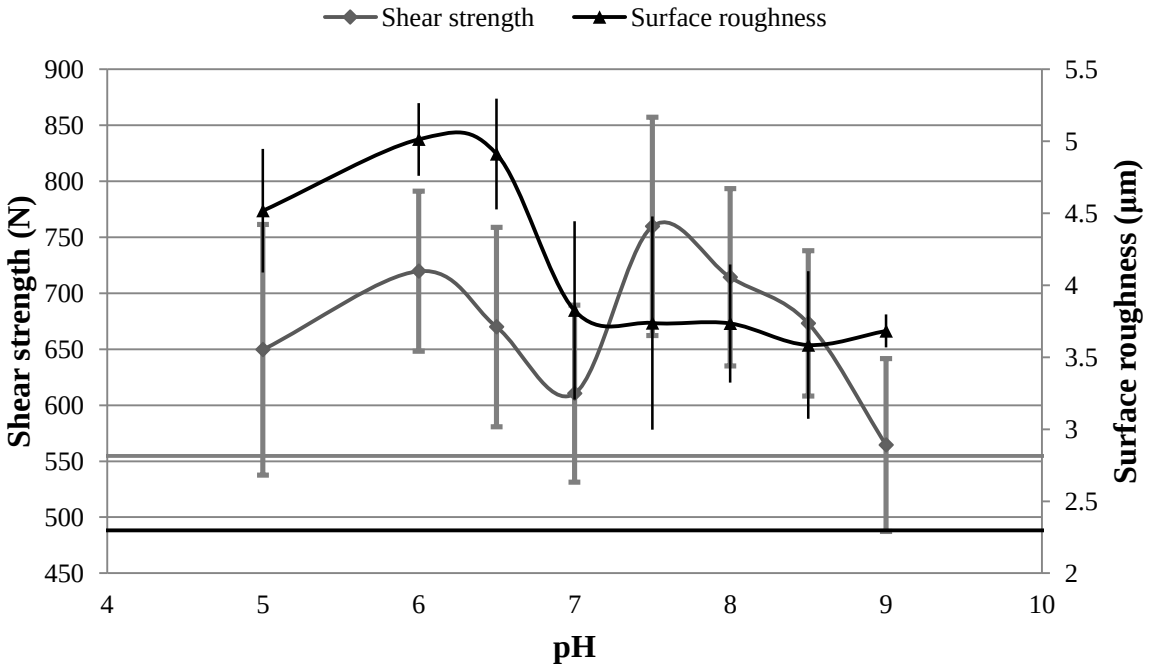

Figure 5.1: Hydrogen peroxide treatment shear strength and surface roughness chart. The linear lines present the shear strength (gray line) and the surface roughness (black line) control values. Error bars represent the SD (+/-1).

The surface roughness seems to follow a similar trend to the shear strength line for the acidic solution samples (pH 5 to pH 7 and control). Above pH 7 the roughness was more or less constant but the shear strength peaked at pH 7.5 and declined. The highest shear strength is observed at surface roughness mean value around 5 μm for pH 6.5 solution, whereas in alkali treatments the maximum was 4 μm for the pH 7.5 treatment solution. Even though the samples treated in pH 7 solution had roughness values of about 4 μm, the shear strength had dropped to values similar to the control samples. Therefore the surface roughness could not be considered as the only factor that affects the shear strength of the WPC surface modification which agrees with Oporto et al (2007).

For the hot air treated samples, the surface roughness means (Figure 5.2) do not show a clear trend with adhesive bond shear strength, unlike the samples treated with acidic hydrogen peroxide solution. The observed surface roughness of the hot air treated samples are low (1.9-2.7 μm) and many were lower than the untreated control. Changes within the sample population were only minor, so it is very difficult to notice a possible trend. Once again there is no noticeable relation of the surface roughness and the shear strength as the roughness values are not significantly different. The highest shear strength value is observed at 2X75 mm s^{-1} with surface roughness about 2. The lowest shear strength at 18.5 mm s^{-1} with surface roughness just below 3 μm.

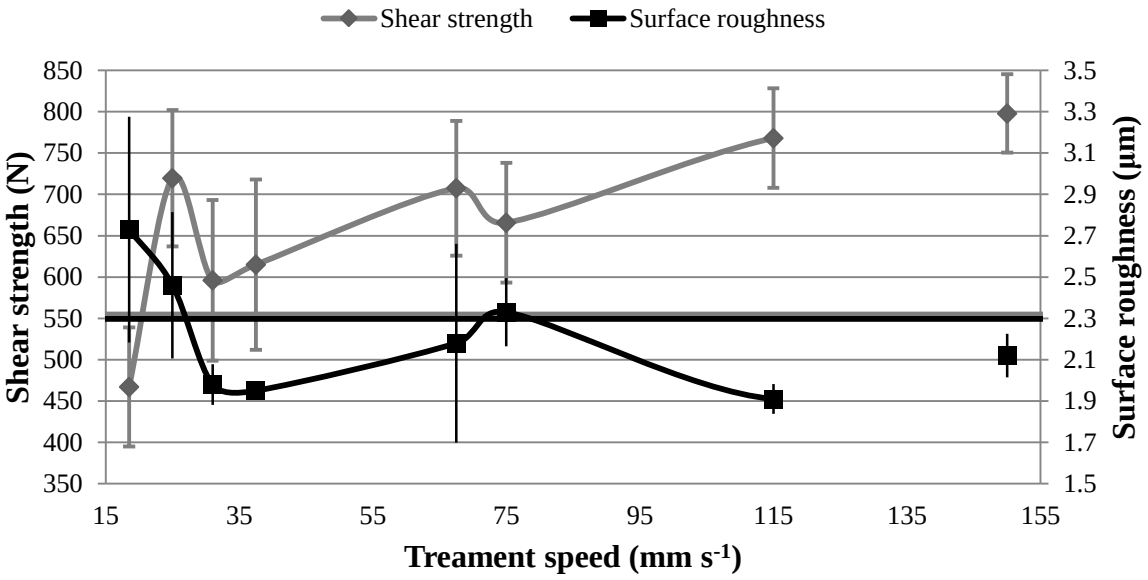

Figure 5.2: Hot air treatment shear strength and surface roughness chart. The values at the treatment speed of 150mm s^{-1} are referring to the treatment with 2 times pass of the hot air gun with the speed of 75 mm s^{-1}. The linear lines present the shear strength (gray line) and the surface roughness (black line) control values. Error bars represent the SD (+/-1).

By comparing the Figure 5.1 with Figure 5.2 it is obvious that the roughness values are unrelated to the shear strength values. In particular, samples treated in solution pH 7.5 have shear strength mean value around 750 N and surface roughness around 4 μm and samples treated with hot air at 115 mm s^{-1} have shear strength around 750 N as well but the surface roughness mean value is much lower (2 μm).

Flame treatment on the other hand gave high values of surface roughness, especially at low speeds. When the samples were treated with the speed of 125 mm s^{-1} the roughness was around 7.5 μm, but the shear strength was reduced to below the control values (Figure 5.3). Then as the surface roughness decreased to values around 5.5 μm for faster treatment speeds like 150 mm s^{-1} and 175 mm s^{-1} the shear strength increased to values around 750 N (175 mm s^{-1}). For treatment speeds from 175 mm s^{-1} to 200 mm s^{-1} as the surface roughness decreases further to a surface mean roughness of 4.5 μm at 200 mm s^{-1} and 250 mm s^{-1}, and the shear strength decreased too, to values only slightly higher than the control. At high speeds the roughness value stabilized at around the same values, but the shear strength did not follow the pattern, and increased slightly to values of around 650 N and 700 N at treatment speed of 250 mm s^{-1}. The surface roughness does looks to have a small correlation with shear strength in the flame treatment method, but still it is just an indication and not a proof.

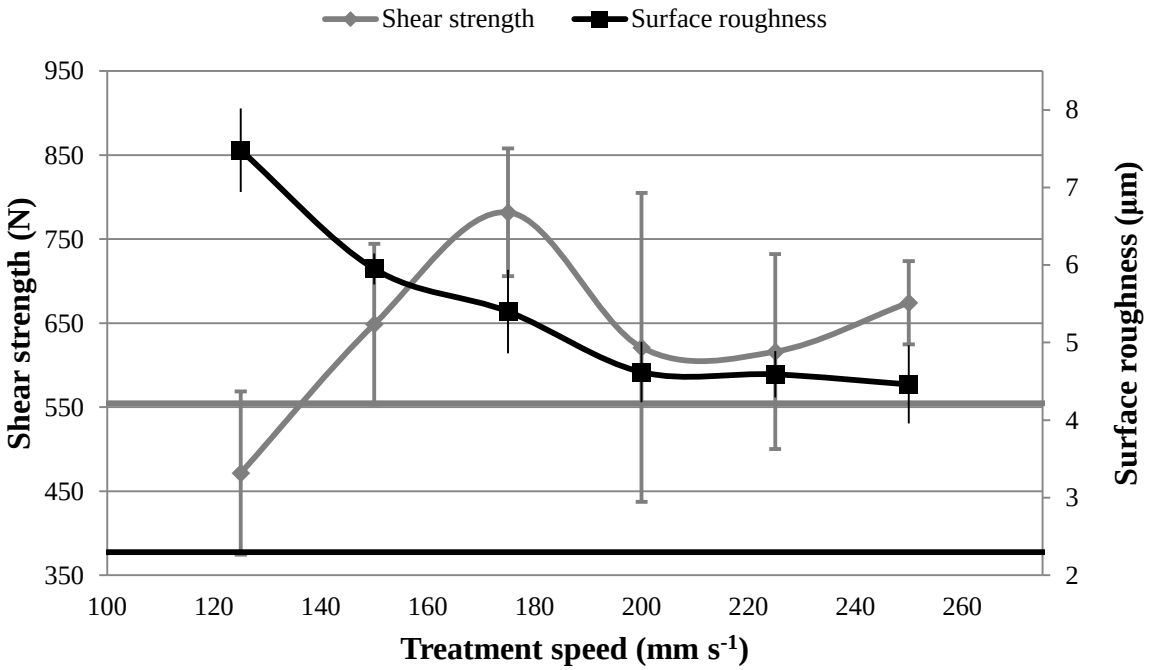

Figure 5.3: Flame treatment shear strength and surface roughness chart. The linear lines present the shear strength (gray line) and the surface roughness (black line) control values. Error bars represent the SD (+/-1).

In the case of the halogen heating lamp treatment, there was also a noticeable pattern (Figure 5.4). When the surface roughness increased the shear strength decreased. This pattern was observed in all halogen lamp treated samples, with an exception of samples treated at 30 mm s^{-1}. There appears to be a clear relationship between surface roughness and shear strength. It seems that the ideal roughness value to produce the best adhesion strength according Figure 5.4 is around 2.2 μm and 2.6 μm. However the halogen heating lamp treatment did not have a beneficial effect on the shear strength of the WPC. In fact all treatment parameters caused the adhesion shear strength to decrease to values lower than the control. Surface roughness on the other hand did not statistically differ from the control values (Table 4.29). Therefore despite the fact that there appears to be a clear pattern observed in Figure 5.4 between shear strength and surface roughness, it could not be considered as true because the roughness mean values are only slightly different and it is not possible to ensure that there is a real difference in roughness among the treated samples. The only difference that one way ANOVA confirmed was between the samples treated with the speed of 20 mm s^{-1} with the samples treated with the speed of 30 mm s^{-1} but still there were not any statistically significant differences from the control samples.

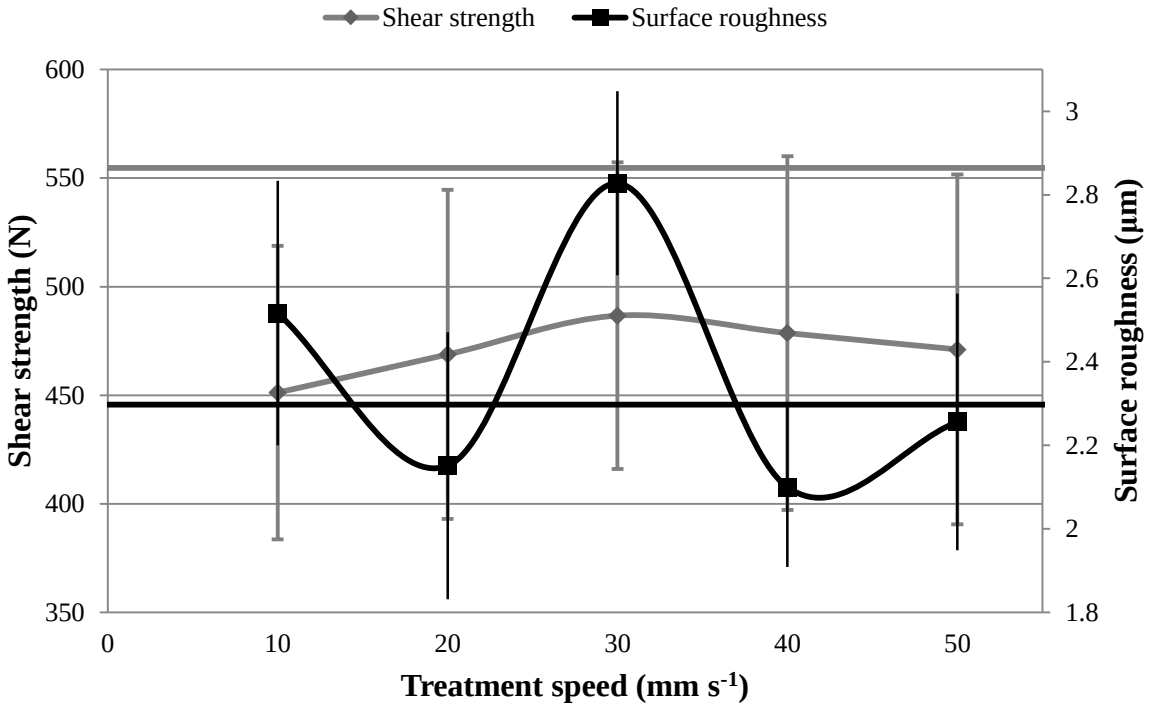

Figure 5.4: Halogen heating lamp treatment shear strength and surface roughness chart. The linear lines present the shear strength (gray line) and the surface roughness (black line) control values. Error bars represent the SD (+/-1).

The Figure 5.5 presents the surface roughness and the adhesion strength of all the tested samples. The surface roughness values around 1.5 µm and 3 µm include the control samples and the treated samples with no statistically significant differences. According to Figure 5.5 there was no noticeable trend across all treatments and therefore there was no noticeable link between the surface roughness and the adhesion strength. There were adhesion strength values observed scattered in the whole surface roughness values range.

It seems that that the adhesion strength of the samples treated with hot air gun and halogen heating lamps is not significantly affected by the surface roughness. The samples treated in hydrogen peroxide had a rougher surface, and the flame treated samples had the roughest.

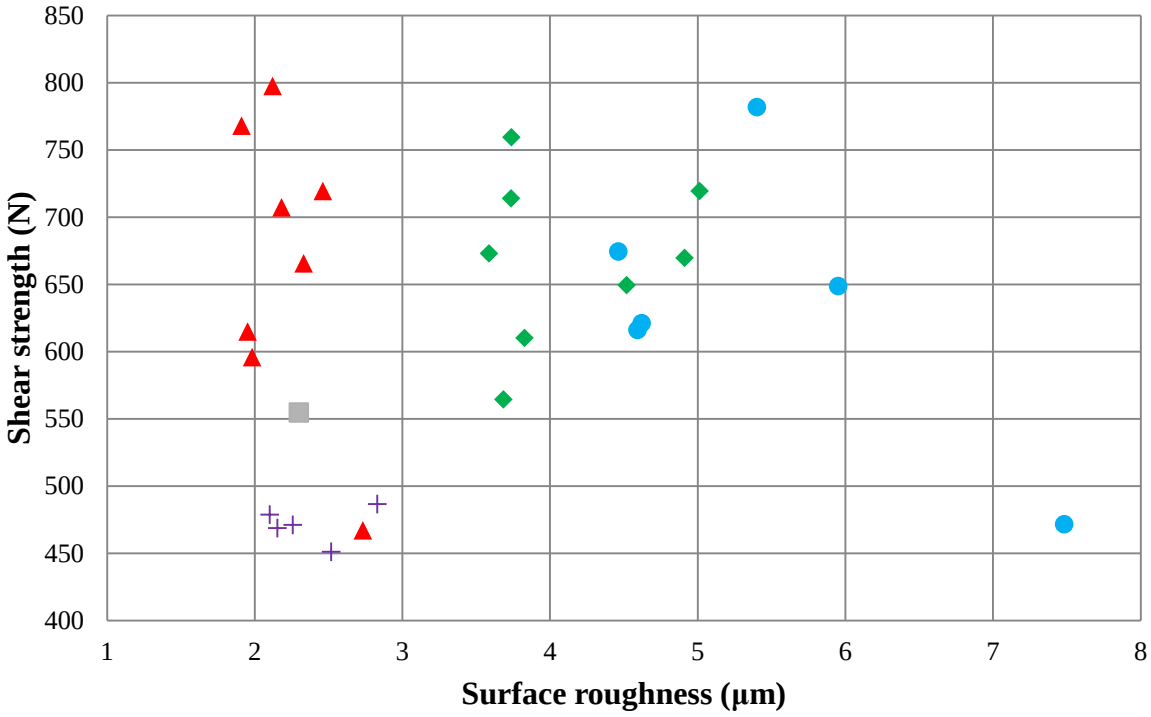

Figure 5.5: Surface roughness and adhesion strength of all the treated and control samples. Grey colour (■) Control, blue (●)flame treatment, red (▲) hot air gun treatment, green (◆) hydrogen peroxide treatment and purple (+) halogen heating lamps treatment.

The surface roughness should be related to the SEM and light microscopy observation. The SEM clearly showed that the samples treated with flame had an increase in roughness because of the pits formed on the sample surfaces. Light microscopy also showed peaks and troughs formed on the surface of the samples treated with the flame. The surface roughness increase of the samples treated in hydrogen peroxide solution could be also be explained by the wood degradation, which was observed by SEM and it was very intense is some cases. However intense degradation which was seen in samples treated in high pH solutions did not

gave higher surface roughness. On the other hand, for the samples treated with the hot air and the halogen heating lamps, despite the fact that SEM and light microscopy showed some very small differences among the treated samples, there was no visible reason that could cause surface roughness change. Thus the roughness tests confirmed the SEM and light microscopy observations for the hot air and halogen heating lamps treatment, as the samples roughness changes were not statistically significant for both treatment methods.

5.3 CHEMICAL ANALYSIS AND SURFACE ENERGY RELATION

The surface energy and the FTIR analysis was used to understand the chemical changes that might be responsible for the adhesion strength improvement. Figure 5.6 presents the adhesion strength and the surface energy of the samples treated in hydrogen peroxide solutions.

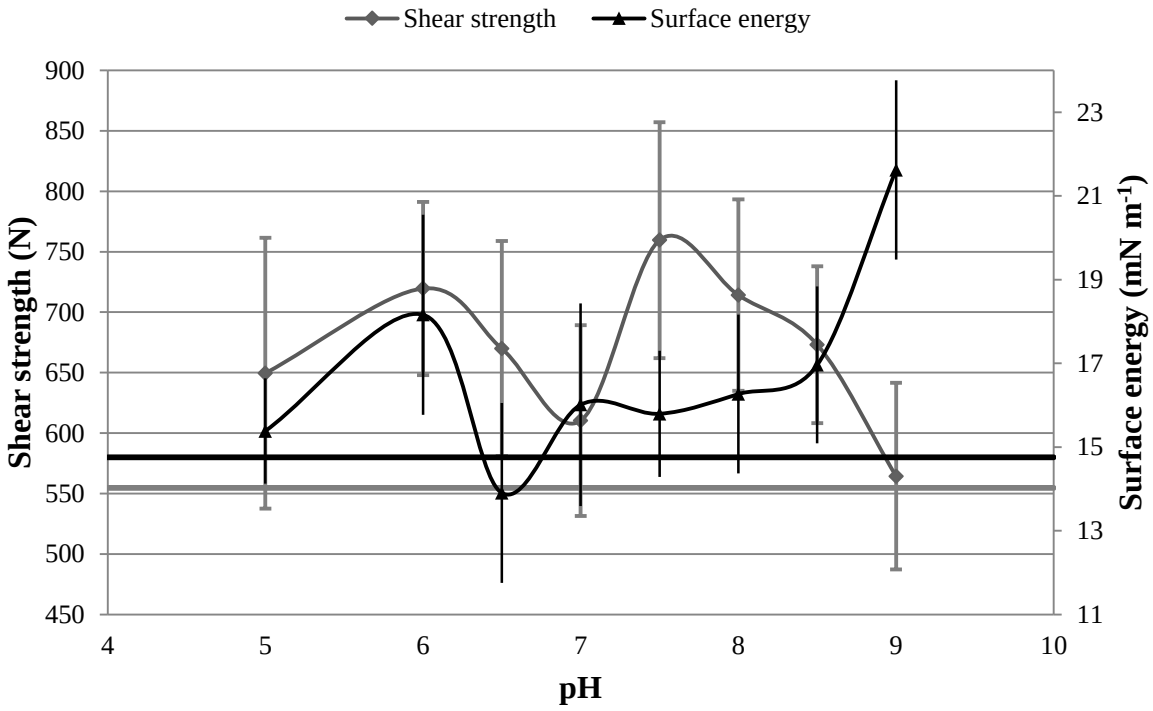

Figure 5.6: Adhesion strength compared to surface energy of hydrogen peroxide treated samples. The linear lines present the shear strength (gray line) and the surface energy (black line) control values. Error bars represent the SD (+/-1).

The adhesion strength did not seem to be related to the surface energy. There were some cases in which the surface energy seems to have a specific trend with the adhesion strength, but the trend was not observed with the other treated samples. The surface energy of the treated samples in acidic solutions appears to follow the same trend with the adhesion strength. The shear strength increased from the control to the samples treated in pH 6 solution.

The same increase was observed to the surface energy from the control samples to the samples treated in pH 6 solution. Then the adhesion strength and the surface energy decreased as the pH solution increased to pH 6.5. Even though the adhesion strength and the surface energy were reduced, as the treatment solution pH increased from pH 6 to pH 6.5, the shear strength was not decreased to mean values lower than the samples treated in pH 5 solution, as it happened with the surface energy which was reduced to mean value even lower than the control. The surface energy of the samples treated in pH 7 was increased from the samples treated in pH 6.5 solution, but the adhesion strength was reduced.

The surface energy of the samples treated in alkaline solutions was almost the same for all samples treated in the pH range from 7 to 8.5. On the other hand, the adhesion strength was significantly increased as the pH of the treatment solution increased from pH 7 and pH 7.5. Then, as the pH solution increased to pH 9 the adhesion strength was reduced to mean value similar to control. In contrast to the adhesion strength, the surface energy of the samples treated in pH 9 solution was greatly increased, to the highest surface energy mean value of all the hydrogen peroxide treated samples. However, it could be possible to notice a reverse trend between the surface energy and the adhesion strength of the samples treated in alkaline solutions. The adhesion strength was reduced as the solution pH increases from pH 7.5 to pH 9, but the surface energy was increased as the pH increases to pH 9.

It was expected that an increase of the surface energy would be related to the increase of the adhesion strength, which was not confirmed for peroxide treatments. Despite the fact that there was an increase of the adhesion strength in almost all treated samples the surface energy did not follow the same trend. In particular, the samples treated at pH 6.5 had higher adhesion strength as compared to the control, but the surface energy was reduced to values lower than the control. Furthermore, the samples treated in pH 9 solution had the lowest adhesion strength among the treated samples but the highest surface energy. Lu (2006) observed a similar reversed trend of the shear strength and the contact angle of ma bamboo samples treated in alkaline hydrogen peroxide solution in presence of NaOH. The contact angle and the shear strength were reduced for the ma bamboo samples treated in pH 7, pH 8 and pH 9 solutions. Also the ma bamboo samples treated in pH 6 solution appeared to have contact angle higher than the control, but the shear strength was higher than the untreated samples. In this study the same effect was observed in the samples treated in pH 6.5 solution.

The surface roughness of the samples treated in pH 7, pH 7.5, pH 8 and pH 8.5 hydrogen peroxide solutions seemed to have a very similar trend with the surface energy. It

seems that the pH of those alkaline solutions did not cause any major morphological difference on the WPC surface. Consequently, the adhesion strength was not affected by the surface roughness or the surface energy. It seems that there is a more complex relationship which is involving various interactive mechanisms on the material surface which are affecting the adhesion strength and not just the surface energy or the surface roughness.

The relationship between shear strength and the ester ratio of the hydrogen peroxide treated samples are presented in Figure 5.7.

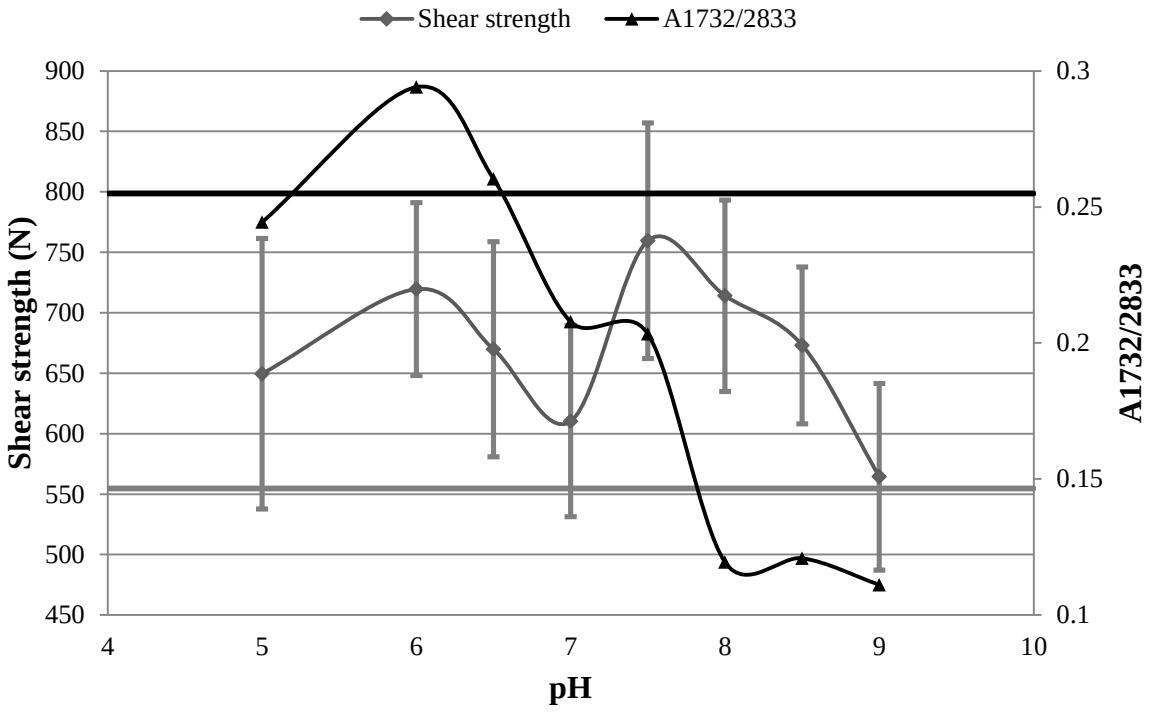

Figure 5.7: Shear strength and ester ratio ($A_{1732/2833}$) comparison of hydrogen peroxide treated samples. The linear lines present the shear strength (gray line) and the ester ratio (black line) control values. Error bars represent the SD (+/-1).

The ester ratios of the samples treated in pH 5 - 7 solutions followed a similar plot line to the shear strength and at pH 5 are similar to, although slightly lower than the control. However the shear strengths were markedly greater than the control, particularly at pH 6. Thus it is not clear whether the ester formation contributes to increases in the adhesion strength.

The ester ratios of the samples treated in alkaline solutions were lower than the control and followed a more or less linear decline from pH 6 to pH 8. Above pH 8 little change in ester ratios occurred. The ester ratios of samples treated in pH 8, pH 8.5 and pH 9 solutions were about 50% of the control values. The samples treated in pH 7 and pH 7.5 had similar

ester ratios, but their shear strength was significantly different, and the highest overall shear strength was at pH 7.5. By contrast, the samples treated in pH 8, pH 8.5 and pH 9 solutions had similar very low ester ratios, yet their shear strength reduced linearly as the pH increased. There was no clear relation of the esters to the shear strength of the hydrogen peroxide treated samples in the alkaline region tested. It is however clear that the hydrogen peroxide treatment in alkaline solutions lowers the ester group content. This is likely to be by the alkali having a dramatic effect on the esters. Caudill and Halek (1992) also report that there were not able to confirm any increase of carbonyls by FTIR after PP surface exposure to hydrogen peroxide. Figure 5.8 presents the average spectra of treated in alkali solution and untreated spruce samples. It is obvious that the esters are significantly reduced, which is also supporting the hypothesis that the esters are dramatically cleaved from the structure of the wood fibres.

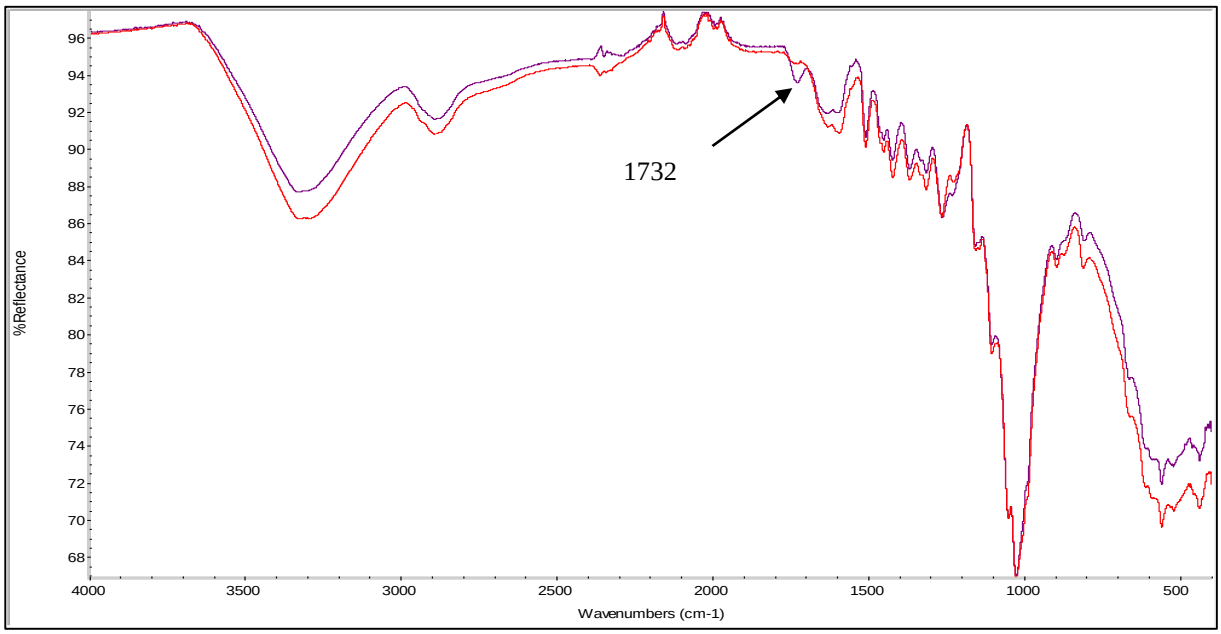

Figure 5.8: Treated (red line) and untreated (blue line) spruce in alkali solution of hydrogen peroxide.

The chemical changes that which were took place on the PP surface after the treatment were not known. However, a polymer scission process could be possible during the oxidation. Lazar et al (2000) reported that double bonds were formed on PP after peroxide decomposition. The possible chemical reactions as shown:

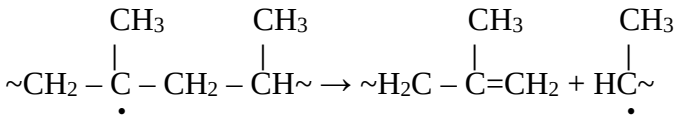

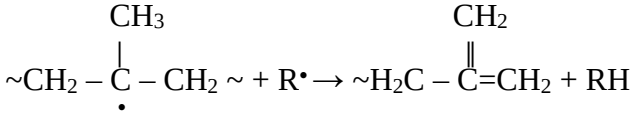

In order to investigate this chemical reaction raw PP was also subjected to hydrogen peroxide treatment in alkali solution (pH 8.5 at 20^{o}C). The average spectra are presented in Figure 5.9.

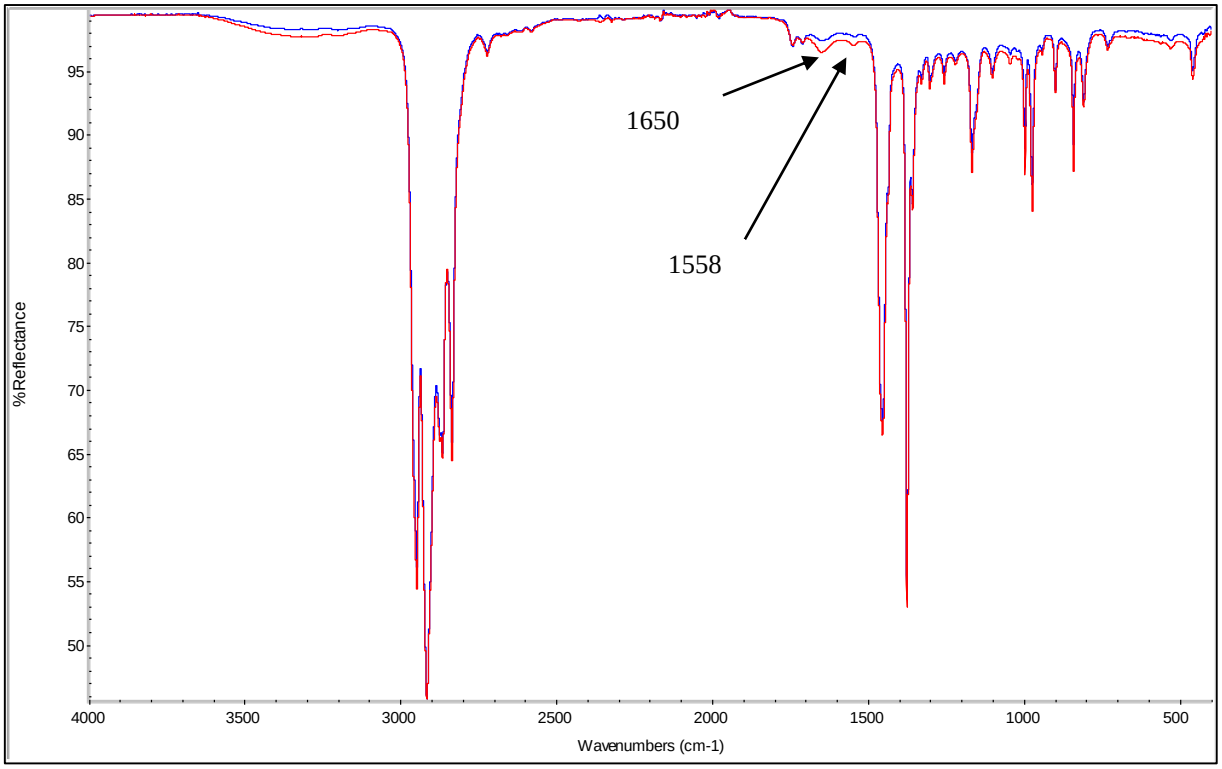

Figure 5.9: Treated (red line) and untreated (blue line) PP in alkali solution of hydrogen peroxide.

An increase in the peak at 1650 cm^{-1} was noticed which refers to C=C bonds (Pretsch et al 2000). This observation agrees with the PP scission and formation of alkene chemical reaction which reported by Lazar et al (2000). In the polypropylene, the esters and carbonyls do not seem to change, which also agrees with the observations of Gaudill and Halek (1992) observations.

Furthermore, there was a slight difference in the peak at 1558 cm^{-1} which refers to sodium carboxylate salts (R-COONa) (Lobo and Bonilla 2003). This could be explained that there was some carboxylic acid formations that reacted with the NaOH and produce the sodium salts.

There does not appear to be any obvious relationship between the surface energy and the ester ratio of the samples treated in hydrogen peroxide solutions (Figure 5.10). However in some of the acidic solutions, the ester ratio increased as the surface energy also increases, i.e. when the pH increased from pH 5 to pH 6 and subsequently from pH 6 to pH 7 both of the lines decreased.

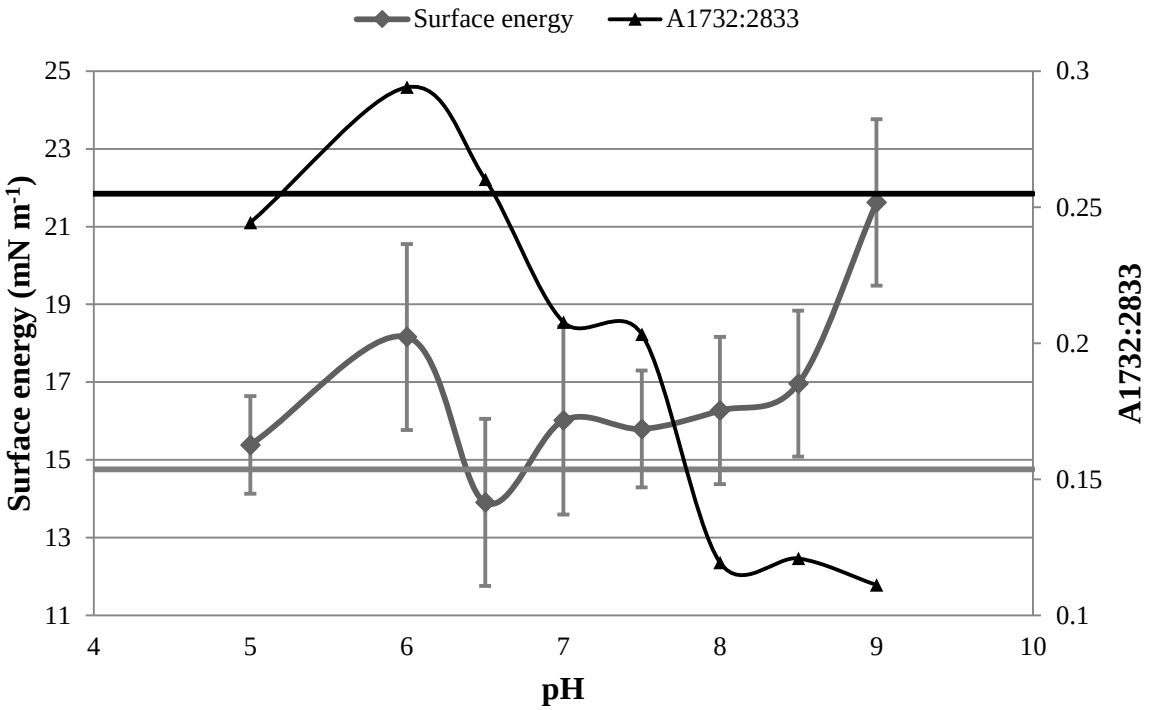

Figure 5.10: Ester ratio ($A_{1732/2833}$) compared to surface energy of the samples treated in hydrogen peroxide solutions. The linear lines present the surface energy (gray line) and the ester ratio (black line) control values. Error bars represent the SD (+/-1).

At pH 7 and 7.5 both of the surface energy and the ester ratio are similar, stabilized to the same values. For the higher pH values there was no relationship; as the ester group content diminished to level off, the surface energy increased.

In general terms the ester content decreased with increasing pH in the hydrogen peroxide solutions whilst the surface energy increased. It is possible that the esters and the carbonyls might be transformed to another group which produces the higher surface energy.

It is clear that the lignin content has a relationship to surface roughness (Figure 5.11). The curves of all of the treatments follow each other. The pH 5 samples had surface roughness higher than the control, while the lignin was lower than the control and with neutral and alkaline treatments the lignin content was reduced. This may have contributed to the wood degradation and fibres decomposition observed by SEM.

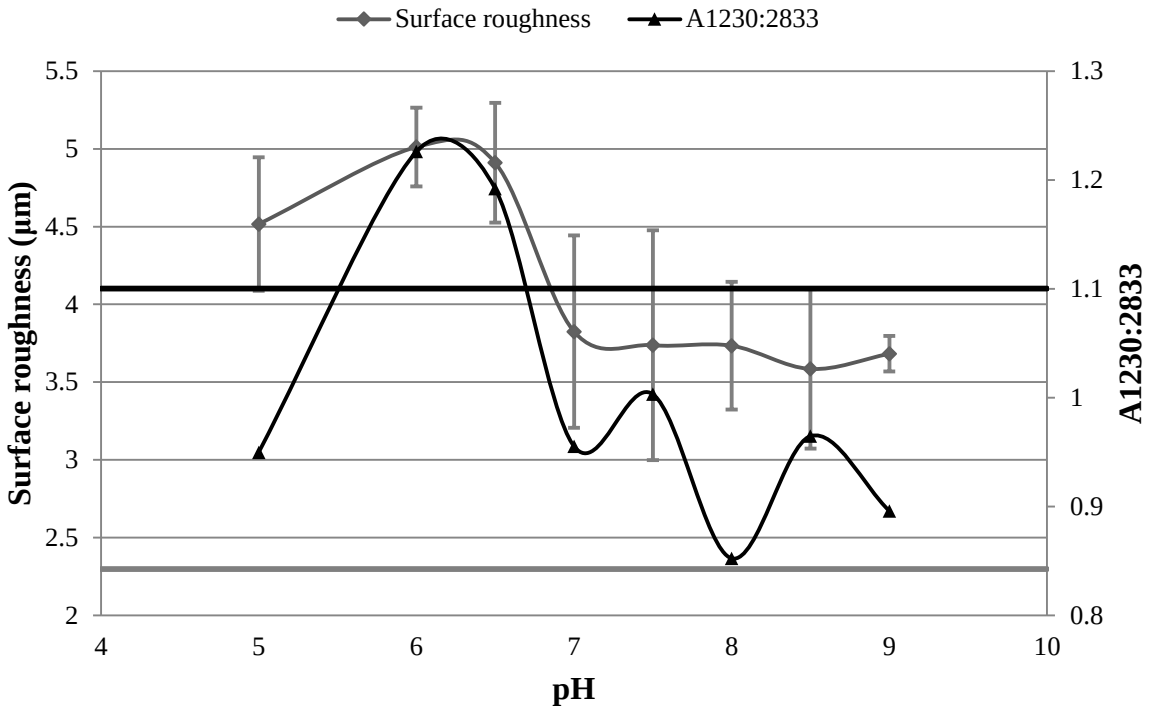

Figure 5.11: Lignin ratio ($A_{1230:2833}$) compared to surface roughness of the samples treated in hydrogen peroxide solutions. The linear lines present the surface roughness (gray line) and the $A_{1230:2833}$ (black line) control values. Error bars represent the SD (+/-1).

The relationships between the surface energy and the adhesion strength of the hot air treated samples are presented in Figure 5.12.

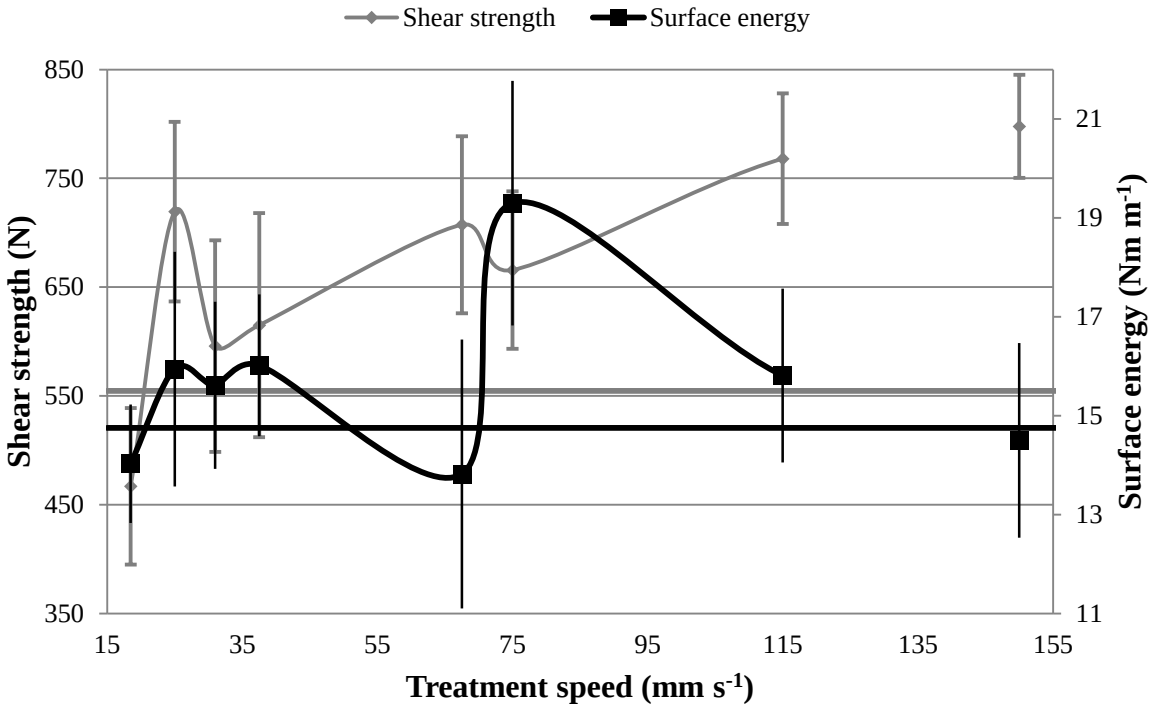

Figure 5.12: Adhesion strength compared to surface energy of hot air treated samples. The values at the treatment speed of 150mm s^{-1} are referring to the treatment with 2 times pass of the hot air gun with the speed of 75 mm s^{-1}. The linear lines present the shear strength (gray line) and the surface energy (black line) control values. Error bars represent the SD (+/-1).

Slow treatment (18.5 mm s^{-1}) caused reductions in surface energy and adhesion strength but at a faster speed (25 mm s^{-1}) they both increased. As speed increased (25 - 37.5 mm s^{-1}) the surface energy showed little change while the adhesion strength decreased. Faster treatment speeds above 37.5 mm s^{-1} the surface energy and the adhesion strength oscillated: where one increase the other decreased, i.e. when the adhesion strength increased the surface energy reduced. The samples treated at the speed of 25 mm s^{-1} and 67.5 mm s^{-1} had similar adhesion strength mean values, but the surface energy was higher than the control for the 25 mm s^{-1} treated samples and lower than the control for the 67.5 mm s^{-1} treated samples. Therefore there was no obvious relationship between the surface energy and the adhesion strength.

The relationships between the adhesion strength and the ester ratio of the hot air treated samples are presented in Figure 5.13.

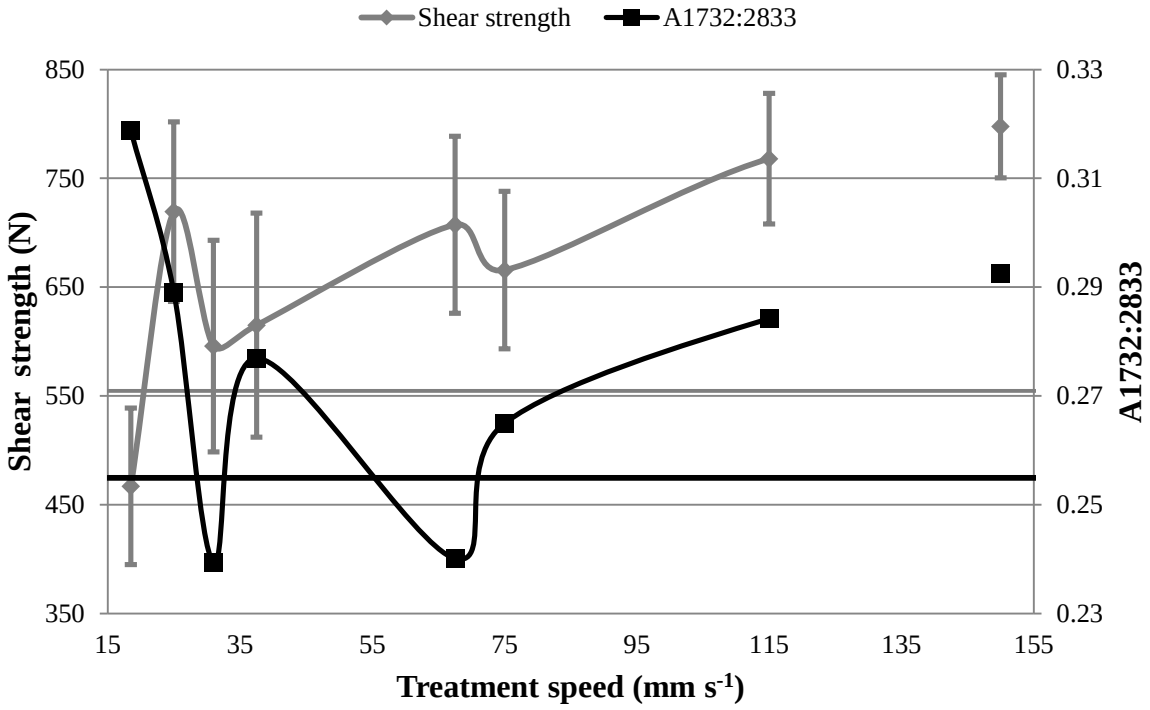

Figure 5.13: Adhesion strength and ester ratio ($A_{1732:2833}$) comparison of hot air treated samples. The values at the treatment speed of 150mm s^{-1} are referring to the treatment with 2 times pass of the hot air gun with the speed of 75 mm s^{-1}. The linear lines present the shear strength (gray line) and the ester ratio (black line) control values. Error bars represent the SD (+/-1).

The adhesion strength and the ester ratios also showed no obvious trends. The slowest treatment speed resulted in a low adhesion strength and a high ester ratio and this also occurred at 67.5 mm s^{-1}. However, at 25 mm s^{-1} the adhesion strength was considerably better than the control but only had a slightly lower ester ratio. At a marginally higher treatment speed (31 mm s^{-1}) the strength was reduced, but so was the ester ratio and faster treatment speeds the greater strength increased but the ester ratios fluctuated. At fast treatment speeds (75, 115 mm s^{-1}) both the strength and ester ratios increased. When two passes were used, 2 X 75 mm s^{-1}, resulted in an increase of both. Therefore only at the slow treatment speeds it is possible to relate the ester content with the adhesion strength with hot air treatment speed.

The relationships between the surface energy and the ester ratio of the hot air treated samples are presented in Figure 5.14.

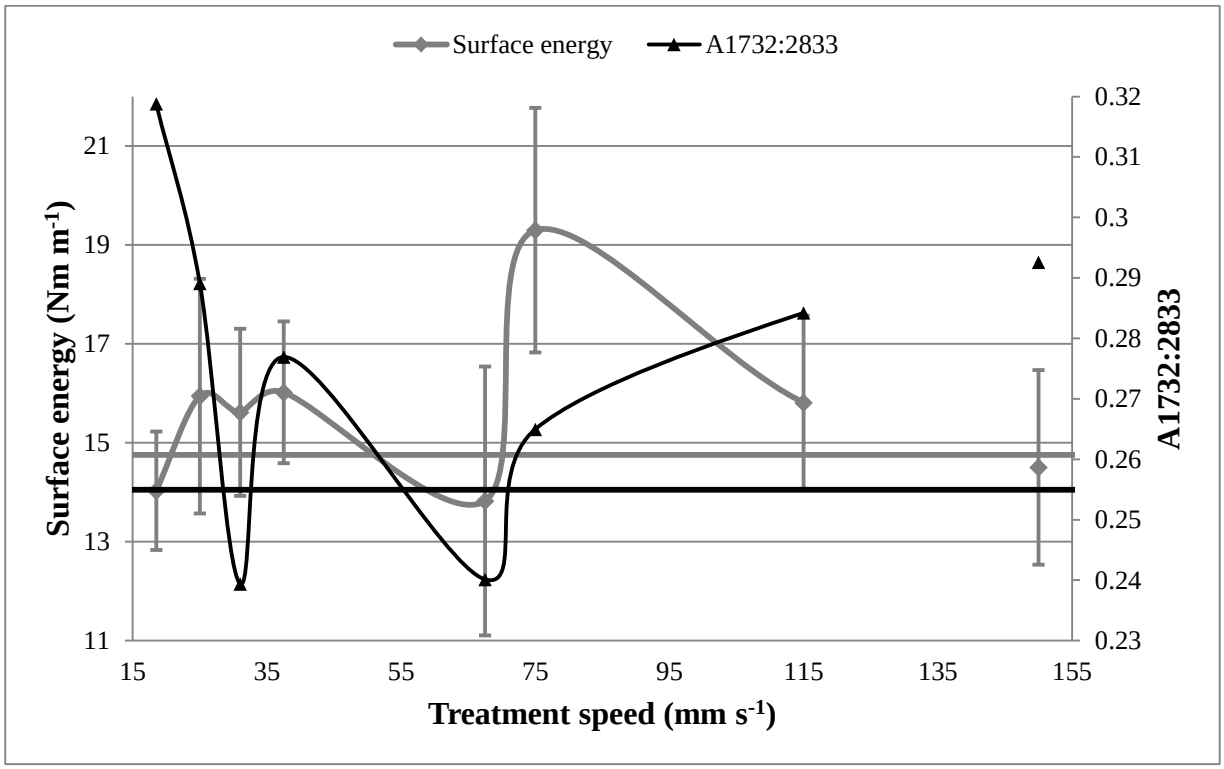

Figure 5.14: Ester ratio ($A_{1732:2833}$) compared to surface energy of the samples treated with hot air. The values at the treatment speed of 150mm s^{-1} are referring to the treatment with 2 times pass of the hot air gun with the speed of 75 mm s^{-1}. The linear lines present the surface energy (gray line) and the ester ratio (black line) control values. Error bars represent the SD (+/-1).

Given the highly fluctuating nature of the results it is difficult to see any trends. High ester ratios were associated with low surface energy at 18 mm s^{-1} and the converse was seen at 75 mm s^{-1} but the other values did not follow this trend. The rest of the treated samples showed a completely different picture with no specific trend. The surface energy of the samples treated with hot air did not appear to have a specific relationship to the ester ratio.

The relationships between the surface roughness to the lignin ratio of hot air treated samples are presented in Figure 5.15.

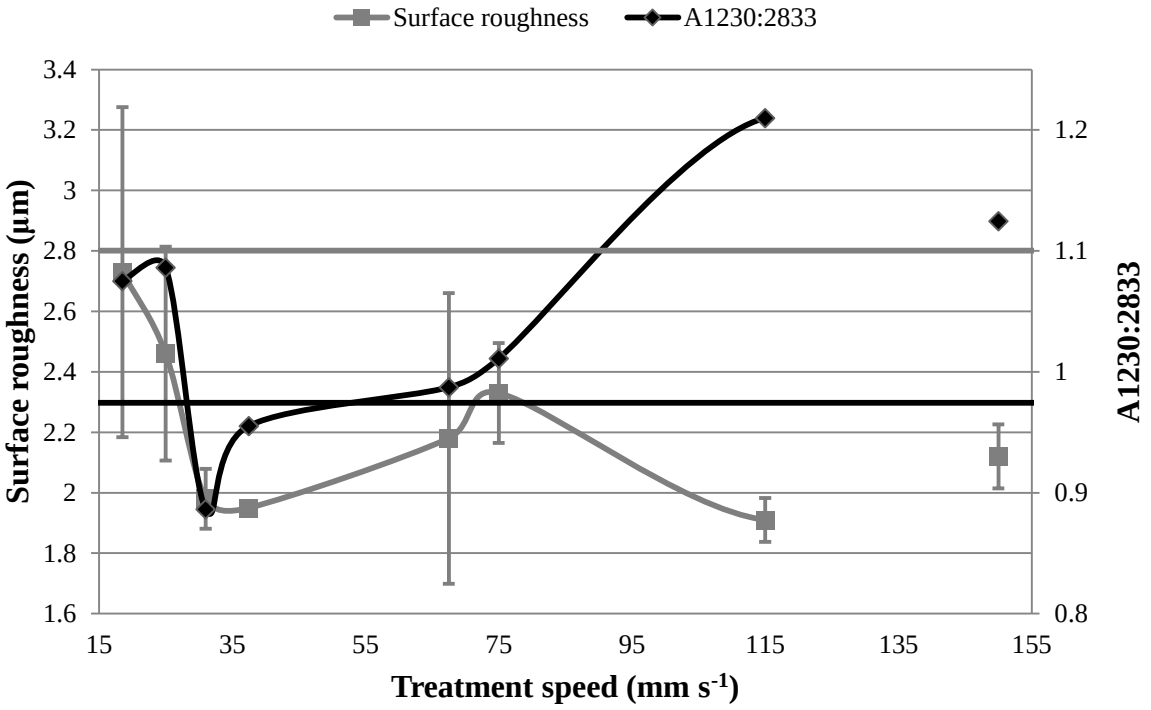

Figure 5.15: Lignin ratio ($A_{1230:2833}$) compared to surface roughness of the samples treated with hot air. The values at the treatment speed of 150mm s^{-1} are referring to the treatment with 2 times pass of the hot air gun with the speed of 75 mm s^{-1}. The linear lines present the surface roughness (gray line) and the $A_{1230/2833}$ (black line) control values. Error bars represent the SD (+/-1).

At the slower treatment speeds surface roughness increased relative to the control while lignin was little different. At faster speeds, 31 to 115 mm s^{-1}, the lignin content dropped to a value lower than the control values at the slower speeds, and increased steadily to a value greater than the control for the fastest treatment speed. Over this range a relationship between surface roughness and lignin content was noticed, but at the highest treatment speed a high lignin content was associated with a low surface roughness. Therefore a relationship between the lignin and the surface roughness was not confirmed in the case of the hot air treated samples.

The relationships between the surface energy and the adhesion strength of the flame treated samples are presented in Figure 5.16.

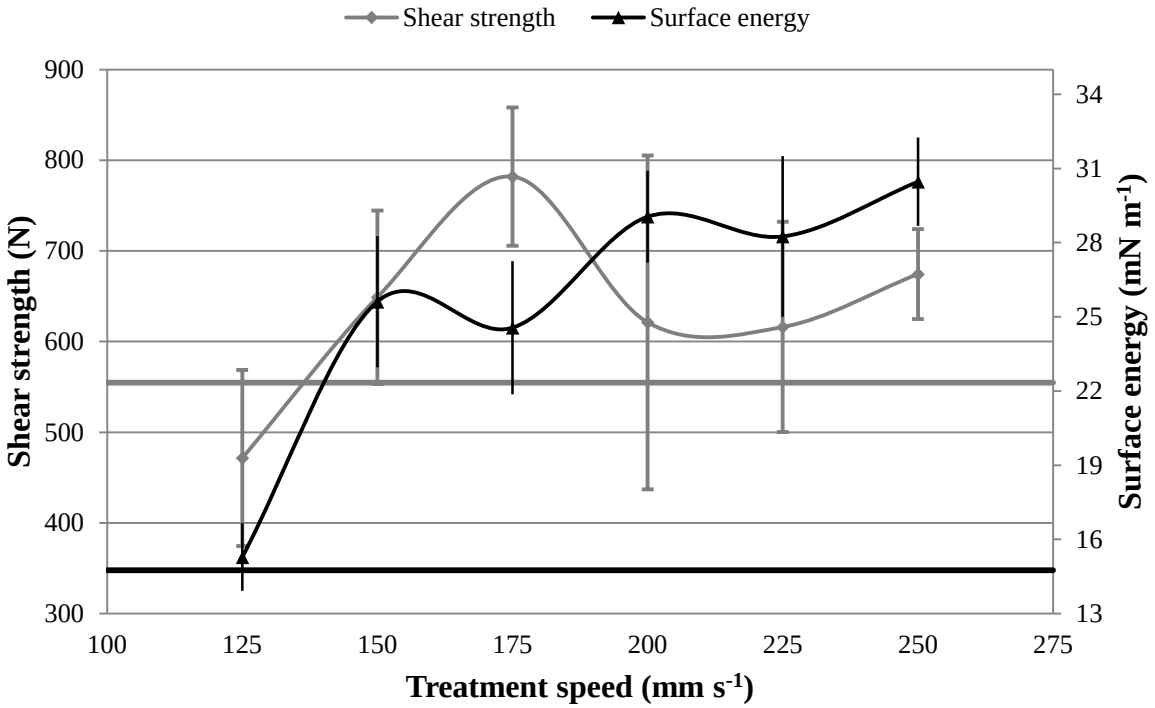

Figure 5.16: Adhesion strength compared to surface energy of flame treated samples. The linear lines present the shear strength (gray line) and the surface energy (black line) control values. Error bars represent the SD (+/-1).

The surface energy of the flame treated samples showed some relation with the adhesion strength: generally as treatment speed increased, surface energy and adhesion strength increased. However the adhesion strength peaked at a speed of 175 mm s^{-1} and at this speed, surface energy, although greater than the controls, showed a small dip in the overall trend of increase with increasing speed.

It is interesting that the adhesion strength of the samples treated with the slowest speed of 125 mm s^{-1} was lower than the control values, while the surface energy was very similar to the control. By contrast, at fast speeds above the peak of strength, further increases in speed resulted in increases in surface energy but the strength values, although increasing with further treatment speed, did not recover to approach the peak values. However the flame treated samples did show a relationship with the adhesion strength of the lap joint samples and the surface energy.

The relationships between the adhesion strength and the ester ratio ($A_{1732:2833}$) of the samples treated with flame are presented in Figure 5.17.

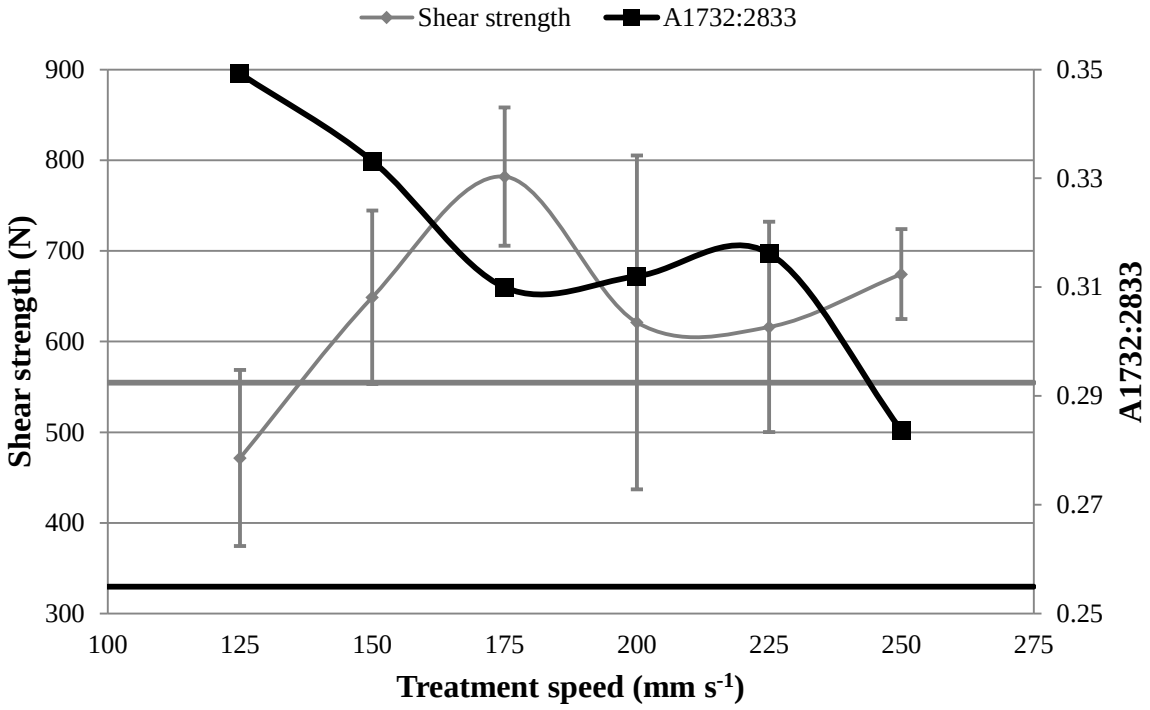

Figure 5.17: Shear strength and ester ratio ($A_{1732:2833}$) comparison of flame treated samples. The linear lines present the shear strength (gray line) and the ester ratio (black line) control values. Error bars represent the SD (+/-1).

In the case of the flame treated samples it was clear that there was a reverse trend of the ester ratio and the adhesion strength. The samples treated with the slowest speed of 125 mm s^{-1} had the highest ester ratio and this increase in ester ratio was large, yet the lowest adhesion strength was lower than the controls. It is possible the slow speed to give wrong level of oxidation which might lead to weaker bonds. All other treated samples showed an improvement of adhesion strength and had ester ratios higher than the untreated samples.

The ester increscent except by the polymer oxidation, could be due to polymer melting which might result to wood fibres exposure on the surface. The forming pits on the surface could support this hypothesis because it is possible to expose wood fibres in greater depth (Figure 4.41 b). However Garbassi et al (1987) reported that there was carbonyl formations due to oxidation on polypropylene surface after flame treatment which could be explain the ester ratio increscent of this study. Papirer and Schultz (1993), and Pijpers and Meier (2001) also report that flame treatment increases the oxygen on polymer surface due to oxidation which also agrees with this study ester ratio results.

The relationships between the surface energy and the ester ratio ($A_{1732:2833}$) of the flame treated samples are presented in Figure 5.18.

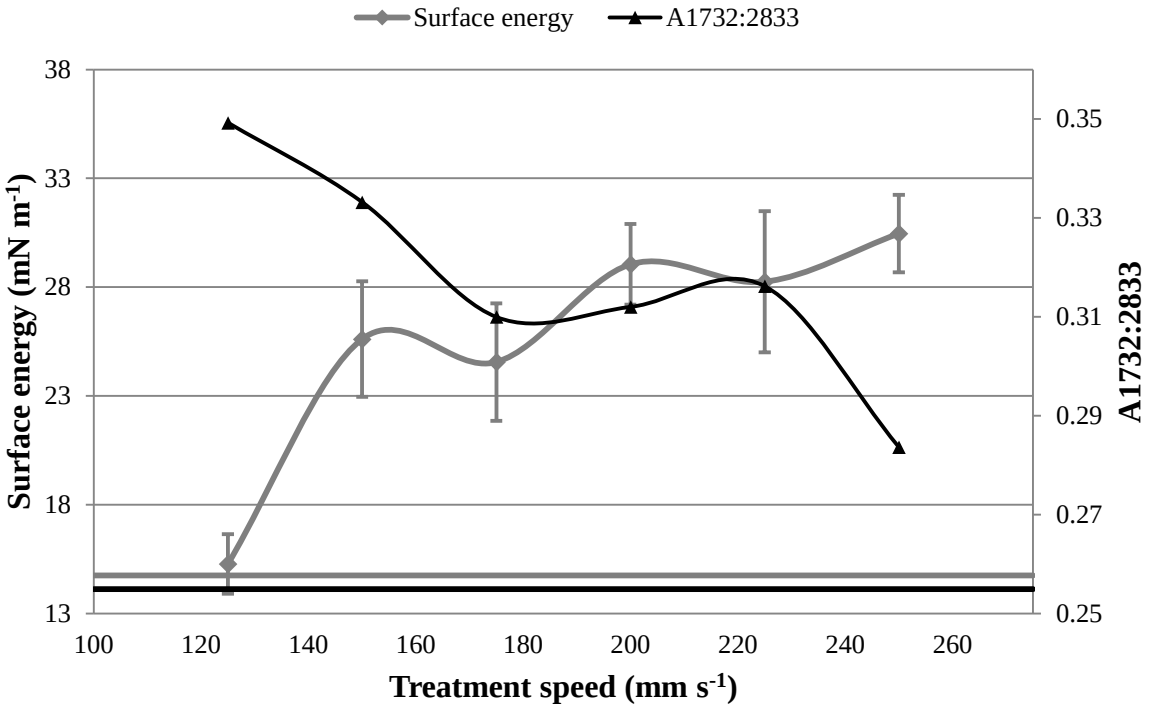

Figure 5.18: Ester ratio ($A_{1732:2833}$) compared to surface energy of the samples treated with flame. The linear lines present the surface energy (gray line) and the ester ratio (black line) control values. Error bars represent the SD (+/-1).

The surface energy also showed a reversed trend when compared to the ester ratio. The main difference was the samples treated with the speed of 175 mm s^{-1}, where both of the points were lower than for 150 mm s^{-1}. However, both the ester and the surface energy were higher than the controls. Thus there is some relationship between the esters and the surface energy but it was not clearly observed for the samples treated with flame. Again, the possible exposure of wood fibres due polymer melting and the formed pits could result in increase of the surface energy. The surface energy was determined by contact angle goniometer which is affected by the water absorption of the surface. Therefore, a more complex interaction involving esters and other chemical changes on the flame treated surface were probably responsible for the increase of the surface energy of the samples.

The relationships of the surface roughness and the lignin ratio ($A_{1230/2833}$) of the flame treated samples are presented in Figure 5.19.

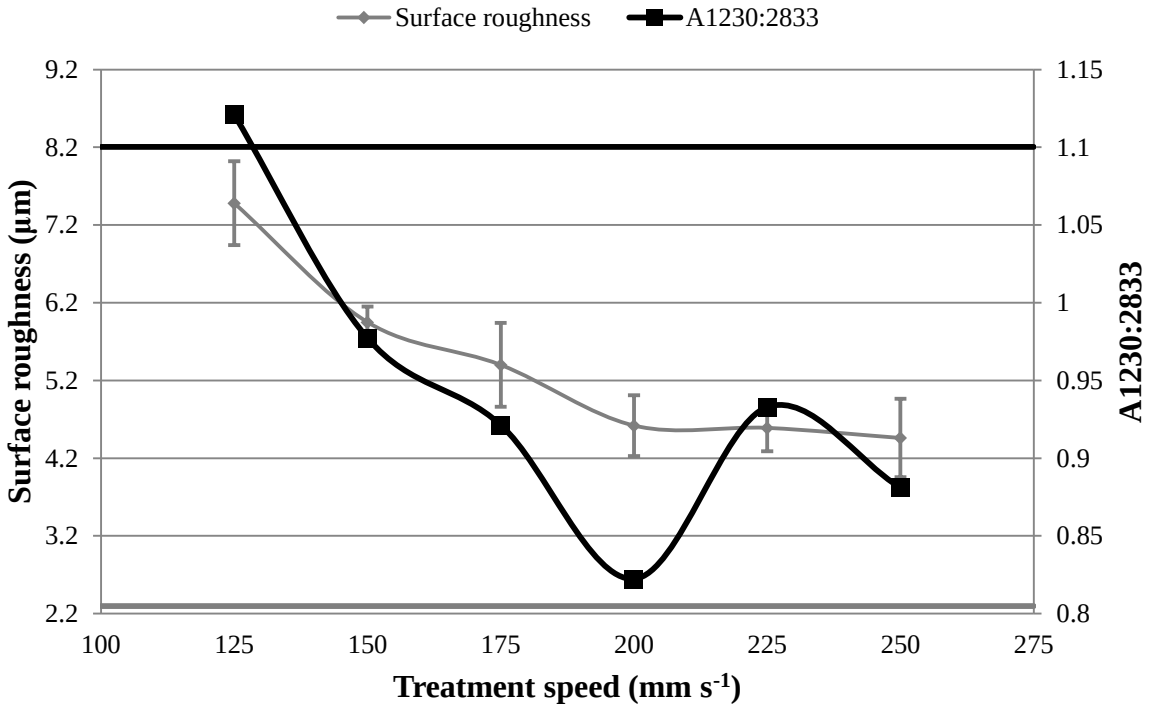

Figure 5.19: Lignin ratio ($A_{1230:2833}$) compared to surface roughness of the samples treated with flame. The linear lines present the surface roughness (gray line) and the $A_{1230:2833}$ (black line) control values. Error bars represent the SD (+/-1).

The surface roughness and the lignin ratio of the flame treated samples seemed to follow a similar trend. Flame treatment duration caused an almost linear increase in surface roughness. This was accompanied by changes in lignin. All lignin contents were lower than the control, except the slowest speed. Yet, the slowest speed showed greatest increase in surface roughness (and lowest shear strength, see Figure 5.16). Control values and slow treatment speeds were similar but increasing speed caused a linear lowering of lignin ratio but only up to 200 mm s^{-1}. Above this speed (225 mm s^{-1} and 250 mm s^{-1}) the lignin ratios were higher. However, in all the flame treated samples, except the 125 mm s^{-1}, the lignin ratios were lower than the control while the surface roughness was higher than the control. The same observation was noticed with the samples treated in hydrogen peroxide solutions and is different to the hot air treated samples. However, the surface roughness of the samples treated with hot air was not found to have statistically significant differences with the untreated samples.

The relationships between the surface energy and the adhesion strength of the halogen heating lamps treated samples are presented in Figure 5.20.

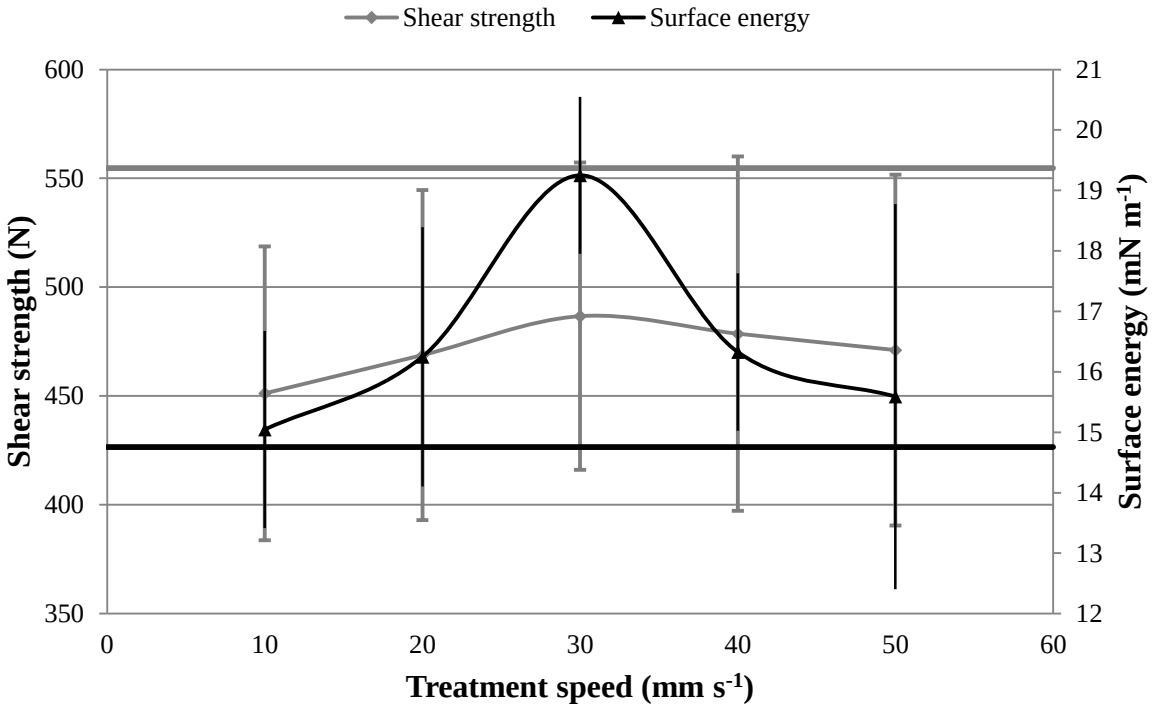

Figure 5.20: Adhesion strength compared to surface energy of halogen heating lamp treated samples. The linear lines present the shear strength (gray line) and the surface energy (black line) control values. Error bars represent the SD (+/-1).

Despite the fact that the shear strength of the adhered joints of the samples treated with halogen heating lamps was considerably lower than the control values the surface energy increased and had a similar trend to the changes in strength, reaching peaks at 30 mm s^{-1}. The samples treated with the speed of 10 mm s^{-1} had adhesion strength lower than the control and surface energy slightly higher than the control. As the treatment speed increases to 30 mm s^{-1} both surface energy and adhesion strength were increased to the highest values among the treated samples. Then, as the treatment speed increases to 50 mm s^{-1} both of the lines decreased.

The relationships between the adhesion strength and the ester ratio ($A_{1732/2833}$) of the halogen heating lamps treated samples are presented in Figure 5.20.

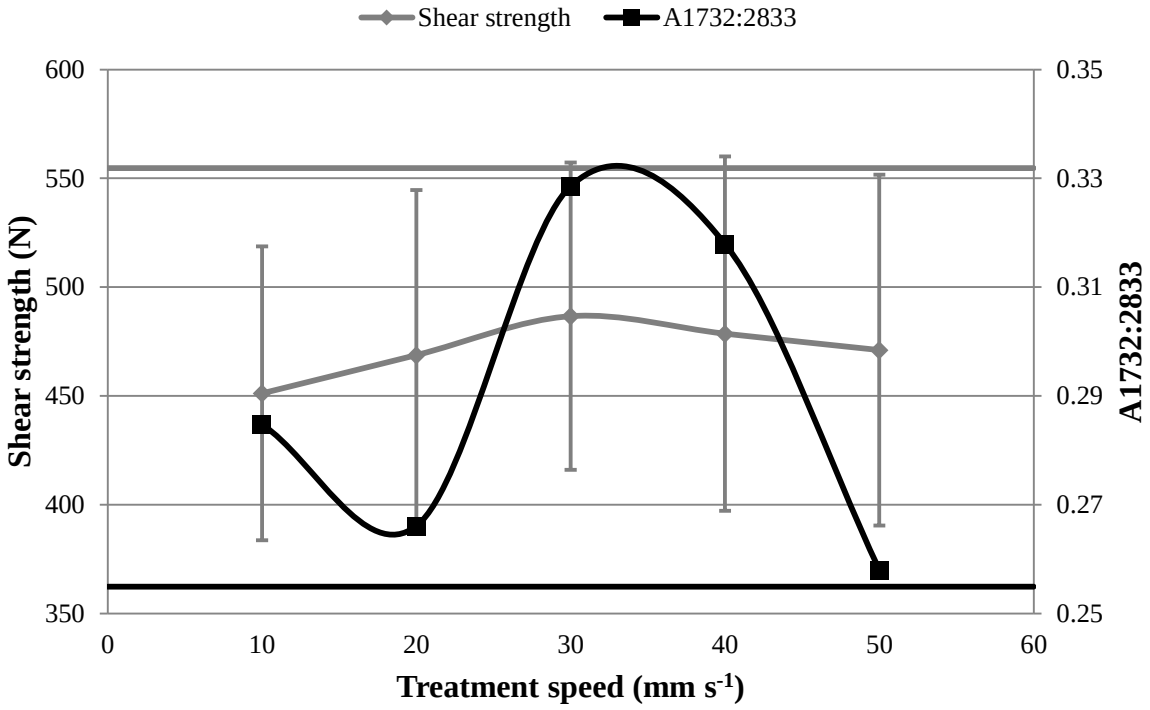

Figure 5.21: Shear strength and ester ratio ($A_{1732:2833}$) comparison of halogen heating lamps treated samples. The linear lines present the shear strength (gray line) and the ester ratio (black line) control values. Error bars represent the SD (+/-1).

The esters also had a similar trend to the adhesion strength. The only dissimilarity was that the ester ratio of the samples treated with the speed of 10 mm s^{-1} was higher than the ester ratio of the 20 mm s^{-1} treated samples. However despite the fact that the esters were higher than the control in all the treated samples, the shear strength of all the treated samples was lower than the control. It seems that the increase of the esters was not able to produce a surface with greater adhesion strength.

The relationships between the surface energy and the ester ratio ($A_{1732/2833}$) of the halogen heating lamps treated samples are presented in Figure 5.22.

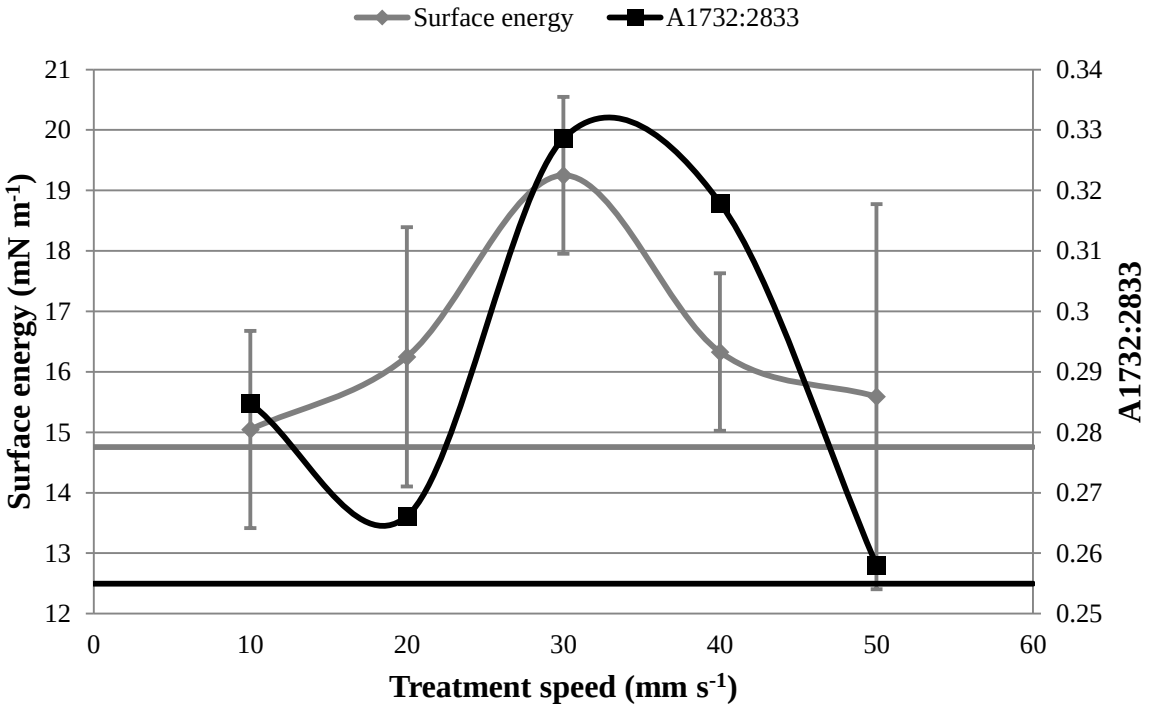

Figure 5.22: Ester ratio ($A_{1732:2833}$) compared to surface energy of the samples treated with halogen heating lamps. The linear lines present the surface energy (gray line) and the ester ratio (black line) control values. Error bars represent the SD (+/-1).

The surface energy and the ester ratio had the same relationship which was observed with the shear strength and the ester ratio. The samples treated with the speed of 10 mm s^{-1} had an ester ratio higher than the samples treated with the speed of 20 mm s^{-1}, but the surface energy of the samples treated with the speed of 10 mm s^{-1} was lower than the samples treated with the speed of 20 mm s^{-1}. However, both surface energy and ester ratio were mainly higher than the untreated samples and there seemed to be a similar trend which could relate the esters with the surface energy.

The relationships between the surface roughness and the lignin ratio ($A_{1230:2833}$) of the halogen heating lamps treated samples are presented in Figure 5.23.

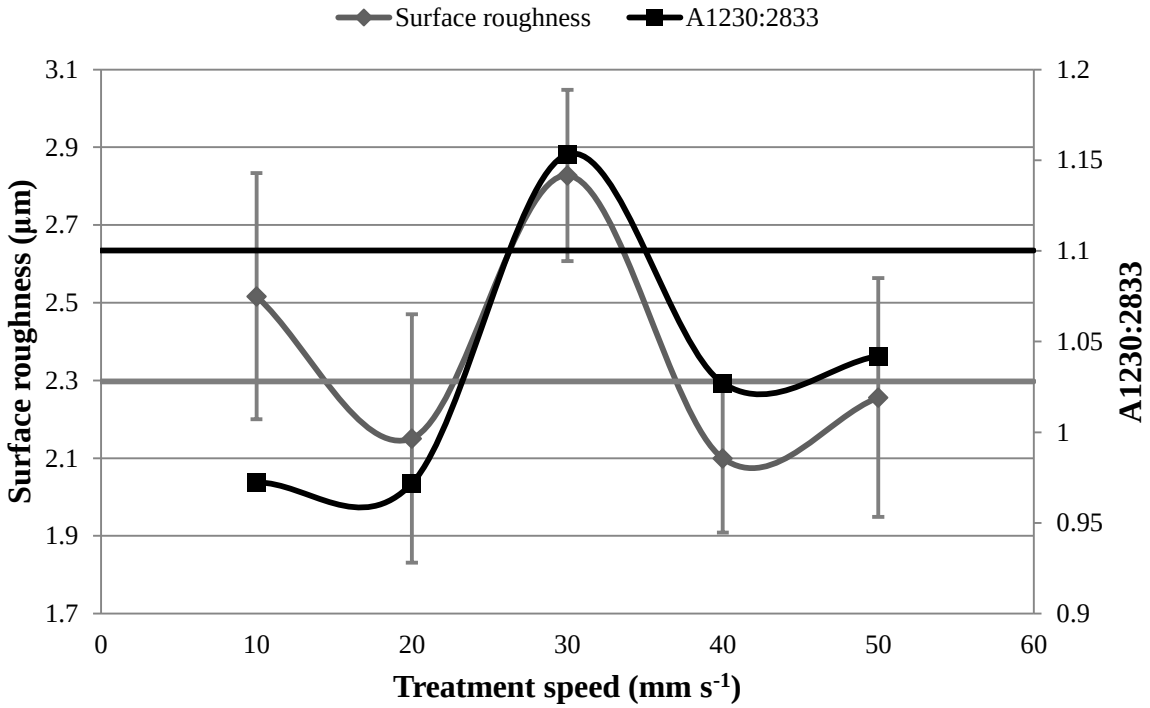

Figure 5.23: Lignin ratio ($A_{1230:2833}$) compared to surface roughness of the samples treated with halogen heating lamps. The linear lines present the surface roughness (gray line) and the $A_{1230:2833}$ (black line) control values. Error bars represent the SD (+/-1).

There was clearly a similar relationship between the lignin and the surface roughness. Again the only outlier was the samples treated at 10 mm s^{-1}. The surface roughness of the samples treated at 10 mm s^{-1} was higher than the untreated samples but the lignin ratio was lower than the control. Also the lignin ratios of the samples treated with the speeds of 40 mm s^{-1} and 50 mm s^{-1} were higher than the samples treated at 10 mm s^{-1} and 20 mm s^{-1}. On the other hand, the surface roughness of the samples treated with the speed of 40 mm s^{-1} were lower than the samples treated at 20 mm s^{-1}, and the roughness of the samples treated at 50 mm s^{-1} were lower than the samples treated with the speed of 10 mm s^{-1}. However, it is important to mention that the halogen heating lamps did not produce statistically significant changes in the WPC surface roughness.

When all of the strength data is pooled and relationships for surface energy are examined (Figure 5.24) no overall trend between all treatments were noted. There was no overall general relationship between the surface energy and the adhesion strength for the hydrogen peroxide treatment and the hot air treatments, while the halogen lamp treatment had a positive relationship on surface energy, despite having no beneficial effect on bond strength.

The flame treated samples seemed to form a distinct cluster of vales where high surface energy and high bond strength are seen. It seems that the flame treatment does significantly affect the surface energy in contrast to the rest of the treatments. However most, except for the most severe, of the flame treatment samples appear to show a strong increase in surface energy associated with increases in adhesion strength.

Furthermore, the halogen heating lamp treated samples and the less effective samples of the flame treated samples and the hot air gun treated samples are forming a cluster with low adhesion strength and similar surface energy.

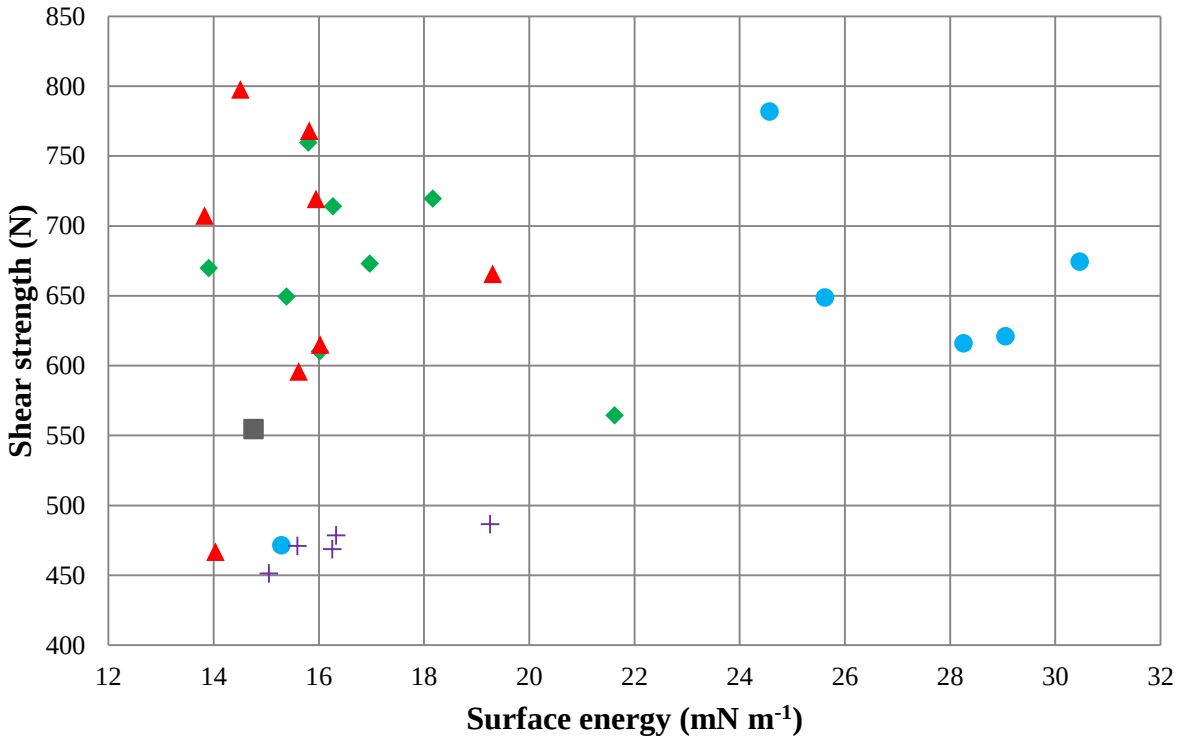

Figure 5.24: Adhesion strength and surface energy scatter graph of all the tested samples. Grey colour (■) Control, blue (●)flame treatment, red (▲) hot air gun treatment, green (◆) hydrogen peroxide treatment and purple (┼) halogen heating lamps treatment.

Figure 5.25 plots the ester ratio and the adhesion strength. Again, at a first glance, no specific trend was apparent. There are values scattered in all areas of the graph. However, the effect on esters, which is caused by the hydrogen peroxide treatment seemed to differ from the other treatment methods. The data of the hydrogen peroxide treatment are spread within the graph with the lowest ester ratio values, and these have the biggest range, in contrast to the rest of the samples. The ester ratio of the other treated samples seemed to be more concentrated in a smaller range. It seems that the hydrogen peroxide treatment affects the esters with a very different way than the heat treatment; as the other treatments are manly heat application.

The hydrogen peroxide treated samples could be exclude from the overall trend because of the ester reaction with the H_2O_2 and the NaOH. Also the flame treated and the hot air treated samples are forming two clusters with almost the same adhesion strength but with slightly different ester ratio. The hot air gun treatment seems to produce a slightly higher ester ratio than the flame treatment.

In addition the slowest treated samples of both flame (125mm s^{-1}) and hot air gun (18.5 mm s^{-1}) samples are outliers compared to samples treated at other speeds. These again form a cluster of least effective treatment with the halogen heating lamp treated samples.

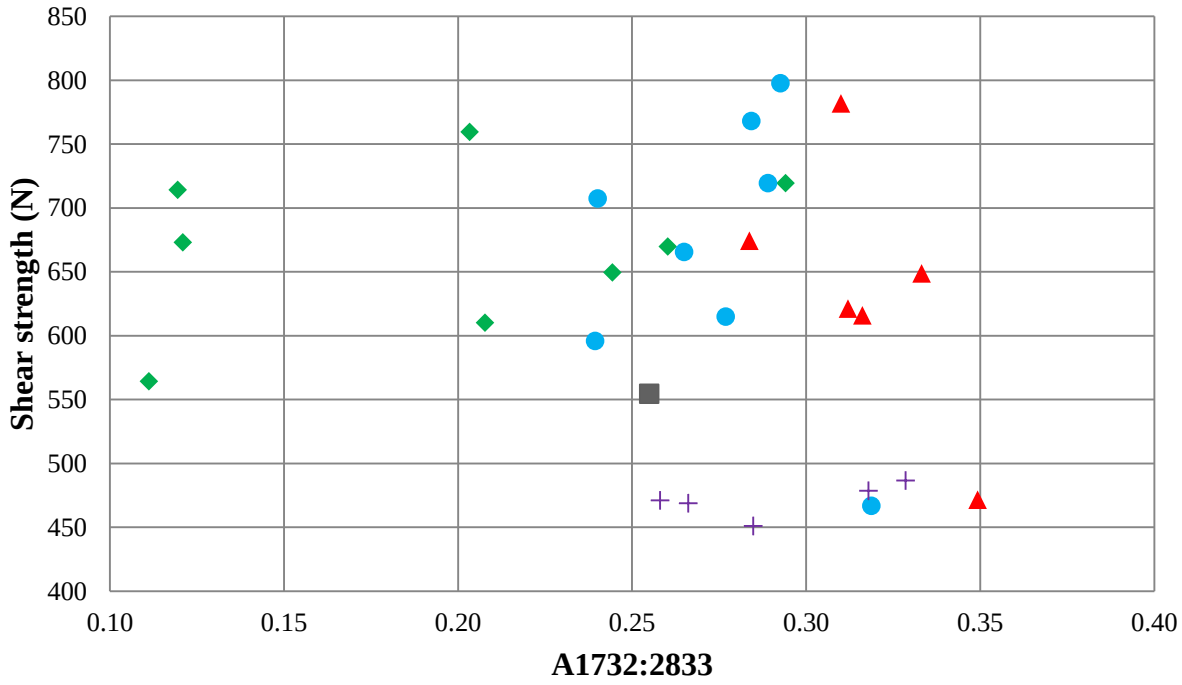

Figure 5.25: Shear strength and ester ratio scatter graph of all the tested samples. Grey colour (■) Control, blue (●)flame treatment, red (▲) hot air gun treatment, green (◆) hydrogen peroxide treatment and purple (+) halogen heating lamps treatment.

Another correlation examined which showed no general correlation was that between surface energy and ester ratios (Figure 5.26). However, surface energy values higher than 24 mN m^{-1}, which is significantly greater than the control (14.76 mN m^{-1}), were only observed at ester ratios from 0.25 to 0.35 which were the flame treated samples. On the other hand, at the same ester values the heat gun and halogen lamp samples showed surface energies lower than 20 mN m^{-1} and in some cases almost similar to the control values. Hydrogen peroxide treatment shows again a different image, with data scattered mainly at lower values of ester ratio than the control, unlike the rest of the treatments which were concentrated in smaller groups.

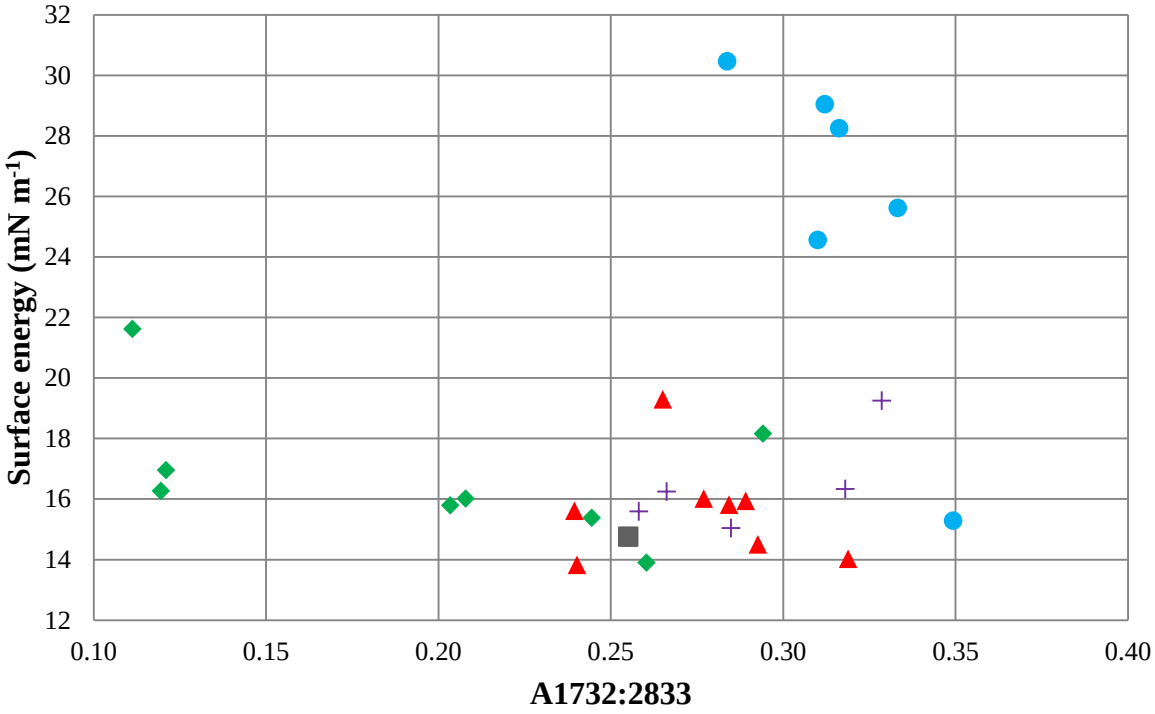

Figure 5.26: Surface energy and ester ratio scatter graph of all the tested samples. Grey colour (■) Control, blue (●)flame treatment, red (▲) hot air gun treatment, green (◆) hydrogen peroxide treatment and purple (+) halogen heating lamps treatment.

5.4 TREATMENT METHODS AESTHETIC IMPACT

The aesthetic appearance of the treated samples is also an important factor, if the material is going to be used for furniture and frame constructions. Colour change was measured and the light microscopy was used to provide information about the surface appearance after each treatment. The surface morphology showed no noticeable changes when the samples were observed by the naked eye. The surface roughness and the

morphology difference were only evident when the samples were examined under SEM and light microscopy. However the colour changes were obvious after each treatment and were confirmed by the colorimetry using the CIE Lab measuring system.

The samples treated with hydrogen peroxide became whiter as the peroxide acts as a bleaching agent. The colour change test confirmed the colour difference of the samples treated in the hydrogen peroxide solutions. In fact the hydrogen peroxide treatment method caused the highest colour difference among the treatment methods, which were tested in this study, with ΔE values of between 9.27 to 11.79 (Figure 4.65). This was typically an increase in ΔL of 10, and a decrease in both a* and b* (Figure 4.66).

The hot air treated samples also had colour differences but these were smaller than that seen at the hydrogen peroxide samples. The samples appeared to become slightly whiter than the control. ΔE of the hot air treated samples confirmed that there was a colour change, with values ranging from 5.66 to 7.24 (Figure 4.69) but those were considerably lower than the ΔE values observed at hydrogen peroxide treated samples. Here the change in luminance was smaller (ΔL 6 to 7) and the reduction in a* and b* varied with speed.

The flame treated samples colour was also different from the control samples. With the naked eye it was clear that the samples treated with the speed of 125 mm s^{-1} had become darker, because the surface was slightly burnt. The colour determination test confirmed that there were colour differences between treated and untreated samples, as the ΔE values varied from 5.89 to 6.77 (Figure 4.73). Here an increase in L*, a* and b* was seen. The highest ΔE value was observed at the samples treated with the slowest speed of 125 mm s^{-1}, as was expected in this sample ΔL was negative, unlike all other speeds. In fact the samples treated with the speed of 125 mm s^{-1} appeared to have the lowest L^* value among all the treated samples of every treatment method and the control samples, which corresponds with the burning of the surface in this set (Figure 4.74). Likewise the colour of the samples treated with halogen heating lamps was slightly different and it was also confirmed by the ΔE values, which varied from 4.87 to 6.14 (Figure 4.77). Halogen heating lamps treatment samples appeared to have the smallest colour differences among all the treatment methods.

5.5 COMPARING OPTIMAL TREATMENTS AND THEIR ADHESION MECHANISMS

From each of the four treatments investigated, it was possible to find an optimal treatment rate or reaction condition. Figure 5.27 shows the data for the optimal treatment of

each method, and present the percentage material failure which was observed for each of the sample population. For the hot air treatment two options are presented. The samples treated at the speed of 115 mm s^{-1} and the samples treated with two passes at the speed of 75 mm s^{-1}. This is because they had similar material failure and therefore both of the treatment cases were considered to have similar beneficial effect to adhesion strength.

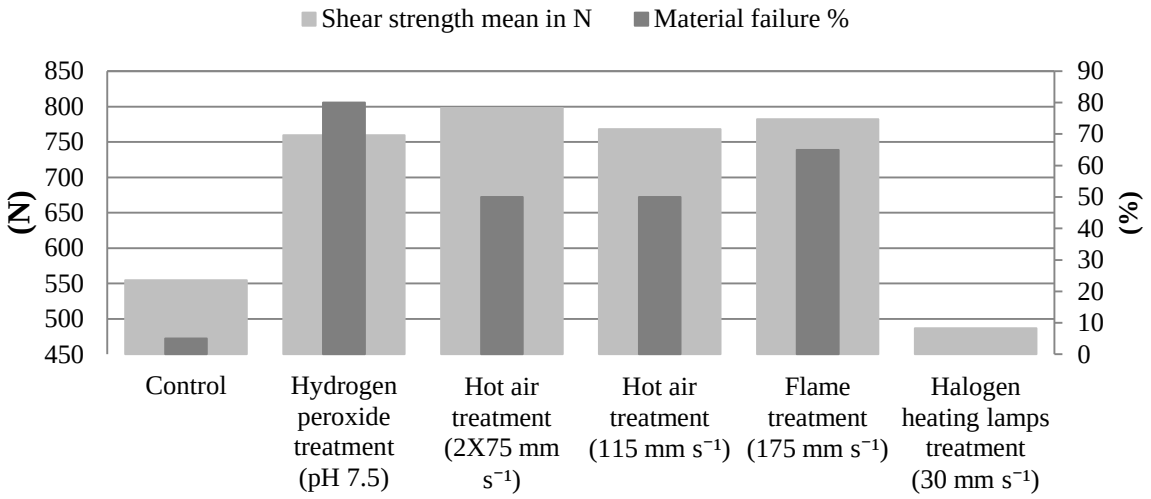

Figure 5.27: Treatments methods shear strength means and material failure percentage. Light grey bars are showing the highest shear strength mean observed of every treatment. Darker bars are showing the percentage of the samples that failed at the material rather to the bonding.

All the treatment methods, except the halogen heating lamp, are able to increase the adhesion strength of the WPC material. Figure 5.27 shows that the highest adhesion strength was achieved when the WPC was treated with two passes of 75 mm s^{-1} hot air at 797.78 N from the shear strength mean of 554.7 N of the untreated samples. The flame treatment at 175 mm s^{-1} was a close second at 781.93 N, followed by the hydrogen peroxide treatment 759.59 N. There were no significant differences between these treatments. The shear strength mean values, excluding the halogen heating lamps treatment, vary from 759.59 N (Hydrogen peroxide treatment) to 797.78 N (Hot air treatment). Therefore, despite the fact that the hot air treatment appears to have the highest adhesion shear strength mean, it is not possible to be sure if this is the best treatment method for improving the WPC adhesion ability. However the lowest deviation (SD=47.45) was achieved for the hot air treatment 2 X 75 mm s^{-1} as compared to 60.11 for the single pass hot air treatment (115 mm s^{-1}), 76.14 for the flame treatment (175 mm s^{-1}) and 97.53 for the hydrogen peroxide system.

In order to compare the effectiveness of every treatment method the material failure percentage could also be considered as a measuring factor that could provide helpful information about the adhesion strength improvement. The hydrogen peroxide treatment had

the highest material failure percentage of 80%. The flame treatment followed with 65% and then the hot air treatment with 50%. By the material failure percentage examination a completely different view of the best treatment method for adhesion improvement is observed as this indicates good cohesion of the cured adhesive, and good adhesion between the adhesive and the WPC, leading to failure in the WPC. According to the shear strength means, the hydrogen peroxide treatment provides the lowest advantageous adhesion effect, which disagrees with the material failure evaluation, according to which hydrogen peroxide has the highest percentage of 80%. Likewise, the hot air treatment has the highest shear strength mean, but it has the lowest percentage of 50% of the samples failed at the material. It is also observed that the samples treated with hot air with the speeds of 2X75 mm s^{-1} and 115 mm s^{-1} had the same percentage of material failure, but the shear strength means were different (797.78 N and 781.93 N respectively). However, the shear strength mean values of both 2X75 mm s^{-1} and 115 mm s^{-1} hot air treated samples still have the highest shear strength means among the rest of the treatment methods.

Consequently, it is not possible to conclude with confidence which of the treatment methods is best for improving the WPC adhesion ability. However, it is clear that all the treatments methods, except the halogen heating lamps, are advantageous, affecting the adhesion ability to almost similar shear strength mean values.

The material failure could be an indication of the adhesion improvement, but it could lead to incorrect conclusions, because there is also a possibility that the WPC surface could have been degraded by the treatment, resulting in a more frangible surface, which would also lead to high material failure. SEM observation revealed that in some cases, like in hydrogen peroxide treated samples, there were clearly visible degraded wood particles. This degradation of the samples treated in hydrogen peroxide solution, most possibly occurred because the wood particles absorb the H_2O_2 treatment solution, and lost adhesion due to swelling and subsequent shrinkage effects. Also, hydrogen peroxide treated samples have the highest material failure percentage among all treated samples. Therefore, it could be possible to link the wood degradation of the treated samples with the material failure.

Figure 5.28 presents the mean shear strength values of the lap joint samples that failed in the material which were excluded from the men values discussed in previous chapter according to the standard. There was a difference between the adhesion strength means, but it is not clear if they really differ because of the low sample number and high standard deviation. One way ANOVA also confirms that there is no statistically significant difference

among the shear strength of the samples that failed on the material (Table 5.1). For that reason, it could not be confirmed whether the sample surface had became fragile due to the oxidation effect of the treatments. Further investigation of surface degradation, which could lead to more fragile surface, is necessary for better evaluation of WPC pre-treatments for adhesion ability improvement.

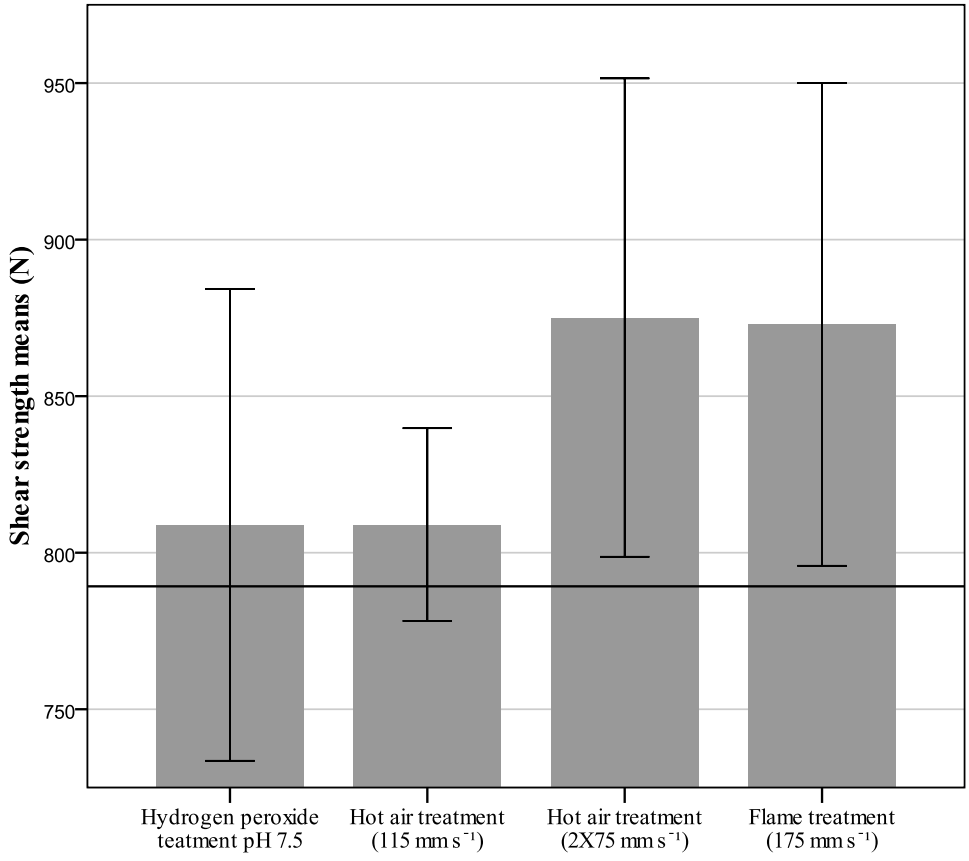

Figure 5.28: Mean values of the samples failed on the material rather the bonding line. The linear line present the shear strength of the only control sample which failed in the material (789.26 N). Error bars presenting the SD (+/-1).

Table 5.1: Best treatments multiple comparison test results. Statistical significant differences for p<0.05. Values with fainter text are >0.05.

	Hot air treatment 115 mm s^{-1}	Hot air treatment 2X75 mm s^{-1}	Flame treatment 175 mm s^{-1}
Hydrogen peroxide treatment pH 7.5	1.000	0.099	0.079
Hot air treatment 115 mm s^{-1}		0.161	0.143
Hot air treatment 2X75 mm s^{-1}			1.000

The pits on the flame treated WPC surface were most probably formed because the polymer component was melted by the heat of the flame and caused the surface roughness to increase. The hydrogen peroxide treated samples did not seem to become rougher under SEM and light microscopy examination, except for the wood particle degradation which could explain the increasing surface roughness. On the other hand, hot air treatment did not cause an increase in surface roughness and the surface roughness of the hot air treated samples was slightly lower than the untreated samples, but with no statistically significant difference according to one way ANOVA analysis. The halogen heating lamp treatment also created samples which retained the same surface roughness.

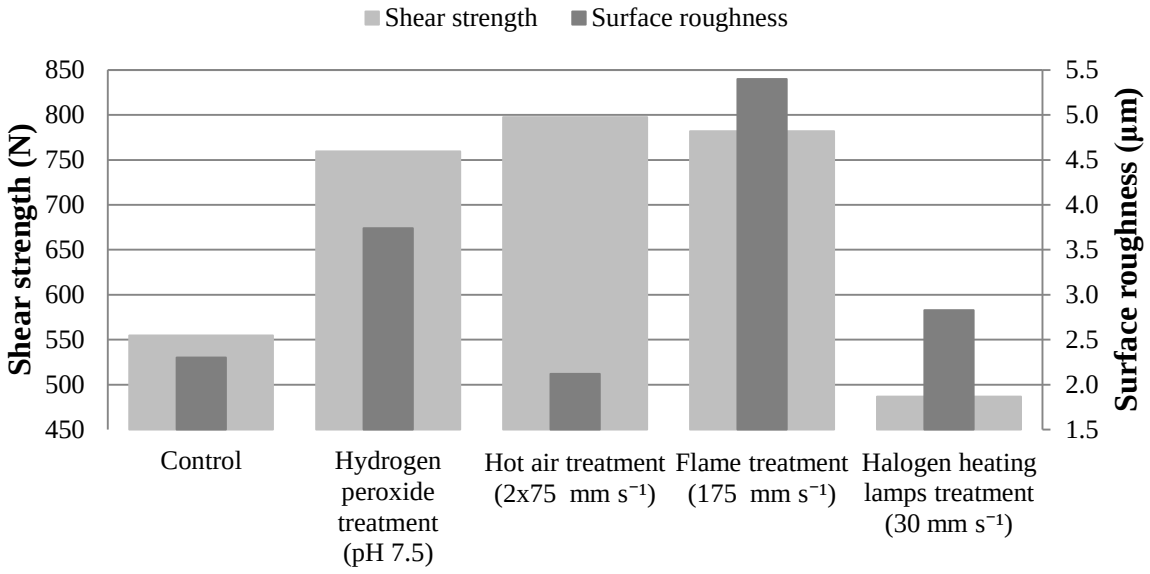

Figure 5.29: Treatments methods shear strength means and surface roughness. Light grey bars shows the shear strength means and the darker bars represent the surface roughness

Therefore the relationship between surface roughness and adhesion strength could not be confirmed and each method caused different surface modification. The adhesion mechanism is not only affected by the surface roughness. Even for hydrogen peroxide and flame treatment which increased the surface roughness, there was no consistent relationship between the surface roughness and the lap joint shear strength. It could be therefore be assumed that more complicated mechanisms like chemical and electrostatic bonds and not just morphological reasons are affecting the adhesion ability of the WPC, because the samples treated with hot air had an advantageous effect on the adhesion ability, but the surface roughness showed no statistically significant changes.

The SEM observation showed the appearance of the sample surfaces, after each treatment, in order to examine the morphological changes which occurred. In the samples

treated in hydrogen peroxide solution, a serious wood particle degradation was noticed. It was also observed that the wood particles partially detached from the polymer. Those damages could lead to water absorption on the surface when the material is exposed to wet or humid weather conditions and might result in reduced joint durability in weathering. However, the wood degradation did not seem to differ between the samples treated in pH 7.5 solution and pH 9. Therefore the pH of the solutions did not seem to cause any obvious differences that could explain why pH 7.5 had the highest adhesion shear strength and pH 9 the lowest among the samples treated in hydrogen peroxide various pH solutions.

On the sample surfaces which were treated with flame the only difference between the samples treated with the speed of 175 mm s^{-1}, which had the highest adhesion shear strength, and the samples treated with the speed of 125 mm s^{-1}, which had the lowest shear strength, was the size of the pitting. The pits which were formed on the surface of the samples treated with the speed of 125 mm s^{-1} were significantly larger than those formed on the samples treated at 175 mm s^{-1}. The pit size as mentioned before could explain the surface roughness difference, but could not be linked with the adhesion behaviour as the pit formation was only observed in the flame treated samples and therefore could not be compared with any similar phenomenon on the other treatment methods. However Zhang et al (1998) reported that there were pits formed on the polymer surface due to electron attack by the corona discharge treatment, which might increase the bonding area resulting in improved adhesion strength.

The sample surfaces treated with the hot air and by the halogen heating lamps did not seem to differ under SEM observation from the untreated samples. Therefore there was no visible morphological change that could explain the adhesion differences with those treatment methods. Consequently, the WPC surface morphology of the pre-treatments presented in this study could not be clearly linked to a specific reason that could explain the adhesion behaviour. In contrast, the SEM observation shows that the flame and the hydrogen peroxide pre-treatments caused surface damage which could be expected to lead to adhesion problems and material durability problems in weather exposure. It is important to further investigate the surface degradation to understand if the damage caused by the pre-treatments is possible to degrade the material quality and reduce its durability.

The surface energy of almost all the treated samples of all the treatment methods was higher than the untreated samples. Also, the adhesion strength of all the treated samples, except of the samples treated with halogen heating lamps, was mainly higher than the control samples. Therefore, it could be possible to link the surface energy to the adhesion strength,

but there was no clear trend supporting this. In some cases similar surface energies produced completely different adhesion strength values, for example, the samples treated in pH 9 hydrogen peroxide solution had the highest surface energy of the samples treated in hydrogen peroxide solution, but also had the lowest adhesion strength among the treated samples. Moreover, the samples treated with hot air with the speed of 75 mm s^{-1} and the samples treated with halogen heating lamps with the speed of 30 mm s^{-1} had similar surface energy of around 19 mN m^{-1}, but the adhesion strength of the hot air treated samples was around 660 N and the halogen heating lamps around 480 N, which was lower than the control values.

The hot air treatment did not produce surface energies higher than the control surface energy according to one way ANOVA, except for the samples treated at the speed of 75 mm s^{-1}. However the adhesion strength of the majority of the treated samples was statistically significantly higher than the control samples. Thus the surface energy did not clearly affect the adhesion strength of the samples treated with hot air, and therefore other reasons were responsible for the adhesion improvement of the hot air treated WPC samples. The surface roughness of the hot air treated samples was also not statistically significant different from the untreated samples. Therefore the surface morphology which was tested by surface roughness in this study was also not responsible for the adhesion strength improvement of the hot air treated samples. Thus there should be chemical differences which should effect the adhesion of the hot air treated WPC.

The most typical product of the oxidation is the esters, which were mainly increased when the WPC was treated with hot air. The ester content values had similar trends to the adhesion strength but there were points where this behaviour was different. For example, the samples treated with hot air at speeds of 18.5 mm s^{-1} and 67.5 mm s^{-1} had exactly the opposite trend than that was expected. The samples treated at the speed of 18.5 mm s^{-1} had the lowest adhesion strength, lower than the control values, and the ester ratio was the highest of the treated samples. Also, as the treatment speed increased from 37.5 mm s^{-1} to 67.5 mm s^{-1} the adhesion strength increased, but the ester ratio decreased to lower than the control. Moreover there were hot air treated samples which had ester ratios lower than the untreated samples, but yet the adhesion strength was higher than the control. Consequently, the esters of the hot air treated samples should be most probably the main reason of which the adhesion strength was improved, but there was no clear trend to relate the adhesion strength and the esters on the surface.

On the other hand, the hydrogen peroxide treatment mainly produces WPC surfaces with lower ester ratios than the control. When the samples were treated in acidic solutions the ester ratio seemed to follow a similar pattern with the adhesion strength. However for the samples treated in alkaline solutions a more insufficient decreasing trend of the ester ratio was observed. Therefore the hydrogen peroxide treatment did not produce better adhesion by the same ester effect which was observed at the samples treated with hot air. The surface energy of the hydrogen peroxide treated samples was mainly higher than the control, but there was no specific trend to explain the adhesion strength improvement. Examination of the surface chemistry did not reveal a number of reasons for the improvement but esters, considered to be the main oxidation products, were reduced. However, it was observed in the hot air gun treatment that the duration of the treatment was not the only factor that changes that surface chemistry but also the treatment repetition. Papirer et al (1993) showed that repetition of flame treatment causes an increase in ester content in polypropylene but there was not in this study any comparison with single and multiple treatment method.

However the surface energy was increased when the samples were treated in hydrogen peroxide solutions. Therefore, a hypothesis that the ester groups were converted further by oxidation causing the surface energy to increase. The surface roughness which was increased after the hydrogen peroxide treatment might also affect the adhesion strength of the samples. Thus, the reasons that cause the increase of the adhesion strength, were a complex combination of both chemical and morphological aspects, which could not be deconvoluted by this study. The lignin reduction of the samples treated in hydrogen peroxide solution could be related to the wood degradation which was observed by the SEM.

The flame treated samples gave the best relationship between the surface energy and the adhesion strength. The surface energy changes followed the adhesion strength, giving similar trends, although this did not occur with all treatment speeds. The ester ratio also, was increased when the samples treated with flame, but the ester trend did not follow the shear strength line and it followed a reversed trend from the adhesion strength. Therefore, it was not possible to understand the exactly contribution of the ester to the adhesion strength improvement of the WPC. This study was also not able to clearly understand the relation of esters with the surface energy of the samples treated with flame.

The halogen heating lamps treatment gave confusing results. The surface energy followed exactly the same trend as the adhesion strength of the treated samples. However, the adhesion strength of all the treated samples was lower than the controls and the surface energy

was higher. The ester ratio was also increased from the control samples and also had a similar trend to the adhesion strength, with an exception of the samples treated with the speed of 10 mm s^{-1}. The increase of the esters and the surface energy in the samples treated with the speed of 30 mm s^{-1} was most possibly related to the adhesion strength, which agrees with the hypothesis that the oxidation would increase the esters and the surface energy and therefore the adhesion strength would be increased. However halogen heating lamp treatment causes the adhesion strength to reduce, which totally disagrees with the hypothesis mentioned before. The surface roughness on the other hand, seems to follow the same trend with the adhesion strength and the surface energy of the halogen heating lamp treated samples, with an exception the samples treated with the speed of 10 mm s^{-1} just like the ester ratio trend. However, the only halogen heating lamp treated samples which had surface roughness higher than the control were the samples treated with the speeds of 10 mm s^{-1} and 30 mm s^{-1}. Also the surface roughness was not statistically significantly different from the control values. Thus it could not be confirmed that the surface roughness was responsible for the lower of the control adhesion strength values.

The aesthetic aspect of the pre-treatments for improving the adhesion ability was mostly monitored by the colour difference which was occurred after each treatment. Figure 5.30 shows the colour differences that occurred in the most beneficial cases of each treatment.

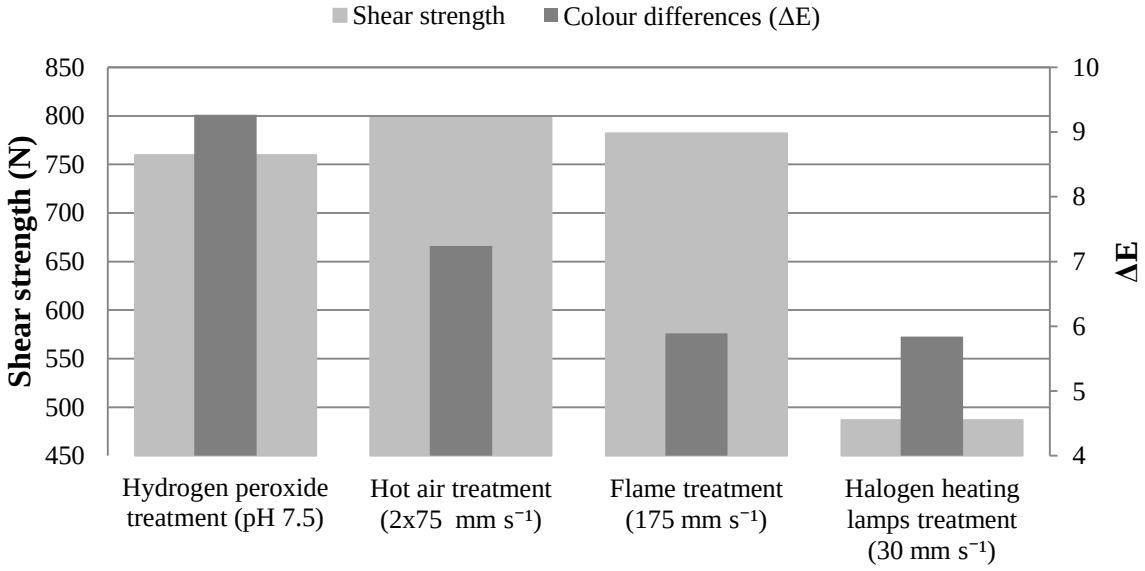

Figure 5.30: Treatments methods shear strength means and surface roughness. Light grey bars shows the shear strength means and the darker bars represent the colour differences.

According to Figure 5.30, the samples treated with halogen lamps appeared to have the smallest colour difference. The flame treated samples had a slightly higher colour difference than the halogen heating lamp treated samples. The hot air treated samples had a higher colour difference than the flame treated samples and the hydrogen peroxide treated samples appear to have had the greatest colour difference. Consequently, among the pre-treatment which benefit adhesion the method which has least affection the colour of the treated samples, is the flame treatment method and the hot air method, with small differences.

5.6 SUGGESTIONS FOR FUTURE WORK

It could be interesting to look the treatment effectiveness of the WPC without rinsing with water in order to avoid possible alteration of the wood flour within the composite and cross check the results with this study for potential differences.

Another factor that needs to be tested is the tension strength of the material after the treatments. There could be a degradation during the pre-treatments that leads to material failure in lower shear strengths.

Moreover SEM microscopy on the adhesive boundary could provide information about the mechanical grafting of the glue on the material surface.

Expanding the treatment parameters could also be interesting to fully evaluate the possibilities of the treatments. Distance of heating equipments, higher treatment speeds and repetition process could result to also beneficial effects on the adhered bond strength.

The halogen heating lamps is a very interesting treatment and the examination of the reasons that results to the lower adhesion strength could provide valuable information about the mechanisms of adhesion.

Finally the chemical reactions during the hydrogen peroxide treatment needs to be further investigated. It could be more interesting to study the effect of the treatment in wood and the polymer separately in order to indentify the different chemical impact on the material.

CHAPTER 6: CONCLUSIONS

1. The reasons which are affecting the adhesion strength of the treated samples were not clearly confirmed by this study. There were more complicated and interactive reasons which were responsible for the adhesion improvement. There were some indications between the surface energy and the adhesion strength where the hypothetical relationship could not be confirmed with certainty. Also there were some indications that the ester content was related with the adhesion strength and the surface energy, but there were cases in which those indications were totally at odds with the rest of the obtained data. For example the samples treated in hydrogen peroxide solution caused the ester ratios to reduce to values lower than the control because of the reactions between esters and H_2O_2 and NaOH, yet showed good bonding.

However it is possible to hypothesise the main factors that affect the adhesion on a treatment by treatment basis.

- The mechanical factor is not affected by the heat gun treatment. No increase in roughness was seen, unlike the observation for flame and hydrogen peroxide treatment.
- The heat gun treated sample improved adhesion appears to be influenced by the chemical bond adhesion theory in particular relating to the ester formation.
- The flame treatment acts by the thermodynamic theory as it produces a surface with high surface energy in contrast to the other treatments.
- The hydrogen peroxide treatment is more adequately explained by mechanical and chemical bonding factors as both the surface roughness and the chemical analysis were significantly altered.
- Finally the halogen heating lamps treatment changes the surface chemistry which results in an adhesion strength decrease.

To understand the mechanism under of which the treated WPC samples had adhesion strength improvement, a further and a more specific research on the chemical and the morphological properties should be undertaken. This study was mainly undertaken to investigate the effectiveness of the pre-treatments in the adhesion strength improvement of the WPC, and not to clarify the exact reasons which result in the adhesion strength improvement of the treated samples.

2. The pre-treatments that were examined in this study were chosen to be easily applicable and without the need of complicated and expensive equipment. The usage of low cost, non-sophisticated equipment and simple methods for applying each treatment method was essential, because the pre-treatments are meant to be used in small workshops by typical furniture and frame construction manufacturers. All treatments which were investigated in this study were advantageous, enhancing the adhesion ability of the WPC, with the exception of the samples treated with halogen heating lamps. The lap joint shear strength means of the optimal for each type of treated samples were around the same values (750 N to 800 N, see Figure 5.27) and therefore all pre-treatment methods, except the halogen heating lamp, could be considered as having a similar improvement in adhesion. The easiest treatment to perform is the hydrogen peroxide solution method, because it is easy to monitor the parameters of the procedure. A timer and a pH meter is the only equipment needed. The disadvantage of this procedure is that the treatment is applied to the whole material and not just to the desired area for bond formation and this could affect the subsequent weathering performance. However, surely a product could be developed for correct pH and easy application only to the desired for bonding area. Furthermore, the wood particles on the surface were degraded and might affect the surface mechanical properties and stability. The material colour also appears changed to a greater degree. Moreover, despite the fact that there is only a small amount of NaOH used there may be some health and safety issues to relating to its usage and storage. Peroxide can under some circumstances be hazardous.

3. The hot air treatment appears to be a very effective surface treatment for adhesion improvement. The shear strength was significantly increased due to the hot air treatment, and had the highest adhesion strength mean value among the rest of the treatment methods. In addition the hot air treatment did not seem to cause any damage of the treated surface, in contrast to the hydrogen peroxide and flame treatment methods. The treatment procedure can be restricted to the area to be bonded and not the whole material (as opposed to the hydrogen peroxide method). The method requires simple equipment with low cost. The only equipment required is a hot air gun which is very easy to use and easy to purchase. Furthermore the colour of the treated samples was not significantly changed. The colour difference was just higher than the colour difference that occurred of the flame treated samples, but was significantly lower than the colour difference that occurred at the samples treated in hydrogen peroxide solution. Moreover, the hot air treatment can also be a very accurate procedure but it is important to control the rate: the slowest treatment speed (18.5 mm s^{-1}) caused low

adhesion strength values. An interesting result was that the two pass treatment provided the best bond.

4. The flame treatment produces adhesion strength improvement values similar to hot air and hydrogen peroxide treatments when done at the optimal speed. It has the advantage that the treatment is restricted to the desired surface, as with the hot air treatment. Flame treatment is easy and the only equipment needed is a flame torch with a MAPP gas tank. The colour change due to flame treatment had the smallest difference among the treatment methods. However, the flame treatment causes pitting degradation on the material surface which might have an effect on the material properties in service. Furthermore, the flame application is a potentially hazardous procedure; the WPC is a flammable material, it could also produce toxic fumes during treatment if polypropylene (as used in this study) is contaminated with additives or replaced with other polymers such as PVC. The treatment speed as well needs to be optimised for any chosen system because a too slow rate produces low adhesion strength results, while too fast is sub-optimal.

5. Consequently, the safest treatments for improving WPC adhesion strength were the hydrogen peroxide and the hot air treatment. However, the hot air treatment seems to be a better procedure than hydrogen peroxide, because there is no need for chemical usage and the surface is modified only at the desirable area and not at the whole material. Furthermore, the samples treated with the hot air do not seem to have a degraded surface, and there was less colour difference in comparison to the samples treated with hydrogen peroxide solutions. Also the procedure of the hot air treatment is significantly faster than the hydrogen peroxide method.

6. The most interesting case however, was the halogen heating lamp treatment method. The treatment using halogen heating lamps caused the adhesion strength to decrease to values lower than the control, without any obvious morphological change. Therefore this method is not recommended. Further investigation of the halogen heating lamps would be whoever interesting to understand the reasons behind this less effective adhesion. It could also worth to investigate the halogen heating lamp as a treatment method to reduce the adhesion ability of polymer materials, for surface protection from paints and adhesives, in uses like workbenches.

REFERENCES

Adhikary B. K., Pang S. and Staiger P. M. 2008a. Long-term moisture absorption and thickness swelling behaviour of recycled thermoplastic reinforced with *Pinus radiata* sawdust. Chem. Eng. J. 142:190-198.

Adhikary B. K., Pang S. and Staiger P. M. 2008b. Dimensional stability and mechanical behaviour of wood-plastic composites based on recycled and virgin high-density polyethylene (HDPE). Compos. Part B-Eng 39:807-815.

Ashori A. 2008. Wood-plastic composites as promising green-composites for automotive industries. Bioresource Technol. 99:4661-4667.

Bengtsson M. and Oksman K. 2006. Silane cross-linked wood plastic composite: Processing and properties. Compos. Sci. Technol. 66:2177-2186.

Bengtsson M., Gatenholm P. and Oksman K. 2005. The effect of crosslinking on the properties of polyethylene/wood flour composites. Compos. Sci. Technol. 65:1468-1479.

Bengtsson M., Oksman K. and Stark M. N. 2006. Profile extrusion and mechanical properties of cross-linked wood-thermoplastic composites. Polym. Compos. 27(2):184-194.

Bledzki K. A. and Gassan J. 1999. Composites reinforced with cellulose based fibres. Prog. Polym. Sci. 24:221-274.

Briggs D., Brewis D.M., Konieczo M.B. 1976. X-ray photoelectron spectroscopy studies of polymer surfaces. Part1 Chromic acid etching of polyolefins. J. Mater. Sci. 11:1270-1277.

Bykov, I., 2008. Characterization of natural and technical lignins using FTIR spectroscopy. D, Master Thesis, Lulea University

Chotirat L., Chaochanchaikul K. and Sombatsompop N. 2007. On adhesion mechanisms and interfacial strength in acrylonitrile-butadiene-styrene/wood sawdust composites. Int. J. Adhes. Adhes. 27:669-678.

Clemons C. 2002. Wood-plastic composites in the United States: The interfacing of two industries. Forest Prod. J. 52(6):10-18.

Clemons C. and Stark N. 2007. Use of saltcedar and Utah juniper as fillers in wood-plastic composites. Forest Products Laboratory Research Paper 641, 17 pp.

Clemons M. C. and Ibach E. R. 2004. Effects of processing method and moisture history on laboratory fungal resistance of wood-HDPE composites. Forest. Prod. J. 54(4):50-57.

Cui Y., Lee S., Noruziaan B., Cheung M. and Tao J. 2008. Fabrication and interfacial modification of wood/recycled plastic composite materials. Part A. Compos. Appl. Sci. 39: 655-661.

De Carvalho A. J. F., Zambon M. D., Curvelo A. A. S. and Gandini A. 2003. Size exclusion chromatography characterization of thermoplastic starch composites: 1. Influence of plasticizer and fibre content. Polym. Degrad. Stabil. 79:133-138.

Du Toit F.J. and Sanderson R.D. 1999. Surface fluorination of polypropylene 1. characterization of surface properties. J. Fluorine Chem. 98:107-114

Falk H. R., Vos J. D., Cramer M. S. and English W. B. 2001. Performance of fasteners in wood flour-thermoplastic composite panels. Forest Prod. J. 51(1):55-61.

Farid S. I., Kortschot M. T. and Spelt J. K. 2002. Wood-flour-reinforced polyethylene: viscoelastic behaviour and threaded fasteners. Polym. Eng. Sci. 42(12):2336-2350.

Faruk O. and Matuana M. L. 2008. Nanoclay reinforced HDPE as a matrix for wood-plastic composites. Compos. Sci. Technol. 68:2073-2077.

Garbassi F., Occhiello E., Polato F. and Brown A. 1987. Surface effect of flame treatments on polypropylene: Part 2 SIMS (FABMS) and FTIR-PAS studies. J. Mater. Sci. 22:1450-1456

Gatenholm P., Bonnerup C. and Wallstrom E. 1990. Wetting and adhesion of water-borne printing inks on surface-modified polyolefins. J. Adhes. Sci. Technol. 10:817-827

Georgopoulos S. T., Tarantili P. A., Avgerinos E., Andreopoulos A. G. and Koukios E. G. 2005. Thermoplastic polymers reinforced with fibrous agricultural residues. Polym. Degrad. Stabil. 90: 303-312.

Gaudill V. E. And Halek G. W. 1992. Polypropylene surface characteristics after exposure to hydrogen peroxide and heat processing. J. Plastic Film and Sheeting. 8(2):140-145

Gijsman P., Kroon M, and Oorschot M. 1995. The role of peroxides in the thermoxidative degradation of polypropylene. Polym. Degrad. Stabil. 51:3-13.

Grigoriou E. A. 1999. Composite products made by lignocellulosic and polymer raw materials. Geotechnical scientific issues 10(2):212-222. (In Greek)

Guimond S., and Wertheimer M. R., 2004. Surface degradation and hydrophobic recovery of polyolefins treated by air corona and nitrogen atmospheric pressure glow discharge. J. Appl. Polym. Sci. 94, 1291-1303

Gupta B. S., Reiniati I. and Laborie M-P. G. 2007. Surface properties and adhesion of wood fiber reinforced thermoplastic composites. Colloid. Surf. A: Physicochem. Eng. Aspects. 303:338-395

Ibach E. R. and Clemons M. C. 2002. Biological resistance of polyethylene composites made with chemically modified fiber or flour. In: Proceedings of the sixth pacific rim bio-based composites symposium and workshop on the chemical modification of cellulosics. Oregon State University, Portland, Oregon, pp. 19-25.

Jaaskelainen, A., Nuopponen, M., Axelsson, P., Loija, M., and Vuorinen, T., 2003. Determination of lignin distribution in pulps by FTIR ATR spectroscopy. J. pulp paper Sci. 29 (10) 328-331.

Jiang H. and Kamdem D. P. 2004. Development of poly(vinyl chloride)/wood composites. A literature review. J. Vinyl Addit. Technol. 10(2):59-69.

Jiang L., Wolcott P. M., Zhang J. and Englund K. 2007. Flexural properties of surface reinforced wood/plastic deck board. Polym. Eng. Sci. 47:281-288.

Johnson M., Tucker N., Barnes S. and Kirwan K. 2005. Improvement of the impact performance of a starch based biopolymer via the incorporation of *Miscanthus giganteus* fibres. Ind. Crops Prod. 22:175-186.

Jones V., Strobel M. and Prokosch M. J. 2005. Development of poly(propylene) surface topography during corona treatment. Plasma Process. Polym. 2:547-553

Kamdem D. P., Jiang H., Cui W., Freed J. and Matuana M. L. 2004. Properties of wood plastic composites made of recycled HDPE and wood flour from CCA-treated wood removed from service. Part A. Compos. Appl. Sci. 35:347-355.

Kiguchi M., Kataoka Y., Matsunaga H., Yamamoto K. and Evans D. P. 2007. Surface deterioration of wood-flour polypropylene composites by weathering trials. J. Wood Sci. 53:234-238.

Kruss GmbH, Hamburg 2004-2011, Software for drop shape analysis DSAI V.1.92 for contact angle measurement systems. User manual. V. 1.92-05

Kumari R., Ito H., Takatani M., Uchiyama M. and Okamoto T. 2007. Fundamental studies on wood/cellulose-plastic composites: effects of composition and cellulose dimension on the properties of cellulose/PP composite. J. Wood Sci. 53:470-480.

La Mantia F.P. and Morreale M. 2008. Accelerated weathering of polypropylene/wood flour composites. Polym. Degrad. Stabil. 93(7):1252-1258

Lazar M., Hrckova L., Borsig E., Marcinin A. And Reichelt N. 2000. Course of degradation and built-up reaction in isotactic polypropylene during peroxide decomposition. J. App. Polym. Sci. 78:886-893

Lee S-Y., Yang H-S., Kim H-J., Jeong C-S., Lim B-S. and Lee J-N. 2004. Creep behavior and manufacturing parameters of wood flour filled polypropylene composites. Compos. Struct. 65:459-469.

Liu, C., Xu, J., Sun, J., Ren, J., Curling, S., Sun, R., Fowler P., and Baird, M., 2006. Physicochemical characterization of cellulose from perennial ryegrass leaves (*Lolium perenne*). Carbohydrate research. 341 2677-2687

Lobo H. And Bonilla J. V. Handbook of plastics analysis. 2003. ISBN 0-8247-0708-7

Lu K. T. 2006. Effects of hydrogen peroxide treatment on the surface properties and adhesion of ma bamboo (*Dendrocalamus latiflorus*). J. Wood Sci. 52:173-178.

Mirabedini S. M., Rahimi H., Hamedifar Sh. and Mohseni S. M. 2004. Microwave irradiation of polypropylene surface: a study on wettability and adhesion. Int. j. Adhes. Adhes. 24:163-170

Nachtigall M.B. S., Cerveira S. G. and Rosa M.L. S. 2007. New polymeric-coupling agent for polypropylene/wood-flour composites. Polym. Test. 26:619-628.

Najafi S.K., Kiaeifar A., Tajvidi M. and Hamidinia E. 2008. Hydroscopic thickness swelling rate of composites from sawdust and recycled plastics. Wood Sci. Technol. 42:161-168.

Najafi S.K., Tajvidi M. and Hamidina E. 2007. Effect of temperature, plastic type and virginity on the water uptake of sawdust/plastic composites. Holz Roh Werkst 65:377-382.

Neagu R. C., Gamstedt E. K. and Lindström M. 2005. Influence of wood-fibre hydroexpansion on the dimensional instability of fibre mats and composites. Part A. Compos. Appl. Sci. 36:772-788.

Nourbakhsh A. and Ashori A. 2008. Fundamental studies on wood-plastic composites: Effects of fiber concentration and mixing temperature on the mechanical properties of poplar/PP composite. Polym. Compos. 29(5):569-573.

Norusis M. J. 2005. SPSS 13.0 guide to data analysis. ISBN 978-0131865358.

Oporto S. G., Gardner J. D., Bernhardt G. and Neivandt J. D. 2007. Characterizing the mechanism of improved adhesion of modified wood plastic composite (WPC) surfaces. J. Adhes. Sci. Technol. 21(11):1097-1116.

Papirer E., Wu D.Y. and Schultz J. 1993. Adhesion of flame-treated polyolefins to styrene butadiene rubber. J. Adhes. Sci. Technol. 7:343-362

Pijpers A.P. and Meier R.J. 2001. Adhesion behavior of polypropylenes after flame treatment determined by XPS(ESCA) spectral analysis. J. Electron. Spectrosc. Relat. Phenom. 121:299-313

Pinto A. M. G., Magalhaes A. G., Silva F. G. and Baptista A. P. M. 2008. Shear strength of adhesively bonded polyolefins with minimal surface preparation. Int. J. Adhes. Adhes. 28:452-456

Pizzi A. And Mittal K. L. 1994. Handbook of adhesion technology. ISBN 0-8247-8974-1

Premalal G.B. H., Ismail H. and Baharin A. 2002. Comparison of the mechanical properties of rice husk powder filled polypropylene composites with talc filled polypropylene composites. Polym. Test. 21:833-839.

Pretsch E., Buhlmann P. and Affolter C. 2000. Structure determination of organic compounds. Tables and spectral data. ISBN 3-540-67815-8

Ritter W. G. 2000. Surface preparation IV: Treatment for plastics II. ASI (Adhesives & Sealants Industry magazine)

Romhány G., Karger-Kocsis J. and Czigány T. 2003. Tensile fracture and failure behavior of thermoplastic starch with unidirectional and cross-ply flax fiber reinforcements. Macromol. Mater. Eng. 288:699-707.

Rowell M. R. 2007. Challenges in biomass-thermoplastic composites. J. Polym. Environ. 15:229-235.

Rowell R. M. 1996. Composites from agri-based resources. In: Proceedings No. 7286: The use of recycled wood and paper in building applications. Forest products society, Madison, Wisconsin. pp. 217-222.

Selke E. S. and Wichman I. 2004. Wood fiber/polyolefin composites. Part A. Compos. Appl. Sci. 35:321-326.

Sjostrom E. 1993. Wood chemistry Fundamentals and applications. TS932.S5813.

Sombatsompop N. and Chaochanchaikul K. 2004. Effect of moisture content on mechanical properties, thermal and structural stability and extrudate texture of poly(vinyl chloride)/wood sawdust composites. Polym. Int. 53:1210-1218.

Son J., Kim H. and Lee P. 2001. Role of Paper Sludge Particle Size and Extrusion Temperature on Performance of Paper Sludge-Thermoplastic Polymer Composites. J Appl. Polym. Sci. 82:2709-2718.

Son J., Yang H-S. and Kim H-J. 2004. Physico-mechanical Properties of Paper Sludge Particle-Thermoplastic Polymer Composites. J. Thermoplast. Compos. 17:509-522.

Stark M. N. and Matuana M. L. 2003. Ultraviolet weathering of photostabilized wood-flour-filled high-density polyethylene composites. J. Appl. Polym. Sci. 90:2609-2617.

Stark M. N. and Matuana M. L. 2006. Influence of photostabilizers on wood flour-HDPE composites exposed to xenon-arc radiation with and without water spray. Polym. Degrad. Stabil. 91:3048-3056.

Stark M. N. and Matuana M. L. 2007a. Characterization of weathered wood-plastic composite surfaces using FTIR spectroscopy, contact angle and XPS. Polym. Degrad. Stabil. 92:1883-1890.

Stark M. N. and Matuana M. L. 2007b. Coating WPCs using co-extrusion to improve durability. In: Proceedings on coating wood and wood composites: Designing for durability. Federation of societies for coatings technology, Seattle, WA, pp. 1-12.

Stark M. N., Matuana M. L. and Clemons M. C. 2004. Effect of processing method on surface and weathering characteristics of wood-flour/HDPE composites. J. Appl. Polym. Sci. 93:1021-1030.

Stark M. N., White H. R. and Clemons M. C. 1997. Heat release rate of wood-plastic composites. Sampe. J. 33(5):26-31.

Stark N. 2001. Influence of moisture absorption on mechanical properties of wood flour-polypropylene composites. J. Thermoplast. Compos. 14:421-432.

Steckel V., Clemons M. C. and Thoemen H. 2007. Effects of material parameters on the diffusion and sorption properties of wood-flour/polypropylene composites. J. Appl. Polym. Sci. 103:752-763.

Stokke D. D. and Gardner J. D. 2003. Fundamental aspects of wood as a component of thermoplastic composites. J. Vinyl Addit. Technol. 9(2):96-104.

Strobel J. M., Strobel M., Lyons C. S., Dunatov C. and Perron S. J. 1991. Aging of air-corona-treated polypropylene film. J. Adhes. Sci. Technol. 2:119-130

Sun et al 2004. Comparative study of hemicellulose isolated with alkaline peroxide from lignocellulosic materials. J. Wood Chem. Technol. 24 (3) 239-262

Sun Q. C., Zhang D. and Wadsworth L. C. 1999. Corona treatment of polyolefin films-A review. Adv. Polym. Technol. 2:171-180

Tajvidi M., Najafi S. K. Shekaraby M. M. and Motiee N. Effect of chemical reagents on the mechanical properties of natural fiber polypropylene composites. Polym. Compos. 27(5):563-569.

Tungjitpornkull S. and Sombatsompop N. 2009. Processing technique and fiber orientation angle affecting the mechanical properties of E-glass fiber reinforced wood/PVC composites. J. Mater. Process. Technol. 209(6):3079-3088

Urbaniak-Domagala, W., 2011. Pretreatment of polypropylene films of creation of thin polymer layers, part 1: The use of chemical, electrochemical, and UV methods. J. Appl. Polym. Sci. 122:2071-2080

Wang W. and Morell J. J. 2004. Water sorption characteristics of two wood-plastic composites. Forest Prod. J. 54(12):209-212.

Wechsler A. and Hiziroglou S. 2007. Some of the properties of wood-plastic composites. Build. Environ. 42:2637-2644.

Winandy E. J., Stark M. N. and Clemons M. C. 2004. Considerations in recycling of wood-plastic composites. In: Proceedings of the fifth global wood and natural fibre composites symposium. Institut fur Werkstofftechnnik Kunststoff- und Recyclingtechnik, Kassel, Germany, pp. A6:1-9.

Yang H-S., Kim H-J., Son J., Park H-J, Lee B-J. and Hwang T-S. 2004. Rice-husk flour polypropylene composites; mechanical and morphological study. Compos. Struct. 64:305-312.

Youngquist A. J. 1995. Unlikely partners? The marriage of wood and nonwood materials. Forest Prod. J. 45(10):25-30.

Zhang D., Sun Q. and Wadsworth L. C. 1998. Mechanism of corona treatment on polyolefin films. Polym. Eng. Sci. 6:965-970